



689
2015

Berichte

zur Polar- und Meeresforschung

Reports on Polar and Marine Research

The Expedition PS89 of the Research Vessel POLARSTERN to the Weddell Sea in 2014/2015

Edited by

Olaf Boebel

with contributions of the participants

Die Berichte zur Polar- und Meeresforschung werden vom Alfred-Wegener-Institut, Helmholtz-Zentrum für Polar- und Meeresforschung (AWI) in Bremerhaven, Deutschland, in Fortsetzung der vormaligen Berichte zur Polarforschung herausgegeben. Sie erscheinen in unregelmäßiger Abfolge.

Die Berichte zur Polar- und Meeresforschung enthalten Darstellungen und Ergebnisse der vom AWI selbst oder mit seiner Unterstützung durchgeführten Forschungsarbeiten in den Polargebieten und in den Meeren.

Die Publikationen umfassen Expeditionsberichte der vom AWI betriebenen Schiffe, Flugzeuge und Stationen, Forschungsergebnisse (inkl. Dissertationen) des Instituts und des Archivs für deutsche Polarforschung, sowie Abstracts und Proceedings von nationalen und internationalen Tagungen und Workshops des AWI.

Die Beiträge geben nicht notwendigerweise die Auffassung des AWI wider.

Herausgeber

Dr. Horst Bornemann

Redaktionelle Bearbeitung und Layout

Birgit Reimann

Alfred-Wegener-Institut
Helmholtz-Zentrum für Polar- und Meeresforschung
Am Handeshafen 12
27570 Bremerhaven
Germany

www.awi.de

www.reports.awi.de

Der Erstautor bzw. herausgebende Autor eines Bandes der Berichte zur Polar- und Meeresforschung versichert, dass er über alle Rechte am Werk verfügt und überträgt sämtliche Rechte auch im Namen seiner Koautoren an das AWI. Ein einfaches Nutzungsrecht verbleibt, wenn nicht anders angegeben, beim Autor (bei den Autoren). Das AWI beansprucht die Publikation der eingereichten Manuskripte über sein Repositorium ePIC (electronic Publication Information Center, s. Innenseite am Rückdeckel) mit optionalem print-on-demand.

The Reports on Polar and Marine Research are issued by the Alfred Wegener Institute, Helmholtz Centre for Polar and Marine Research (AWI) in Bremerhaven, Germany, succeeding the former Reports on Polar Research. They are published at irregular intervals.

The Reports on Polar and Marine Research contain presentations and results of research activities in polar regions and in the seas either carried out by the AWI or with its support.

Publications comprise expedition reports of the ships, aircrafts, and stations operated by the AWI, research results (incl. dissertations) of the Institute and the Archiv für deutsche Polarforschung, as well as abstracts and proceedings of national and international conferences and workshops of the AWI.

The papers contained in the Reports do not necessarily reflect the opinion of the AWI.

Editor

Dr. Horst Bornemann

Editorial editing and layout

Birgit Reimann

Alfred-Wegener-Institut
Helmholtz-Zentrum für Polar- und Meeresforschung
Am Handeshafen 12
27570 Bremerhaven
Germany

www.awi.de

www.reports.awi.de

The first or editing author of an issue of Reports on Polar and Marine Research ensures that he possesses all rights of the opus, and transfers all rights to the AWI, including those associated with the co-authors. The non-exclusive right of use (einfaches Nutzungsrecht) remains with the author unless stated otherwise. The AWI reserves the right to publish the submitted articles in its repository ePIC (electronic Publication Information Center, see inside page of verso) with the option to "print-on-demand".

Titel: Polarsterns vergeblicher Versuch das Schelfeis nahe der Neumayer-Station III zur Übergabe von Treibstoff zu erreichen: Ein ca. 500m breiter Kanal im etwa 3 m dicken Meereis der Atka Bucht.

© Steffen Spielke, Reederei F. Laeisz G.m.b.H.

Cover: Polarstern's vain attempt to reach the ice shelf near Neumayer Station III for its refueling: a quarter-mile wide channel into Atka Bay's fast ice of typically 10 feet thickness.

© Steffen Spielke, Reederei F. Laeisz G.m.b.H.

The Expedition PS89 of the Research Vessel POLARSTERN to the Weddell Sea in 2014/2015

Edited by

Olaf Boebel

with contributions of the participants

Please cite or link this publication using the identifiers

hdl:10013/epic.45857 or <http://hdl.handle.net/10013/epic.45857> and

doi:10.2312/BzPM_0689_2015 or http://doi.org/10.2312/BzPM_0689_2015

ISSN 1866-3192

PS89

(ANT-XXX/2)

2 December 2014 - 1 February 2015
Cape Town – Cape Town



Chief scientist
Olaf Boebel

Coordinator
Rainer Knust

Contents

Contents

1.	Zusammenfassung und Fahrtverlauf	2
	Summary and Itinerary	6
2.	Weather Conditions During PS89 (ANT-XXX/2)	8
3.	Scientific Programmes	10
3.1	Oceanography	10
3.1.1	Implementation of the HAFOS Observation System in the Antarctic	10
3.1.2	Biogeochemical Argo-type floats for SOCCOM (Southern Ocean Carbon and Climate Observations and Modelling)	40
3.1.3	The carbon system of the Southern Meridian GoodHope Section	49
3.1.4	Ocean Acoustics	57
3.1.5	Transport variations of the Antarctic Circumpolar Current	66
3.1.6	Sound levels as received by whale during a ship's passage	73
3.2	Sea Ice Physics	76
3.2.1	Sea ice mass and energy budgets in the Weddell Sea	76
3.3	Biology	102
3.3.1	Sea ice ecology, pelagic food web and top predator studies	102
3.3.2	Cetaceans in ice	127
3.4	Geobiosciences	132
3.4.1	Culture experiments on trace metal incorporation in deep-sea benthic foraminifers from the Southern Ocean	132

Appendix

A.1	Teilnehmende Institute / Participating Institutes	133
A.2	Fahrtteilnehmer / Cruise Participants	136
A.3	Schiffsbesatzung / Ship's Crew	138
A.4	Stationsliste / Station List PS89	140

1. ZUSAMMENFASSUNG UND FAHRTVERLAUF

Olaf Boebel

AWI

Die Antarktisexpedition PS89 mit FS *Polarstern* sollte ursprünglich von Kapstadt über die Atka-Bucht (*Neumayer-Station III*) in das Weddellmeer und weiter nach Punta Arenas führen. Ein während des logistischen Aufenthaltes in der Atka-Bucht entstandenes, irreparables Problem an der Verstelleinheit des Backbord-Propellers führte jedoch zu signifikanten Einschränkungen in der Leistungs- und Manövrierfähigkeit des Schiffes, die Anlass gaben, die Expedition abubrechen und über Kapstadt nach Bremerhaven zurückzukehren, um dort die notwendigen Reparaturarbeiten schnellstmöglich durchzuführen. Somit ergab sich ein Expeditionsverlauf Kapstadt – Atka-Bucht – Kapstadt.

Die Expedition beinhaltete logistische und wissenschaftliche Vorhaben. Hiervon wurden die logistischen Aufgaben (Versorgung *Neumayer-Station III* mit Treibstoff und Vorräten) vollständig umgesetzt, während von den geplanten wissenschaftlichen Arbeiten nur der Teil realisiert werden konnte, der vor Anlaufen der Atka-Bucht lag und damit weniger als die Hälfte des geplanten Programms beinhaltete.

Die wissenschaftlichen Arbeiten lassen sich in stationsgebundene, meereisbasierte, vom fahrenden Schiff aus durchgeführte sowie helikoptergestützte Arbeiten unterteilen.

Folgende stationsgebundene Aufgaben wurden durchgeführt:

- Aufnahme von 13 Tiefseepegeln entlang des GoodHope-Schnittes; (geplant: 14)
- Aufnahme/Auslage von 6/6 Verankerungen östlich *Neumayer-Station III*; (geplant: 7/5)
- Aufnahme/Auslage von 0/0 Verankerungen westlich *Neumayer-Station III*; (geplant: 14/11)
- Auslegung von 15 Argo-Floats; (geplant 28)
- Auslegung von 12 SOCCOM-Floats
- Fahren von 94 CTD Stationen mit Rosette
- Kalibration von 6 RAFOS-Schallquellen
- Analyse von ca. 4000 Wasserproben
- Beprobung des Meeresbodens mit dem Multicorer (2).

Folgende Arbeiten wurden vom fahrenden Schiff aus durchgeführt:

- Erfassung des Vorkommens von Vögeln, Robben und Walen
- Erfassung von Temperatur, Salzgehalt und Strömungsprofilen
- 18 SUIF-Fänge, davon 8 unter dem Meereis (geplant > 30)
- 15 RMT-Fänge, davon 6 in eisbedeckten Gebieten (geplant > 20).

Folgende Arbeiten wurden vom Meereis aus durchgeführt:

- 5 ROV-Eisstationen (davon 2 auf frei driftendem Meereis, geplant 12)
- Auslegung von 12 Meereisbojen (div. Typen, geplant 22)
- 3 Eiskernstationen (geplant 6)
- 2 Eisdicken-Transekte per Schlitten (geplant 0).

Weitere Arbeiten nutzten die Helikopter als Plattform. Insgesamt ergaben sich 116 Flüge mit 84:32 h kumulativer Dauer. Hiervon entfallen u.A.:

- 20 Flüge auf Tierbeobachtungen (geplant ca. 60)
- 5 Flüge auf EM Bird-Transekte (geplant 15).

Weitere wissenschaftliche Flüge erfolgten zur Markierung von Schollen, Erprobung von Geräten, logistischen Unterstützung der eisgebundenen Arbeiten sowie zum Personen- und Materialtransport bei *Neumayer III*.

Die Reise begann am 02. Dezember 2014, 18:00 h Ortszeit in Kapstadt. Die zunächst anstehende Aufnahme der Tiefseepegel verlief problemlos, was auch dem bemerkenswert gut funktionierenden POSIDONIA-System (Sendeeinheit im Brunnenschacht mit USBL-Box) zuzuschreiben ist. Einen großen Fortschritt stellt dabei die PosiSoft-Software dar, mit der sich der Aufstieg der Geräte zuverlässig verfolgen ließ. So konnte noch während des Aufsteigens der Verankerung das Schiff so positioniert werden, dass Tiefseepegel bzw. Verankerung an optimaler Position relativ zum Schiff auftauchen, was weiteres Suchen überflüssig machte und die Aufnahme (u.a. sehr effizient vom Schlauchboot aus) beschleunigte.

Im weiteren Expeditionsverlauf wurden entlang der Fahrtroute an den Verankerungspositionen sowie südlich von 55°S in Abständen von 60 nm CTDs gefahren und an ausgewählten Positionen mit biogeochemischen Sensoren ausgestattete Argo-Floats ausgelegt.

Begünstigt durch die sich um Maud Rise herum schnell öffnende Polynja war der Reisefortschritt entlang des 0°-Schnittes zügig. Am südlichsten Ende dieses Schnittes herrschte jedoch wie schon vor 2 Jahren starker Eisgang, wodurch sich sehr zeitintensive Verankerungsaufnahmen ergaben. Durch parallele Eisstationen konnte der Verlust an Stationszeit jedoch kompensiert werden, sodass der 0°-Schnitt zum 23. Dezember verlassen und die Atka-Bucht wie geplant zum 25. Dezember abends angelaufen werden konnte, um mit den Ladearbeiten zu beginnen.

Da der Zugang zum Nordanleger von stark zerklüftetem Meereis blockiert war, sollte versucht werden, den längeren Weg durch das weitgehend unzerklüftete Eis vor dem Nordostanleger freizubrechen (Beginn 26. Dezember 01:00 h). Nach 2½-tägigem Brechen musste dieser Versuch jedoch ca. 1 nm vor dem Nordostanleger am 28. Dezember 16:30 h wegen des oben erwähnten technischen Schaden abgebrochen werden. Alternativ wurde daraufhin am 31. Dezember 2014 10:00 h mit einer Meereisentladung der Feststoffe begonnen. Aufgrund der vorausschauenden Planung und des engagierten Einsatzes von sowohl Stations- als auch Schiffspersonal konnten die Löscharbeiten nach 2 Tagen abgeschlossen werden (Ablegen Atka-Bucht am 1. Januar 2015 16:00 h). Hierauf wurde das Schiff etwa 20 nm nach Westen verlegt, um Brennstoff für die *Neumayer-Station III* an der dort zugänglichen Schelfeiskante zu löschen. Eine erste Charge konnte zwischen dem 2. Januar 14:00 h und 22:00 h abgegeben werden. Weitere Arbeiten konnten dann aber wegen Wetter- und Eisbedingungen erst am 8. Januar 15:00 h wieder aufgenommen und am 9. Januar 06:30 h endgültig abgeschlossen werden. Der eingeschränkten Eisgängigkeit geschuldet konnte der Rückweg erst am 13. Januar 2015 angetreten werden, nachdem die Wetterlage zumindest kleinräumige Eisaufklärungsflüge erlaubte, um einen Weg durch den dichten Eisgürtel vor der Küste zu finden. Mit Erreichen des offenen Wassers am 15. Januar 2015 06:00 h konnten stationsgebundene Arbeiten wieder aufgenommen werden. Die nach Erreichen des freien Wassers verbliebene Stationszeit konnte jedoch aufgrund der eingeschränkten Manövrierfähigkeit und Eisgängigkeit nur begrenzt wissenschaftlich genutzt werden, da nahe der Eiskante keine zur Beprobung geeigneten Schollen zu finden waren und starker Seegang und Wind soweit möglich vermieden wurden.

Während des insgesamt 21-tägigen Aufenthaltes (vorgesehen 3 Tage) im Bereich der Atka-Bucht wurde, soweit die logistischen und meteorologischen Randbedingungen es zuließen, während der Wartezeiten ein Ersatzprogramm von Eisstationen, RMT- und SUI-Netzfängen, CTD-Stationen sowie Schallquellen-Kalibrationen durchgeführt. Mit diesem Programm konnten am Rande des ursprünglichen Expeditionsplans ergänzende Daten erhoben werden. Zusammenfassend ist festzuhalten, dass während des Zeitraumes, in dem das Schiff voll operabel war, nahezu alle gesteckten Ziele in bewährter Zusammenarbeit zwischen Schiff und Wissenschaft erreicht wurden. Alle geplanten Stationen im Weddellmeer westlich der Atka-Bucht wurden jedoch aufgrund des Abbruchs der Expedition nicht angelaufen. Wissenschaftliche Projektziele, die auf Arbeiten in diesem Gebiet angewiesen sind, konnten somit nicht erreicht werden und sind auf eine alternative Expedition angewiesen.

Die Reise endete am 1. Februar 2015 8:00 h Ortszeit in Kapstadt.

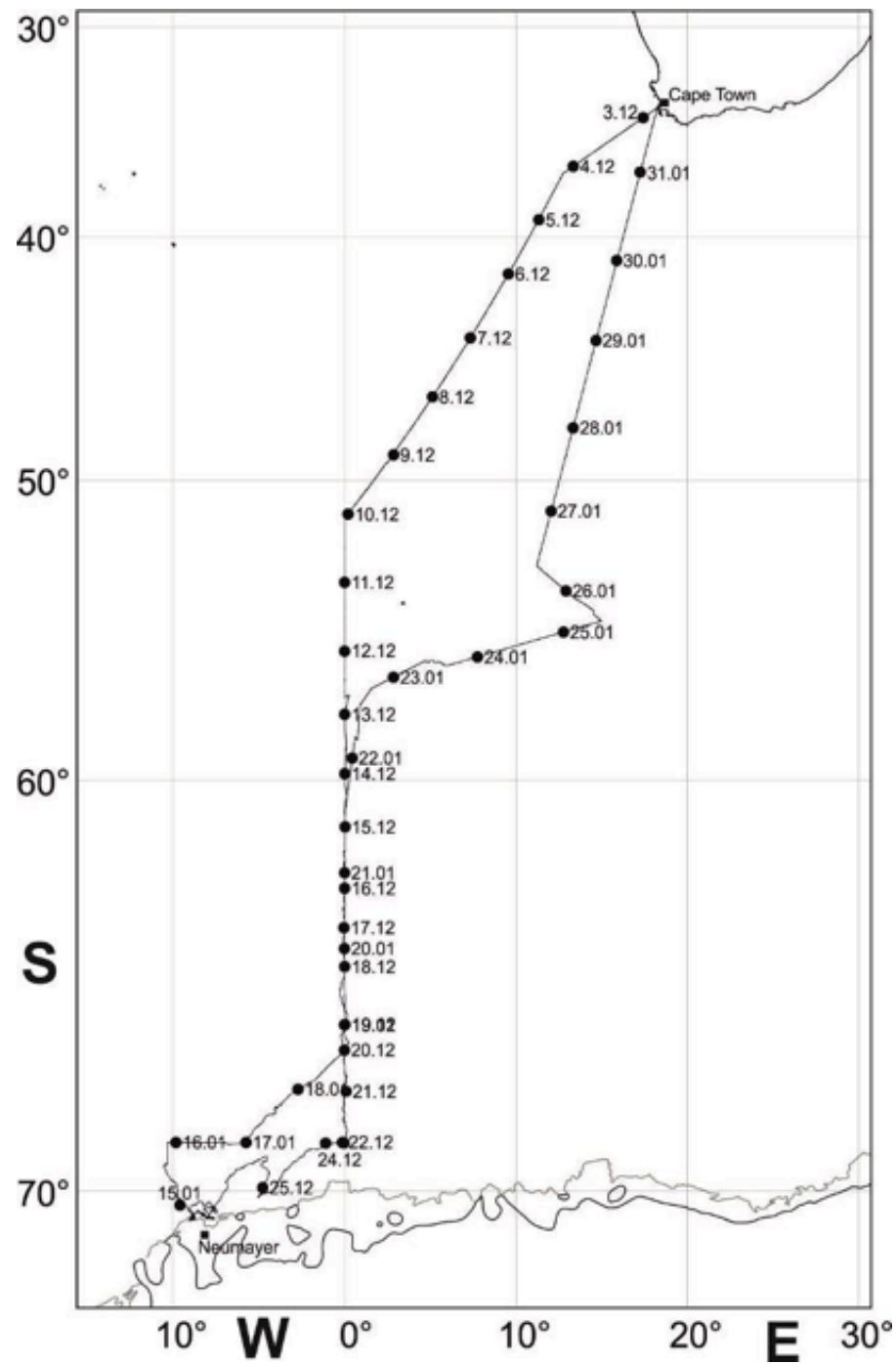


Abb. 1.1: Fahrtverlauf der Expedition PS89 (ANT-XXX-2) ins Weddellmeer; Start und Ende der Reise war Kapstadt.

Fig 1.1: Cruise plot of expedition PS89 (ANT-XXX-2) to the Weddell Sea; starting and ending in Cape Town.

SUMMARY AND ITINERARY

The *Polarstern* expedition PS89 to the Antarctic was initially routed from Cape Town via Atka Bay (*Neumayer Station III*) through the Weddell Sea to Punta Arenas. However, the pitch control system of the portside propeller of the ship suffered an irreparable damage during our stay at Atka Bay, which we had entered to provide for *Neumayer Station III*. This failure reduced the vessel's performance and manoeuvrability to such degree that the decision was taken to cease the expedition and return to Bremerhaven via Cape Town to have the necessary repairs undertaken as soon as possible. This resulted in a rerouting of this expedition from Cape Town to Atka Bay and back to Cape Town.

The expedition had been dedicated to logistic and scientific purposes. All logistic aims (supply of *Neumayer Station III* with fuel and goods) were achieved successfully whereas it had only been possible to carry out less than half of the scientific programme, i.e. the part prior to reaching Atka Bay.

The scientific work was characterised by station-based, sea ice-based, ship-based and helicopter-borne activities.

The station-based work comprised:

- Recovery of 13 deep sea pressure gauges along the Good Hope section, (of 14 planned)
- Recovery/deployment of 6/6 moorings east of *Neumayer Station III* (of 7/5 planned)
- Recovery/deployment of 0/0 moorings west of *Neumayer Station III* (of 14/11 planned)
- Deployment of 15 Argo floats (of 28 planned)
- Deployment of 12 SOCCOM floats (of 12 planned)
- 94 CTD casts with rosette
- Calibration of 6 RAFOS sound sources
- Analyses of approximately 4,000 water samples
- Sampling of deep sea bottom using multicore (2).

Ship-based research consisted of:

- Surveys of birds, seals, and whales
- Measurement of temperature, salinity, and current profiles
- 18 SUIT hauls, 8 out of those under sea ice (of >30 planned)
- 15 RMT hauls, 6 out of those in ice covered areas (of >20 planned)

Sea ice-based research included:

- 5 ROV ice stations (2 out of those on drifting sea ice, of 12 planned)
- Deployment of 12 sea ice buoys (of different types, of 22 planned)
- 3 ice core stations (of 6 planned)
- 2 ice thickness transects using sledge (of 0 planned)

Helicopter-borne work amounted to 116 flights with 84:32 h of cumulative flying time. Out of the 116 flights we carried out:

- 20 flights for animal observations (out of approximately 60 planned)
- 5 flights for EM bird transects (out of 15 planned).

Other flights were undertaken to mark ice floes, for testing of instruments, logistic flights for ice stations, and for transportation of researchers and material to and from *Neumayer Station III*.

The expedition set off on December 2, 2014 at 18:00 LT in Cape Town. The recovery of the deep sea pressure gauges along the route was performed in a timely manner – a fact in large parts to be attributed to the remarkably well operating POSIDONIA system (mobile unit in the moon pool and USBL box). The user interface, PosiSoft, allowed reliable tracking of the ascending moorings and constitutes a significant step forward. Using PosiSoft, the ship could be positioned in an apt position for recovery of moorings and gauges, rendering further searches unnecessary and significantly speeding up the recovery process (most effective from the Zodiac).

On the way south CTDs were cast at the mooring sites along the route and every 60 nm south of 55°. Furthermore, bio-geochemically enhanced Argo floats were deployed at selected positions for the SOCCOM project.

A rapidly opening polynya around Maud Rise allowed quick travelling along the 0° transect. At the southernmost tip of this transect, however, we met heavy ice coverage similar to the situation we had encountered two years before, rendering the mooring recoveries very time-consuming. However, the loss of station time could be compensated by introducing ice stations in parallel. Thus, we were able to leave the zero-meridian on 23 December and enter Atka Bay on 25 December, with the intention to start provisioning *Neumayer Station III* in accordance with the time schedule.

Since the berthing site at the “North Pier” was blocked by heavily ridged sea ice, the decision was taken to break the longer way through primarily one-year old sea ice towards the north-easterly berthing site, which started 26 December, 01:00 h. After two and a half days of breaking the ice, this effort came to an end just 1 nm off the “North East Pier” due to the technical failure mentioned above. Due to this circumstance, the unloading of solid provisions was started on 31 December, 10:00 h via the sea-ice. Thanks to the remarkable preparation and commitment of both the station’s and the ship’s personnel, the loading procedures were completed within two days. Leaving Atka Bay on January 1, 2015, 16:00 h, the ship was positioned about 20 nm to the west, to commence bunkering of fuel for *Neumayer Station III*. A first share was pumped on 2 January between 14:00 h and 22:00 h. However, due to unfavourable weather and ice conditions, bunkering could only be resumed on 8 January, to be completed by 9 January. Only four days later, on 13 January, we were able to start heading back to Cape Town, when the weather conditions finally allowed reconnaissance flights near the ship to find a suitable way through the thick belt of ice encircling the coast. Having reached open waters on 15 January, 06:00 h, some scientific station work was resumed. The remaining station time however could only be exploited in parts, as the technical impairments constrained our ability to find suitable ice floes near the ice edge or to reach specific locations.

During the 21-days-stay in Atka Bay (with 3 days initially planned) the waiting time was filled with a substitution programme of ice stations, RMT hauls, SUIT catches, CTD casts and sound source calibrations, whenever the logistics and meteorological conditions permitted. On the sidelines of the original expedition plan this programme allowed to collect complementary data. In summary, one needs to acknowledge that during the ship’s unrestraint operability almost all of the goals set were reached in the usual mutual cooperation of the science and the ship crews. However, with the cancellation of the further expedition, none of the stations planned for the Weddell Sea west of Atka Bay could be reached. Any of the project goals basing on research work in that area could not be achieved and will completely rely on an alternate expedition.

The cruise ended on February 1, 2015, 08:00 h LT, in Cape Town.

2. WEATHER CONDITIONS DURING PS89 (ANT-XXX/2)

Dipl.-Met. Max Miller, Hartmut Sonnabend

DWD

During Monday (Dec. 01, 2014) a typical “Cape-Doctor” situation developed in Cape Town and intensified on Tuesday. On Tuesday, December 02, 2014, 18:30 pm *Polarstern* left Cape Town for the campaign PS89 (ANT-XXX/2). South-easterly winds at Bft 8 to 9 and gusts 10, scattered clouds and 18° C were registered. During the night and near the coast we got wind force 9. Only away from the coast wind abated to Bft 7 on Wednesday morning (Dec. 03). A sea state around 4 m forced some stronger rolling of the vessel. Afterwards we reached the Subtropical High off South Africa and sailed at light and variable winds until Thursday. On Friday (Dec. 05) a first low within the frontal zone hit us only for short times with north-westerly winds Bft 7.

While continuing south, several storm lows crossed our track from Sunday evening (Dec. 07) until Thursday (Dec 11). Sea state increased temporarily up to 6 m at wind force 9. On Wednesday evening, *Polarstern* crossed the centre of a storm at 53° 20' S on the Greenwich Meridian. Stormy northerly winds abated to light and variable and increased rapidly up to Bft 9 again, now from south to southeast.

During the night to Sunday (Dec. 14) we reached the ice near 60° S. A secondary low at Bouvet Island intensified and moved southeast. Sailing south along the Greenwich Meridian, *Polarstern* passed at its west side from Monday (Dec. 15) on. Southerly winds freshened and reached their maximum at Bft 7 to 8 on Wednesday (Dec. 17).

From Saturday (Dec. 20) until turn of the year, weak pressure gradient combined with moist air masses were prevailing along DROMLAN coast. Therefore low level clouds temporarily hampered the flight operations. On Christmas Day (Thursday) we reached the large ice field in front of the berth off *Neumayer Station III*.

Off the British Antarctic Station *Halley* a small low formed on New Year's Day. It moved north, deepened and became stationary northwest of *Neumayer Station III*. From Saturday (Jan. 03) until Tuesday (Jan. 06) easterly to north-easterly winds freshened up to wind force 7. Afterwards the low weakened and winds abated for two days. However, a new low near South Georgia moved southeast and replaced the latter one from Friday (Jan. 09) onwards. Again we registered strong winds from east to northeast, on Saturday for short times up to force 8.

Only on Monday evening (Jan. 12) winds abated and snowfall ended. During the following days *Polarstern* operated between above mentioned low and a ridge along the eastern DROMLAN coast. North-easterly winds hardly exceeded Bft 5. A low at Bouvet Island moved south, intensified and was located as storm north of the Russian Antarctic Station *Novolazarevskaya* on Saturday (Jan. 17). We got at its west side with southerly winds Bft 7. On Sunday (Jan. 18) another storm approached and caused only temporarily winds from northeast at force 9 combined with a sea state around 5 m. Already on Sunday evening winds abated Bft 6. But during the following days a swell of 4 m remained while steaming north.

During the night to Thursday (Jan. 22) the next storm passed by north of us. Winds increased only for short times up to Bft 7. Due to the high speed of the storm several swells were driven and caused cross sea. On Thursday we sailed the main swell of 5 m.

Again a storm approached at the beginning of the final week of the expedition. On Sunday evening (Jan. 25) north-easterly winds freshened up to Bft 7 only for short times. During the night to Monday *Polarstern* crossed the storm's centre and winds abated clearly. But from Monday morning on south-westerly winds increased Bft 7 to 8 and caused a sea state around 5 m. Later we entered the frontal zone between a low east of the South Sandwich Islands and the subtropical high which forced steady north-westerly winds at Bft 6 to 7 and a swell around 3 m until Thursday (Jan. 29). On Friday the cold front crossed our area. Winds veered southwest to south and abated gradually to Bft 5 on Saturday.

On Sunday morning, February 01, 2015, *Polarstern* reached Cape Town at temporarily gusty winds from southeast. Fig. 2.1 – Fig. 2.4 depict the statistical distributions of wind direction and force, wave height and cloud coverage.

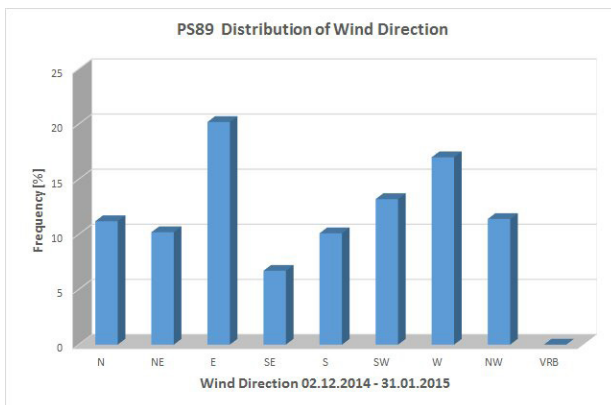


Fig. 2.1: Distribution of wind directions during PS89

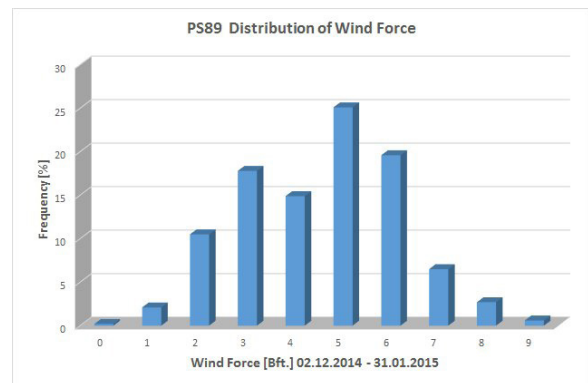


Fig. 2.2: Distribution of wind force during PS89

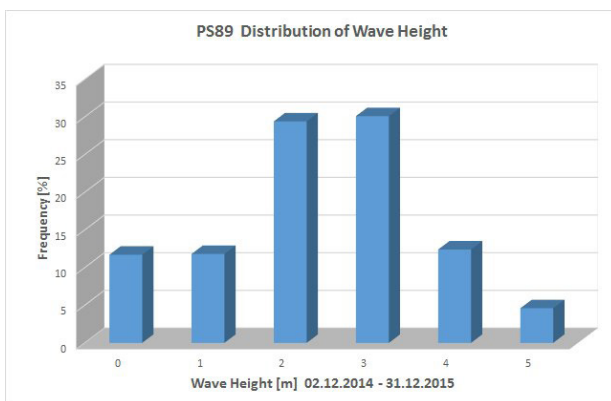


Fig. 2.3: Distribution of wave heights during PS89

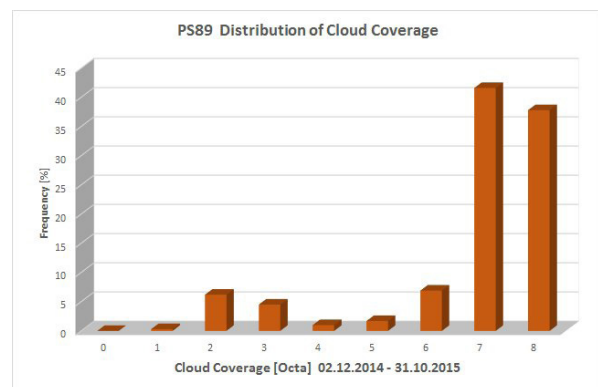


Fig. 2.4: Distribution of cloud coverage during PS89

3. SCIENTIFIC PROGRAMMES

3.1 Oceanography

3.1.1 Implementation of the HAFOS Observation System in the Antarctic

Olaf Boebel¹, Rainer Graupner¹, Ioana Ivanciu²,
Stefanie Klebe¹, Katerina Lefering³, Peter
Lemke¹, Christoph Lerchl⁴, Tim Meinhardt⁵,
Matthias Monsees¹, Friederike Rohardt⁶, Gerd
Rohardt¹, Jan Rohde⁷, Stefanie Spiesecke¹,
Karolin Thomisch¹, Sarah Zwicker¹

¹AWI

²Geomar

³U of Strathclyde, Glasgow, UK

⁴Ludwig-Max. Univ. München

⁵TU Hamburg-Harburg

⁶TU Bergakademie Freiberg

⁷TU Braunschweig

Grant No: AWI-PS89_01

Outline and objectives

The ocean is a key element of the global climate system because of its storage and transport of heat, its ability to act as a sink of CO₂ and due to the sea ice ocean albedo effect. The response of the ocean to changes in the forcing is both expressed and controlled by its stratification, which is governed by the vertical distribution of temperature and salinity. Previously, shipborne observations were the only means of obtaining vertical profiles of water mass properties with sufficient accuracy, but progress in sensor technology now allows using automated systems since this century as well. The current backbone of the Global Ocean Observing System (GOOS) is the Argo system, which is founded on an international array of more than 3,000 profiling floats, the Argo array. However, Argo in its current form is restricted to oceanic regions that are ice free year-round, as the floats need to surface regularly to be localized and to transmit the data via satellite link. HAFOS (Hybrid Antarctic Float Observing System) constitutes an extension of this system into seasonally ice covered waters of the Weddell Gyre, overcoming the limitations through a novel combination of well tested technologies to close the observational gaps in the Antarctic Ocean.

To determine trends and fluctuations in the characteristics of the main Antarctic water masses (Warm Deep Water, WDW and Antarctic Bottom Water, ABW), a set of more than a dozen hydrographic moorings (Fig. 3.1.1.1) has been maintained and expanded throughout the past 30 years by AWI. HAFOS builds on this backbone by having added RAFOS sound sources for under-ice tracking of Argo floats since 2002. Near bottom recorders continue the truly climatological time series as sentinels for climate change in the formation areas of bottom waters whereas the profiling floats record the water mass properties in the upper ocean layers. Passive acoustic monitoring allows linking marine mammal distribution in the open ocean to ongoing ecosystem changes, thereby complementing the physical measurements with biosphere observations at its highest trophic level. The effort constitutes the first basin wide monitoring effort (with the exception of the US Navy's SOSUS array) and focuses on a region where year-round observations are notoriously sparse and difficult to obtain. HAFOS complements international efforts to establish an ocean observing systems in the Antarctic as a legacy of the International Polar Year 2007/2008 (IPY) and the Southern Ocean Observing System (SOOS), which is presently under development under the auspices of the Scientific Committee of Antarctic Research (SCAR) and the Scientific Committee on Oceanic Research (SCOR).

Sound sources and other oceanographic instruments are, by and large, designed for deployment periods of maximal 3 years before they need to be recovered for maintenance and battery replacement. One major goal of *Polarstern* expedition PS89 (ANT-XXX/2) was to recover and redeploy these moorings to be able to continuing these observations for another 2-3 years. During transits between mooring locations, hydrographic profiles were to be collected and order of 27 NEMO floats should have been released. Combined with currently active floats from AWI and other institutions, it was expected to thereby extend the data density as requested by Argo (1 float every $3^\circ \times 3^\circ$ box, i.e. ca. 150 floats for the area under consideration).

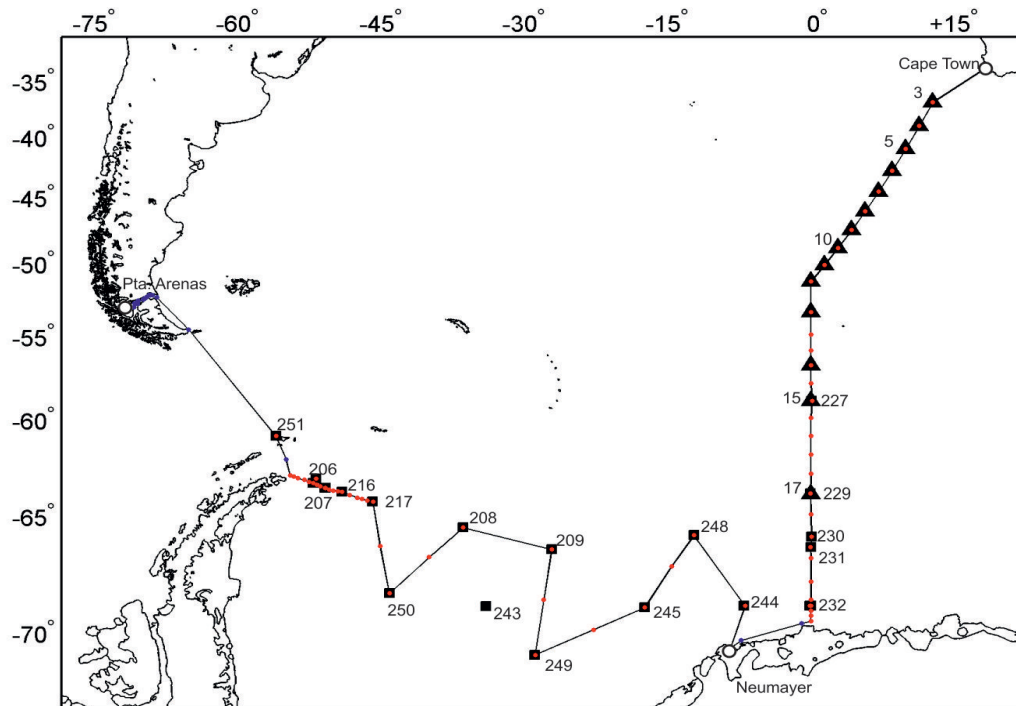


Fig. 3.1.1.1: Layout of array of oceanographic deep-sea moorings (squares) throughout the Weddell Sea and along the Greenwich Meridian. Red dots indicate moorings scheduled for turnaround during this expedition. Triangles indicate locations of pressure sensor equipped inverted echosounders (PIES) scheduled for recovery.

Work at sea

Hydrographic moorings

Due to the early termination of the expedition any, activities west of *Neumayer Station III* had to be cancelled and hence the majority of moorings could not be recovered and redeployed (Table 3.1.1.1 and Fig. 3.1.1.2). East of *Neumayer Station III*, a total of 6 moorings were recovered (Table 3.1.1.2 and Fig. 3.1.1.2) along and in the vicinity of the Greenwich Meridian. A total of 6 moorings were redeployed (Table 3.1.1.3 and Fig. 3.1.1.2).

Tab. 3.1.1.1: Pending mooring recoveries

Mooring	Latitude	Longitude	depth [m]	Deployment	
AWI232-10	69° 00.11' S	00° 00.11' W	3370	19.12.2010	10:20
AWI243-1	68° 00.67' S	34° 00.15' W	4443	31.01.2007	06:15
AWI248-1	65° 58.09' S	12° 15.12' W	5011	27.12.2012	08:50
AWI245-3	69° 03.47' S	17° 23.32' W	4746	28.12.2012	21:04
AWI249-1	70° 53.55' S	28° 53.47' W	4364	30.12.2012	12:41
AWI209-7	66° 36.45' S	27° 07.26' W	4830	01.01.2013	15:05
AWI208-7	65° 37.23' S	36° 25.32' W	4732	03.01.2013	13:20
AWI250-1	68° 28.95' S	44° 06.67' W	4100	05.01.2013	14:53
AWI217-5	64° 22.94' S	45° 52.12' W	4410	09.01.2013	14:16
AWI216-5	63° 53.61' S	49° 05.17' W	3513	10.01.2013	00:17
AWI207-9	63° 43.57' S	50° 51.64' W	2500	12.01.2013	08:23
AWI207-8	63° 43.20' S	50° 49.54' W	2500	06.01.2011	12:26
AWI206-8	63° 15.51' S	51° 49.59' W	917	14.01.2013	05:06
AWI206-7	63° 28.93' S	52° 05.87' W	950	06.01.2011	20:52
AWI251-1	61° 00.88' S	55° 58.53' W	319	15.01.2013	02:11

Tab. 3.1.1.2: Mooring recoveries during PS89

Mooring	Latitude	Longitude	depth [m]	Deployment		Recovery	
AWI227-12	59° 02.57' S	00° 04.91' E	4600	11.12.2012	14:41	13.12.2014	07:14
AWI229-10	63° 59.66' S	00° 02.67' W	5172	14.12.2012	12:34	16.12.2014	15:04
AWI230-8	66° 02.12' S	00° 02.98' E	3552	15.12.2012	14:39	18.12.2014	11:21
AWI231-10	66° 30.93' S	00° 00.65' W	4524	17.12.2010	12:00	19.12.2014	09:26
AWI232-11	68° 59.86' S	00° 06.51' W	3319	18.12.2012	06:00	21.12.2014	21:52
AWI244-3	69° 00.35' S	06° 58.97' W	2900	25.12.2012	10:27	17.01.2015	07:28

Tab. 3.1.1.3: Mooring deployments during PS89

Mooring	Latitude	Longitude	depth [m]	Deployment	
AWI227-13	59° 02.67' S	00° 05.37' E	4600	13.12.2014	16:38
AWI229-11	64° 00.31' S	00° 00.22' W	5165	17.12.2014	11:43
AWI229-12	63° 54.94' S	00° 00.16' E	5172	20.01.2015	11:38
AWI231-11	66° 30.41' S	00° 00.66' W	4472	19.12.2014	17:59
AWI232-12	68° 58.89' S	00° 05.00' W	3360	23.12.2014	09:52
AWI244-4	69° 00.34' S	06° 58.94' W	2900	16.01.2015	14:20

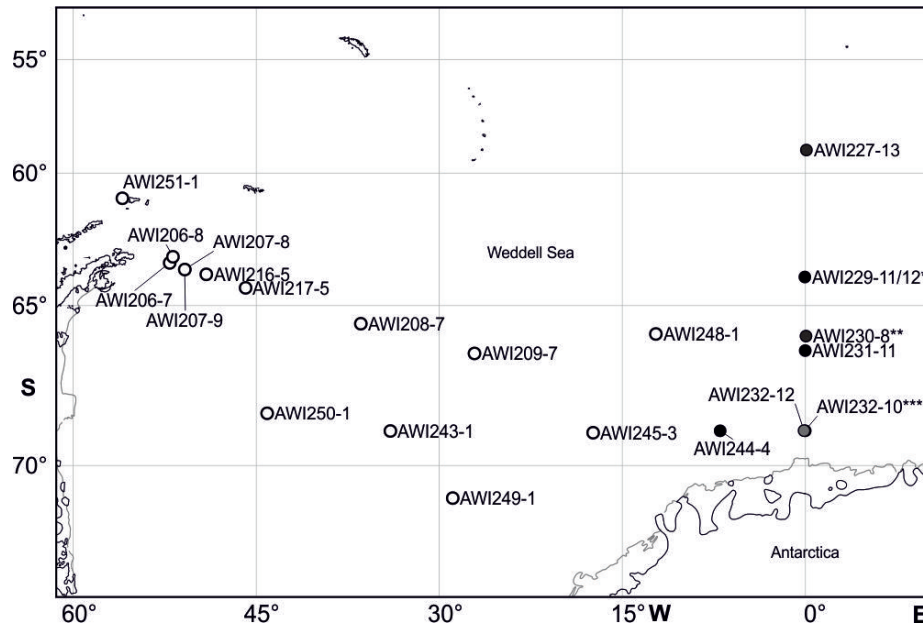


Fig. 3.1.1.2: Map of mooring locations occupied since 2012/13 or earlier. Black dots indicate moorings exchanged or recovered during this expedition (PS89). Note: *) AWI229-12 was deployed during the return leg to Cape Town, hosting a sound source and an acoustic recorder. **) AWI230-8 was recovered only. ***: AWI232-10 was located and released but did not surface.

Details regarding the instrumentation of the moorings recovered and deployed are listed in Table 3.1.1.4 and 3.1.1.5.

Tab. 3.1.1.4: Instrumentation of recovered moorings

Mooring	Latitude Longitude	Water Depth [m]	Date / Time - deployed - recovered	Instrument Type	Serial Number	Instrument Depth [m]	Record length (days) [Remarks]
AWI227-12	59° 02.57' S	4600	11.12.2012	PAM	1025	1020	
	00° 04.91' E		14:41 13.12.2014 07:14	SBE16	319	4557	731
AWI229-10	63° 59.66' S	5172	14.12.2012	AVTP	8050	200	732
	00° 002.67' W		12:34	SBE37	9834	200	732
				SBE37	447	250	732
			16.12.2014	SBE37	237	300	[2]
			15:04	SBE37	240	350	732
				SBE37	435	400	732
				SBE37	9838	450	732
				SBE37	438	500	732
				SBE37	439	550	732
				SBE37	2086	600	732
				SBE37	449	650	732
				SBE37	245	700	732
				RCM 11	452	706	732

3.1 Oceanography

Mooring	Latitude Longitude	Water Depth [m]	Date / Time - deployed - recovered	Instrument Type	Serial Number	Instrument Depth [m]	Record length (days) [Remarks]
				SOSO	0026	807	[1]
				PAM	1010	969	[1]
				RCM 11	475	1977	[3]
				SBE37	9833	5126	[3]
				RCM 11	144	5127	[3]
AWI230-8	66° 02.12' S	3552	15.12.2012	AVTP	10491	200	732
	00° 02.98' E		14:39	SBE37	2088	200	732
				SBE37	2090	300	456
			18.12.2014	SBE37	2091	400	732
			11:21	SBE37	2092	500	732
				SBE37	2093	600	732
				SBE37	2094	700	732
				AVT	6856	725	732
				PAM	1009	949	[1]
				AVTP	9213	1657	732
				SBE37	2095	3508	732
				AVT	9179	3509	732
AWI231-10	66° 30.93' S	4524	17.12.2010	AVTP	10541	200	732
	00° 00.65' W		12:00	SBE37	2096	200	732
				SBE37	2098	250	732
			19.12.2014	SBE37	2099	300	732
			09:26	SBE37	2100	350	732
				SBE37	2101	400	732
				SBE37	2385	450	732
				SBE37	2234	500	732
				SBE37	2386	550	732
				SBE37	2389	600	732
				SBE37	2391	650	732
				SBE37	3813	700	732
				AVT	9184	729	732
				SOSO	0024	830	[1]
				RCM 11	509	1812	703
				SBE37	7726	4413	732
				AVT	9180	4414	732
AWI232-11	68° 59.86' S	3319	18.12.2012	AVTP	10925	250	733
	00° 06.51' W		06:00	RCM 11	469	757	733
			21.12.2014	PAM	1011	958	[1]
			21:52	RCM 11	512	1765	664
				SBE37	7727	3265	733

Mooring	Latitude Longitude	Water Depth [m]	Date / Time - deployed - recovered	Instrument Type	Serial Number	Instrument Depth [m]	Record length (days) [Remarks]
				AVT	10499	3266	[2]
AWI244-3	69° 00.35' S	2900	25.12.2012	SOSO	29	806	[1]
	06° 58.97' W		10:27	PAM	0001	998	[1]
				SBE16	2419	2857	751

Remarks: [1] to be processed [2] flooded [3] lost due to broken mooring rope

Tab. 3.1.1.5: Instrumentation of deployed moorings

Mooring	Latitude Longitude	Water Depth [m]	Date Time	Instrument Type	Instrument Serial Number	Instrument Depth [m]
AWI227-13	59° 02.67' S	4600	13.12.2014	PAM	1056	1020
	00° 05.37' E		16:38	SBE37	8125	4557
AWI229-11	64° 00.31' S	5165	17.12.2014	AVTP	8395	202
	00° 00.22' W		11:43	SBE37	8129	203
				SBE37	9831	300
				SBE37	10943	400
				SBE37	10944	500
				SBE37	11419	600
				SBE37	11420	700
				RCM11	501	709
				PAM	1057	970
				SBE37	227	5121
AWI229-12	63° 54.94' S	5172	20.01.2015	SOSO	0048	798
	00° 00.16' E		11:38	PAM	1055	1001
				SBE37	228	5167
AWI231-11	66° 30.41' S	4472	19.12.2014	SOSO	0026	851
	00° 00.66' W		17:59	PAM	1058	973
				SBE37	11421	4429
AWI232-12	68° 58.89' S	3360	23.12.2014	AVT	8367	290
	00° 05.00' W		09:52	AVT	9211	798
				PAM	1059	999
				RCM11	472	1806
				SBE37	11422	3306
				RCM11	25	3307
AWI244-4	69° 00.34' S	2900	16.01.2015	SOSO	0047	806
	06° 58.94' W		14:20	PAM	1061	998
				SBE37	12470	2857

3.1 Oceanography

Abbreviations:

AVTP	Aanderaa Current Meter with Temperature- and Pressure Sensor
AVT	Aanderaa Current Meter with Temperature Sensor
DCS	Aanderaa Doppler Current Sensor
PAM	Passive Acoustic Monitor (Type: AURAL or SONOVAULT)
PIES	Pressure Inverted Echo Sounder
RCM11	Aanderaa Doppler Current Meter
SBE16	SeaBird Electronics Self Recording CTD to measure Temp., Cond. and Pressure
SBE37	SeaBird Electronics, Type: MicroCat, to measure Temperature and Conductivity
SOSO	Sound Source for SOFAR-Drifter

Sound source array

A major goal of this expedition was to refurbish the sound sources used for tracking the NEMO floats under the ice. Due to the early termination of this expedition, however, only 3 sources could be replaced. With the originally planned focus of float deployments in the inner Weddell Sea, we had initially decided not to redeploy the north-easternmost source W1 on our southbound leg from Cape Town to *Neumayer Station III*, while W2 and W11 were replaced as planned. However, based on the decision to launch a large number of floats into the coastal current to compensate for our inability to reach the inner Weddell Sea, W1 was redeployed during the northbound leg. Hence our array is unchanged, with 3 sources having been refurbished during this expedition. A summary of sound source activities is given in Tables 3.1.1.6 and 3.1.1.7 as well as Fig. 3.1.1.3.

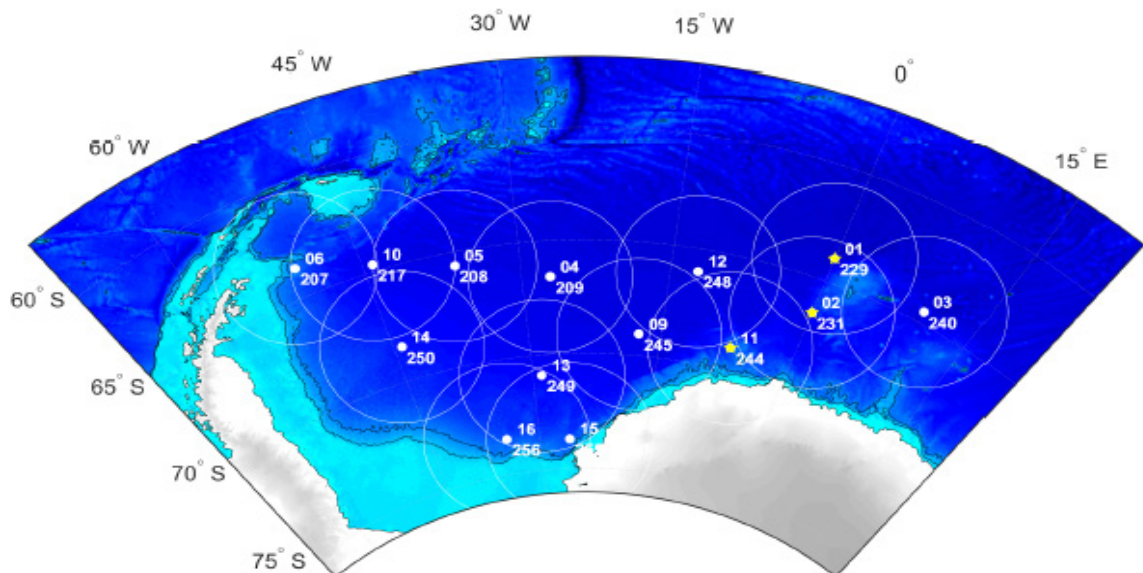


Fig. 3.1.1.3: HAFOS sound source array. White dots with concentric circles: sources launched in 2011 or early with 300 km range. Yellow stars: Sources refurbished during PS89

Tab. 3.1.1.6: Recovery of sound sources during PS89

Mooring SoSo site	Type SN	Water depth Deploy depth [m]	Position	Deployment Recovery dates	Schedule [GPS]	Recov. Time [GPS]	Recov Time [SoSo]	total drift [s]	Mission length [days]	drift [s/day]	Comments
229-10 W1	Develogic D0026, EI.0040	5172 807	63°59.66'S 00°02.65'W	2012-12-14 2015-01-16	12:30:16 [*]	09:50:10 (UTC)	09:50:08 (UTC)	-2	732	-0.0027	communication ok, mechanically in very good condition
231-10 W2	Develogic D0024, EI.0033	4456 830	66°30.93'S 00°00.65'W	2012-12-16 2014-12-19	13:00	11:48:10 11:49:16	11:48:10 11:49:16	0.00	733	0.0000	communication ok, mechanically in very good condition
244-03 W11	R0029	2900 806	69°00.35'S 06°58.97'W	2012-12-25 2015-01-20	12:40	09:51:30 09:52:05	09:45:03 09:45:39	-387	753	-0.5139	communication ok, mechanically in very good condition

*) Clock set to 12:30 UTC at to deployment; GPS=UTC+16s. Sign of offsets: positive (+): unit is late, negative (-): unit is early.

Tab. 3.1.1.7: Deployment of sound sources during PS89

Mooring / SoSo site	Type / SN	water depth /m	Latitude	Longitude	Deployment date	Soso depth [m]	Schedule GPS time	Comments
W1 229-12	D0048, EI0064	5209	63° 54.94' S	000° 00.17' W	2015-01-20	798	12:30	1st Sweep 2015-01-21 ^{1),2),4)}
W2 231-11	D0026, EI.0066	4472	66° 30.41' S	000° 00.66' W	2014-12-19	851	13:00	1st Sweep 2014-12-20 ^{2),3),4)}
W11 244-4	D0047	2900	69° 00.34' S	006° 58.95' W	2015-01-16	806	12:40	1st Sweep 2014-12-20, ^{1),2),4)}

1) Tuning for resonance frequency during ANT-XXIX/2; 2) Additional Battery Pack; 3) Recovered resonance tube with new electronics; 4) Firmware V2.2; General comment: GPS = UTC+16s during this expedition.

RAFOS source calibration

A detailed description of the objectives and approach of tuning the RAFOS sources *in-situ* is given in the expedition report of ANT-XXIX/2 (Boebel et al., 2014). During this expedition, we tuned newly acquired sources, intended for the refurbishment of the array, directly at sea under hydrographic conditions similar to the deployment site. Differing from the procedure used during ANT 29.2 (3 iterative cuts) we now only used 2 iterative cuts to adjust the resonator tube's length. In total, the frequency response of 9 sound sources was determined using 25 runs: 3 previously tuned systems and 6 new Develogic NTSS sound source systems.

Tuning (i.e. shortening) of the 6 new resonator tubes to a resonance frequency near 260 Hz was performed in 5 steps as follows:

1. Determination of frequency response of resonator "off works" by using seven consecutive 5-Hz wide, 80s sweeps covering 225 Hz to 260 Hz.

3.1 Oceanography

2. First cut of resonator tube by about 70 % of length reduction as estimated to reach target frequency.
3. Determination of frequency response after first cut by using seven 5-Hz wide, 80s sweeps from 225 Hz to 260 Hz.
4. Second and final cut to reach target frequency.
5. Determination of frequency response of final tube length by using a single 80s long 5 Hz sweeps from 248 Hz – 263 Hz and a single RAFOS sweep (259.38 Hz – 260.9 Hz, duration 80s).

Additionally, the resonance frequency of 3 systems (D00017 and D0018) tuned previously in Hamburg harbour by the manufacturer were determined by sweeping from 230 Hz – 265 Hz, in analogy to step 1, along with the resonance frequency of unit D0024 (recovered at W2 during PS89) which had been tuned during ANT-XXVIII/2.

Prior to 20 Dec 2014, sound sources were calibrated in deep water using the CTD winch on *Polarstern's* starboard side, lowering the sound sources horizontally to 200 m. To avoid entangling of the winch's cable, an extra weight of 50 kg was added below the sound source, followed by an acoustic recorder (iCListen, by OceanSonics, Canada) strapped on a rope 6m beneath the sound source. During the prolonged stay at Atka Bay (water depth 200 m) a mobile capstan and the ship's crane at the port side near the stern were used to lower the sound sources to 150 m depth with the iCListen acoustic recorder 25 m beneath the sound source. After repositioning the ship westwards near the Antarctic shelf ice edge with water depths of about 400 m, the sound sources were lowered to 200m, with the recorder suspended 25 m beneath the sound source. When no CTD cast was performed at or close to the tuning location, a Microcat CTD Recorder (SM37, SeaBird) was attached near the sound source to the rope to obtain local sound speed.

After completion of the tuning procedure, 30-min long recordings from the iCListen HF acoustic recorder were saved from the internal storage to harddisk. Using Adobe Audition, sweeps belonging to a given sound source were manually cut at their boundaries from the displayed spectrogram and saved as single files. Later these single sweeps were merged and saved as a single file containing the complete sweep from 225 Hz to 260 Hz. A custom MATLAB™ script was used to determine the (current) resonance frequency of the highest root-mean-square amplitude. A second MATLAB™ script used the current resonance frequency, current tube length and environmental parameters (e.g. sound velocity at tuning depth, water density) to derive the target resonance length and the excess length to be cut from the current tube.

During tuning activities, a marine mammal watch was conducted from the ship's bridge to shut down tuning activities in case marine mammals were to approach the ship closer than 1,000 m. This was not the case. Singly on 31.12.2014 at 12:49, while preparing the sound source for the last calibration run of the day, an Antarctic minke whale was sighted at about 1000 m distance from the ship, moving away. During calibration (13:03 to 13:35) the animal was not resighted.

CTD observations

CTD casts were conducted pursuing 3 independent objectives:

- To extend the spatially highly resolved repeat CTD section along the Greenwich meridian by another 2 years;
- To collect temperature and salinity data at PIES and mooring positions for the estimation of the drifts of the moored sensors;
- To provide calibration for the biogeochemical Argo floats.

Time constraints did not allow repeating the CTDs section's deep casts every 30 m (56 km) as during previous expeditions. Rather, a spacing of 60 m had to be chosen. In addition by matching deep cast positions to those of moorings and float deployment, the necessity for additional CTD deep casts was minimized.

The rosette assembly comprised a SBE 911plus CTD system, combined with a carousel type SBE32 with 24 Niskin water samplers of 12 liter volume. Additionally, the assembly was equipped with an oxygen sensor SBE43, a Wetlabs C-Star transmissometer (wave length 650 nm; path length 25 cm), a Wetlabs Eco-FLR fluorometer, and a Benthos/DataSonics altimeter type PSA 916D.

CTD data was logged with Seabird's *SeaSaveV7* data acquisition software to a local PC in raw format. *ManageCTD*, a Matlab™ based script developed at AWI, was employed to execute Seabird's *SBEDataProcessing* software, producing CTD profiles adjusted to 1-dbar intervals. *ManageCTD* additionally embedded metadata (header) information extracted from the DShip-Electronic Station Book before conducting a preliminary de-spiking and data validation of the profile data.

Preprocessed data were saved in OceanDataView compatible format, to provide near real-time visualization of e.g. potential temperature and salinity, particularly to provide *enroute* (i.e. during the expedition) visualization of the unfolding hydrographic section.

The CTD was equipped with double sensors (Table 3.1.1.8) for temperature (SBE3plus) and conductivity (SBE4C). These sensors were calibrated prior to the expedition. *Enroute* comparison of the calibrated sensors nevertheless revealed differences of about 0.1 mK in temperature and 1 $\mu\text{S}\cdot\text{cm}^{-1}$ in conductivity for *in-situ* measurements between the sensors.

Tab. 3.1.1.8: CTD-Sensor configuration

	#1 (primary); calibrated	#2 (secondary); calibrated
Temperature (SBE3plus)	2929; Apr. 2013	4127; Jun. 2014
Conductivity (SBE4c)	3885; Apr. 2013	3290; Apr. 2013

During this expedition, data from 38 full ocean depth CTD profiles were collected (Table 3.1.1.9 and Fig. 3.1.1.4). In addition, 2 shallow (52 and 70 m) CTDs were cast for the calibration of a SUIT's CTD-unit and 52 CTDs were cast at hourly intervals (with some interruptions for logistic reasons) at the shelf ice edge.

3.1 Oceanography

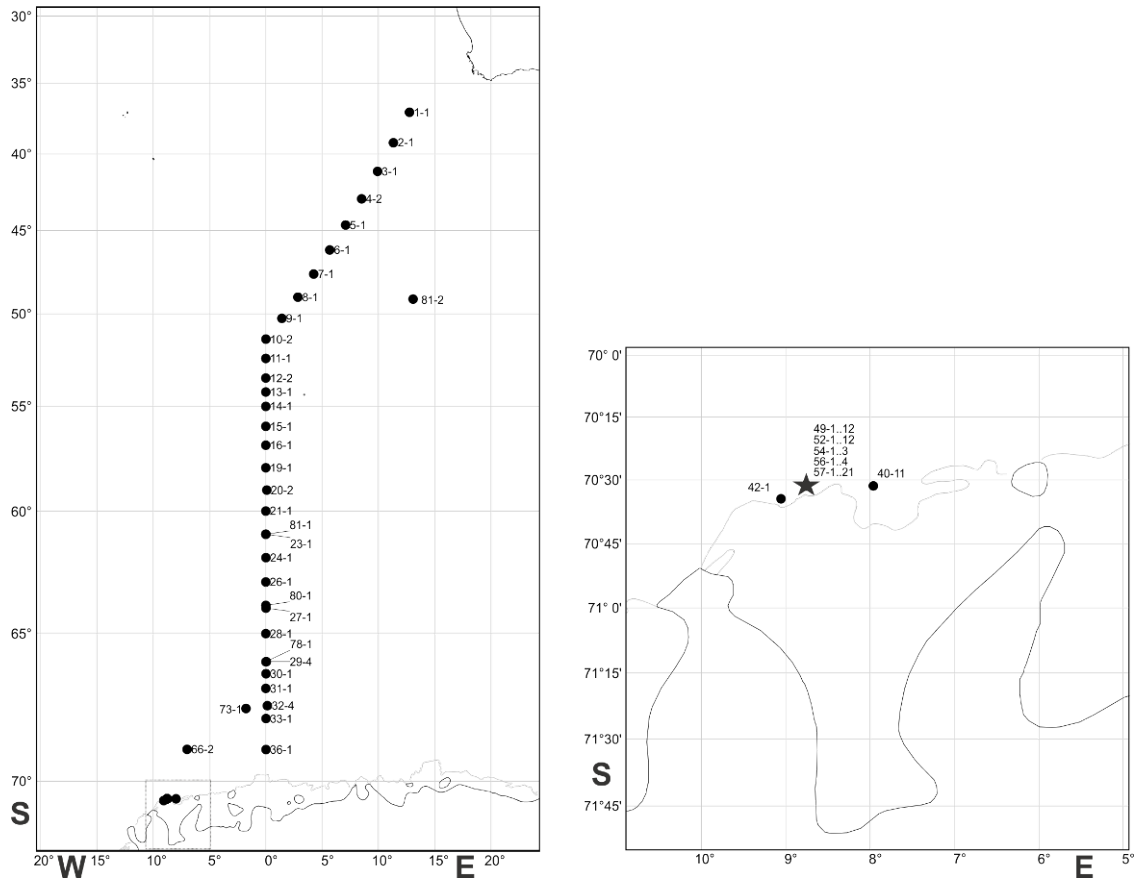


Fig. 3.1.1.4: Left: Map of locations of CTD stations. Labels indicate station and cast numbers as given in the station list. Right: Enlarged map of Atka Bay, with a star indicating the position of the hourly CTD time series.

Tab. 3.1.1.9: List of CTD profiles taken during PS89

Station - Cast	Date /time	Latitude	Longitude	Water depth [m]	max pres. [dbar]
1-1	04-Dec-2014 04:57	37 6.168 S	12 45.618 E	4890	4904
2-1	05-Dec-2014 00:56	39 13.662 S	11 20.028 E	5129	5226
3-1	05-Dec-2014 18:12	41 9.882 S	9 55.602 E	4610	4702
4-1	06-Dec-2014 09:05	42 58.542 S	8 30.558 E	3928	70
4-2	06-Dec-2014 10:59	42 58.788 S	8 30.348 E	3931	3969
5-1	07-Dec-2014 03:44	44 39.468 S	7 5.538 E	4585	4655
6-1	07-Dec-2014 18:04	46 12.900 S	5 40.500 E	4831	4877
7-1	08-Dec-2014 07:43	47 40.278 S	4 15.222 E	4541	4587
8-1	08-Dec-2014 23:19	49 2.118 S	2 51.600 E	4218	4239
9-1	09-Dec-2014 14:51	50 15.300 S	1 25.530 E	3893	3902
10-2	10-Dec-2014 03:41	51 25.308 S	0 0.582 E	2683	2678
11-1	10-Dec-2014 11:48	52 28.722 S	0 0.060 E	2598	2558
12-2	10-Dec-2014 21:21	53 31.458 S	0 0.180 E	2647	2596
13-1	11-Dec-2014 08:19	54 15.258 S	0 0.120 E	2734	2721
14-1	11-Dec-2014 15:13	54 59.988 S	0 0.018 E	1705	1663

3. Scientific Programmes

Station - Cast	Date /time	Latitude	Longitude	Water depth [m]	max pres. [dbar]
15-1	11-Dec-2014 23:38	55 59.958 S	0 0.162 E	3685	3695
16-1	12-Dec-2014 08:11	56 55.620 S	0 0.348 E	3646	3670
19-1	12-Dec-2014 23:17	58 0.078 S	0 0.120 E	4528	4574
20-2	13-Dec-2014 11:25	59 2.238 S	0 5.628 E	4639	4683
21-1	14-Dec-2014 03:20	59 59.088 S	0 0.078 E	5375	5451
23-1	14-Dec-2014 16:50	60 59.862 S	0 0.378 E	5393	5467
24-1	15-Dec-2014 07:11	61 59.580 S	0 0.840 E	5368	5454
26-1	16-Dec-2014 00:14	62 59.370 S	0 0.360 E	5311	5391
27-1	16-Dec-2014 11:06	64 1.578 S	0 1.038 E	5193	5271
28-1	18-Dec-2014 01:24	65 0.018 S	0 0.018 E	3735	3748
29-4	18-Dec-2014 18:25	66 1.890 S	0 2.868 E	3615	3621
30-1	19-Dec-2014 02:05	66 27.708 S	0 1.488 E	4500	4538
31-1	20-Dec-2014 00:52	66 58.752 S	0 0.228 E	4710	4762
32-4	20-Dec-2014 15:23	67 34.182 S	0 8.472 E	4154	4123
33-1	21-Dec-2014 02:49	68 0.030 S	0 1.260 E	4513	4557
36-1	22-Dec-2014 23:23	69 0.612 S	0 1.620 E	3369	3373
42-1	03-Jan-2015 00:24	70 34.458 S	9 3.330 W	467	462
40-11	03-Jan-2015 05:17	70 31.398 S	7 57.720 W	232	232
49-1	07-Jan-2015 22:17	70 31.308 S	8 45.462 W	156	162
49-2	07-Jan-2015 23:10	70 31.320 S	8 45.450 W	156	164
49-3	08-Jan-2015 00:09	70 31.278 S	8 45.288 W	154	155
49-4	08-Jan-2015 01:07	70 31.248 S	8 45.330 W	151	155
49-5	08-Jan-2015 02:06	70 31.308 S	8 45.462 W	155	161
49-6	08-Jan-2015 03:09	70 31.308 S	8 45.522 W	158	162
49-7	08-Jan-2015 04:14	70 31.290 S	8 45.438 W	153	159
49-8	08-Jan-2015 05:22	70 31.320 S	8 45.552 W	172	167
49-9	08-Jan-2015 06:22	70 31.350 S	8 45.522 W	174	170
49-10	08-Jan-2015 07:16	70 31.338 S	8 45.552 W	174	169
49-11	08-Jan-2015 08:10	70 31.392 S	8 45.528 W	178	171
49-12	08-Jan-2015 09:12	70 31.380 S	8 45.582 W	179	171
52-1	09-Jan-2015 21:06	70 31.392 S	8 45.582 W	168	173
52-2	09-Jan-2015 22:04	70 31.398 S	8 45.558 W	168	173
52-3	09-Jan-2015 23:04	70 31.392 S	8 45.480 W	164	173
52-4	10-Jan-2015 00:09	70 31.320 S	8 45.420 W	155	161
52-5	10-Jan-2015 01:09	70 31.308 S	8 45.498 W	157	164
52-6	10-Jan-2015 02:08	70 31.308 S	8 45.378 W	154	158
52-7	10-Jan-2015 03:06	70 31.320 S	8 45.390 W	154	158
52-8	10-Jan-2015 04:12	70 31.320 S	8 45.480 W	157	163
52-9	10-Jan-2015 05:09	70 31.350 S	8 45.378 W	157	161
52-10	10-Jan-2015 06:09	70 31.380 S	8 45.390 W	159	167
52-11	10-Jan-2015 07:10	70 31.398 S	8 45.438 W	162	173
52-12	10-Jan-2015 08:04	70 31.380 S	8 45.492 W	163	173
54-1	10-Jan-2015 13:11	70 31.308 S	8 45.498 W	169	164

3.1 Oceanography

Station - Cast	Date /time	Latitude	Longitude	Water depth [m]	max pres. [dbar]
54-2	10-Jan-2015 14:09	70 31.308 S	8 45.468 W	166	162
54-3	10-Jan-2015 15:07	70 31.290 S	8 45.450 W	164	160
56-1	10-Jan-2015 19:08	70 31.350 S	8 45.450 W	*)	167
56-2	10-Jan-2015 20:02	70 31.362 S	8 45.432 W	157	167
56-3	10-Jan-2015 21:04	70 31.338 S	8 45.450 W	157	167
56-4	10-Jan-2015 22:04	70 31.368 S	8 45.360 W	157	164
57-1	11-Jan-2015 01:08	70 31.278 S	8 45.468 W	165	161
57-2	11-Jan-2015 02:07	70 31.290 S	8 45.510 W	167	163
57-3	11-Jan-2015 03:06	70 31.302 S	8 45.498 W	167	163
57-4	11-Jan-2015 04:07	70 31.278 S	8 45.450 W	165	160
57-5	11-Jan-2015 05:06	70 31.362 S	8 45.420 W	*)	166
58-1	11-Jan-2015 07:07	70 31.302 S	8 45.420 W	*)	161
58-2	11-Jan-2015 08:09	70 31.320 S	8 45.462 W	156	167
57-8	11-Jan-2015 09:06	70 31.320 S	8 45.510 W	158	166
57-9	11-Jan-2015 10:07	70 31.350 S	8 45.528 W	161	170
57-10	11-Jan-2015 11:07	70 31.338 S	8 45.432 W	157	165
57-11	11-Jan-2015 12:11	70 31.338 S	8 45.402 W	156	162
57-12	11-Jan-2015 13:06	70 31.308 S	8 45.468 W	155	163
57-13	11-Jan-2015 14:09	70 31.260 S	8 45.498 W	152	160
57-14	11-Jan-2015 16:09	70 31.302 S	8 45.528 W	156	164
57-15	11-Jan-2015 17:08	70 31.302 S	8 45.510 W	156	163
57-16	11-Jan-2015 19:10	70 31.302 S	8 45.492 W	154	162
57-17	11-Jan-2015 20:09	70 31.308 S	8 45.468 W	155	163
57-18	11-Jan-2015 21:07	70 31.320 S	8 45.510 W	158	166
57-19	11-Jan-2015 22:07	70 31.332 S	8 45.558 W	161	169
57-20	11-Jan-2015 23:06	70 31.350 S	8 45.480 W	159	168
57-21	12-Jan-2015 00:06	70 31.350 S	8 45.492 W	159	169
66-3	16-Jan-2015 10:55	69 0.312 S	6 59.190 W	2949	2944
73-1	18-Jan-2015 04:18	67 39.990 S	1 45.168 W	4508	4548
78-1	19-Jan-2015 05:45	66 2.130 S	0 0.798 E	3642	3639
80-1	20-Jan-2015 07:41	63 55.068 S	0 0.438 E	*)	5282
81-1	21-Jan-2015 12:34	61 0.090 S	0 0.138 E	5385	5463
82-1	27-Jan-2015 14:01	49 0.018 S	12 56.052 E	4121	52
82-2	27-Jan-2015 15:40	49 0.000 S	12 55.950 E	4121	4134

*) Due to environmental regulation, the EK60 echosounder was generally switched off while on station, resulting in deep-water soundings occasionally being unavailable when the CTD reached the sea floor.

Salinometer measurements

To monitor the accuracy and precision of the CTD's conductivity sensors, salinity/conductivity of 281 water samples was determined using an Optimare Precision Salinometer (OPS) for 17 CTD stations (Table 3.1.1.10) between 04.12.2014 and 27.01.2015. Water samples were

measured in reference to Standard Water batch no. P152; K15 = 0.99981, valid until date: 2013-05-05.

Enroute comparisons between *in-situ* CTD data and salinometer based salinity measurements of water samples indicated that the conductivity sensors (SBE4c #3290) used in the secondary sensor pair featured the higher accuracies (Fig. 3.1.1.5). In addition, their drifts were smaller than that of the primary sensor for the duration of the expedition.

A definitive determination of sensors' drifts however requires post-expedition lab calibrations, for which the sensors will be returned to Seabird Electronics after leg PS89. Hence all results reported hereinafter must be considered preliminary.

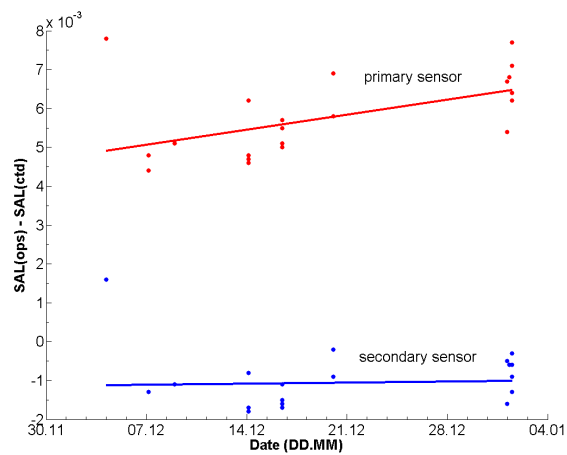


Fig. 3.1.1.5: Deviation in salinity between OPS measurements and *in-situ* CTD measurements for samples below 4,000 m depth. The correction for the secondary sensor (blue line) is about -0.0011, and constant over time, contrasting a notable drift of the primary sensor.

Tab. 3.1.1.10: Salinity samples from the water sampler and measured with the OPS

Station	Cast	PRES	SAL1	SAL2	OPS	OPS-SAL1	OPS-SAL2
1	1	4685,33	34,7295	34,7357	34,7373	0,0078	0,0016
1	1	2532,392	34,8307	34,8356	34,8375	0,0068	0,0019
2	1	5221,684	34,7144	34,7208	34,7295	0,0151	0,0087
2	1	2535,527	34,8325	34,8373	34,8394	0,0069	0,0021
5	1	4650,843	34,6938	34,6999	34,6986	0,0048	-0,0013
5	1	4073,404	34,7125	34,7182	34,7169	0,0044	-0,0013
5	1	3558,331	34,732	34,7374	34,7363	0,0043	-0,0011
5	1	3048,601	34,7545	34,7597	34,7588	0,0043	-0,0009
5	1	2845,22	34,7623	34,7672	34,7672	0,0049	0
5	1	2535,105	34,7769	34,7816	34,7811	0,0042	-0,0005
5	1	2332,578	34,7767	34,7809	34,781	0,0043	1E-04
5	1	2025,961	34,7619	34,7665	34,7654	0,0035	-0,0011
5	1	1821,695	34,7325	34,7369	34,7361	0,0036	-0,0008
5	1	1517,67	34,6379	34,6418	34,6412	0,0033	-0,0006

3.1 Oceanography

Station	Cast	PRES	SAL1	SAL2	OPS	OPS-SAL1	OPS-SAL2
5	1	1213,912	34,4938	34,4976	34,4989	0,0051	0,0013
5	1	1009,719	34,3919	34,3951	34,3961	0,0042	0,001
5	1	907,022	34,3221	34,3257	34,3252	0,0031	-0,0005
5	1	808,521	34,2781	34,2819	34,2813	0,0032	-0,0006
5	1	605,137	34,1889	34,1924	34,1929	0,004	0,0005
5	1	403,382	34,168	34,1718	34,1702	0,0022	-0,0016
5	1	302,76	34,2272	34,2298	34,2308	0,0036	0,001
5	1	202,306	34,3839	34,39	34,3871	0,0032	-0,0029
5	1	151,313	34,4487	34,4521	34,4541	0,0054	0,002
5	1	101,078	34,426	34,4278	34,431	0,005	0,0032
5	1	75,41	34,4146	34,4176	34,4184	0,0038	0,0008
5	1	50,821	34,0617	34,0607	34,0935	0,0318	0,0328
5	1	24,52	34,0299	34,0337	34,0339	0,004	0,0002
8	1	4236,423	34,6839	34,6901	34,689	0,0051	-0,0011
8	1	3558,288	34,6942	34,7002	34,6993	0,0051	-0,0009
8	1	3352,179	34,6984	34,7039	34,7028	0,0044	-0,0011
8	1	3047,934	34,7138	34,7196	34,7191	0,0053	-0,0005
8	1	2844,892	34,7318	34,737	34,7366	0,0048	-0,0004
8	1	2535,953	34,7465	34,7514	34,7513	0,0048	-1E-04
8	1	2232,269	34,764	34,7688	34,7689	0,0049	0,0001
8	1	2028,088	34,7683	34,773	34,7731	0,0048	1E-04
8	1	1823,47	34,7634	34,7681	34,768	0,0046	-1E-04
8	1	1519,173	34,7308	34,7349	34,7338	0,003	-0,0011
8	1	1212,244	34,6622	34,666	34,6663	0,0041	0,0003
8	1	1010,283	34,5924	34,5964	34,598	0,0056	0,0016
8	1	908,852	34,533	34,5371	34,5372	0,0042	1E-04
8	1	811,834	34,4931	34,4971	34,4963	0,0032	-0,0008
8	1	603,845	34,3489	34,3529	34,3561	0,0072	0,0032
8	1	404,681	34,174	34,1789	34,1774	0,0034	-0,0015
8	1	304,117	34,1124	34,1164	34,1169	0,0045	0,0005
8	1	204,722	34,102	34,1065	34,1074	0,0054	0,0009
8	1	152,457	33,948	33,9517	33,9502	0,0022	-0,0015
8	1	101,675	33,7945	33,798	33,8003	0,0058	0,0023
8	1	74,318	33,7924	33,7961	33,7972	0,0048	0,0011
8	1	56,114	33,7902	33,794	33,7947	0,0045	0,0007
8	1	27,906	33,7902	33,7941	33,7946	0,0044	0,0005
8	1	28,573	33,79	33,7938	33,7946	0,0046	0,0008
11	1	2553,745	34,6796	34,685	34,6847	0,0051	-0,0003
11	1	1215,108	34,7222	34,7264	34,7262	0,004	-0,0002
12	2	2590,594	34,6761	34,6815	34,6804	0,0043	-0,0011
12	2	2232,511	34,6776	34,6826	34,682	0,0044	-0,0006
12	2	2027,24	34,6797	34,6845	34,6837	0,004	-0,0008
12	2	1823,869	34,6821	34,6868	34,6859	0,0038	-0,0009
12	2	1620,535	34,6855	34,69	34,6897	0,0042	-0,0003

3. Scientific Programmes

Station	Cast	PRES	SAL1	SAL2	OPS	OPS-SAL1	OPS-SAL2
12	2	1417,848	34,6917	34,6957	34,6955	0,0038	-0,0002
12	2	1214,154	34,6993	34,7035	34,7034	0,0041	-1E-04
12	2	1011,205	34,7053	34,7094	34,7092	0,0039	-0,0002
12	2	912,104	34,7067	34,7108	34,7111	0,0044	0,0003
12	2	809,978	34,7084	34,7121	34,7122	0,0038	0,0001
12	2	708,457	34,7052	34,7091	34,7085	0,0033	-0,0006
12	2	606,248	34,6957	34,6996	34,6993	0,0036	-0,0003
12	2	504,58	34,6785	34,6822	34,6834	0,0049	0,0012
12	2	405,133	34,6507	34,6547	34,6546	0,0039	-1E-04
12	2	304,615	34,5938	34,5981	34,5951	0,0013	-0,003
12	2	251,958	34,5126	34,5155	34,5157	0,0031	0,0002
12	2	203,916	34,3358	34,3395	34,3387	0,0029	-0,0008
12	2	151,783	34,1413	34,147	34,1499	0,0086	0,0029
12	2	126,581	33,9243	33,9269	33,9137	-0,0106	-0,0132
12	2	101,462	33,8631	33,8668	33,8691	0,006	0,0023
12	2	77,109	33,8609	33,8648	33,8663	0,0054	0,0015
12	2	51,892	33,8574	33,8611	33,8647	0,0073	0,0036
12	2	25,532	33,8562	33,8601	33,8631	0,0069	0,003
16	1	3669,751	34,6492	34,6553	34,6542	0,005	-0,0011
16	1	3279,143	34,6521	34,6578	34,6567	0,0046	-0,0011
16	1	3048,858	34,6538	34,6593	34,658	0,0042	-0,0013
16	1	2845,208	34,6546	34,66	34,6593	0,0047	-0,0007
16	1	2537,206	34,6572	34,6623	34,6622	0,005	-0,0001
16	1	2230,486	34,6608	34,6658	34,6654	0,0046	-0,0004
16	1	2027,846	34,6632	34,6679	34,6679	0,0047	0
16	1	1722,965	34,6672	34,6719	34,672	0,0048	1E-04
16	1	1519,596	34,6707	34,6752	34,6754	0,0047	0,0002
16	1	1214,407	34,6753	34,6795	34,6797	0,0044	0,0002
16	1	1011,356	34,6792	34,6835	34,6833	0,0041	-0,0002
16	1	911,1	34,6808	34,6846	34,6852	0,0044	0,0006
16	1	808,609	34,6824	34,6864	34,6868	0,0044	0,0004
16	1	606,305	34,6792	34,6831	34,6836	0,0044	0,0005
16	1	505,024	34,6831	34,6869	34,6875	0,0044	0,0006
16	1	391,158	34,6843	34,6881	34,6884	0,0041	0,0003
16	1	302,615	34,6348	34,6378	34,6402	0,0054	0,0024
16	1	200,869	34,4726	34,4763	34,4779	0,0053	0,0016
16	1	151,685	34,3799	34,3838	34,385	0,0051	0,0012
16	1	100,758	34,2372	34,2468	34,2595	0,0223	0,0127
16	1	74,818	34,1779	34,1712	34,1762	-0,0017	0,005
16	1	59,947	34,087	34,088	34,0902	0,0032	0,0022
16	1	20,318	34,073	34,0766	34,0782	0,0052	0,0016
16	1	20,994	34,073	34,0759	34,0788	0,0058	0,0029
21	1	5450,653	34,6399	34,6469	34,6461	0,0062	-0,0008
21	1	4900,58	34,6407	34,6473	34,6455	0,0048	-0,0018

3.1 Oceanography

Station	Cast	PRES	SAL1	SAL2	OPS	OPS-SAL1	OPS-SAL2
21	1	4592,734	34,6418	34,6483	34,6465	0,0047	-0,0018
21	1	4384,752	34,6431	34,6495	34,6477	0,0046	-0,0018
21	1	4075,647	34,6459	34,6522	34,6505	0,0046	-0,0017
21	1	3871,64	34,6477	34,6538	34,6521	0,0044	-0,0017
21	1	3562,539	34,6497	34,6556	34,6536	0,0039	-0,002
21	1	3048,632	34,6524	34,6579	34,6564	0,004	-0,0015
21	1	2028,176	34,6589	34,6638	34,663	0,0041	-0,0008
21	1	1516,638	34,665	34,6697	34,6692	0,0042	-0,0005
21	1	1313,548	34,6675	34,672	34,6725	0,005	0,0005
21	1	1011,476	34,6729	34,677	34,6771	0,0042	0,0001
21	1	911,915	34,6745	34,6786	34,6785	0,004	-0,0001
21	1	807,95	34,6768	34,6808	34,6802	0,0034	-0,0006
21	1	606,377	34,6805	34,6844	34,6838	0,0033	-0,0006
21	1	402,31	34,6826	34,6865	34,6852	0,0026	-0,0013
21	1	202,721	34,6825	34,6863	34,6847	0,0022	-0,0016
21	1	152,417	34,658	34,6647	34,6689	0,0109	0,0042
21	1	101,881	34,3234	34,3407	34,3014	-0,022	-0,0393
21	1	76,784	34,2087	34,2127	34,2112	0,0025	-0,0015
21	1	51,641	34,149	34,1526	34,1502	0,0012	-0,0024
21	1	24,751	33,9894	33,9931	34,0193	0,0299	0,0262
21	1	14,515	33,9342	33,9305	33,9712	0,037	0,0407
21	1	13,017	33,9317	33,936	33,9644	0,0327	0,0284
27	1	5270,853	34,64	34,6471	34,6455	0,0055	-0,0016
27	1	4902,366	34,6412	34,648	34,6469	0,0057	-0,0011
27	1	4593,36	34,6429	34,6496	34,648	0,0051	-0,0016
27	1	4386,773	34,6447	34,6514	34,6497	0,005	-0,0017
27	1	4077,989	34,6473	34,6539	34,6524	0,0051	-0,0015
27	1	3872,555	34,6485	34,655	34,6534	0,0049	-0,0016
27	1	3563,875	34,6503	34,6566	34,655	0,0047	-0,0016
27	1	3051,139	34,6532	34,6591	34,6575	0,0043	-0,0016
27	1	2540,271	34,6568	34,6623	34,6619	0,0051	-0,0004
27	1	2029,575	34,6626	34,6676	34,6674	0,0048	-0,0002
28	1	3747,814	34,6489	34,655	34,6547	0,0058	-0,0003
28	1	3307,272	34,6524	34,6584	34,6576	0,0052	-0,0008
28	1	3051,645	34,654	34,6602	34,659	0,005	-0,0012
28	1	2847,166	34,6556	34,6616	34,6606	0,005	-0,001
28	1	2540,172	34,6585	34,6642	34,6635	0,005	-0,0007
28	1	2233,914	34,6617	34,6673	34,6668	0,0051	-0,0005
28	1	2029,553	34,6649	34,6705	34,6697	0,0048	-0,0008
28	1	1723,914	34,6701	34,6753	34,6749	0,0048	-0,0004
28	1	1520,597	34,6733	34,6785	34,6783	0,005	-0,0002
28	1	1215,741	34,6794	34,6844	34,6841	0,0047	-0,0003
28	1	1012,33	34,6838	34,6882	34,6886	0,0048	0,0004
28	1	911,09	34,6858	34,6905	34,6912	0,0054	0,0007

3. Scientific Programmes

Station	Cast	PRES	SAL1	SAL2	OPS	OPS-SAL1	OPS-SAL2
28	1	809,674	34,6882	34,6926	34,6934	0,0052	0,0008
28	1	607,188	34,6923	34,6961	34,696	0,0037	-0,0001
28	1	505,884	34,6942	34,6985	34,6985	0,0043	0
28	1	404,669	34,6944	34,6988	34,699	0,0046	0,0002
28	1	303,385	34,6964	34,7008	34,7008	0,0044	0
28	1	202,171	34,6906	34,6955	34,6057	-0,0849	-0,0898
28	1	151,758	34,6834	34,6879	34,6876	0,0042	-0,0003
28	1	101,338	34,6624	34,6648	34,6662	0,0038	0,0014
28	1	50,758	34,2834	34,2911	34,3097	0,0263	0,0186
28	1	35,503	34,1402	34,145	34,2157	0,0755	0,0707
28	1	14,752	33,6421	33,6463	33,6635	0,0214	0,0172
28	1	14,751	33,6422	33,6464	33,6844	0,0422	0,038
31	1	4761,53	34,644	34,6511	34,6509	0,0069	-0,0002
31	1	4078,949	34,6487	34,6554	34,6545	0,0058	-0,0009
31	1	3564,693	34,6509	34,6573	34,6564	0,0055	-0,0009
31	1	3050,689	34,6544	34,6604	34,66	0,0056	-0,0004
31	1	2846,713	34,6562	34,6619	34,6624	0,0062	0,0005
31	1	2540,503	34,6594	34,6651	34,6649	0,0055	-0,0002
31	1	2335,944	34,6614	34,6669	34,667	0,0056	0,0001
31	1	2030,001	34,6653	34,6706	34,671	0,0057	0,0004
31	1	1825,848	34,6686	34,6736	34,6746	0,006	0,001
31	1	1520,822	34,6739	34,6789	34,6792	0,0053	0,0003
31	1	1215,345	34,6797	34,6843	34,685	0,0053	0,0007
31	1	1013,228	34,6836	34,6882	34,6888	0,0052	0,0006
31	1	911,115	34,6858	34,6899	34,6915	0,0057	0,0016
31	1	810,115	34,6867	34,6912	34,6924	0,0057	0,0012
31	1	607,023	34,6928	34,6971	34,6978	0,005	0,0007
31	1	404,557	34,6981	34,7021	34,703	0,0049	0,0009
31	1	303,459	34,698	34,7022	34,7026	0,0046	0,0004
31	1	202,575	34,693	34,6972	34,6985	0,0055	0,0013
31	1	151,795	34,6862	34,6904	34,6911	0,0049	0,0007
31	1	101,065	34,6716	34,6759	34,6764	0,0048	0,0005
31	1	75,643	34,6512	34,6563	34,6504	-0,0008	-0,0059
31	1	40,596	34,1396	34,1398	34,1822	0,0426	0,0424
31	1	20,106	33,9733	33,9779	33,9769	0,0036	-0,001
31	1	20,133	33,9728	33,9769	33,9765	0,0037	-0,0004
66	2	2847,454	34,654	34,6604	34,6595	0,0055	-0,0009
66	2	1012,617	34,6806	34,6855	34,6859	0,0053	0,0004
73	1	4547,225	34,646	34,6532	34,6527	0,0067	-0,0005
73	1	4079,424	34,6483	34,6553	34,6537	0,0054	-0,0016
73	1	3565,034	34,6504	34,657	34,6561	0,0057	-0,0009
73	1	3051,94	34,6538	34,6602	34,6593	0,0055	-0,0009
73	1	2847,487	34,6555	34,6615	34,6612	0,0057	-0,0003
73	1	2540,47	34,6587	34,6646	34,6637	0,005	-0,0009

3.1 Oceanography

Station	Cast	PRES	SAL1	SAL2	OPS	OPS-SAL1	OPS-SAL2
73	1	2336,528	34,6608	34,6667	34,6659	0,0051	-0,0008
73	1	2029,565	34,6651	34,6707	34,6697	0,0046	-0,001
73	1	1825,912	34,6685	34,6736	34,6727	0,0042	-0,0009
73	1	1520,707	34,6737	34,679	34,6777	0,004	-0,0013
73	1	1216,056	34,6795	34,6845	34,6833	0,0038	-0,0012
73	1	1012,835	34,6838	34,6888	34,6871	0,0033	-0,0017
73	1	911,253	34,6855	34,6903	34,6882	0,0027	-0,0021
73	1	810,15	34,687	34,6919	34,6891	0,0021	-0,0028
73	1	606,798	34,692	34,6965	34,6932	0,0012	-0,0033
73	1	404,538	34,6919	34,6964	34,6936	0,0017	-0,0028
73	1	303,649	34,692	34,6967	34,692	0	-0,0047
73	1	202,313	34,6799	34,6844	34,6801	0,0002	-0,0043
73	1	141,764	34,6559	34,6605	34,6509	-0,005	-0,0096
73	1	101,14	34,5928	34,6032	34,5796	-0,0132	-0,0236
73	1	50,625	34,3159	34,3192	34,3121	-0,0038	-0,0071
73	1	25,003	34,1307	34,123	34,1163	-0,0144	-0,0067
73	1	14,883	33,8604	33,8856	33,8185	-0,0419	-0,0671
73	1	14,988	33,8308	33,841	33,8242	-0,0066	-0,0168
78	1	3635,723	34,6491	34,6559	34,6545	0,0054	-0,0014
78	1	3305,743	34,6519	34,6583	34,6554	0,0035	-0,0029
78	1	3050,459	34,6535	34,66	34,6568	0,0033	-0,0032
78	1	2843,745	34,6555	34,6617	34,6576	0,0021	-0,0041
78	1	2539,618	34,6586	34,6646	34,6603	0,0017	-0,0043
78	1	2234,938	34,6614	34,6671	34,6625	0,0011	-0,0046
78	1	2030,232	34,6637	34,6692	34,6641	0,0004	-0,0051
78	1	1724,283	34,6689	34,6741	34,6687	-0,0002	-0,0054
78	1	1520,881	34,6723	34,6776	34,6714	-0,0009	-0,0062
78	1	1216,793	34,6785	34,6837	34,6766	-0,0019	-0,0071
78	1	1013,488	34,6824	34,6874	34,68	-0,0024	-0,0074
78	1	910,298	34,6841	34,6891	34,6909	0,0068	0,0018
78	1	808,504	34,686	34,6909	34,692	0,006	0,0011
78	1	606,642	34,6903	34,695	34,6952	0,0049	0,0002
78	1	506,311	34,6894	34,6941	34,695	0,0056	0,0009
78	1	405,473	34,6889	34,6935	34,6908	0,0019	-0,0027
78	1	303,85	34,6869	34,6914	34,6863	-0,0006	-0,0051
78	1	201,436	34,6782	34,6832	34,6772	-0,001	-0,006
78	1	151,053	34,6602	34,6658	34,6571	-0,0031	-0,0087
78	1	100,215	34,5619	34,5709	34,5664	0,0045	-0,0045
78	1	51,452	34,3133	34,2951	34,3228	0,0095	0,0277
78	1	20,682	33,3444	33,3533	33,4433	0,0989	0,09
78	1	20,745	33,3549	33,356	33,405	0,0501	0,049
78	1	15,122	33,3282	33,332	33,404	0,0758	0,072
80	1	4902,049	34,6405	34,6479	34,6473	0,0068	-0,0006
80	1	1519,955	34,67	34,6752	34,6755	0,0055	0,0003

3. Scientific Programmes

Station	Cast	PRES	SAL1	SAL2	OPS	OPS-SAL1	OPS-SAL2
81	1	5461,819	34,6386	34,6466	34,6463	0,0077	-0,0003
81	1	5106,805	34,6393	34,647	34,6464	0,0071	-0,0006
81	1	4593,489	34,6401	34,6476	34,6463	0,0062	-0,0013
81	1	4078,167	34,6436	34,6509	34,65	0,0064	-0,0009
81	1	3871,611	34,6464	34,6534	34,6523	0,0059	-0,0011
81	1	3563,477	34,6488	34,6555	34,6542	0,0054	-0,0013
81	1	3050,526	34,6511	34,6575	34,6568	0,0057	-0,0007
81	1	2538,305	34,6544	34,6603	34,6603	0,0059	0
81	1	2028,359	34,6585	34,6642	34,6634	0,0049	-0,0008
81	1	1518,3	34,6643	34,6698	34,6695	0,0052	-0,0003
81	1	1011,658	34,6719	34,677	34,6775	0,0056	0,0005
81	1	911,825	34,6739	34,6791	34,6792	0,0053	0,0001
81	1	809,09	34,6754	34,6805	34,6808	0,0054	0,0003
81	1	607,855	34,6798	34,6846	34,6844	0,0046	-0,0002
81	1	405,695	34,6819	34,6869	34,6863	0,0044	-0,0006
81	1	304,356	34,6816	34,6865	34,6866	0,005	1E-04
81	1	204,764	34,6788	34,6838	34,6829	0,0041	-0,0009
81	1	151,081	34,6576	34,6586	34,6621	0,0045	0,0035
81	1	101,372	34,2741	34,2794	34,2622	-0,0119	-0,0172
81	1	75,678	34,1869	34,1915	34,1892	0,0023	-0,0023
81	1	51,124	34,1193	34,1227	34,1209	0,0016	-0,0018
81	1	24,767	33,6711	33,724	33,6684	-0,0027	-0,0556
81	1	14,771	33,6023	33,6063	33,6108	0,0085	0,0045
81	1	14,652	33,6022	33,6069	33,609	0,0068	0,0021
82	2	2536,299	34,746	34,7519	34,7534	0,0074	0,0015
82	2	2280,335	34,747	34,7525	34,7532	0,0062	0,0007
82	2	2025,13	34,7628	34,7685	34,7686	0,0058	1E-04
82	2	1770,775	34,7611	34,7665	34,7667	0,0056	0,0002
82	2	1520,608	34,7458	34,7511	34,7519	0,0061	0,0008
82	2	1265,154	34,6987	34,7037	34,7051	0,0064	0,0014
82	2	1014,546	34,6355	34,6403	34,6391	0,0036	-0,0012
82	2	910,587	34,586	34,5908	34,5915	0,0055	0,0007
82	2	809,081	34,5399	34,5444	34,5436	0,0037	-0,0008
82	2	707,743	34,5071	34,5118	34,5116	0,0045	-0,0002
82	2	605,856	34,4393	34,4438	34,4403	0,001	-0,0035
82	2	504,504	34,3475	34,3523	34,3516	0,0041	-0,0007
82	2	403,204	34,2524	34,2579	34,2542	0,0018	-0,0037
82	2	303,946	34,1717	34,1764	34,1756	0,0039	-0,0008
82	2	251,583	34,1161	34,1204	34,1219	0,0058	0,0015
82	2	202,473	34,0742	34,0814	34,0820	0,0078	0,0006
82	2	151,15	34,0158	34,0203	34,0210	0,0052	0,0007
82	2	126,259	33,886	33,8838	33,8799	-0,0061	-0,0039
82	2	100,175	33,7758	33,7856	33,7938	0,018	0,0082
82	2	75,464	33,7498	33,7542	33,7566	0,0068	0,0024

3.1 Oceanography

Station	Cast	PRES	SAL1	SAL2	OPS	OPS-SAL1	OPS-SAL2
82	2	49,987	33,7489	33,7535	33,7547	0,0058	0,0012
82	2	14,959	33,7488	33,7534	33,7546	0,0058	0,0012
82	2	14,253	33,749	33,7537	33,7540	0,005	0,0003

Argo float deployments

On the southbound leg, one Argo float (type Webb APEX) was deployed for the Royal Netherlands Meteorological Institute (KNMI, contact point sterl@knmi.nl, Table 3.1.1.11).

Tab. 3.1.1.11: APEX float deployments on behalf of KNMI

Float type	Deployment Date Time [UTC]	Station ID	T water @ keel [°C]	Latitude	Longitude	Water Depth [m]	Ship's Speed [kn]	Ship's course [°]	Wind Direction [°]	Wind Speed [m/s]
Apex	12.12.14 1:11	PS89/0015-2		55° 59,98' S	0° 0,08' E	3697.4	1.3	233	230	6

During the northbound leg, 15 Argo floats (type Optimare NEMO) were deployed near the continental shelf into the Antarctic coastal current (Table 3.1.1.12).

Tab. 3.1.1.12: NEMO float deployments

Nemo Ser. No.	Deployment Date Time [UTC]	Station ID	Temp water @ keel [°C]	Latitude	Longitude	Water Depth [m]	Ship's Speed [kn]	Ship's course [°T]	Wind Direction [°T]	Wind Speed [m/s]
293	15.1.15 11:40	PS89/0060-1	-1.6815	69° 46,55' S	10° 06,49' W	*)	1.3	286	60	10
291	15.1.15 13:52	PS89/0061-1	-1.638	69° 30,15' S	10° 32,60' W	*)	4.8	348	55	10
294	15.1.15 21:00	PS89/0063-1	-1.6135	69° 13,71' S	10° 20,37' W	3979.6	3.2	2	270	2
297	15.1.15 22:39	PS89/0064-1	-1.5096	69° 00,05' S	10° 18,39' W	4513.7	3.6	99	262	4
290	16.1.15 04:17	PS89/0065-1	-1.1126	68° 59,98' S	08° 00,04' W	3543.6	2.5	112	327	3
282	16.1.15 23:41	PS89/0068-1	-1.6591	69° 00,24' S	05° 46,09' W	*)	2.6	86	217	6
281	17.1.15 03:01	PS89/0069-1	-1.2644	68° 40,04' S	05° 05,38' W	*)	2.7	57	223	10
285	17.1.15 15:03	PS89/0070-3	-1.2802	68° 15,20' S	04° 00,40' W	4093.4	1.2	297	258	14
280	17.1.15 22:07	PS89/0072-1	-1.472	67° 59,93' S	03° 14,23' W	4213.5	2.5	299	284	10
284	18.1.15 06:15	PS89/0073-3	-0.6915	67° 39,92' S	01° 45,17' W	*)	1.2	55	47	12
288	18.1.15 09:34	PS89/0074-1	-0.1743	67° 20,17' S	00° 56,43' W	*)	2.2	38	60	16
289	18.1.15 13:52	PS89/0075-1	-0.396	67° 00,17' S	00° 00,84' W	*)	3.1	320	66	19
286	18.1.15 20:23	PS89/0076-1	0.1834	66° 39,89' S	00° 00,56' E	*)	1.1	16	2	11
287	19.1.15 00:35	PS89/0077-1	-0.1823	66° 20,23' S	00° 00,02' W	4021.8	2.8	357	23	14
276	19.1.15 07:45	PS89/0078-3	0.0431	66° 01,31' S	00° 02,30' E	*)	1.5	46	18	13

*) Due to environmental regulation, the EK60 echosounder was generally switched off while on station, resulting in deep-water soundings frequently being unavailable at the time of float launch.

Operational results

Hydrographic moorings

Details of the moorings scheduled for recovery, their instrumentation and the length of each associated data record are listed in Table 3.1.1.13. In general, the instruments performed well, providing, with few exceptions, data for the full deployment period.

Tab. 3.1.1.13: Moorings **recovered** between Cape Town and *Neumayer III* and on the Greenwich meridian. The date and time of the recovery is the date and time of the first release command

Mooring	Latitude Longitude	Water Depth (m)	Date Time a. deployed b. recovered	Instrument Type	Serial Number	Instrument Depth (m)	Record Length (days) [Remarks]
AWI229-10	63° 59.66' S	5172	14.12.2012	AVTP	8050	200	732
	00° 002.67' W		12:34	SBE37	9834	200	732
				SBE37	447	250	732
			16.12.2014	SBE37	237	300	[2]
			15:04	SBE37	240	350	732
				SBE37	435	400	732
				SBE37	9838	450	732
				SBE37	438	500	732
				SBE37	439	550	732
				SBE37	2086	600	732
				SBE37	449	650	732
				SBE37	245	700	732
				RCM 11	452	706	732
				SOSO	0026	807	[1]
				PAM	1010	969	[1]
				RCM 11	475	1977	[3]
				SBE37	9833	5126	[3]
				RCM 11	144	5127	[3]
AWI230-8	66° 02.12' S	3552	15.12.2012	AVTP	10491	200	732
	00° 02.98' E		14:39	SBE37	2088	200	732
				SBE37	2090	300	456
			18.12.2014	SBE37	2091	400	732
			11:21	SBE37	2092	500	732
				SBE37	2093	600	732
				SBE37	2094	700	732
				AVT	6856	725	732
				PAM	1009	949	[1]
				AVTP	9213	1657	732
				SBE37	2095	3508	732
				AVT	9179	3509	732
AWI231-10	66° 30.93' S	4524	17.12.2010	AVTP	10541	200	732
	00° 00.65' W		12:00	SBE37	2096	200	732
				SBE37	2098	250	732

3.1 Oceanography

Mooring	Latitude Longitude	Water Depth (m)	Date Time a. deployed b. recovered	Instrument Type	Serial Number	Instrument Depth (m)	Record Length (days) [Remarks]
			19.12.2014	SBE37	2099	300	732
			09:26	SBE37	2100	350	732
				SBE37	2101	400	732
				SBE37	2385	450	732
				SBE37	2234	500	732
				SBE37	2386	550	732
				SBE37	2389	600	732
				SBE37	2391	650	732
				SBE37	3813	700	732
				AVT	9184	729	732
				SOSO	0024	830	[1]
				RCM 11	509	1812	703
				SBE37	7726	4413	732
				AVT	9180	4414	732
AWI232-11	68° 59.86' S	3319	18.12.2012	AVTP	10925	250	733
	00° 06.51' W		06:00	RCM 11	469	757	733
				PAM	1011	958	[1]
			21.12.2014	RCM 11	512	1765	664
			21:52	SBE37	7727	3265	733
				AVT	10499	3266	[2]
AWI244-3	69° 00.35' S	2900	25.12.2012	SOSO	29	806	[1]
	06° 58.97' W		10:27	PAM	0001	998	[1]
				SBE16	2419	2857	751

Remarks: [1] to be processed; [2] flooded; [3] lost due to broken mooring rope.

Tab. 3.1.1.14: Moorings **deployed** during PS89

Mooring	Latitude Longitude	Water depth (m)	Date Time	Instrument Type	Instrument Serial Number	Instrument depth (m)
AWI227-13	59° 02.67' S	4600	13.12.2014	PAM	1056	1020
	00° 05.37' E		16:38	SBE37	8125	4557
AWI229-11	64° 00.31' S	5165	17.12.2014	AVTP	8395	202
	00° 00.22' W		11:43	SBE37	8129	203
				SBE37	9831	300

3. Scientific Programmes

Mooring	Latitude Longitude	Water depth (m)	Date Time	Instrument Type	Instrument Serial Number	Instrument depth (m)
				SBE37	10943	400
				SBE37	10944	500
				SBE37	11419	600
				SBE37	11420	700
				RCM11	501	709
				PAM	1057	970
				SBE37	227	5121
AWI229-12	63° 54.94' S	5172	20.01.2015	SOSO	0048	798
	00° 00.16' E		11:38	PAM	1055	1001
				SBE37	228	5167
AWI231-11	66° 30.41' S	4472	19.12.2014	SOSO	0026	851
	00° 00.66' W		17:59	PAM	1058	973
				SBE37	11421	4429
AWI232-12	68° 58.89' S	3360	23.12.2014	AVT	8367	290
	00° 05.00' W		09:52	AVT	9211	798
				PAM	1059	999
				RCM11	472	1806
				SBE37	11422	3306
				RCM11	25	3307
AWI244-4	69° 00.34' S	2900	16.01.2015	SOSO	0047	806
	06° 58.94' W		14:20	PAM	1061	998
				SBE37	12470	2857

Abbreviations used:

AVTP	Aanderaa Current Meter with Temperature- and Pressure Sensor
AVT	Aanderaa Current Meter with Temperature Sensor
DCS	Aanderaa Doppler Current Sensor
PAM	Passive Acoustic Monitor (Type: SONOVAULT)
RCM11	Aanderaa Doppler Current Meter
SBE16	SeaBird Electronics Self Recording CTD to measure Temp., Cond. and Pressure
SBE37	SeaBird Electronics, Type: MicroCat, to measure Temperature and Conductivity

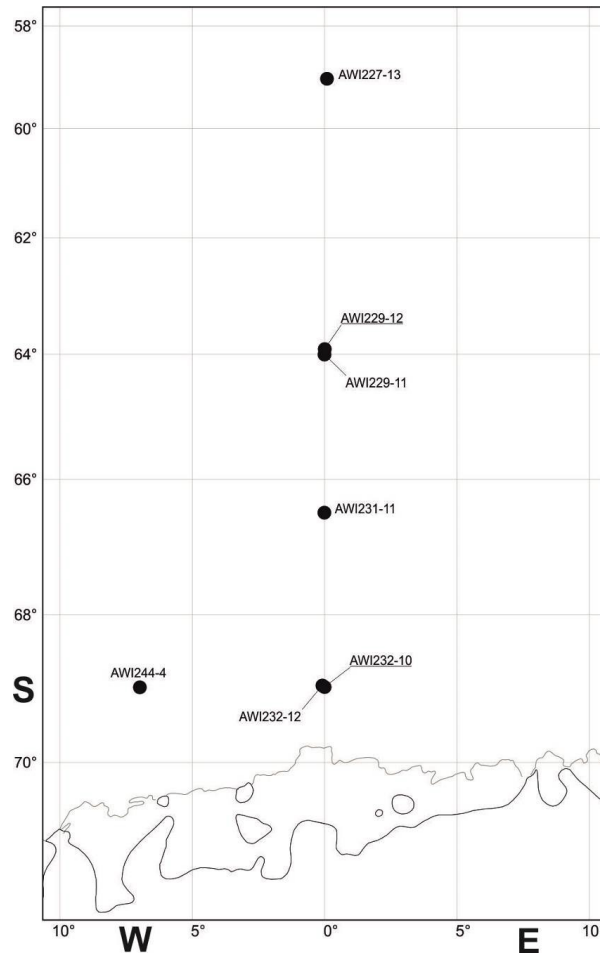


Fig. 3.1.1.6: Position of mooring deployments during PS89

The Posidonia positioning system

A detailed description of mooring recoveries under heavy sea-ice conditions is given in Boebel (2013). Essential to such recoveries is a robust and timely localization of the mooring's transponders by the *Posidonia* hydroacoustic positioning system. During PS89, only the mobile *Posidonia* antenna (deployable on station through the ship's well) was available. With this antenna installed in the ship's well, *Polarstern* cannot move in ice covered area to avoid the risk of damaging the antenna. Deploying the antenna through the ship's well lasts about 45 minutes, a time span during which *Polarstern* necessarily drifts with the ice floes. For *Polarstern* to be within the acoustic range (a downward directed cone of an opening angle of about $\pm 60^\circ$) of the mooring's transducers at the time of operability of the antenna, the ship hence has to be placed at a location upstream (with regard to the tide and wind driven ice-drift) of a distance equaling drift speed x 45min. Determining this drift (including an understanding of the tidal cycle's phase) requires at least 2 hours, preferably longer prior to positioning the ship and deploying the antenna.

Posidonia's main electronic unit *POSIDONIA 6000* had been replaced with the new USBL-BOX prior to our expedition. This proved to be a substantial improvement as valid localizations were obtained immediately upon the first interrogating ping. Additionally, after its release, the transponder can be tracked to within $\pm 60^\circ$ (measured from the vertical), i.e. up to 100 m below the surface under practical conditions. Together with the visualization software *PosiView*

(provided by Ralf Krockner, AWI), the system now meets all requirements necessary for mooring recoveries, even under adverse sea-ice conditions. Nevertheless the current deployment/recovery procedure of the *Posidonia* antenna is extremely time consuming (lasting a total of 1.5 h at least) during which the ship has to remain immobile.

Sea ice borne mooring recoveries

Severe ice situations can bar *Polarstern* from reaching a mooring's location and breaking of the ice nearby to allow the mooring to surface (Boebel, 2013). Under such circumstances, recovering the mooring directly from the floe with limited assistance from the ship is necessary. The approach bases on the notion that once the mooring is released, its floatation will assemble under the sea ice and drift with it. Hence, if the mooring's position at the time of surfacing is known in a sea ice based reference frame, one would have plenty of time to provide access to it through the sea ice.

To penetrate the sea ice, a small modified earthmover with a 90 cm diameter drill was mobilized for this expedition. In general, sea ice borne mooring recoveries comprise the following steps:

- Locate, release and track the mooring with USBL-BOX and mark the presumed under-ice position on the ice floe.
- Place the earthmover on the ice floe and proceed to the marked point.
- Drill a hole through the ice and verify that the mooring is close by.
- Deploy diver or ROV to retrieve part of the mooring rope through the bore hole.
- Recover the mooring without assistance from the ship's winches using a portable capstan and a tripod over the hole to lift heavy instruments.

During PS89 we did not encounter conditions that rendered the above approach necessary; However, the overall operation was tested on December 29, 2014 during our stay in Atka Bay. This test of our equipment for sea-ice borne mooring recovery was positive, yet some specific aspects require reconsideration or improvement to reduce the effort and time. Specifically, we gained the following insights:

Earthmover/drill and plates:

The earthmover has a weight of about 2,000 kg. The chain drive is too small to propel the unit on snow (rather than ice). Standard synthetic plates, used typically in road construction and sized 1 x 2m, were positioned on the snow in front of the earthmover to provide a skid-free foundation for the chain drives. At a minimum 3 plates are needed to be able to repeatedly shift the plate left behind the earthmover to its front. With 5 plates and enough helpers the earthmover can proceed continuously without a stop, see Fig. 3.1.1.7.



Fig. 3.1.1.7: The earthmover drives on plates to the drill site. The plates are necessary if the ice floes are covered with high and soft snow.

Drilling operation

The drill has a diameter of 90 cm. A total of 4 holes need to be drilled side by side to create an opening large enough to ensure a safe diving operation. Deployment of ROV and recovery of instruments might be achieved with 2 holes. The drill can be extended by meter-long segments, allowing drilling ice thicknesses up to 3 meters. However, with the lifting cranes height remaining limited, the ice slush (Fig. 3.1.1.8) near the bottom of the drill well cannot be lifted out of the drilling hole requiring an alternative solution, possibly by pumps. In addition the assembly of the drill and its extension segments too long and proved rather complicate.



Fig. 3.1.1.8: Drilling a 90 cm diameter hole. Larger holes need to be created by overlapping several holes.

Tripod, rope guidance and portable capstan:

Raising the tripod and assembling the rope guidance and capstan (Fig. 3.1.1.9) takes about 1 – 2 hours. Five people were needed for this job.



Fig. 3.1.1.9: Left: The tripod (test set-up, ultimately to be placed over the hole for lifting heavy instruments). The area covered by black plates (2 x 2 m) indicating the approximate size of the hole. Right: The rope-guidance at the edge of the hole for the recovery of the mooring rope. Pulling out the rope is supported by the portable capstan (behind the rope-guidance).

RAFOS source calibration

During calibration runs, all but two sources performed sweeps as scheduled. Two electronics did not transmit all sweeps or truncated sweeps early, requiring their replacement with new electronics. Table 3.1.1.15 lists details on the calibration process.

During calibration at 200 m depth, the amplitude of the RAFOS signal from the new sound sources exceeded that of the ship noise, both in spectral as well as in terms of broad band levels as recorded by the iCListen (samplingrate: 4 kHz) suspended below the source.

Generally, with increasing resonance frequencies (while approaching the target frequency), peak amplitudes increased, confirming the desired resonance behaviour.

Shallow water conditions, however, may have interfered with the determination of the resonance frequency. While it was planned to conduct the final measurement of each sound source in deep water, due to the discontinuing of the cruise and the short time remaining, this was not possible. For sound sources calibrated in shallow waters (see Table 3.1.1.15) it is hence advisable to check the final resonance frequency measurements prior to their deployment during the next expedition.

Argo floats

Unfortunately, none of the Optimare Nemo floats transmitted any data (so far as of June 2015). When this problem became apparent while still on board on the way back to Cape Town, additional test were performed, revealing that the floats performed the full mission, but aborted communications via Iridium only few seconds after they had attempted to establish satellite communication. This problem reproducibly occurred when the parameter “Transmission Time”, a time-out defining the maximum period a float would be transmitting data when uploading multiple profiles, was set to 720 min (rather than 90 min when the system works fine), even though the valid parameter range is reported as 5 min up to “mission_cycle_time” (4,320 min (3 days) and 14,400 min (10 days) in this case) in the instruments manual (160 6 01 00 000). So far, the manufacturer did not respond to our questions regarding the detailed origin of this behaviour. While the floats thus appear to conduct their mission as intended, they appear incapable of transmitting the data they collected, and hence must be considered lost for all practical terms.

Tab. 3.1.1.15: Calibration runs by serial number of sound sources with date of measurement and resulting resonance frequency.

Nr	Device	tuning electronics	Measurement 1 start length		Measurement 2 after 1st cut		Measurement 3 after final cut	
			Date	fres [Hz]	Date	fres [Hz]	Date	fres [Hz]
1	D0043	Ei0049	09.01.2015 ²⁾	237,4	10.01.2015 ²⁾	253,4	--	--
2	D0045	Ei0049 / Ei0064	31.12.2014 ^{1,3)} 07.01.2015 ²⁾	244,8	09.01.2015 ²⁾	249,8	10.01.2015 ²⁾	261,2
3	D0047	Ei0047	13.12.2014 ¹⁾	238,2	14.12.2014 ¹⁾	253	20.12.2014 ¹⁾	260,8
4	D0048	Ei0064	13.12.2014 ¹⁾	242,1	14.12.2014 ^{1,3)} 20.12.2014 ^{1,3)} 31.12.2015 ²⁾ 01.01.2015 ²⁾	252	07.01.2015 ²⁾	260,2
5	D0049	Ei0049 / Ei0064	31.12.2014 ²⁾	232,5	01.01.2015 ²⁾	244,2	05.01.2014 ^{2);} 07.01.2015 ²⁾	260,4
6	D0050	Ei0049 / Ei0064	07.01.2015 ²⁾	239,8	09.01.2015 ²⁾	252,4	10.01.2015 ²⁾	261,2
7	D0017	Ei0035	15.12.2014 ¹⁾	-- ³⁾	-	-	-	-
8	D0018	Ei0038	15.12.2015 ¹⁾	262,2	-	-	-	-
9	D0024	Ei0033	01.01.2015 ²⁾	260,2	-	-	-	-

1) deepwater tuning, 2) shallow water tuning (waterdepth <400m), 3) failure of electronics.

Preliminary scientific results

CTD Observations

The temperature section along the Greenwich Meridian (Fig. 3.1.1.10) displays an overall thermal structure resembling that of earlier cruises. However, a warming of the deep water masses, continuing the general trend as documented in this long term time series for some 20 plus years is revealed in direct comparisons.

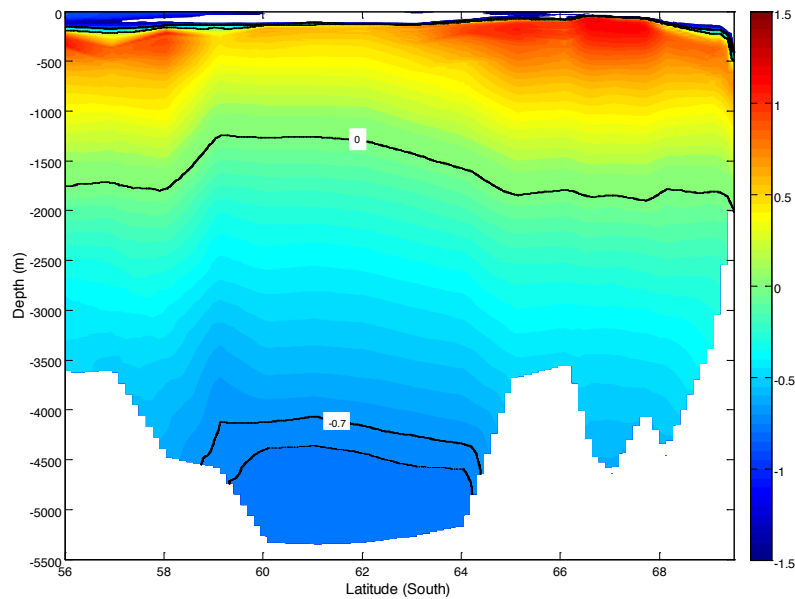


Fig. 3.1.1.10: Temperature section along the Greenwich Meridian

The hourly time series of CTD profiles close to the shelf ice edge (Fig. 3.1.1.11) shows a clear tidal cycle in the hydrographic structure.

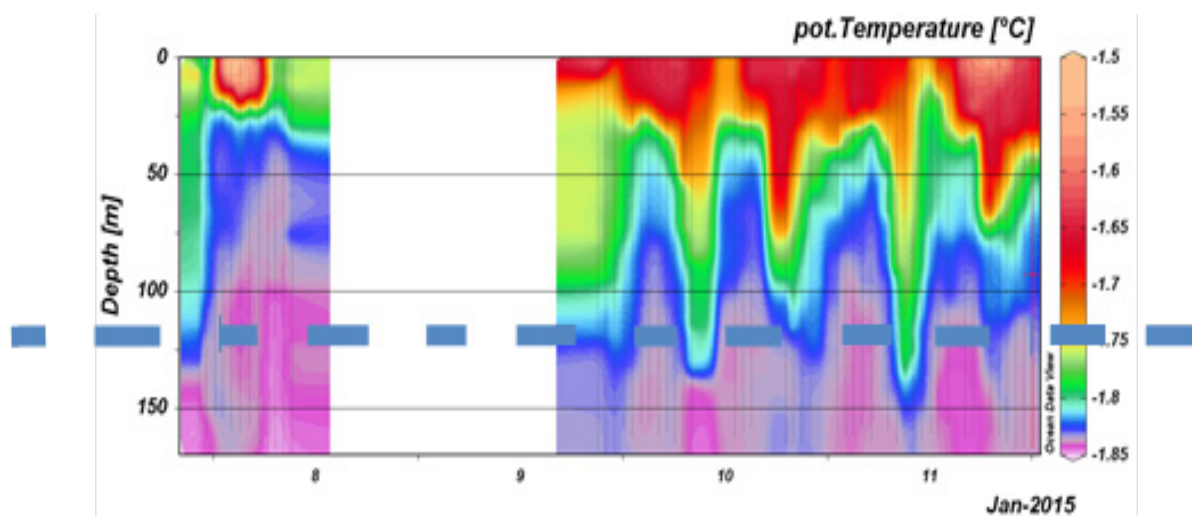


Fig. 3.1.1.11: Contour plot of the CTD profiles over time. The period of the low tide sea level are overlaid as dashed blue line.

Data management

The final records from moored instruments (CTD-recorders and current meters) will be processed after post-expedition calibrations were finished. All data will be stored and available through the PANGAEA data base. P.I.: Olaf Boebel and Gerd Rohardt.

The final processing of CTD-data will be conducted after post-expedition calibrations are finished. All data will be stored and available through the PANGAEA data base. AWI. P.I.: Gerd Rohardt

References

Boebel O (ed) (2013) The Expedition of the Research Vessel "Polarstern" to the Antarctic in 2012/13 (ANT-XXIX/2), hdl:10013/epic.40136.

3.1.2 Biogeochemical Argo-type floats for SOCCOM (Southern Ocean Carbon and Climate Observations and Modelling)

Daniel Schuller¹, Hannah Zanowski⁸

not on board: Lynne Talley², Steve Riser³, Andrew Dickson², Kenneth Johnson⁴, Emmanuel Boss⁵, Richard A. Feely⁶, Lauren Juranek⁷, Jorge Sarmiento⁸, Robert Key⁸

¹SIO-ODF

²SIO

³U Washington

⁴MBARI

⁵U Maine

⁶NOAA/PMEL

⁷OSU

⁸Princeton University

Grant No: AWI-PS89_06

Funding: NSF Polar Programs PLR-1425989 and NASA NNX14AP49G

Objectives

The Southern Ocean surrounding Antarctica is the primary window through which the intermediate, deep, and bottom waters of the ocean interact with the surface and thus the atmosphere. In the past 20 years, observational analyses and model simulations have transformed understanding of the Southern Ocean, suggesting that the ocean south of 30°S, occupying just 30 % of the total surface ocean area, has a profound influence on the Earth's climate and ecosystems. Prior results suggest that:

- the Southern Ocean accounts for up to half of the annual oceanic uptake of anthropogenic carbon dioxide from the atmosphere;
- vertical exchange in the Southern Ocean supplies nutrients that fertilize up to three-quarters of the biological production in the global ocean north of 30°S;
- the Southern Ocean accounts for about 75 % ± 22 % of the excess heat that is transferred from the atmosphere into the ocean each year; and
- Southern Ocean winds and buoyancy fluxes are the principal source of energy for driving the global large-scale deep meridional overturning circulation.

Model studies also project that changes in the Southern Ocean will have profound influence on future climate trends, with corresponding alteration of the ocean carbon cycle, heat uptake, and ecosystems. Projections include:

- due to ocean acidification, the Southern Ocean south of ~60°S will become undersaturated with respect to aragonite (a form of calcium carbonate) by ~2030 with a potentially large impact on calcifying organisms and Antarctic ecosystems; and
- the vertical exchange of deep and surface waters may either increase as winds over the Southern Ocean increase, or decrease as higher rainfall results in more stratification. More vertical exchange would be expected to result in more anthropogenic carbon uptake from the atmosphere, but less storage of carbon through biological cycling, while its impact on heat uptake depends on whether it brings anomalously warm or cold waters to the ocean surface.

The SOCCOM (Southern Ocean Carbon and Climate Observations and Modelling) project is implementing sustained observations of the carbon cycle, together with mesoscale eddying models linked to the observations. 180 to 200 autonomous profiling floats with biogeochemical

sensors (oxygen, nitrate, pH and optical sensors in addition to temperature/salinity) and sea-ice avoidance software are being deployed throughout the Southern Ocean over a period of six years. These will extend current seasonally limited observations of biogeochemical properties into nearly continuous coverage in time, with horizontal spatial coverage over the entire Southern Ocean and vertical coverage to 2,000 m. These float deployments must take place from research ships with CTD/rosette sampling in order to collect water samples (to be analyzed for oxygen, nutrients, pH, alkalinity, HPLC, POC) for float profile calibration, and to collect *in-situ* fluorescence and transmissometer profiles, also for float calibration. The first set of 6 prototype floats with this configuration of biogeochemical sensors was deployed in the Ross Sea and southern South Pacific in March-April, 2014 from GO-SHIP section P16S on the *RV Nathaniel B. Palmer*; the floats are operating well, with data reported in near real-time and publicly available from <http://soccom.princeton.edu/soccomviz.php>. The pH sensor technology, which was developed recently, is proving to be very robust. The T/S data are part of the Argo float data set.

All SOCCOM floats and calibration measurements, with the exception of the optical measurements, are supported by the U.S. National Science Foundation Polar Programs. Optical measurements instrumentation on the floats and HPLC/POC calibrations are supported by U.S. NASA.

The 12 floats deployed from *Polarstern* PS89 are the first large-scale SOCCOM deployment, and are the first of our international collaborations. These floats will contribute to the international Southern Ocean Observing System (SOOS), and the Argo database.

Work at sea

Profiling floats

Twelve SOCCOM floats were deployed according to Table 3.1.2.1 and Fig. 3.1.2.1. All of these Argo-equivalent floats were equipped with state-of-the-art biogeochemical instrumentation. All but two have sea ice-avoidance software. All but three have pH sensors. Eight were Apex floats built at U. Washington from components purchased from Teledyne/Webb. Four were Navis floats from Sea-Bird Electronics (SBE), and are prototypes for SBE's new biogeochemical float programme. Details of each float's capabilities are provided in Table 3.1.2.2. PS89 deployments were carried out by Dan Schuller (SIO Oceanographic Data Facility) and Hannah Zanowski (Princeton U. graduate student), at the conclusion of the CTD/rosette cast.

As of 28 January, 2015, all 12 floats had been deployed, and were reporting good profiles, with the exceptions of 9,125 and 9,260 which have not yet reported, and of the pH sensor on float 0508, which failed on deployment. Several have already encountered sea ice but then successfully re-emerged, with resulting programmed delays in profile reporting. The first 8 floats were deployed along the Greenwich meridian, with locations chosen to sample each major oceanographic regime, based on previous hydrographic sections, and also tracer release and particle release numerical experiments in the Southern Ocean State Estimate (SOSE at SIO; M. Mazloff and J. Wang) and in the Hycom model (RSMAS U. Miami; I. Kamenkovich). The last 4 floats were intended for deployment across the Weddell Sea, but were released at the specified locations when it was decided that *Polarstern* would return directly to Cape Town. The first two of this group were released far to the south hoping that they would travel westward into the Weddell Sea. The third was released to increase density of the array and to supplement this region with a pH sensor. The fourth was released at the latitude of float 0508 to provide pH measurements in the polar frontal zone.

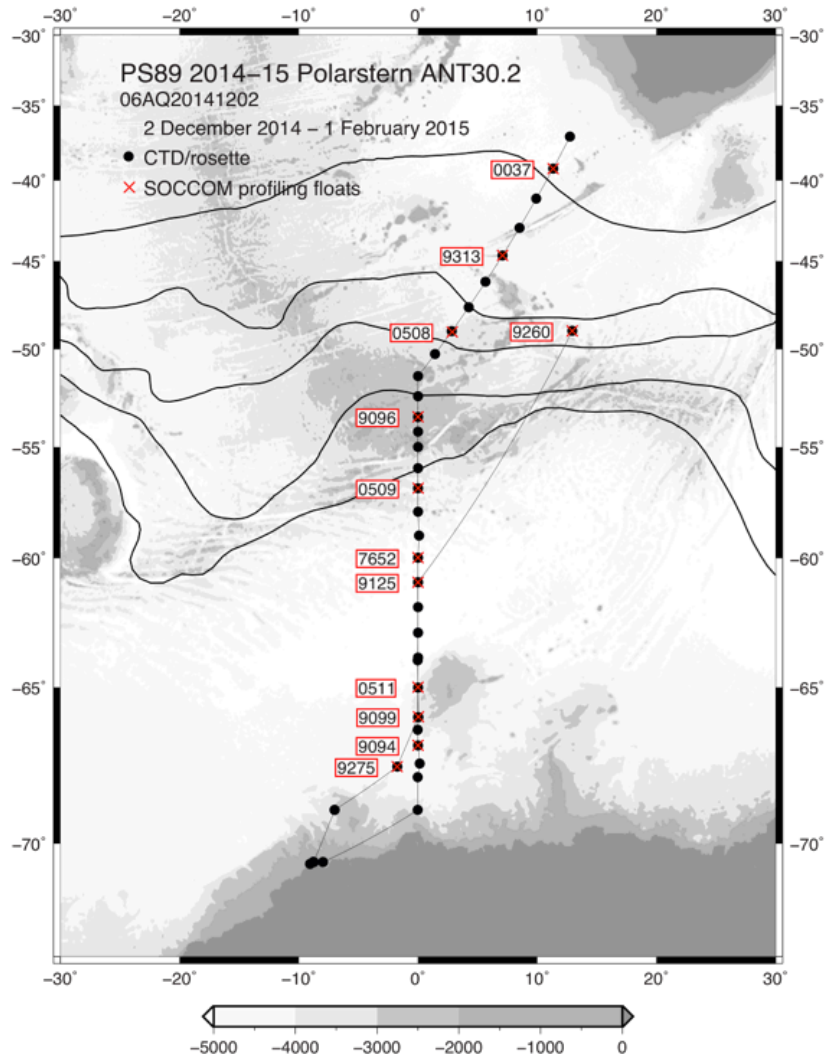


Fig. 3.1.2.1: SOCCOM float deployments from Polarstern PS89 (red x's) with PS89 CTD stations (black dots) (2 December 2014 – 1 February 2015). Light curves are the standard Orsi fronts (subtropical, subantarctic, polar and southern boundary, from north to south).

Tab. 3.1.2.1: SOCCOM float deployment details

Float ID	Latitude Longitude	Sensors	Station #	Deployment date	Deployment time
0037 Navis	39° 13.9' S 11° 20.3' E	ONF	2-1	5-12-2014	0350Z
9313 Apex	44° 39.5' S 07° 05.6' E	ONFp	5-1	7-12-2014	0554Z
0508 Navis	49° 03.2' S 02° 52.1' E	IONFp*	8-1	9-12-2014	0100Z
9096 Apex	53° 31.0' S 00° 00.2' E	IONFp	12-2	10-12-2014	2234Z

Float ID	Latitude Longitude	Sensors	Station #	Deployment date	Deployment time
0509 Navis	56° 55.8' S 00° 00.9' E	IONFp	16-1	12-12-2014	1100Z
7652 Apex	59° 59.0' S 00° 00.0' E	IONF	21-1	14-12-2014	0505Z
0511 Navis	64° 59.7' S 00° 00.1' E	IONFp	28-1	18-12-2014	0255Z
9094 Apex	66° 58.7' S 00° 00.6' W	IONFp	31-1	20-12-2014	0246Z
9275 Apex	67° 40.0' S 01° 45.2' W	IONFp	73-1	18-1-2015	0611Z
9099 Apex	66° 01.5' S 00° 02.0' E	IONFp	78-1	19-1-2015	0739Z
9125 Apex	61° 00.2' S 00° 00.1' W	IONFp	81-1	21-1-2015	1436Z
9260 Apex	49° 00.1' S 12° 56.1' E	IONFp	82-2	27-1-2015	1708Z

I = ice enabled; O = oxygen sensor; N = nitrate sensor; F = FLbb; p = pH
 *pH sensor failed on deployment

Table 3.1.2.2: SOCCOM float specifications

Float Number	Typ ⁽¹⁾	max. depth	O ₂ ⁽²⁾	NO ₃ ⁽³⁾	pH	optics ⁽⁴⁾	ice capable ⁽⁵⁾
7652	APEX	1750	✓	✓	✓	✓	✓
9094	APEX	1750	✓	✓	✓	✓	✓
9096	APEX	1750	✓	✓	✓	✓	✓
9099	APEX	1750	✓	✓	✓	✓	✓
9125	APEX	1750	✓	✓	✓	✓	✓
9260	APEX	1750	✓	✓	✓	✓	✓
9275	APEX	1750	✓	✓	✓	✓	✓
9313	APEX	1750	✓	✓	✓	✓	
0037	Navis	2000	✓	✓		✓	
0509	Navis	2000	✓	✓	✓	✓	✓
0511	Navis	2000	✓	✓	✓	✓	✓
0508	Navis	2000	✓	✓	✓	✓	✓

Notes:

1. APEX denotes floats built at UW from components purchased from Teledyne/Webb; Navis denotes floats purchased by UW in ready-to-deploy condition from SBE.
2. O₂ sensor on APEX floats is Aanderaa 4330; on Navis floats it is SBE-63.
3. NO₃ sensor on APEX floats is MBARI/ISUS; on Navis floats it is Satlantic/SUNA.

3.1 Oceanography

4. OPTICS denotes WetLabs FLBB fluorometer and backscatter capability on APEX floats; on Navis floats, the optical sensor is ECO-MCOMC and includes a CDOM fluorometer in addition to chlorophyll fluorometer and backscattering.
5. Ice capability is from field-tested software developed at UW on APEX floats; on Navis floats it is from contributed software developed at UW but being tested in the field for the first time from this *Polarstern* set of float deployments.

CTD/Rosette Sampling

CTD casts were completed at each SOCCOM float deployment location for a total of 12 profiles. Full water column bottle samples were taken by SIO-ODF for pH, alkalinity, nutrients, HPLC and POC at each station. ULPGC sampled and analysed water samples for oxygen and DIC, while AWI sampled and analysed water samples for salinity at these locations. As SOCCOM's reciprocal contribution to the overall PS89 cruise, SIO-ODF collected and analysed nutrient samples on board on all of the CTD/rosette stations (NSF funding). pH and alkalinity samples are being shipped to Andrew Dickson's laboratory at SIO (NSF funding). HPLC and POC samples are being shipped to Emmanuel Boss at U. Maine (NASA funding).

Nutrients

Summary

1130 samples from SOCCOM and other CTD casts were analysed for nutrients. The cruise started with new pump tubes and they were changed once during the cruise, after *station 36-1*. Two sets of Primary/Secondary standards were made up over the course of the cruise. The cadmium column efficiency was checked periodically and was greater than 98 %.

Equipment and Techniques

Nutrient analyses (phosphate, silicate, nitrate+nitrite, and nitrite) were performed on a Seal Analytical continuous-flow AutoAnalyzer 3 (AA3). The methods used are described by Gordon et al (1992) Hager et al. (1968), and Atlas et al. (1971). Details of modification of analytical methods used in this cruise are also compatible with the methods described in the nutrient section of the GO-SHIP repeat hydrography manual (Hydes et al., 2010)

Nitrate/Nitrite Analysis

A modification of the Armstrong et al. (1967) procedure was used for the analysis of nitrate and nitrite. For nitrate analysis, a seawater sample was passed through a cadmium column where the nitrate was reduced to nitrite. This nitrite was then diazotized with sulfanilamide and coupled with N-(1-naphthyl)-ethylenediamine to form a red dye. The sample was then passed through a 10mm flowcell and absorbance measured at 540 nm. The procedure was the same for the nitrite analysis but without the cadmium column.

Reagents

Sulfanilamide

Dissolve 10g sulfanilamide in 1.2N HCl and bring to 1 liter volume. Add 2 drops of 40 % surfynol 465/485 surfactant.

Store at room temperature in a dark poly bottle.

Note: 40 % Surfynol 465/485 is 20 % 465 plus 20 % 485 in DIW.

N-(1-Naphthyl)-ethylenediamine dihydrochloride (N-1-N)

Dissolve 1g N-1-N in DIW, bring to 1 liter volume. Add 2 drops 40 % surfynol 465/485 surfactant.

Store at room temperature in a dark poly bottle. Discard if the solution turns dark reddish brown.

Imidazole Buffer

Dissolve 13.6g imidazole in ~3.8 liters DIW. Stir for at least 30 minutes to completely dissolve. Add 60 ml of CuSO₄ + NH₄Cl mix (see below). Add 4 drops 40 % Surfynol 465/485 surfactant. Let sit overnight before proceeding

Using a calibrated pH meter, adjust to pH of 7.83-7.85 with 10 % (1.2N) HCl (about 10 ml of acid, depending on exact strength). Bring final solution to 4L with DIW.

Store at room temperature.

NH₄Cl + CuSO₄ mix:

Dissolve 2g cupric sulfate in DIW, bring to 100 ml volume (2 %)

Dissolve 250 g ammonium chloride in DIW, bring to 1 liter volume.

Add 5 ml of 2 % CuSO₄ solution to this NH₄Cl stock. This should last many months.

Phosphate Analysis

Ortho-Phosphate was analyzed using a modification of the Bernhardt and Wilhelms (1967) method. Acidified ammonium molybdate was added to a seawater sample to produce phosphomolybdic acid, which was then reduced to phosphomolybdous acid (a blue compound) following the addition of dihydrazine sulfate. The sample was passed through a 10 mm flowcell and absorbance measured at 820 nm (880 nm after station 10, see section on analytical problems for details).

Reagents

Ammonium Molybdate

H₂SO₄ sol'n:

Pour 420 ml of DIW into a 2 liter Erlenmeyer flask or beaker, place this flask or beaker into an ice bath. SLOWLY add 330 ml of conc H₂SO₄.

This solution gets VERY HOT!! Cool in the ice bath. Make up as much as necessary in the above proportions.

Dissolve 27 g ammonium molybdate in 250 ml of DIW. Bring to 1 liter volume with the cooled sulfuric acid sol'n. Add 3 drops of 15 % DDS surfactant. Store in a dark poly bottle.

Dihydrazine Sulfate

Dissolve 6.4g dihydrazine sulfate in DIW, bring to 1 liter volume and refrigerate.

Silicate Analysis

Silicate was analyzed using the basic method of Armstrong et al. (1967). Acidified ammonium molybdate was added to a seawater sample to produce silicomolybdic acid which was then reduced to silicomolybdous acid (a blue compound) following the addition of stannous chloride. The sample was passed through a 10mm flowcell and measured at 660 nm.

Reagents

Tartaric Acid

Dissolve 200g tartaric acid in DW and bring to 1 liter volume. Store at room temperature in a poly bottle.

Ammonium Molybdate

Dissolve 10.8 g Ammonium Molybdate Tetrahydrate in 1,000 ml dilute H₂SO₄*.

*(Dilute H₂SO₄ = 2.8 ml conc H₂SO₄ or 6.4 ml of H₂SO₄ diluted for PO₄ moly per liter DW)

3.1 Oceanography

(dissolve powder, then add H_2SO_4)

Add 3-5 drops 15 % SDS surfactant per liter of solution.

Stannous Chloride

stock: (as needed)

Dissolve 40g of stannous chloride in 100 ml 5N HCl. Refrigerate in a poly bottle.

NOTE:

Minimize oxygen introduction by swirling rather than shaking the solution. Discard if a white solution (oxychloride) forms.

working: (every 24 hours)

Bring 5 ml of stannous chloride stock to 200 ml final volume with 1.2N HCl. Make up daily - refrigerate when not in use in a dark poly bottle.

Sampling

Nutrient samples were drawn into 30 mL polypropylene screw-capped centrifuge tubes.

The tubes and caps were cleaned with 10 % HCl and rinsed 3 times with sample before filling. Samples were analyzed within 12 hours after sample collection, allowing sufficient time for all samples to reach room temperature. The centrifuge tubes fit directly onto the sampler.

Data collection and processing

Data collection and processing was done with the software (ACCE ver 6.07) provided with the instrument from Seal Analytical. After each run, the charts were reviewed for any problems during the run, any blank was subtracted, and final concentrations (micro moles/liter) were calculated, based on a linear curve fit. Once the run was reviewed and concentrations calculated a text file was created. That text file was reviewed for possible problems and then converted to another text file with only sample identifiers and nutrient concentrations for merging with other bottle data.

Standards and Glassware calibration

Primary standards for silicate (Na_2SiF_6), nitrate (KNO_3), nitrite (NaNO_2), and phosphate (KH_2PO_4) were obtained from Johnson Matthey Chemical Co. and/or Fisher Scientific. The supplier reports purities of >98 %, 99.999 %, 97 %, and 99.999 respectively.

All glass volumetric flasks and pipettes were gravimetrically calibrated prior to the cruise. The primary standards were dried and weighed out to 0.1mg prior to the cruise. The exact weight was noted for future reference. When primary standards were made, the flask volume at 20°C, the weight of the powder, and the temperature of the solution were used to buoyancy-correct the weight, calculate the exact concentration of the solution, and determine how much of the primary was needed for the desired concentrations of secondary standard. Primary and secondary standards were made up twice during the cruise. The new standards were compared to the old before use.

All the reagent solutions, primary and secondary standards were made with fresh distilled deionized water (DIW).

Standardizations were performed at the beginning of each group of analyses with working standards prepared prior to each run from a secondary. Working standards were made up in low nutrient seawater (LNSW). LNSW was collected off shore of coastal California and treated in the lab. The water was first filtered through a 0.45 micron filter then re-circulated for ~8 hours through a 0.2 micron filter, passed a UV lamp and through a second 0.2 micron filter. The actual concentration of nutrients in this water was empirically determined during the standardization calculations.

The concentrations (micro-mole per liter) of the working standards used were:

	uM	uM	uM	uM
	N+N	PO4	SiO3	NO2
0)	0.0	0.0	0.0	0.0
1)	15.50	1.2	60	0.50
2)	31.00	2.4	120	1.00
3)	46.50	3.6	180	1.50

Analytical Problems

No major analytical problems were noted. No samples were lost.

Oxygen

Although ULPGC group was responsible for the determination of dissolved oxygen, the SIO-ODF system was made available in order to compare methodologies. The ULPGC system is a potentiometric endpoint detection system whereas the SIO-ODF system uses a photometric endpoint detection based on the absorption of 365 nm wavelength UV light. Potassium iodate standards were swapped between the two groups and used to confirm the calibration concentration of the thiosulfate titrating solution. The results from both groups determined the concentration of thiosulfate to an error on the order of 0.03 %, well within the precision of the instruments. On three stations (40, 42, and 66) dissolved oxygen was sampled and analyzed by both groups, each using their own calibrated glass bottles and thiosulfate titration solution. The results are plotted in section 3.1.3, Fig. 3.1.3.3. The results of the three stations indicate a standard deviation of $\pm 0.43 \mu\text{mol kg}^{-1}$, an error determination of less than 0.11 %, well within the precision of the instruments. These results indicate both groups prepared their potassium iodate standard solution satisfactorily and that both systems are reliable for at-sea determination of dissolved oxygen concentration. Dissolved oxygen values reported for all stations, including SOCCOM stations, are from the ULPGC data.

Alkalinity/pH

335 samples from SOCCOM CTD stations were taken for alkalinity/pH. Approximately 10 % of samples were duplicates. Samples were drawn from the Niskin bottles, preserved with mercury (II) chloride and packed for shipping via air freight back to SIO (Andrew Dickson).

HPLC and POC

36 near-surface samples from SOCCOM CTD stations were taken for HPLC analysis. 1-2 L of sample was filtered in the dark through glass fiber filters. Filters were immediately stored in aluminum foil packages in a Dewar of liquid nitrogen. 36 near-surface samples from SOCCOM CTD stations were also taken for POC analysis. 1-2 L of sample was filtered in the dark through pre-combusted glass fiber filters. Filters were immediately stored in pre-combusted aluminum foil packages in a Dewar of liquid nitrogen. At each station one set each of HPLC and POC samples was a duplicate. Samples were packed for shipping (dry shipper) via air freight back to University of Maine (Emmanuel Boss).

Salinity

Salinity samples were collected at all depths from the SOCCOM CTD stations. Samples were analyzed by H. Zanowski using AWI's shipboard OPS system.

Preliminary (expected) results

All floats reporting back to shore successfully. pH sensor malfunctioned on float 0508.

Data management

SOCCOM will make all ODF nutrient analyses available immediately after collection and onboard quality control, for merging with the other data sets collected on the ship, whether they are collected at float locations or at other stations. We will make all pH/alkalinity data sets available after they are analyzed at SIO.

Rosette sample data for SOCCOM float calibration is being assembled and merged by Robert Key at Princeton U. CTD and fluorometer/transmissometer profile data for SOCCOM float calibration is being assembled by Sharon Escher at SIO.

For profiles at float locations, including all discrete rosette samples and CTD/fluorometer profiles: it is important that these data be available to us for calibration of the floats, in preliminary form and then later with quality control/calibration. SOCCOM can assist with discrete data merging. It would be highly preferable that the data from these stations be publicly available as soon as possible. SOCCOM would like to post these data on its own website as part of the float programme (R. Key).

For datasets collected at other stations, where floats are not deployed, but where SIO ODF has performed nutrient analyses, it would be advantageous to us to have access to the profile data for quality control. For stations with full carbon measurements, it would be highly advantageous to collaborate with ULPGC and AWI to extend the SOCCOM empirical algorithm for carbon profiles based on the float data; the algorithm will be developed by SOCCOM (L. Juranek, Oregon State University; R. Feely, NOAA/PMEL). SOCCOM can assist with discrete data merging and quality control. Data release policy will be according to the Chief Scientist (O. Boebel).

References

- Armstrong FAJ, Stearns CA & Strickland JDH (1967) The measurement of upwelling and subsequent biological processes by means of the Technicon Autoanalyzer and associated equipment. *Deep-Sea Research*, 14, pp.381-389.
- Atlas EL, Hager SW, Gordon LI & Park PK (1971) A Practical Manual for Use of the Technicon AutoAnalyzer in Seawater Nutrient Analyses Revised. Technical Report 215, Reference 71-22, p.49, Oregon State University, Department of Oceanography.
- Bernhardt H & Wilhelms A (1967) The continuous determination of low level iron, soluble phosphate and total phosphate with the AutoAnalyzer. *Technicon Symposia*, I, pp.385-389.
- Gordon LI, Jennings JC, Ross AA & Krest JM (1992) A suggested Protocol for Continuous Flow Automated Analysis of Seawater Nutrients in the WOCE Hydrographic Program and the Joint Global Ocean Fluxes Study. Grp. Tech Rpt 92-1, OSU College of Oceanography Descr. Chem Oc.
- Hager SW, Atlas EL, Gordon LI, Mantyla AW & Park PK (1972) A comparison at sea of manual and autoanalyzer analyses of phosphate, nitrate, and silicate *Limnology and Oceanography*, 17, pp.931-937.
- Hydes DJ, Aoyama M, Aminot A, Bakker K, Becker S, Coverly S, Daniel A, Dickson AG, Grosso O, Kerouel R, Ooijen J van, Sato K, Tanhua T, Woodward EMS & Zhang JZ (2010). Determination of Dissolved Nutrients (N, P, Si) in Seawater with High Precision and Inter-Comparability Using Gas-Segmented Continuous Flow Analysers, In: *GO-SHIP Repeat Hydrography Manual: A Collection of Expert Reports and Guidelines*. IOCCP Report No. 14, ICPO Publication Series No 134.

3.1.3 The carbon system of the Southern Meridian GoodHope Section

Melchor Gonzalez-Davila¹, Magdalena Santana-Casiano¹, Eric Wurz²

¹IOCAG
²AWI

Grant No: AWI-PS89_05

Objectives

The role of the Southern Ocean (SO) remains a key issue in our understanding of the global carbon cycle and how it will respond under predicting future climate change. Recent studies have suggested that SO is uptaking around 30 to 40 % of the anthropogenic excess CO₂ (C_{ant}) followed also by an important and efficient transport of this C_{ant} by intermediate-deep water formation in this area. The uptake and accumulation of C_{ant} is mainly controlled by the ocean circulation and water mass mixing, in particular the deepest penetrations associated with convergence zones. This is why the Southern Ocean is one of the most conspicuous places of the global ocean. The formation of intermediate, deep and bottom water masses together with the upwelling of old waters take place through complex dynamical processes that will be one of the main objectives of the HAFOS project and this research cruise. North of the polar Front (around 51° S) the deep winter ventilation that produces the formation of Sub-Antarctic Mode Water (SAMW) and Antarctic Intermediate Water (AIW) inject C_{ant} down to more than 1,000 m depth. To the south, the intrusion of C_{ant} can reach deep and bottom water below 2,000 m during the complex formation of Antarctic Bottom Water (AABW). This cruise has provided a new set of carbon dioxide data for this area that will increase our knowledge of the amount of anthropogenic carbon being incorporated by the different water masses and will be compared with previous results for this area in order to compute anthropogenic carbon inventory, the concentration in deep and bottom layers and its storage and evolution. The main objectives of this cruise have been, then:

- Contribute to the maintenance of AWI's GoodHope and Weddell Sea sections.
- Analyze of the data and compare them with the previous Bonus GoodHope cruise (Meridian section). Special focus on the changes, shortening of the calcium carbonate saturation states and in the variation of the anthropogenic carbon concentration and inventory.
- Analysis of the long-term trends and inter-annual variability.
- Collaborate with other research groups involved in the cruise.

In order to achieve these objectives, the Marine Chemistry group (QUIMA) from the Instituto de Oceanografía y Cambio Global (IOCAG) at the Universidad de Las Palmas de Gran Canaria (ULPGC) and one AWI-student assigned to our group have measured at all locations for each CTD cast and along the water column three carbon dioxide parameters: the pH in total scale, the total alkalinity (A_T) and the total dissolved inorganic carbon concentration (C_T), making the value traceable to the highest standards by using Certified Reference Material for CO₂ analyzes. Moreover we have included a continuous surface monitoring of partial pressure of CO₂ in order to test its reliability compared with the underwater pCO₂ systems already installed in the *Polarstern*. During the cruise, the QUIMA group analyzed the concentration of dissolved oxygen in each CTD samples by using a potentiometric WINKLER method.

Work at sea

Three variables of the carbonate system were measured along the water column on board of the *Polarstern* cruise in order to achieve the highest level of data quality and resolution, to study the consistency of the variables and to account for the objectives above proposed.

3.1. Oceanography

Moreover, a continuous underway xCO₂ sensor PRO-CO₂TM was added to measure the partial pressure of CO₂ in the surface water following the ship trajectory during the first three weeks of the cruise. The QUIMA group of ULPGC owns a coulometric determination system for total dissolved inorganic carbon, the VINDTA 3C system (MARIANDATM), and an automatic spectrophotometric pH system developed by the QUIMA group.

pH

The pH is measured in total scale ($[H^+]_T = [H^+]_F + [HSO_4^-]$, where $[H^+]_F$ is the free proton concentration), pH_T at a constant temperature of 10°C. An automatized system base on the spectrophotometric technique of Clayton and Byrne (1993) with the m-cresol purple as indicator is used (González-Dávila et al., 2003, Santana-Casiano et al., 2007). A new and compact device has been developed following previous one using ocean optics technology and included in a fully automatic computer controlled system that clean, sample, produce a zero and a blank reading for each sample to be analyzed. Reproducibility of the system is better than 0.002 pH units (after 11 analyses).

Total Alkalinity and Dissolved Inorganic Carbon

A VINDTA 3C system (Mintrop et al., 2000) (www.MARIANDA.com), is used for the titration of the potentiometric total alkalinity and total dissolved inorganic carbon with coulometer determination after phosphoric acid addition, with a system precision of ± 1.0 μmol kg⁻¹. For alkalinity determination, 100 ml of seawater is titrated by adding HCl to the seawater past the carbonic acid end point. For the C_T determination, a calibrated pipette of 20 ml of seawater is filled automatically by pumping the seawater that it is injected in a scrubber containing 20 drops of phosphoric acid (10 % v/v) and the CO₂ released is trapped in a cathodic solution that is titrated coulombimetrically until photometric end point. Each analysis takes about 20 minutes and a titration cell usually is valid for around 60 samples. The titration of CRMs, batch #137, for both parameters is used to test the performance of the equipment after the preparation of each titration cell.

Calcite and aragonite saturation states

The degree of saturation state of seawater with respect to calcite and aragonite was calculated as the ion product of the concentration of calcium and carbonate ions, at the *in-situ* temperature, salinity and pressure divided by the stoichiometric solubility product (K_{sp}^*) for those conditions

$$\Omega_{cal} = [Ca^{2+}][CO_3^{2-}] / K_{sp,cal}^* \quad (1)$$

$$\Omega_{arg} = [Ca^{2+}][CO_3^{2-}] / K_{sp,arg}^* \quad (2)$$

where the calcium concentration is estimated from the salinity, and the carbonate ion concentration is calculated from A_T and C_T, and computed by using CO₂sys.xls v12 (Lewis and Wallace, 1998).

Dissolved oxygen concentration. The oxygen concentration was determined by using a potentiometric titration system with a MethromTM 858 system and a platinum electrode following the WOCE protocols.

Sampling procedure

500 ml glass bottles are used for the determination of both alkalinity and inorganic carbon. Two-100 ml glass bottles will be used to analyze the pH and dissolved oxygen concentration. The bottles are rinsed twice with seawater and over-filled with seawater. Samples are preserved from the light and analyzed between stations. In shallow stations and in case the samples are not possible to be analyzed for C_T in less than 5 hours after sampling, they are poisoned with $HgCl_2$. For oxygen, the bottles were over-filled whilst the temperature is measured in order to account for solubility changes due to temperature variability.

Partial pressure of carbon dioxide

A continuous xCO_2 sensor (PSI CO_2 -Pro) designed by Pro-Oceanus Systems company in Halifax, Canada was installed in a continuous clean seawater output onboard the *Polarstern* and close to the continuous underwater pCO_2 systems General Oceanic and SubCtech that continuously monitor the molar fraction of CO_2 along the trajectory of the vessel, in order to compare the systems. The General Oceanic system uses an equilibrator with a spray chamber while the SubCtech system uses a silicon membrane to determine the equilibrium CO_2 concentration. In order to maintain accuracy, the PSI detector module has an automatic zero point calibration (AZPC) that compensates for changes in optical cell performance and significant changes in environmental parameters such as gas stream temperature. An AZPC is performed each 1 hour. Accuracy provided by the company is 1 ppm and precision of 0.01 ppm.

Preliminary results

In order to achieve the highest standards of accuracy in the water column carbonate system variables and make them traceable to other cruises, a total of 25 Certified Reference Materials, CRMs, for the carbonate system variables were analyzed on board. The CRMs batch #137 was supplied by the Scripps Institution of Oceanography (SIO) Chemistry lab with certified values of 2231.59 and 2031.90 $\mu mol kg^{-1}$ for total alkalinity and total dissolved inorganic carbon concentration, respectively. Fig. 3.1.3.1 shows the results for the analyzes of the A_T as a function of the date the CRMs were analyzed with a average value of 2231.71 $\mu mol kg^{-1}$ and a standard deviation of 1.09 $\mu mol kg^{-1}$. Most of the data were inside $\pm\sigma$, with some of them also inside $\pm 2\sigma$ and no one out this range.

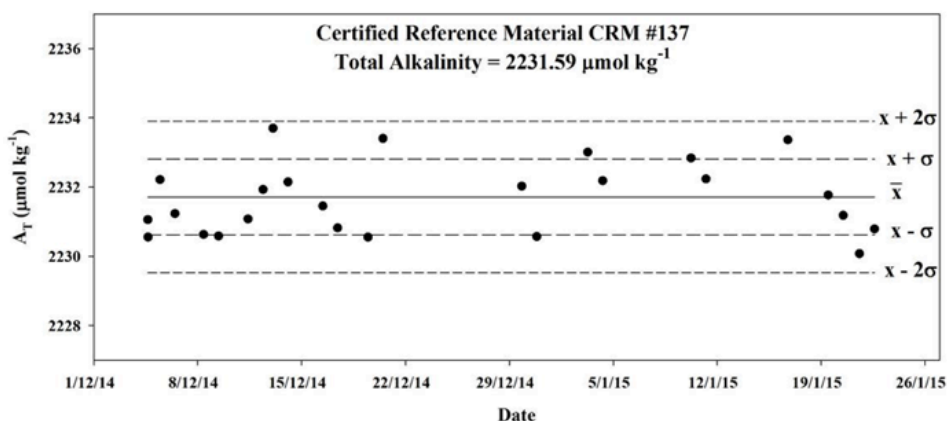


Fig. 3.1.3.1: Total alkalinity, A_T values for the 25 Certified Reference Material samples, CRMs, batch #137 analyzed during the *Polarstern* cruise PS89. The lines indicate the average value and the values at $\pm\sigma$ and $\pm 2\sigma$ standard deviation.

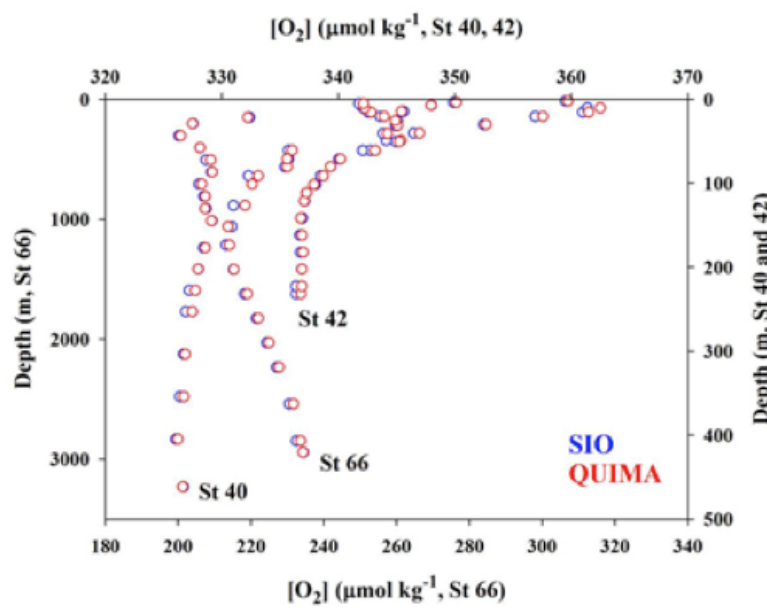


Fig. 3.1.3.3: Dissolved oxygen determination in three selected stations, St. 40, 42 and 66 determined by two titration systems with two different end-point detection probes, a potentiometric electrode (QUIMA, red circles) and a photometric detector (SIO, blue circles).

Cape Town-Greenwich Meridian

The Southern Ocean plays an important role in modulating the global climatic system by transporting and storing heat, fresh water, nutrients, and anthropogenic CO_2 (e.g., Lovenduski and Gruber, 2005). This region is predicted to be greatly influenced by global change, given that polar marine ecosystems are particularly sensitive to carbonate change (Sarmiento et al., 1998; Orr et al., 2005).

Fig. 3.1.3.4 shows the sea surface temperature and salinity determined with the continuous underwater system together with the partial pressure of the dissolved CO_2 concentration. Values for the surface saturation state of Aragonite determined in discrete samples for each CTD station is also included together with the main oceanographic fronts and domains crossed during the cruise, from north to south: (i) the subtropical domain and the northern and southern subtropical fronts (N- and S-STF), (ii) the Antarctic Circumpolar Current (ACC) domain with 3 fronts crossed, the subantarctic front (SAF), the polar front (PF) and the southern ACC front (SACCF), and (iii) the eastern part of the Weddell Sea gyre with the southern boundary (SBdy) separating this domain from the ACC.

During the PS89 cruise, the expected trend of decreasing surface temperature towards the south was observed. This temperature gradient was correlated by a decrease in $\text{pH}_{\text{T},10}$ and an increase in the surface inorganic carbon total concentration C_{T} (data not shown) together with important changes in the partial pressure of CO_2 in the frontal zones associated to both temperature changes and mixing in the shear area of the frontal zone that favor both the arrival of deeper rich CO_2 water and higher biological production that decreases the CO_2 levels.

The levels of the computed saturation state for Aragonite in the surface waters shows that south the SACCF the values of Ω_{Arag} were always below 1.5. In the southernmost zones the values were as low as 1.1. In any case, south of the SACCF the organisms which used calcium carbonate as aragonite (pteropodes) are strongly affected by these low values and their shells could be severely damaged.

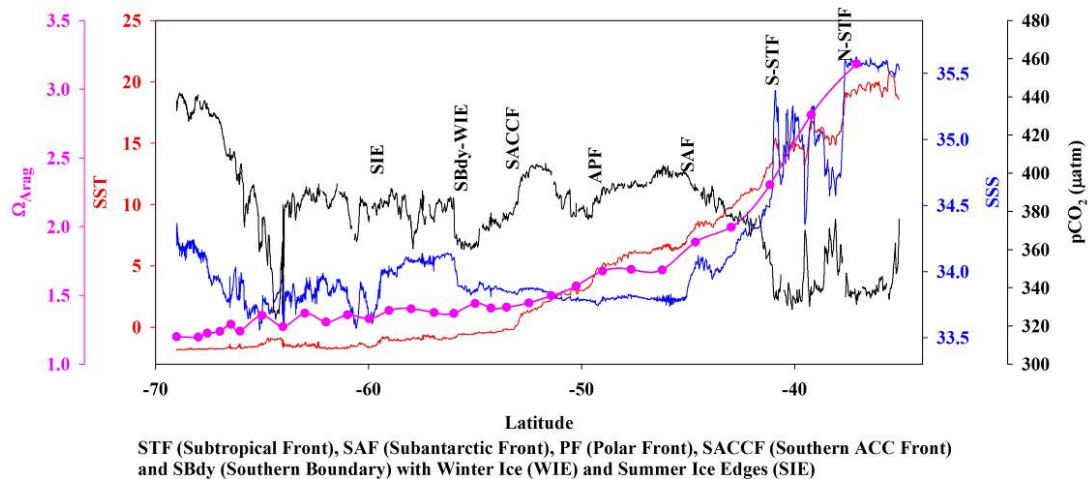


Fig. 3.1.3.4: Sea surface temperature (SST), salinity (SSS), partial pressure of CO₂ continuous determined together with values of surface Aragonite saturation state along the cruise track for samples analyzed in the upper 10 m. The figure shows the position of the major frontal zones during the PS89 (ANT-XXX/2) cruise.

A total of 30 CTD rosette with 24 bottles fired on each of them were carried out along the meridian GoodHope section during the PS89 cruise with a complete determination of the three carbonate system variables. The carbonate system data are now being treated in order to characterize completely the carbon system of the water masses, defining the buffer capacity and their sensitivity to the increase of CO₂ in the ocean. In order to predict the evolution of the carbon cycle in this sensitive area, to quantify the impact of high CO₂ on ocean chemistry and marine biology and to determine the consequences for our future climate, the carbonate properties as a function of the different water masses found in the region will be studied and discussed. Moreover the results from these cruises will be compared with those done previously, in particular with that done during the International Polar Year Bonus GoodHope cruise (González-Dávila et al., 2011) in order to study annual variability in the different carbonate indexes. Fig. 3.1.3.5, shows the values determined for the total dissolved inorganic carbon, C_T, during the PS89 cruise that will be considered in this study.

Atka Bay area

The distribution of A_T and C_T was measured at 4 Ice Stations from 1 m to 20m at 6 depths in order to calculate the saturation grade of aragonite and calcite and the possible effects in the organism living in those conditions. In collaboration with the biological group (Section 3.2.1) six bottles were sampled below the sea ice in 4 stations, station 35, station 40 cast 3 and 4 and station 46. The corresponding saturation state for aragonite is depicted in Fig. 3.1.3.6. The data show a strong variability with the lowest values in station 35, where the Ω_{Arag} reached 1.1 below 5 meters below the sea-ice and the highest in station 46, where the values were 1.6. It is also observed in station 40 an important variability in the determined values in the first 20 meters that can be consequence of tidal effects as it was considered in another experiment. The values determined for Ω_{Arag} are all of them very close to 1, clearly indicating that the organisms living in these waters and using calcium carbonate in their skeletons could be affected. These aspects together with other studies carried out by the biological group and described in Section 3.2.1. will be discussed and published in collaboration.

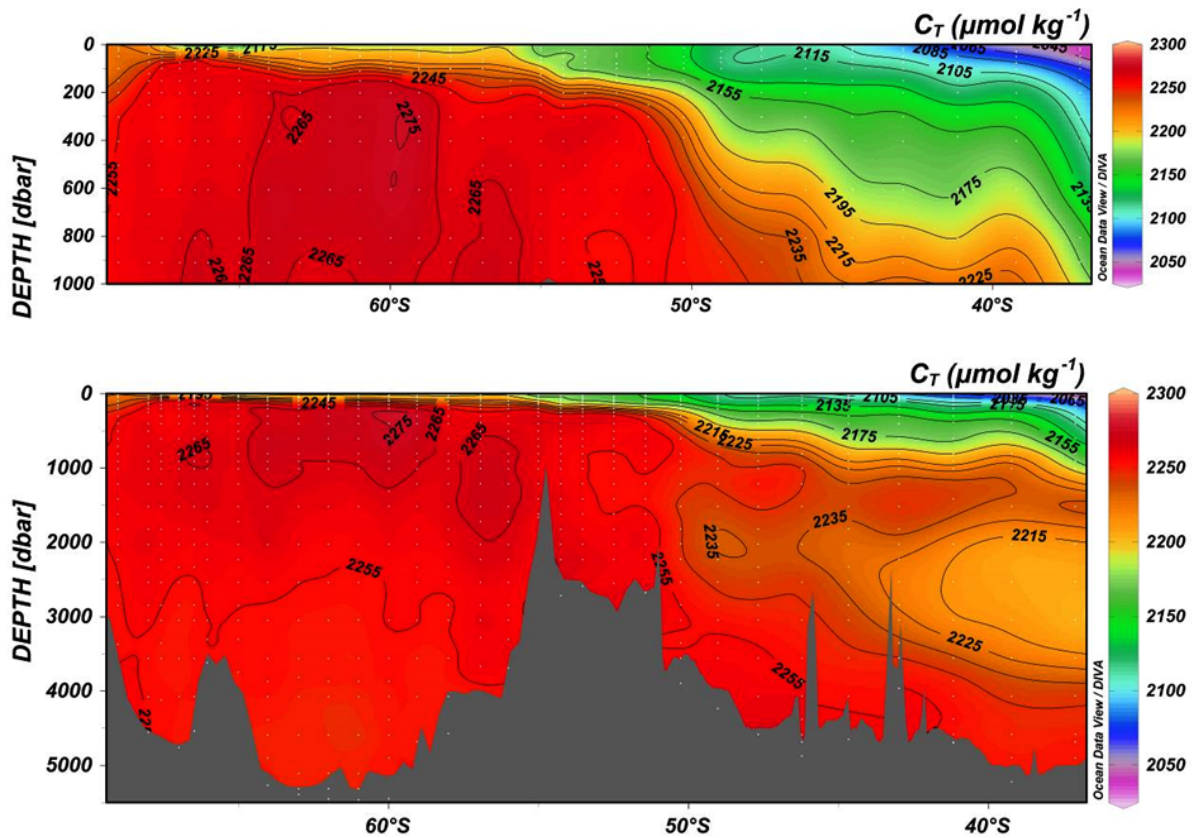


Fig. 3.1.3.5: Vertical distribution of the total dissolved inorganic carbon concentration in the first 1,000 m (top panel) and in the full domain (low panel) along the Southwest Atlantic sector of the Southern Ocean during December 2014.

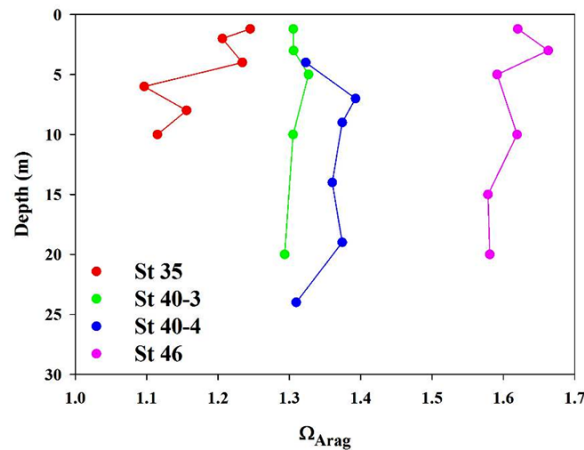


Fig. 3.1.3.6: Saturation state for the calcium carbonate in the form of Aragonite below the sea-ice for the stations 35, 40 cast 3 and 4 and station 46 in the Atka Bay area.

In a second set of studies, a Yo-Yo experiment was carried out in open waters close to the sea-ice at 70° 31.40' S and 8° 45.57' W (Section 3.1.1) in order to study the tidal effect on the pH, A_T and C_T variables. The Yo-Yo study started on January 7, 2015 at 22:00 hours with 12 casts that finished on January 8, at 9:00 am. Carbonate system variables were determined in the last 11 and 12 casts. The Yo-Yo experiment continued in January 9, 21:00 as station 52 with 12 hourly

casts, as station 54 in January 10, at 13:00 hours with 3 casts, station 56 the same day at 18:00 with 4 casts and finished with station 57 with 21 casts starting on January 11 at 1:00 am and finishing January 12 at 0:00 hours. The 40 total casts were sampled for carbonate system variables. The results from these studies are now being processed. The preliminary data (data not shown) indicated an important effect in all the carbonate system variables that affected the full 160 meter profile of the station that can only be explained considering the changes in the water masses due to the tidal effect. Collaboration with the physical oceanography group at AWI has already been established.

Data management

Metadata of recorded data will be made available through the cruise report. CTD sampling data for carbon system variables and oxygen will be made available after validation through the PANGAEA database. Results will be used by a PhD student assigned to our group and published in international journals.

References

- Clayton TD, Byrne RH (1993) Spectrophotometric seawater pH measurements: total hydrogen ion concentration scale calibration of m-cresol purple and at-sea results. *Deep Sea Res.* 40:2115-2129.
- Gonzalez-Dávila M, Santana-Casiano JM, Rueda MJ, Llinás O, Gonzalez-Dávila EF (2003) Seasonal and interannual variability of seasurface carbon dioxide species at the European Station for Time Series in the Ocean at the Canary Islands (ESTOC) between 1996 and 2000. *Global Biogeochem. Cycles* 17(3):1076, doi:10.1029/2002GB001993.
- González Dávila M, Santana-Casiano JM, Fine RA, Happell J, Delille B, Speich S (2011) Carbonate system in the water masses of the Southeast Atlantic sector of the Southern Ocean during February and March 2008. *Biogeosciences* 8:1401–1413.
- Lewis E, Wallace DWR (1998) Program Developed for CO₂ System Calculations. ORNL/CDIAC-105. Carbon Dioxide Information Analysis Center, Oak Ridge National Laboratory, U.S. Department of Energy, Oak Ridge, Tennessee.
- Lovenduski NS, Gruber N (2005) The impact of the Southern Annular Mode on Southern Ocean circulation and biology. *Geophysical Research Letters* 32:L11603, doi:10.1029/2005GL022727.
- Mintrop L, Pérez FF, González-Dávila M, Santana-Casiano JM, Körtzinger A (2000) Alkalinity determination by potentiometry: Intercalibration using three different methods, *Ciencias Marinas* 26: 23-37.
- Orr JC, Fabry VJ, Aumont O, Bopp L, Doney SC, Feely RA, Gnanadesikan A, Gruber N, Ishida A, Joos F, Key RM, Lindsay K, Maier-Reimer E, Matear R, Monfray P, Mouchet A, Raymond G, Najja, RG, Plattner G-, Rodgers KB, Sabine CL, Sarmiento JL, Schlitzer R, Slater RD, Totterdell IJ, Weirig MF, Yamanaka Y, Yool A (2005) Anthropogenic ocean acidification over the twenty-first century and its impact on calcifying organisms. *Nature* 437: doi: 10.1038/nature04095
- Santana-Casiano JM, González-Dávila M, Rueda MJ, Llinás O, González-Dávila EF (2007) The interannual variability of oceanic CO₂ parameters in the northeast Atlantic subtropical gyre at the ESTOC site. *Global Biogeochemical Cycles*, 21:GB1015, doi:10.1029/2006GB002788.
- Sarmiento JL, Hughes TMC, Stouffer RJ, Manabe S (1998) Simulated response of the ocean carbon cycle to anthropogenic climate warming. *Nature* 393:245–249.

3.1.4 Ocean Acoustics

Karolin Thomisch, Stefanie Spiesecke, Katharina
Lefering, Matthias Monsees, Rainer Graupner,
Olaf Boebel;
not on board: Ilse van Opzeeland

AWI

Grant No: AWI-PS89_01

Objectives

The restricted accessibility of the Southern Ocean during most of the year limits our expanding of knowledge on many marine mammal species in terms of their distribution patterns, habitat use and behavior. Most of the polar marine mammals produce species-specific vocalizations during a variety of behavioral contexts. Hence, passive acoustic monitoring (PAM) offers a valuable and frequently used tool for marine mammal research, capable of covering large temporal and spatial scales. Especially in remote areas such as the Southern Ocean, moored PAM recorders are the tool of choice as data can be collected year-round, under poor weather conditions, during darkness and in areas with dense ice cover.

The HAFOS observing system is a large scale array of oceanographic moorings deployed throughout the Weddell Sea in order to investigate the ocean interior of the Atlantic sector of the Southern Ocean. Passive acoustic recorders are part of the moored instrumentation, which is recovered, serviced and redeployed during PS89 to retrieve the data collected and to continue the long-term time series. The basin-wide design of the HAFOS observatory and the multi-year scale of data collection allow an unprecedented investigation of the spatio-temporal patterns in marine mammal biodiversity at the different mooring locations. Species-specific habitat usage of marine mammals can be explored by linking acoustic presence data to information on environmental parameters, such as depth or sea ice coverage. Furthermore, the design of the HAFOS array can provide information on the detection range of the various marine mammal sounds which is of vital importance for interpretation of call rates in the context of local acoustic abundances.

Work at sea

Recovery of moored acoustic recorders

Four SonoVault recorders (produced by Develogic GmbH, Hamburg), which had been deployed during ANT-XXIX/2 in December 2012/Jan 2013, were recovered during PS89. An overview of recovered acoustic recorders and all relevant recovery information is provided in Table 3.1.4.1 and recorder positions are shown in Fig. 3.1.4.1.

After recovery, the acoustic recorders were rinsed with freshwater and cleaned from biological fouling. The mooring frame which facilitates the integration of the acoustic recorders in line with the oceanographic moorings was removed for easy handling and opening of the recorder for data recovery. To check the status of the recovered recorder, it was connected to a laptop through a serial connection and accessed using a custom-built software for the SonoVaults. The recorders were then left to dry overnight to prevent damage to the electronics from water that retained in the threading of the recorder housing. For that reason, any water within the threading was removed by blowing it out using compressed air while opening the housing. After opening the recorder housing, the internal power supply was disconnected. All SDHC-cards, which had been labelled with serial number, module number and SDHC card-slot prior to recorder deployment, were removed and backed up (see below).

Mooring AWI232-10 (69°S, 0°E, deployed during ANT-XXVII/2, containing SonoVault recorder SV1003, Table 3.1.4.1), which had not been accessible during ANT-XXIX/2 due to heavy ice

3.1 Oceanography

conditions at the mooring position, could again not be recovered during this cruise. While communication was established with the mooring release, it failed to release the mooring, even after repeated commands to this effect.

The moorings located in the central Weddell Sea (and hence the acoustic recorders included, Table 3.1.4.1) could not be recovered due to the cancellation of the initially planned cruise track of PS89. Their recovery will be attempted during one of the following cruises to the Weddell Sea.

Tab. 3.1.4.1: Overview of SonoVault recorders recovered (white background) during PS89. Recorders shaded grey could not be retrieved during PS89.

Mooring	Device SN	Wwater depth [m]	Position	Deploy-ment depth [m]	Deployment date	Recovery date	Gain [dB]	Time Signal	Setup
AWI 247-03	SN1019	4235	20°58.54'S 05°59.07'E	736	2012-11-22	2014-11-24	30	--	1), file length 300s
AWI 227-12	SV1025	4600	59°02.63'S 00°04.92'E	1020	2012-12-11	2014-12-13	24	--	1),(3),(7)
AWI 229-10	SV1010	5172	63°59.66'S 00°02.65'W	969	2012-12-14	2014-12-16	24	12:30; daily	1),(3)
AWI 230-8	SV1009	3552	66°02.12'S 00°02.98'E	949	2012-12-15	2014-12-18	24	--	1),(3)
AWI 232-10	SV1003	3344	69°00.11'S 00°00.11'W	987	2010-12-19	postponed	50	--	1), 2)
AWI 232-11	SV1011	3319	68°59.86'S 00°06.51'W	958	2012-12-18	2014-12-22	30	--	1),(3)
AWI 244-03	SV0001	2900	69°00.35'S 06°58.97'W	998	2012-12-25	2015-01-16	30	12:40; daily	1),(3)
AWI 248-01	SV1013	5011	65°58.09'S 12°15.12'W	1081	2012-12-27	postponed	30	14:00; daily	1),(4)
AWI 245-03	SV1012	4746	69°03.48'S 17°23.32'W	1065	2012-12-28	postponed	48	13:10; daily	1),(4)
AWI 249-01	SV1014	4364	70°53.55'S 28°53.47'W	1085	2012-12-30	postponed	48	13:50; daily	1),(4)
AWI 209-07	SV1027	4830	66°36.45'S 27°07.26'W	226	2013-01-01	postponed	48	13:30; daily	1),(4)
	SV1028	4830	66°36.45'S 27°07.26'W	1007	2013-01-01	postponed	48	13:30; daily	1),(4)
	SV1029	4830	66°36.45'S 27°07.26'W	2516	2013-01-01	postponed	48	13:30; daily	1),(4)
AWI 208-07	SV1030	4732	65°37.23'S 36°25.32'W	956	2013-01-03	postponed	48	12:40; daily	1),(4)
AWI 250-01	SV1031	4100	68°28.95'S 44°06.67'W	1041	2013-01-05	postponed	48	13:10; daily	1),(4)
AWI 217-05	SV1020	4410	64°22.94'S 45°52.12'W	960	2013-01-09	postponed	48	13:50; daily	1),(4)
AWI 207-8	AU085LF	2500	63°43.07'S 50°49.91'W	219	2011-01-06	postponed	22	13:10; daily	4)
AWI 207-09	SV1032	2500	63°42.09'S 50°49.61'W	219	2013-01-12	postponed	48	14:10; daily	4), 5)
	SV1033	2500	63°42.09'S 50°49.61'W	1012	2013-01-12	postponed	48	14:10; daily	4), 5)
	SV1034	2500	63°42.09'S 50°49.61'W	2489	2013-01-12	postponed	48	14:10; daily	4), 5)

Mooring	Device SN	Water depth [m]	Position	Deployment depth [m]	Deployment date	Recovery date	Gain [dB]	Time Signal	Setup
AWI 206-7	SV1006	950	63°28.84'S 52°05.77'W	909	2011-01-06	postponed	48	--	1), 2)
AWI 206-08	AU232LF	917	63°15.51'S 51°49.59'W	277	2013-01-14	postponed	22	--	6)
	SV0002	917	63°15.51'S 51°49.59'W	907	2013-01-14	postponed	48	--	2)
AWI 251-01	SV1008	320	61°00.88'S 55°58.53'W	212	2013-01-16	postponed	48	--	1),4)
	AU231LF	320	61°00.88'S 55°58.53'W	210	2013-01-16	postponed	22	--	6)

- 1) Sampling: 5.3 kHz/24 bit, continuously, file duration 600 s;
- 2) 96 kHz/24 bit, Subsampling: 5 minutes every 2 hours;
- 3) CFG: Clock section setting A
- 4) CFG: Clock section setting B; All: No Precision Clock;
- 5) sampling: 9.6 kHz/24 bit, continuously, file duration 600 s;
- 6) Sampling: 32 kHz/16 bit, subsampling: 5 minutes every hour;
- 7) rope shackles

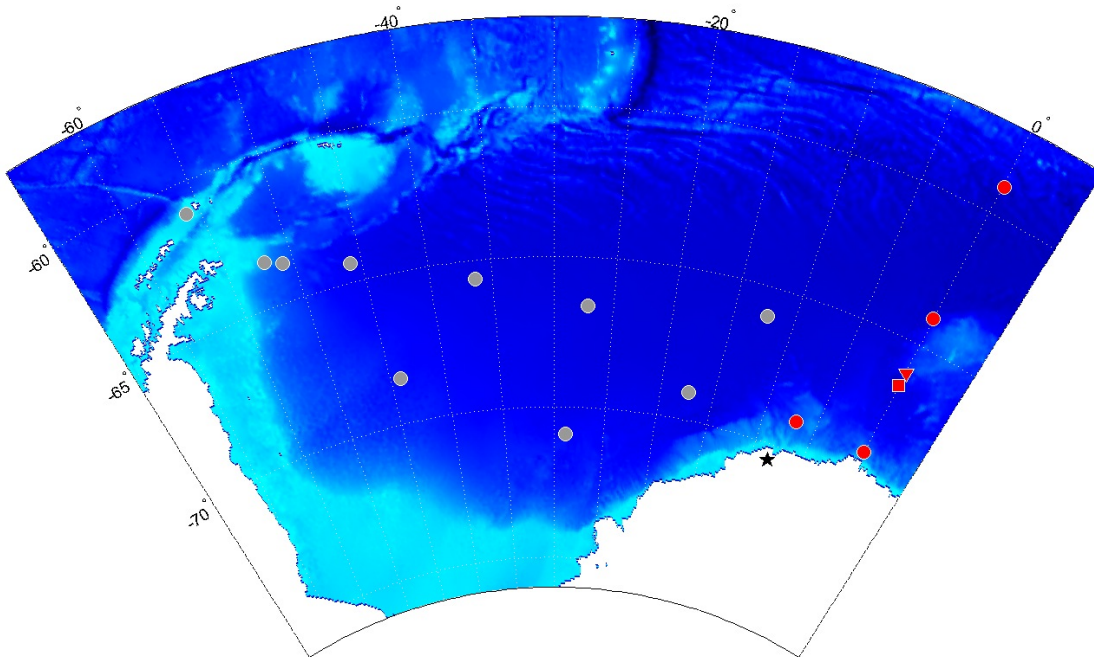


Fig. 3.1.4.1: Locations of acoustic recorders that were recovered and redeployed (red circles) during PS89. The red square and triangle indicate locations where recorders were only deployed or recovered, respectively. Grey dots indicate positions of moorings yet unrecovered. The black star represents the position of the PALAOA observatory.

Data retrieval and backup

All five units (four recorders were recovered during this cruise, while one recorder, moored off Namibia, had been recovered during the previous cruise leg, PS88) did not respond to communications efforts directly after recovery, i.e., stopped recording prior to recovery. Nevertheless, all units recorded for at least part of their deployment period (Fig. 3.1.4.2); further

3.1 Oceanography

details are discussed in section *Preliminary technical results*. A total of 1.7 TB of passive acoustic data was obtained.

The SonoVault recorders stored data on thirty-five 32 GB SDHC cards (allowing a maximum of 1.1 TB of data storage per recorder). After recovery, the SDHC cards were removed from the recorders and the acoustic data were copied using a custom-written shell script. Up to eight SDHC cards were copied simultaneously, with data initially saved to one of two HDD (4 TB) drives which were synchronized after copying was completed. The backup process included the renaming of files based on each files' internal time stamp (WAV-header) to the file name format 'YYYYMMDD-HHMMSS_AWIXXX-ZZ_SVXXXX.wav' (with X representing the IDs of mooring and SonoVault recorder, respectively and Z indicating the consecutive numbering of this mooring (i.e., the number of the current servicing cycle at a respective mooring)).

A total of three SDHC cards (i.e., one of recorder SV1009, SV1010 and SV1011 each) that presumably contain acoustic data were inaccessible during the data backup process. Recovery of those data using professional recovery software will be attempted at AWI Bremerhaven in 2015.

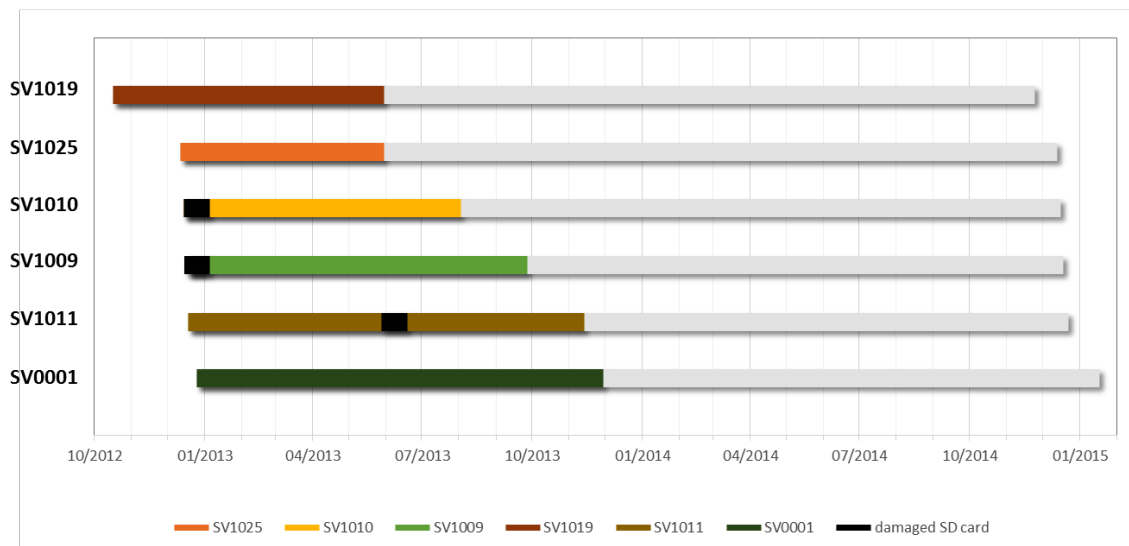


Fig. 3.1.4.2: Overview of deployment and operational period of acoustic recorders recovered during PS89. Grey bars indicate the deployment periods, while colored bars are indicative for actual recording periods of the recorders. Black bars represent periods during which recorders presumably operated but collected data have not yet been retrieved or backed up due to damaged SD cards.

Deployment of moored acoustic recorders

A total of four SonoVault recorders were deployed in four moorings during PS89 along the Greenwich meridian (Fig. 3.1.4.1, Table 3.1.4.2). These recorders are equipped with the latest electronics version V4.0. After the 2012/13, the recovery of the first batch of recorders deployed in 2010/11 revealed that electronic noise was apparent in some of the recorders. Therefore, the manufacturer redesigned the analog part of analog/digital front-end which is now placed on a separate board. All new recorders use the firmware version V4.07. Apart from some bug-fixing, additional features, e.g. the writing of log files and the storage of the configuration from the SD Card to the internal FRAM are implemented now in this version. All SonoVaults now deployed use five recording modules (SVR) with hardware version V2.2 and firmware version V4.05. After flashing the microprocessors, all implemented functions (e.g., changing parameter settings, downloading the configuration and retrieval of the system information) were tested. Subsequently, a test recording was started in the laboratory on board. Additionally, a

functionality test was conducted over several days on board Polarstern to check the transition between SD cards and recording modules during saving of the recorded data. Data were of good quality and properly written to the SD cards. For all recorders, the electronics proved operational.

A calibration of each deployed recorder was performed to ensure the correct calculation of signal levels after recovery. For the calibration a Brüel & Kjaer calibrator (Type 4229) with the custom made adapter SV.PA for the TC 4037 hydrophones was used. The calibration frequency is 251.2 Hz \pm 0.1 % (ISO 266) and the amplitude (at 1013 hPa) is 153.95 dB SPL. For the calibration measurement the recorder was set to the deployment sampling rate of 6857 Hz at 24bit and a file size of 1 minute. Gain setting was then altered from 0 – 7 (system gain settings, representing 6 dB – 48 dB) every minute during the calibration process. All recordings were stored and signal levels were noted.

Prior to the deployment, nine 128 GB SDXC cards and twenty-six 32 GB SDHC cards were placed into the SD card slots on each recording module, resulting in a total storage capacity of 1.9 TB per recorder. All SD cards were formatted to FAT32. 128 GB SDXC cards needed to be formatted using the freeware tool 'SDXCformatterFAT32'. On the first SD card (S0) of the first of five recording modules (M0-M4), the recording configuration (e.g., gain setting, sample rate) was stored. Additionally, the module number was copied onto S0 of every recording module to make the set of seven SD cards of this module available for storage.

The recorders are equipped with batteries (LS33600) and the O-rings were carefully cleaned and greased before closing the housing. All SonoVaults were programmed to record at a sampling rate of 6857 Hz with 24 bit and to store data in files of 600 s duration (Table 3.1.4.2). Internal data storage was structured to store data in folders of 48 files (8h) each. Gain was set to 48 dB in all deployed recorders (Table 3.1.4.2).

Tab. 3.1.4.2: Overview of SonoVault recorders that were deployed during PS89

Mooring	SV	Corr. water depth /m	Position LAT LON	Deployment depth /m	Deployment date /time (UTC)	Gain /dB	Time Signal	Setup
AWI 227-13	SV1056	4600	59° 02.67' S 000° 05.37' E	1020	2014-12-13 16:37	48	--	6857 Hz; 24bit
AWI 229-11	SV1057	5165	64° 00.32' S 000° 00.22' W	970	2014-12-17 10:45	48	--	6857 Hz; 24bit
AWI 231-11	SV1058	4472	66° 30.71' S 000° 01.51' W	973	2014-12-19 17:32	48	13:10; daily	6857 Hz; 24bit
AWI 232-12	SV1059	3360	68° 58.89' S 000° 05.00' W	999	2014-12-23 09:20	48	--	6857 Hz; 24bit
AWI 244-04	SV1061	2900	69° 00.34' S 006° 58.95' W	998	2015-01-16 13:57	48	12:40; daily	6857 Hz; 24bit
AWI 229-12	SV1055	5209	63° 54.94' S 000° 00.17' W	1001	2015-01-20 11:15	48	12:30; daily	6857 Hz; 24bit; Start: 01.01.2016 12:00

Change in hardware setup of the PALAOA observatory

Since 2005, PALAOA ('Perennial Acoustic Observatory in the Antarctic Ocean) is located on the Ekström Ice Shelf (70° 31' S, 8° 13' W) and collects continuous underwater recordings from a coastal Antarctic environment using a hydrophone deployed at ca. 160 m depths.

During the supply of the *Neumayer Station III* from 28 Dec 2014 until 31 Dec 2014, an aluminum box, containing an acoustic recorder, was installed at the position of the former PALAOA container. It was recessed into the snow and is covered with a wooden board and some snow. The box (80cm x 60cm x 60cm) includes a Reson input module EC6073 for the active hydrophone (Reson TC4032) and a SonoVault electronics module, similar to those used in the moored recorders. For power supply, four 90 Ah, 12V batteries were included, two connected in row for each, the active hydrophone and the recording electronics. Storage capacity is 4.4 TB (35 x 128 GB SDXC). With a sampling rate of 80 kHz at 24bit and a file size of 600s the PALAOA system is expected to run up to 6 months. Servicing will be provided by the overwintering team of *Neumayer III* at intervals of 4-6 months.

Preliminary technical results

Four acoustic recorders deployed during ANT-XXIX/2 in 2012 were recovered during PS89, in addition to one recorder already recovered during the previous leg, PS88. One SonoVault recorder deployed during ANT-XXVII/2 in 2010 could not be recovered. Further, the recovery of the moorings in the central Weddell Sea had to be postponed to a later cruise due to the alteration in the destination port of the cruise.

Neither the recovered recorders nor the mooring frames exhibited signs of corrosion. The zinc anodes however were heavily corroded and their residue had in parts clustered near the hydrophone, possibly impeding sound reception from some directions.

All of the recorders were functional during at least parts of the deployment period with recording periods ranging between 7 and 11 months, resulting in cumulative acoustic recordings of more than 42 months (Fig. 3.1.4.2).

However, all SonoVaults had ceased recording prior to recovery. The cause of these failures is yet undetermined. Battery voltage was reduced with respect to new batteries in all of the recovered recorders (Table 3.1.4.3). However, it was still sufficient to theoretically maintain functionality of the recorders which work with a supply voltage range from 7V-33V (Hardware Rev. 3.3). As mentioned before, communication directly after deployment was not possible in any of the recorders. To check the clock drift, the hardware and to post-calibrate the hardware in combination with the hydrophone, a new battery was connected to the hardware. In Table 3.1.4.3 an overview on the hard and software conditions of the recovered recorders is given. The time drift of the real-time-clock, which is powered independently by a lithium cell embedded on the electronics module, was determined.

A post calibration of each recovered recorder was performed to ensure the correct calculation of signal levels after recovery. The procedure was the same as for the calibration, but with only the gain setting used during the deployment period. All recordings were stored and signal levels were noted.

In general, the SonoVault recordings were of good quality. SV1010 and SV1011 contained pronounced low-frequency noise within the frequency range from 3 to 20 Hz which was likely caused by the electronics itself. Such low-frequent noise occurred throughout the recordings without a clear pattern and may therefore not be related to transitions between SDHC cards or modules during data storage. Regularly pulsed electronic noise, as observed in an earlier generation of the recorders, were detected in SV1011 and SV1009. In SV1011, the pulsed noise was only evident a few days before the recorder stopped operating, therefore, its occurrence may be caused by battery voltage related issues. However, for SV1009, the presence of the electronic noise pulses was not confined to the end of the recording period. The recordings of SV0001 contained electronic noise throughout the entire operational period and no sounds seem to have been recorded. The cause of failed recording in SV0001 have yet to be determined.

Tab. 3.1.4.3: Overview of hardware and firmware versions as well as post-recovery conditions of the SonoVault recorders recovered during PS88 and PS89.

Device			Hardware Version		Firmware Version		Condition			
Mooring	Device SN	Electronics SN	Analog Frontend	Recording Modules	Analog Frontend	Recording Modules	remaining Battery Voltage in V	Communi-cation established	Real-time clock* drift in ms/d	Comments
AWI 247-03	SN1019	EI1019	Rev 3.3	Rev.1.5	V3.11	V3.11	destroyed	not possible	--	a), b), c)
AWI 227-12	SV1025	EI1025	Rev.3.3	Rev.1.5	V3.11	V3.11_N1	13.8	Only with new power source	+61.47	a), b)
AWI 229-10	SV1010	EI1039	Rev.3.3	Rev.1.2	V3.11	V3.11_A	14.6	Only with new power source	-376,49	a), b)
AWI 230-8	SV1009	EI1041	Rev.3.3	Rev.1.2	V3.11	V3.11_A	9.88	Only with new power source	-51.31	a), b)
AWI 232-11	SV1011	EI1043	Rev.3.3	Rev.1.2	V3.11	V3.11_A	9.87	Only with new power source	+234.79	a), b)
AWI 244-03	SV0001	EI1035	Rev.3.3	Rev.1.2	V3.11	V3.11_A	destroyed	not possible	--	a), b), c)

a) mechanical condition good; b) no communication established directly after recovery; c) electronics damaged, batteries burned out, SD cards readable

Preliminary scientific results

For the five acoustic recorders retrieved during PS88 and PS89, long-term spectrograms over the entire recording period were calculated using MATLAB™ (Fig. 3.1.4.3).

These long-term spectrogram (totalling approx. 39,000 hours of recordings) provided the basis for a preliminary analysis of the acoustic recorders to investigate data quality of the recordings as well to determine the presence of distinct acoustic events (e.g., temporally dominant frequency bands, repetitive loud events, etc.) during the recording period (Fig. 3.1.4.3).

Visual and aural inspection of single files (i.e., 10 minute files) was conducted using Raven Lite 1.0 in order to provide more detailed information on the acoustic presence of different marine mammals. To this end, the selection of single files was largely balanced across the operational period of the respective recorder. For each recorder, the audible marine mammal species were depicted in preliminary biodiversity maps (Fig. 3.1.4.4) to obtain a first overview of spatial differences in species composition.

All recorders deployed in the Southern Ocean recorded vocalizations of leopard seals, as well as choruses of Antarctic blue whales and fin whales, respectively (Fig. 3.1.4.4). Antarctic minke whales were acoustically present on all recorders except for the northernmost SonoVault at 59°S (Fig. 3.1.4.4). In contrast, humpback whale calls were recorded at all locations except for the southernmost recording site (Fig. 3.1.4.4). Calls of Ross seals and crabeater seals were only detected at the recorder that was moored closest to the Antarctic continent at 68°S (Fig. 3.1.4.4).

The SonoVault that was deployed on the northern edge of the Walvis Ridge in the Southern Angola Basin off Namibia recorded Antarctic blue whale chorus and humpback whale calls (Fig. 3.1.4.5). Furthermore, during most of the 7.5 months recording period, airgun signals and broadband noise, presumably originating from distant ships, were discernible.

We like to emphasize that these results base on a first very coarse screening of the passive acoustic data and that it cannot be excluded that the maps presented here do not reflect the full local marine mammal biodiversity.

3.1 Oceanography

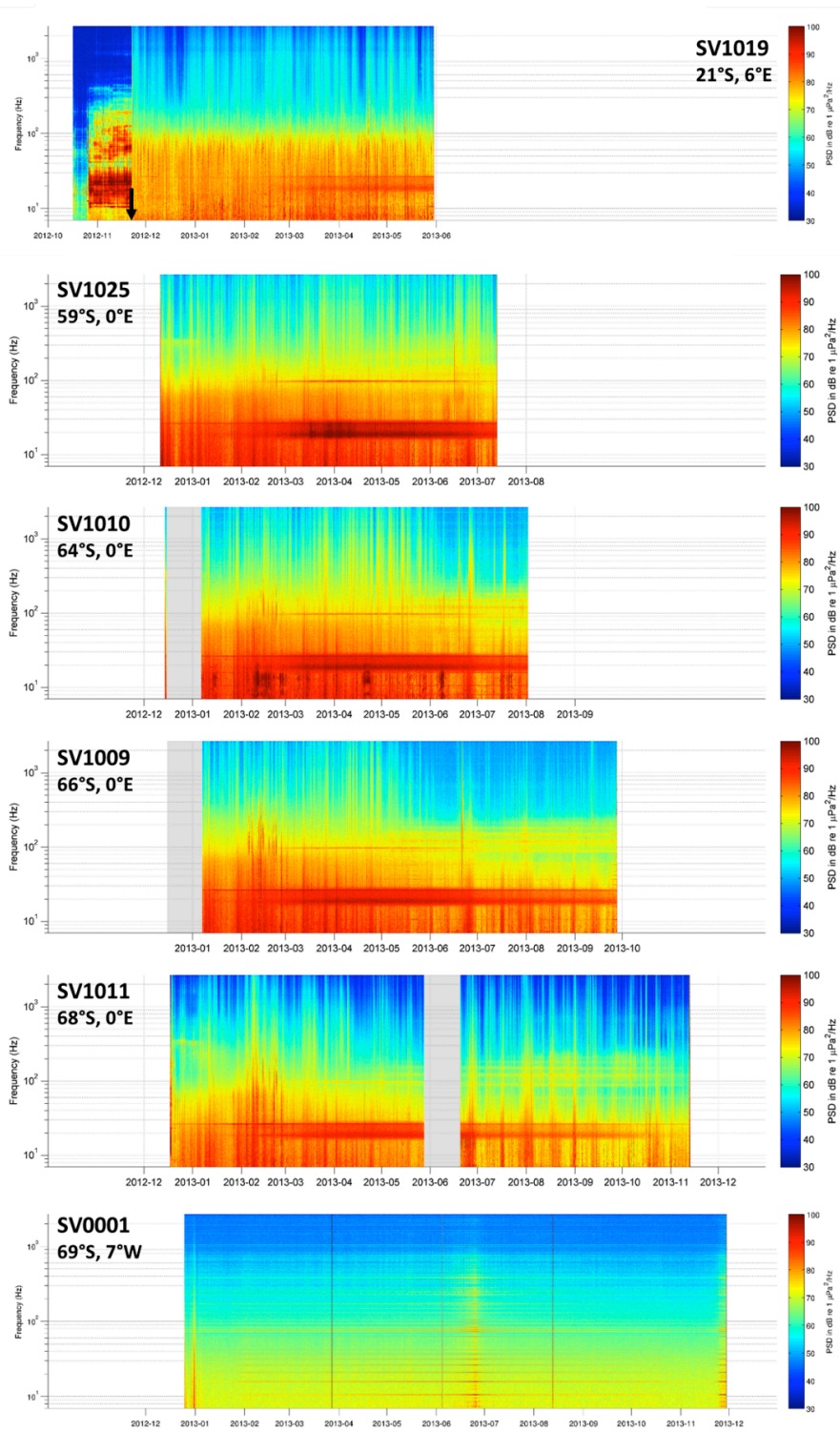


Fig. 3.1.4.3: Long term spectrograms of recorders retrieved during PS89 and PS88 (SV1019). Periods highlighted in grey indicate records stored on SD cards unreadable as yet.

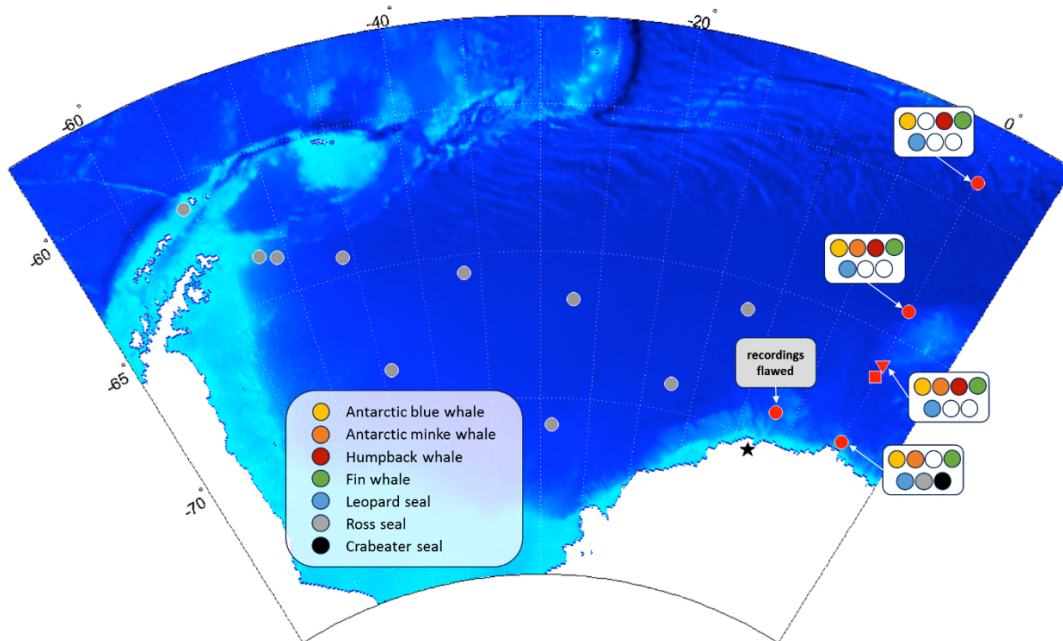


Fig. 3.1.4.4: Preliminary results on acoustic presence of marine mammal species in passive acoustic data recorded by SonoVaults that were recovered during PS89.

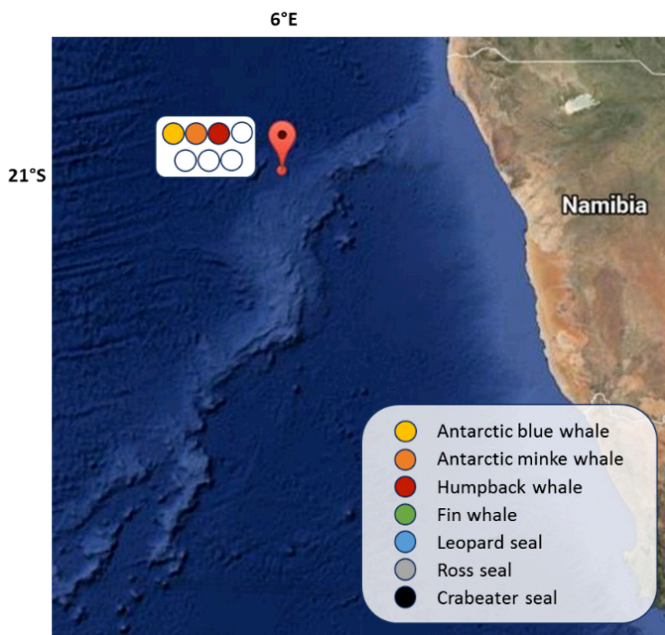


Fig. 3.1.4.5: Preliminary results on acoustic presence of marine mammal species in passive acoustic data recorded by SonoVault deployed at the northern edge of Walvis Ridge off Namibia.

Data management

All passive acoustic data will be transferred to the AWI silo and made accessible through the Pangaea database. P.I.: Ilse van Opzeeland.

3.1.5 Transport variations of the Antarctic Circumpolar Current

Olaf Boebel¹, Ioana Ivanciu², Gerd Rohard¹,
Matthias Monsees¹
not on board: Andreas Macranders³

¹AWI
²HAFRO
³IfM-GEOMAR

Grant No: AWI-PS89_01

Objectives

Pressure Inverted Echo Sounders (PIES) deliver bottom pressure, bottom temperature and travel times of sound signals from the bottom to the sea-surface, effectively providing a measure of average temperature of the water column and sea surface height (SSH). C-PIES additionally provide local current speed 50 m above the bottom by an acoustic DCS current meter. These data are used to evaluate variations of both barotropic and baroclinic geostrophic transport of the Antarctic Circumpolar Current (ACC) as part of the AWI programme to observe the decadal variability of the ACC. The PIES are placed along the GoodHope section between South Africa and Antarctica (Fig. 3.1.5.1), which in large parts coincides with ground track # 133 of the Jason (previously TOPEX/Poseidon) satellite mission to allow direct comparison with altimetry SSH. PIES-to-PIES distances are chosen to resolve the major oceanic fronts of this region.

Work at sea

During PS89, 13 of 14 PIES were recovered successfully, while one PIES (ANT 10 at 49°S) was not released due to severe weather jeopardizing its successful recovery. However, its Posidonia transponder was acoustically contacted and its position confirmed.

All PIES were acoustically released by a mobile EG&G 8011A deck unit connected to a hydrophone lowered over the side of the vessel. Release commands were repeated 3-5 times with 2 minutes spacing to ensure that the PIES is not blocked during its own measurement schedule, and to re-trigger release execution after possible resets. Due to the high underwater noise level of *Polarstern*, acknowledge pings of the PIES were never detected with the exception of the shallowest position ANT15-1. All PIES moorings featured an Ixsea ET861 Transponder, which was used to establish the underwater location and aid the recovery with the ship's Posidonia device (see section 3.1.1, Operational results – The Posidonia positioning system). Contrary to previous experiences (see Appendices A.5 & 6 in Fahrback et al. 2011) the positions obtained via Posidonia proved robust to within -30° under the sea surface. Monitoring the PIES/transponders ascent, the ship was positioned for the PIES to surface at a bearing of 15° and 2 cables distance from the bow, allowing a speedy recovery, mostly by use of the ship's zodiac.

Tab. 3.1.5.1: Deployment and revolver information on the GoodHope PIES array.

PIES SN DCS SN Posidonia SN	Deployment				Recovery				
	Mooring ID Station book	Date time (UTC)	Position (GPS) Depth (DWS)	Deployment CTD	Mooring ID Station book	Release date Release time (UTC)	Position Depth (Posidonia)	Time offset	Recovery CTD
PIES #058 no DCS ET861 #637	ANT 3-3 PS77/013-3	30.11.2010 06:31	37° 5.84' S 12° 45.23' E 4904 m	PS77/013-1	ANT 3-3 PS89/001-2	04.12.2014 07:08	37° 5.90' S 12° 45.56' E 4983 m	PIES:09:45:12 GMT 09:47:20	PS89/001-1
C-PIES #184 DCS #752 ET861 #726	ANT 4-3 PS79/035-2	05.12.2011 12:07	39° 13.07' S 11° 20.04' E 5122	PS79/035-3	ANT 4-2 PS89/002-2	05.12.2014 01:20	39° 13.67' S 11° 20.05' E 5076 m	PIES 13:32:48 GMT 13:34:00	PS89/002-1
C-PIES #182 no DCS ET861 #469	ANT 5-3 PS77/015-3	02.12.2010 08:05	41° 9.77' S 9° 55.31' E 4624 m	PS77/015-1	ANT 5-3 PS89/003-2	05.12.2014 18:32	41° 9.87' S 9° 55.61' E 4605 m	PIES 20:47:00 GMT 20:48:00	PS89/003-1
PIES #069 no DCS ET861 #384	ANT 6-1 PS77/016-1	02.12.2010 22:17	42° 58.80' S 8° 30.15' E 3930 m	PS77/016-2	ANT 6-1 PS89/004-3	06.12.2014 11:23	42° 58.46' S 8° 30.67' E 3882 m	unavailable	PS89/004-2
C-PIES #181 DCS #750 ET861 #639	ANT 7-4 PS77/017-2	03.12.2010 18:37	44° 39.73' S 7° 5.15' E 4593 m	PS77/017-3	ANT 7-4 PS89/005-2	07.12.2014 04:00	44° 39.46' S 7° 5.60' E 4540 m	PIES 06:18:48 GMT 06:18:30	PS89/005-1
C-PIES #183 DCS #751 ET861 #616	ANT 8-1 PS77/018-1	04.12.2010 14:55	46° 12.97' S 5° 40.23' E 4786 m	PS77/018-2	ANT 8-1 PS89/006-2	07.12.2014 18:24	46° 12.91' S 5° 40.51' E 4767 m	PIES 20:28:56 GMT 20:29:40	PS89/006-1
C-PIES #251 DCS #26 ET861 #602	Ant 9-3 PS77/019-2	05.12.2010 10:20	47° 39.87' S 4° 15.22' E 4541 m	PS77/019-3	ANT 9-3 PS89/007-2	08.12.2014 08:31	47° 40.34' S 4° 15.03' E 4504 m	PIES 11:12:32 GMT 11:17:10	PS89/007-1
C-PIES #250 DCS #031 ET861 #617	ANT 10-2 * PS77/020-2	06.12.2010 03:58	49° 0.77' S 2° 50.05' E 4056 m	PS77/020-3	recovery pending	recovery pending	recovery pending	recovery pending	recovery pending
C-PIES #249 DCS # 24 ET861 #385	ANT 11-4 PS77/021-3	07.12.2010 00:13	50° 15.45' S 1° 25.18' E 3901 m	PS77/021-2	ANT 11-4 PS89/009-2	09.12.2014 15:11	50° 15.40' S 1° 25.48' E 3842 m	PIES 16:54:01 GMT 16:59:00	PS89/009-1
PIES #062 no DCS ET861 #612	ANT 12-1 PS77/022-1	07.12.2010 10:52	51° 25.15' S 0° 0.24' E 2713 m	PS77/022-2	ANT 12-1 PS89/010-1	10.12.2014 01:08	51° 25.37' S 0° 0.63' E 2638 m	PIES 02:47:03 GMT 02:48:10	PS89/010-2
C-PIES # 252 DCS # 32 ET861 #391	ANT 13-3 PS77/026-2	08.12.2010 11:23	53° 31.22' S 0° 0.13' E 2642 m	PS77/026-3	ANT 13-1 PS89/012-1	10.12.2014 18:53	53° 31.35' S 0° 0.36' E 2570 m	PIES 20:21:12 GMT 20:26:00	PS89/012-2

PIES SN DCS SN Posidonia SN	Deployment				Recovery				
	Mooring ID Station book	Date time (UTC)	Position (GPS) Depth (DWS)	Deployment CTD	Mooring ID Station book	Release date Release time (UTC)	Position Depth (Posidonia)	Time offset	Recovery CTD
PIES # 191 no DCS ET861 #638	ANT 14-1 PS77/034-1	10.12.2010 04:15	56° 55.71' S 0° 0.01' W 3673 m	PS77/034-2	ANT 14-1 PS89/016-2	12.12.2014 08:43	56° 55.65' S 0° 0.36' E 3714 m	PIES 11:12:51 GMT 11:15:00	PS89/016-1
PIES #189 no DCS ET861 #614	ANT 15-2 PS77/042-2	11.12.2010 18:51	59° 2.37' S 0° 5.29' E 4647 m	PS77/042-2	ANT 15-2 PS89/020-3	13.12.2014 11:48	59° 2.27' S 0° 5.86' E 4594 m	PIES 14:12:52 GMT 14:14:15	PS89/020-2
PIES #125 no DCS ET861 #601	ANT 17-1 PS77/053-1	14.12.2010 23:45	64° 0.70' S 0° 2.72' W 5201 m	PS77/053-2	ANT 17-1 PS89/027-4	17.12.2014 12:50	64° 0.55' S 0° 3.03' W 5164 m	PIES 14:55:02 GMT 14:57:00	PS89/027-1

* PIES auto-release date: 06.04.2017 12:00 UTC REL code: REL 58

GMT+16 s=GPS

Remarks

88

ANT 4-3 - Only three years of record

ANT 6-1 - Connection through thin wire broken, PIES took approximately 3 h to release; no response on "switch on" – PIES opened, memory card removed.

ANT 10-2 - Recovery not possible due to bad weather

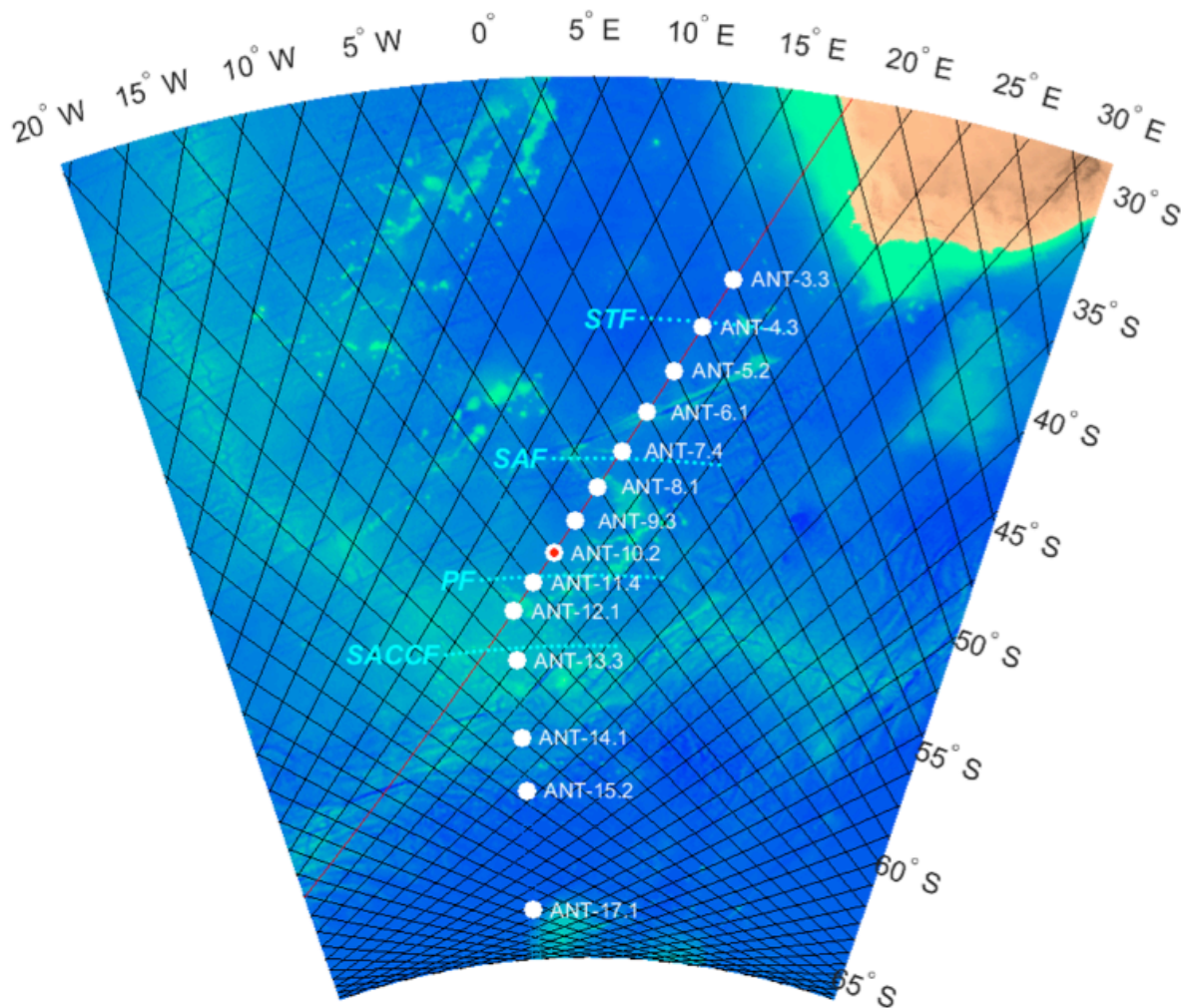


Fig. 3.1.5.1: Location of PIES recoveries during PS89 (white dots) including Jason satellite ground tracks (black line, track 133 marked red) and climatologic locations of major ocean fronts (cyan dots). PIES ANT 10-2 (red dot) was not recovered.

Preliminary results

Data was downloaded from the PIES directly after recovery via RS232 terminal communication and saved to the ship's network drive. Data was processed according to GSO Technical Report No. 2007-02 (Fig. 3.1.5.2, Fig. 3.1.5.3). Travel time data was derived according to the quartile period, pressure was detided and de-drifted and temperature was offsetted by minimizing temperature differences between initial and final PIES data and CTD bottom temperature measurements (Table 3.1.5.2).

All recovered PIES recovered operated flawlessly over the entire deployment period of 3 – 4 years (Table 3.1.5.3). Pressure accuracy and drift is within accepted range of the sensor; also acoustic travel time yields plausible results at most instruments.

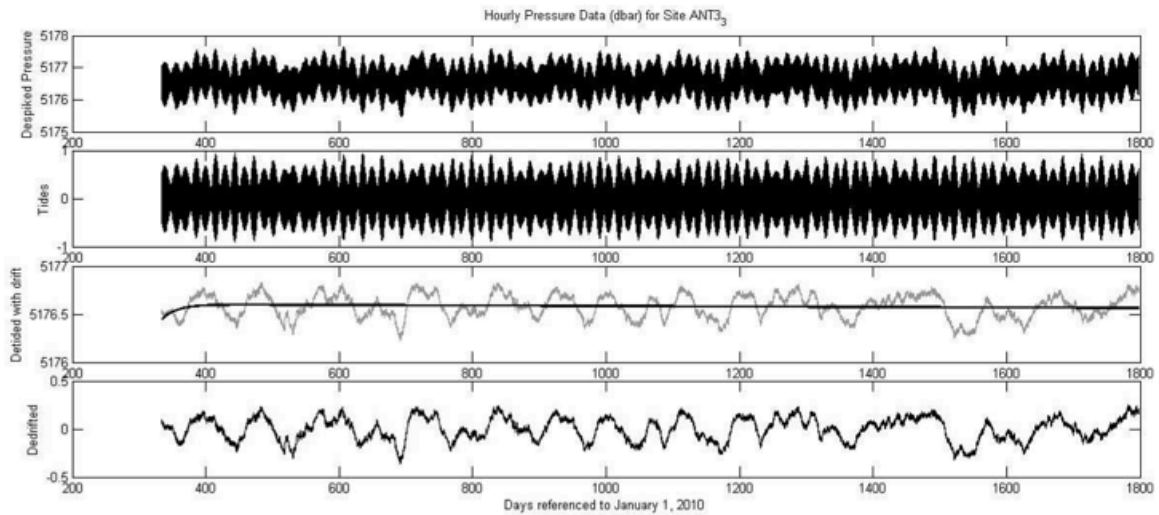


Fig. 3.1.5.2: ANT 3-3 hourly values of raw pressure data, fitted tides, detided pressure data, and detided and de-drifted pressure data (top to bottom).

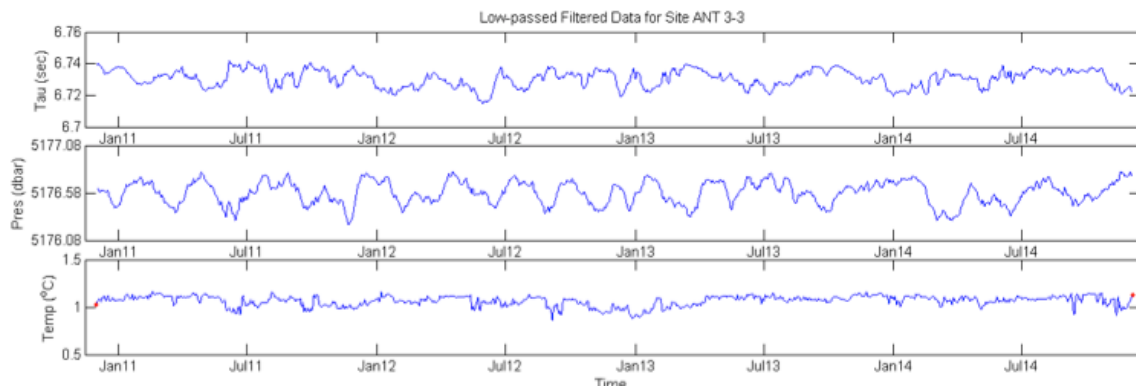


Fig. 3.1.5.3: ANT 3-3 travel time, pressure and temperature data after processing. The red dots at the start and end of the temperature time series indicate the CTD's bottom temperatures.

Tab. 3.1.5.2: Temperature offsets between recovered PIES and deep CTD bottom temperatures

PIES ID Station book	Deployment				Recovery				
	Bottom T (°C)	CTD Pres. (dbar)	CTD Date & Time	CTD Position	Bottom T (°C)	CTD Pres. (dbar)	CTD Date & Time	CTD Position	PIES Pres. (dbar)
ANT 3-3	1.0263	4933	30-Nov-2010 03:38:00	37.0957 S 12.7702 E	1.1279	4904	04-Dec-2014 04:57:00	37.1028 S 12.7603 E	5176
ANT 4-3					1.0207	5226	05-Dec-2014 00:56:00	39.2277 S 11.3338 E	5258

PIES ID Station book	Deployment				Recovery				
	Bottom T (°C)	CTD Pres. (dbar)	CTD Date & Time	CTD Position	Bottom T (°C)	CTD Pres. (dbar)	CTD Date & Time	CTD Position	PIES Pres. (dbar)
ANT 5-3	0.9921	4778	02-Dec-2010 05:07:00	41.1247 S 9.9623 E	1.0258	4702	05-Dec-2014 18:12:00	41.1647 S 9.9267 E	4750
ANT 6-1	1.2557	3968	03-Dec-2010 00:04:00	42.9823 S 8.5013 E	1.2055	3969	06-Dec-2014 10:59:00	42.9798 S 8.5058 E	3986
ANT 7-4	0.8495	4654	03-Dec-2010 20:36:00	44.6693 S 7.0920 E	0.7508	4655	07-Dec-2014 03:44:00	44.6578 S 7.0923 E	4679
ANT 8-1	0.8419	4889	04-Dec-2010 16:55:00	46.2195 S 5.6831 E	0.8067	4877	07-Dec-2014 18:04:00	46.2150 S 5.6750 E	4901
ANT 9-3	0.7160	4604	05-Dec-2010 12:26:00	47.6605 S 4.2555 E	0.8031	4587	08-Dec-2014 07:43:00	47.6713 S 4.2537 E	4623
ANT 11-4	0.6060	3889	06-Dec-2010 22:28:00	50.2602 S 1.4440 E	0.6343	3902	09-Dec-2014 14:51:00	50.2550 S 1.4255 E	3948
ANT 12-1	0.5443	2698	07-Dec-2010 12:28:00	51.4195 S 0.0055 E	0.5348	2678	10-Dec-2014 03:41:00	51.4218 S 0.0097 E	2717
ANT 13-3	0.3843	2619	08-Dec-2010 12:57:00	53.5200 S 0.0008 W	0.4067	2596	10-Dec-2014 21:21:00	53.5243 S 0.0030 E	2645
ANT 14-1	-0.2869	3696	10-Dec-2010 06:04:00	56.9330 S 0.0030 W	-0.2796	3670	12-Dec-2014 08:11:00	56.9270 S 0.0058 E	3686
ANT 15-2	-0.4026	4677	11-Dec-2010 20:48:00	59.0387 S 0.1057 E	-0.4029	4683	13-Dec-2014 11:25:00	59.0373 S 0.0938 E	4701
ANT 17-1	-0.3957	5267	15-Dec-2010 02:01:00	64.0405 S 0.0030 W	-0.3848	5271	16-Dec-2014 11:06:00	64.0263 S 0.0173 E	5291

Tab. 3.1.5.3: Overview of data quality from recovered PIES

PIES ID Station book	C-option	Duration	Data quality	Comment	Depth
ANT 3-3		4 years	all good		
ANT 4-3	yes	3 years	all good		
ANT 5-3		4 years	all good		
ANT 6-1		3.5 years	TT gap in 2012		
ANT 7-4	yes	4 years	all good		
ANT 8-1	yes	4 years	all good		

3.1 Oceanography

PIES ID Station book	C-option	Duration	Data quality	Comment	Depth
ANT 9-3	yes	4 years	all good	warming 0.1°C	4624 dbar
ANT 10-		not recovered			
ANT 11-4	yes	4 years	all good		
ANT 12-1		4 years	all good		
ANT 13-3	yes	4 years	all good	warming 0.02°C	2645 dbar
ANT 14-1		4 years	all good		
ANT 15-2		4 years	all good		
ANT 17-1		4 years	all good	warming 0.02°C	5291 dbar

Data management

PIES data will be validated and made available through the Pangaea database at AWI within one year of this cruise. P.I.: Olaf Boebel (AWI) and Andreas Macrander (HAFRO)

References

Fahrbach E (ed), 2011. The Expedition of the Research Vessel "*Polarstern*" to the Antarctic in 2010/11 (ANT-XXVII2), hdl:10013/epic.38039.

3.1.6 Sound levels as received by whale during a ship's passage

Karolin Thomisch, Stefanie Spiesecke, Katharina AWI
Lefering, Matthias Monsees, Rainer Graupner,
Olaf Boebel;
not on board: Ilse van Opzeeland

Grant No: AWI-PS89_01

Objectives

To minimize risks of collisions between marine mammals and approaching ships, it is important to understand the acoustic perception of an approaching ship from the whale's perspective. As received levels, and their variation with aspect and distance, differ significantly from source level corrected sound fields commonly presented in reports describing a ship's acoustic characteristics, and are furthermore difficult to back-calculate from such data for the frequencies and distances of concern, this project aimed for records of received levels in a close-encounter like situation with shallow hydrophone depths, mimicking the location of whale close to the surface.

Work at sea

To obtain sound levels under such conditions, a hydrophone was deployed twice at shallow depths from a zodiac and received sound levels were measured while RV *Polarstern* passed nearby. The experiment proceeded as follows:

The zodiac was launched on station and positioned nearby, stopping the zodiac's engine. A passive acoustic recorder (ICListen SN U1212, manufactured by OceanSonics, Canada), attached to a rope by cable ties, was lowered to 10 m depth, using an anchor weight about 5 kg. The recorder recorded continuously at 512 kHz, 24 bit. After launch of the zodiac, *Polarstern* resumed cruising speed (10 kn) and steamed to approximately 1 nm distance from the zodiac where she performed a Williamson turn, heading back onto her track without reduction of speed, subsequently passing the zodiac on a straight track and at a relatively constant speed of 10 knots at a PCA (point of closest approach) of about 0.1 nm (180 m).

The acoustic measurements were conducted at 56° 55,32' S, 0° 0,86' E (12th December 2014) and at 59° 2,50' S, 0° 6,33' E (13th December 2014). Periods during which RV *Polarstern* passed by the hydrophone position in a straight line at constant speed lasted for 8 and 7 minutes, respectively (Table 3.1.6.1). Start and end times of these periods were extracted from the station book records of *Polarstern* via DAVIS-Ship ("DShip").

Geographic positions and heading angle of *Polarstern* during these "sound profile periods" were downloaded from DAVIS-Ship with a temporal resolution of 1 s. Geographic positions of *Polarstern* were recorded midships, representing the position of the scientific navigation platform MINS (serving as reference location on RV *Polarstern*). Geographic positions of the hydrophone were recorded every 10 seconds using a GPS device (GPSmap 62stc, by Garmin) which was located on the zodiac. Potential drift of the hydrophone due to vertical current shear (resulting in divergent positions of zodiac and hydrophone) was considered negligible due to the shallow deployment depth/short rope length of the hydrophone.

Tab. 3.1.6.1: Acoustic measurements of RV *Polarstern* sound emissions during PS89

Date	Station ID	Latitude	Longitude	Profile start (UTC)	Profile end (UTC)
12.12.2014	PS89 017-1	56° 55,32' S	0° 0,86' E	10:33	10:41
13.12.2014	PS89 020-4	59° 2,50' S	0° 6,33' E	13:45	13:52

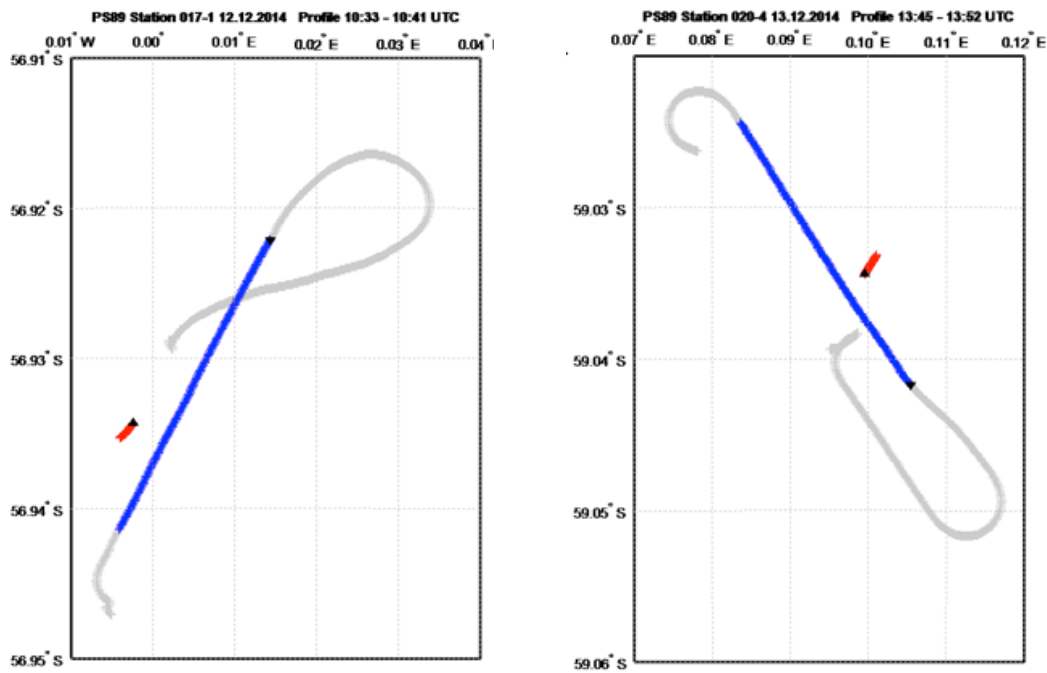


Fig. 3.1.6.1: Tracks of *Polarstern* (grey) with relevant recordings periods marked in blue. Drift of zodiac in red. Positions of both at end of relevant recording period are marked by a black triangle.

Preliminary results

GPS positions of the hydrophone during the sound profile periods were interpolated to 1-second resolution for ship-hydrophone distance and bearing calculations. Acoustic records during the sound profile period were high-pass filter with a Butterworth filter with a cut-off frequency of 40 Hz in order to prevent low-frequency noise originating from wave action influencing the analysis. Amplitudes of instantaneous received sound levels (SPL_{rms}) were calculated for 2-second long intervals for each second over the entire frequency range (i.e., 40 – 256,000 Hz). Ambient noise levels, representative for the acoustic environment conditions during sound profiles for each of the two days were calculated as SPL_{rms} over the entire frequency range using the three to five minutes prior to the start time of the sound profile. Listening to these segments confirmed that no ship noise was audible but only the slapping of small waves onto the zodiac.

Received sound levels were correlated with distance between ship and hydrophone positions as well as with the angle between the ship's track and the hydrophone position at each time step.

The analysis exhibits that the noise floor differed by about $4 \text{ dB}_{\text{rms}}$ re $1 \mu\text{Pa}$ between the two events (Fig. 3.1.6.2). It shows a linear increase of sound pressure levels with distance of about 5-6 dB per cable (1/10 nm or 186m), peaking at a level of about 123-125 dB at the time of CPA. The decrease of the sound pressure level occurs at a lesser rate of about 3-4 dB per cable.

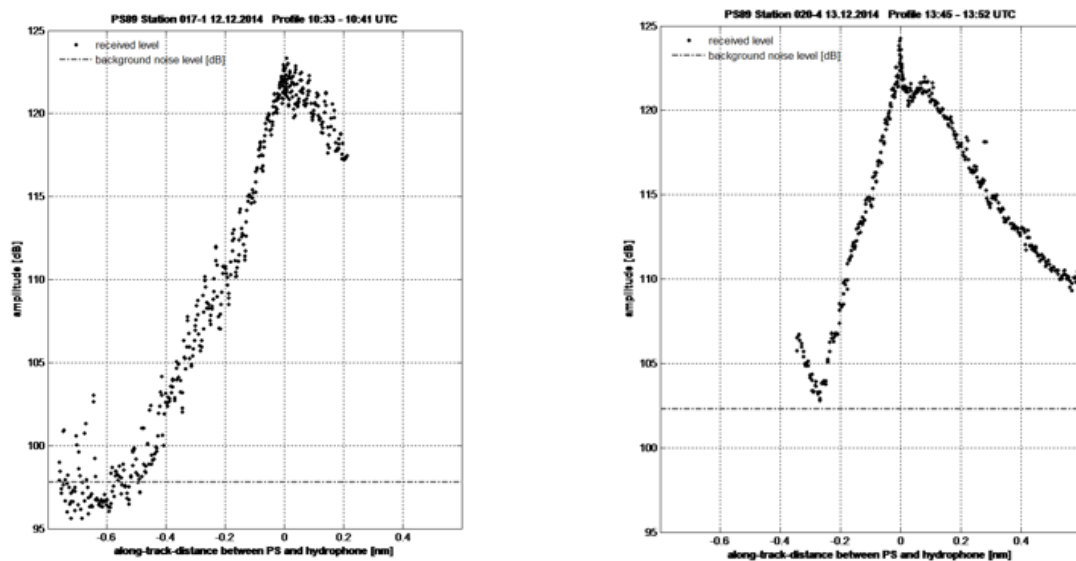


Fig. 3.1.6.2: Received broad band sound pressure levels (dB_{SPL} re $1 \mu\text{Pa}$) as a function of Polarstern's distance from the CPA (closest point of the approach). Values less than zero represent the approach towards, values greater zero the departure from the CPA.

Data management

Data will be stored in the AWI's permanently storage facility. Data will be made available after publication on basis of individual agreement.

3.2 Sea ice physics

3.2.1 Sea ice mass and energy budgets in the Weddell Sea

Marcel Nicolaus¹, Sandra Schwegmann¹,
Stefanie Arndt¹, Martin Schiller¹, Thomas
Hollands¹, Johannes Kainz¹,
not on board: Thomas Busche², Wolfgang
Dierking¹, Bin Cheng³

¹AWI
²DLR
³FMI

Grant No: AWI-PS89_02

The sea ice physics programme during this cruise was a main contribution to the Sea Ice Physics and Ecology Study (SIPES). SIPES was designed as an inter-disciplinary field study focusing on the inter-connection of sea ice physics, sea ice biology, biological oceanography, and top predator ecology. To achieve this, the sea ice physics programme performed sea ice thickness surveys, under-ice investigations with a remotely operated vehicle, deployments of autonomous stations (buoys), along-track ice observations from the bridge, and measurements of physical properties of the sea ice and its snow cover during ice stations. An overview of all stations, flights, and deployments is given in Fig. 3.2.1.1 and Table 3.2.1.1. The programme continued previous studies of Antarctic sea ice with a focus on three main topics:

- 1) Sea ice thickness and snow depth surveys were performed in order to describe the state of sea ice coverage on different temporal and spatial scales in the observation area. We obtained data from *in-situ* measurements, surface transects, airborne measurements (EM-Bird), and through the deployment of autonomous platforms (buoys). All together, the data obtained during the cruise will contribute to improve sea ice mass balance studies from autonomous *in-situ* techniques (buoys), remote sensing products (e.g. CryoSat, SMOS), as well as numerical models (e.g. FESOM).
- 2) The interaction of solar short-wave radiation and sea ice was studied to enable better estimates of heat fluxes through the ice cover into the upper ocean. With this, we aim to better quantify relationships between physical properties of sea ice and its associated ecosystem. Spectral radiation fluxes through sea ice were mapped using radiometers mounted on a remotely operated vehicle (ROV), allowing insights into the spatial variability of sea-ice and light conditions on floe scales.
- 3) Snow and surface conditions of sea ice were studied to improve our ability to interpret SAR data from satellites in order to gain additional knowledge about sea ice deformation and dynamical properties. From the combination of *in-situ* measurements with coordinated satellite data retrievals we aim to directly match both scales of observations.

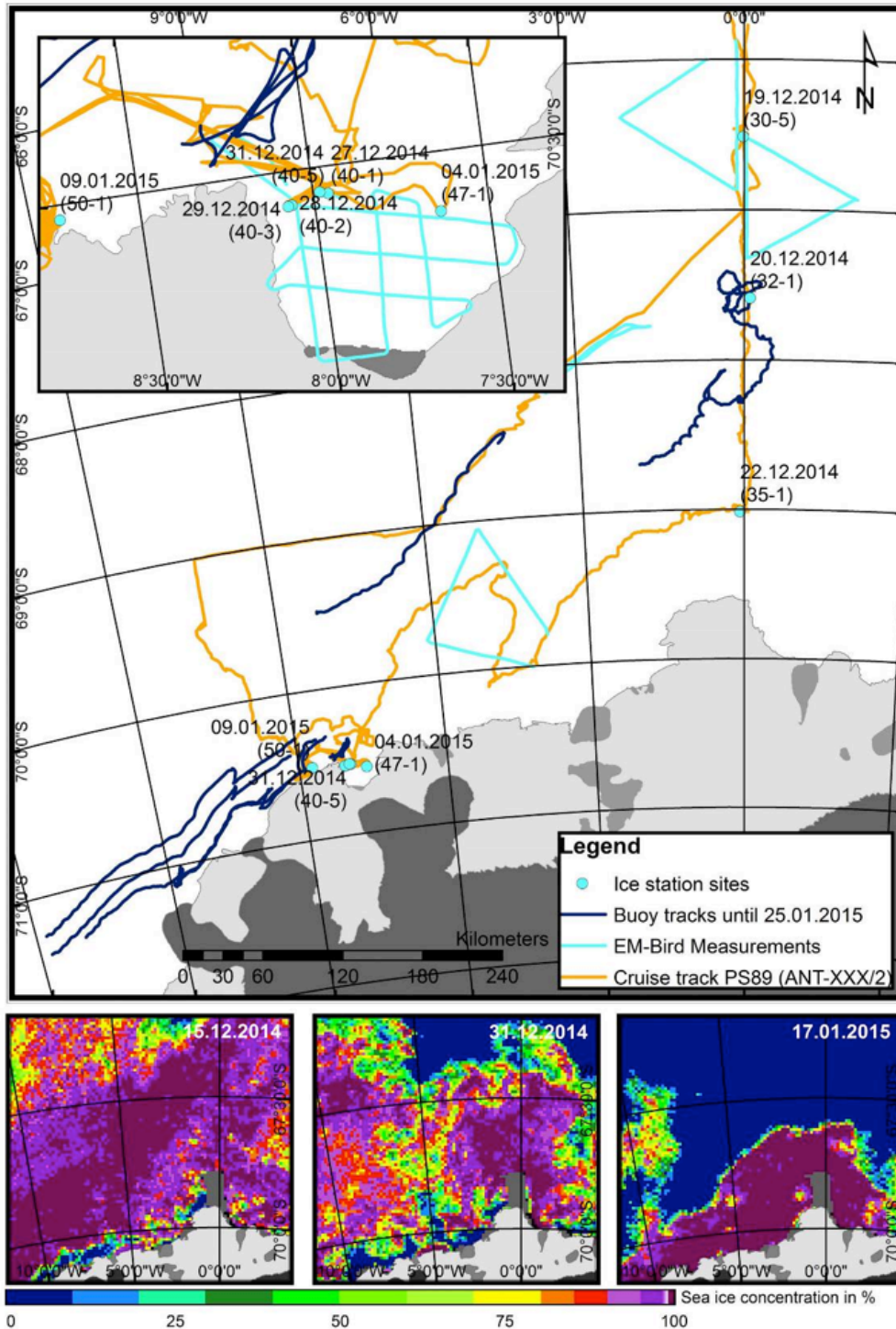


Fig. 3.2.1.1: Overview of all activities of the sea ice physics part of SIPES during PS89 (ANT-XXX/2). The inset (top left) enlarges the Neumayer / Atka Bay region. The three bottom panels show the sea ice concentration from AMSR2 for the three given dates during the expedition. Not shown here: Hourly observations of sea ice conditions along the cruise track between 13 December 2014 (60.4°S, 0.0°E) and 17 January 2015 (68.0°S, 3.25°W).

3.2 Sea ice physics

Tab. 3.2.1.1: Table of all ship stations and helicopter flights with contributions of the sea ice physics part of SIPES during PS89 (ANT-XXX/2). Chapter numbers refer to sub-chapters with additional information, tables, and figures with respect to single methods. Abbreviations: Long.: Geographic Longitude; Lat.: Geographic Latitude; GEM: Ground Electro Magnetics with GEM-2; SDMP: Snow Depth with Magna Probe, SIT: Sea Ice Thickness drilling; SPIT: Snow Pit; ROV: Remotely Operated Vehicle; BUOY: Buoy deployment

Date	Long.	Lat.	Station ID	EM-Bird	GEM	SDMP	SIT	SPIT	ROV	BUOY
12.12.14	0.100	-57.400	PS89/H007	Test						
12.12.14	0.200	-57.400	PS89/H008	Test						
18.12.14	-0.800	-65.900	PS89/H015	Test						
18.12.14	-0.800	-65.900	PS89/H016	YES						
19.12.14	-0.015	-66.513	PS89/H020	YES						
19.12.14	-0.015	-66.513	PS89/030-5			YES	YES	YES		
20.12.14	0.104	-67.588	PS89/032-1		YES	YES	YES	YES	YES	YES
22.12.14	-0.075	-69.015	PS89/035-1		YES	YES	YES	YES	YES	
24.12.14	-4.000	-69.800	PS89/H046	YES						
27.12.14	-7.957	-70.527	PS89/H058	YES						
27.12.14	-7.957	-70.527	PS89/040-1		YES	YES	YES	YES	YES	YES
28.12.14	-8.065	-70.533	PS89/040-2		YES					
31.12.14	-8.065	-70.533	PS89/040-5		YES					
03.01.15	-8.289	-70.438	PS89/044-1							YES
03.01.15	-8.289	-70.438	PS89/H080							YES
03.01.15	-8.065	-70.533	PS89/045-1							YES
04.01.15	-7.641	-70.558	PS89/046-1		YES	YES	YES	YES	YES	
09.01.15	-8.732	-70.515	PS89/050-1						YES	
11.01.15	-8.732	-70.515	PS89/058-1		YES					
17.01.15	-3.600	-68.200	PS89/H111							YES
17.01.15	-3.600	-68.200	PS89/H112	YES						

Tab. 3.2.1.2: Pangaea labels as used for sea ice physics measurements. The list is a continuation from Polarstern expedition ARK-XXVII/3 (IceArc). Devices / methods in italics were used during this expedition.

PANGAEA label	Description
Ship based	
ICEOBS	Ice Observations from ship bridge (along track)
OPT	Optical measurements (spectral, type Ramses) – Crows nest
Helicopter based	
AEM	Airborne EM Ice Thickness Profiler (EM-Bird)
Ice station (ICE)	
<i>ALB</i>	<i>Albedo measurements</i>
<i>AWS</i>	<i>Automatic Weather Station</i>
CTD	CTD (from ice floe)
<i>EMI</i>	<i>Electromagnetic Induction Ice Thickness Profiler (EM31 MkII)</i>
GEM	Ground EM (GEM-2)
OLA	Optical L-Arm measurements
OPT	Optical measurements (spectral, type Ramses)
ROV	ROV
SDMP	Snow Depth measured with Magna Probe
SIC	Sea Ice Corer
SIT	Sea Ice Thickness Drill (Thickness/Freeboard/Snowdepth)
SPIT	Snow Pit
Buoys	
BUOY-IMB	Ice Mass Balance Buoy
BUOY-SNOW	Snow Depth Buoy
BUOY-SVP	Surface Velocity Profiler
Ice Cores	
CORE-ARC	Archive core
CORE-DEN	Parameters: Density
CORE-DNA	Parameters: DNA
CORE-LSI	Parameters: Lipid Stable Isotope Analyses
CORE-MEI	Parameters: Meiofauna
CORE-OPT	Parameters: Bio-optical
<i>CORE-RNA</i>	<i>Parameters: RNA</i>
CORE-SAL	Parameters: Salinity, Chlorophyll-a
CORE-TEX	Parameters: Temperature, Texture

3.2.1.1 Airborne Sea Ice Surveys

Objectives

The sea-ice thickness distribution in the Weddell Sea is poorly investigated and only few observational data exist so far. Over the last decades, most information has only been obtained from upward-looking sonars and few *Polarstern* cruises during summer and winter conditions. Satellite data of sea-ice thickness is currently limited to the ICESat period (2003-2009), but there exist programmes to evaluate sea-ice thickness retrievals from CryoSat-2 and thin ice thickness by SMOS. Hence, one of the objectives of the sea ice thickness surveys during PS89 (ANT-XXX/2) was to obtain validation data for satellite retrieval algorithms of Antarctic sea-ice thickness, in particular expanding the data from the winter campaigns in 2013. In addition, airborne and ground based sea-ice thickness measurements are conducted at the same time and location in order to obtain information on the local (ground), regional (airborne) and large scales (satellites) variability from data with different spatial resolutions. Those data aim to reveal the derivation of statistical sea-ice thickness parameter that arises by the comparisons of data from different sensors.

Work at sea

We used the airborne multi-frequency electromagnetic (AEM) induction sounding system MAiSIE (Multi Sensor Airborne Sea Ice Explorer) to measure total (sea ice + snow) thickness by helicopter surveys. The 4 m long instrument, the EM-Bird, is towed on a 20 m long cable underneath the helicopter and measures the sea-ice thickness in a height of 10-15 m above the surface. Integrated in the EM-Bird system is a laser altimeter, which measures the distance to the surface. Beside its role for sea ice thickness calculation, the laser data allow the calculation of surface roughness and accordingly ridge density and distribution. For the first 4 measurement flights, a KT19 infrared thermometer was additionally integrated in the EM-Bird. The KT19 measures the surface temperature in the footprint of the EM signal. These surface temperatures may be used to better discriminate between thin sea ice and open water (e.g. leads, cracks between floes). In addition, it provides reference data for comparisons with passive remote-sensing data products, which use brightness temperatures to analyse surface processes and patterns. Before the last flight, the KT19 was exchanged with nadir-looking photo camera (Canon EOS 5D Mk II). The camera was installed to document the sea-ice conditions along the flight tracks. However, due to an installation fault, no useful images were recorded.

Preliminary results

In total, we performed 5 survey and 3 test flights with a total length of 1,200 km. Flight operations were significantly hampered by weather conditions with low clouds and low contrast during most times of the cruise. Therefore, flights are spaced by several days and scattered along the cruise track (see Fig. 3.2.1.1 and Table 3.2.1.1.1). We found predominantly first-year sea ice during the surveys with total thicknesses between 1 m and 6 m on average, depending on the location. Fig. 3.2.1.1.1 shows the thickness distribution for each flight. For the survey in the beginning and at the end of the expedition (18 and 19 December 2014 and 19 January 2015), each close to the sea-ice edge, the modal total sea ice thickness was 0.8 and 0.9 m. Closer to the coast / ice-shelf edge, it increased to a mode of 1.8 m. The fast-ice in the Atka Bay was much thicker than the drifting pack ice. Modal fast ice thickness was 6.1 m, but the measurements were certainly impacted by the platelet ice below the sea ice. These effects will be studied in detail in during post-processing of these data. It may be expected that an inverse modelling under consideration of the different EM frequencies will give new insights into the role of platelet ice for sea ice close to ice shelves.

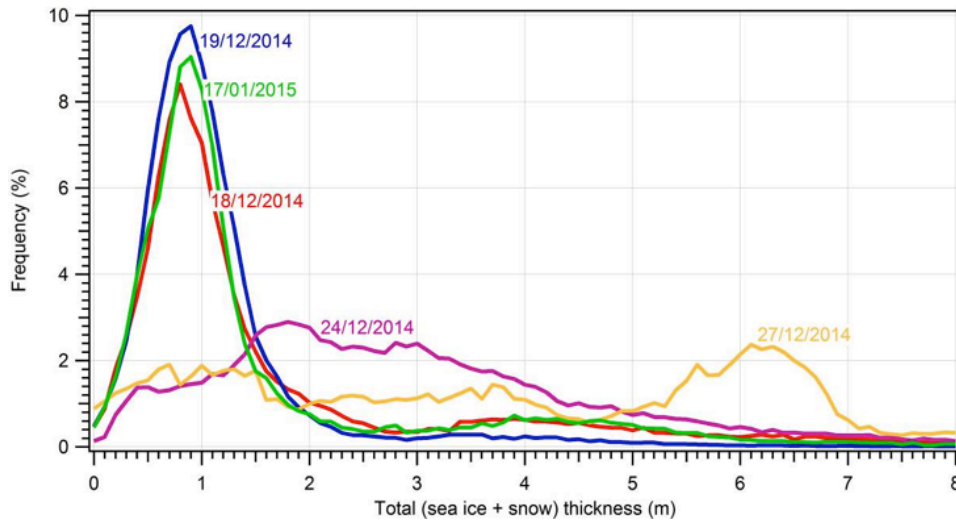


Fig. 3.2.1.1.1: Total ice thickness distribution for the AEM surveys during PS89 (ANT-XXX/2). All flight tracks are shown in Fig. 3.2.1.1.

Tab. 3.2.1.1.1: List of airborne sea-ice thickness surveys during Polarstern cruise PS89 (ANT-XXX/2).

Label	Device	Date	Length (km)
PS89/H007-AEM	EM-Bird, Laser altimeter, KT19	12/12/2014	- , test flight
PS89/H008-AEM	EM-Bird, Laser altimeter, KT19	12/12/2014	- , test flight
PS89/H015-AEM	EM-Bird, Laser altimeter, KT19	18/12/2014	- , test flight
PS89/H016-AEM	EM-Bird, Laser altimeter, KT19	18/12/2014	295.2
PS89/H020-AEM	EM-Bird, Laser altimeter, KT19	19/12/2014	283.1
PS89/H046-AEM	EM-Bird, Laser altimeter, KT19	24/12/2014	277.2
PS89/H058-AEM	EM-Bird, Laser altimeter, KT19	27/12/2014	153.2
PS89/H112-AEM	EM-Bird, Laser altimeter, Camera	17/01/2015	185.3

Data management

The sea-ice thickness and surface temperature data will be released following final processing after the cruise or depending on the completion of competing obligations (e.g. PhD projects), upon publication as soon as the data are available and quality-assessed. Data submission will be to the PANGAEA database and international databases like the Sea Ice Thickness Climate Data Record (Sea Ice CDR).

3.2.1.2 Thickness profiles (snow and sea ice) during ice stations

Objectives

The thickness of Antarctic sea ice and its snow cover is one of the most important parameters in terms of total mass and energy balance, but sea-ice thickness datasets are sparse. In addition, there are rarely data sets that combine high-resolution thickness information and high spatial coverage. This issue can be overcome by the combination of ground-based (instrument: GEM-2) and airborne (instrument: EM-Bird) measurements. This combination aims also to estimate the influence of the different footprints of these instruments on the total (sea ice + snow)

3.2 Sea ice physics

thickness distribution. For the validation of this advanced measurement method, drill hole measurements at particular sites shall reveal the actual sea-ice thickness. Those holes have also the function to reveal the sea ice-freeboard relation, which is needed for the calculation of sea-ice thicknesses from remotely sensed sea-ice freeboard.

However, the sea ice mass distribution and in particular the energy balance depends also on the snow depth distribution. Therefore, snow depths and sea-ice thicknesses were measured concurrently during GEM-transects. Information about the snow depth along the GEM-2 transects will determine the state of the snow depth distribution but will also help to determine the pure sea-ice thickness from GEM-2 data. For this purpose, snow depth measurements with the Magna Probe followed the same track as the GEM-2 measurements.

Work at sea

We used the ground-based multi-frequency electromagnetic device GEM-2 to measure the total (sea ice + snow) thickness. The measurement principle is similar to that of the EM-Bird. The device was mounted in a modified plastic sled for thickness transects and pulled over the snow surface either by hand or, for two long transects in the Atka Bay, by a skidoo. During the hand-held GEM-2 thickness surveys, we simultaneously operated a Magna Probe (Snow Hydro, Fairbanks, USA) in order to obtain the snow-depth distribution along the survey track. These measurements were taken every 2 to 5 steps on the track. The GEM-2 was calibrated several times on different sea-ice thicknesses with the help of a wooden ladder. For validation reasons, bore holes were drilled with 5cm-diameter augers along the ROV-grid (see Chapter 3.2.1.4) and at the calibration sites. Those data will also be used in order to determine the sea ice-freeboard relation.

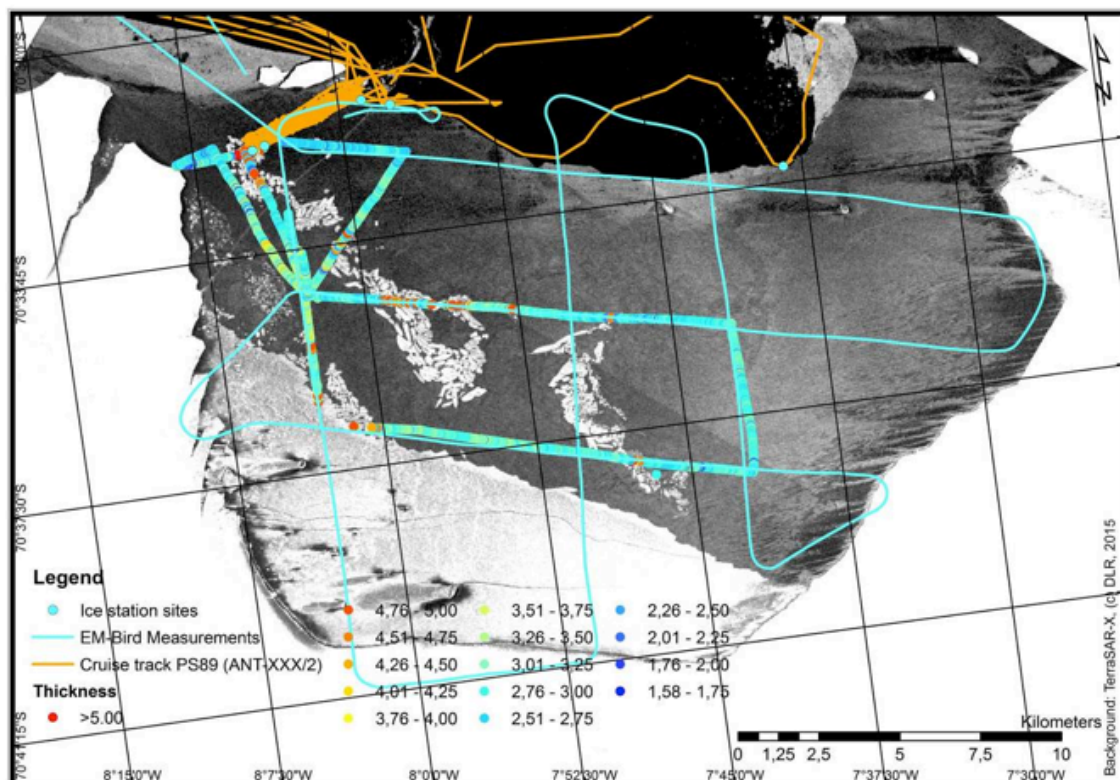


Fig. 3.2.1.2.1: Total ice thickness from GEM-2 skidoo-surveys across the Atka Bay (data compiled from 28.12. and 31.12.2014 surveys). The background shows a TerraSAR-X scene and the EM-Bird survey from 27.12.2014.

Preliminary results

In total, we performed 4 calibrations, 5 hand-held and 2 skidoo-based GEM-surveys. The surveys amount to about 73 km of profile data. 4 of the 5 hand-held GEM-surveys were combined with Magna Probe snow depth measurements on the same track. This was not done for station PS89/058-1 as snow did not exist at the measuring site (due to strong snow drift events before). In addition, snow depth measurements were also performed at ice station PS89/030-5. Total sea ice thicknesses ranged from 0.4 m to 5 m with mean (modal) values between 0.9 and 2.9 m (0.5 and 2.9 m). The mean (modal) snow depth ranged from 22.9 cm to 49.5 cm. Fig. 3.2.1.2.1 shows the sea ice thickness distribution from preliminary results for the skidoo transects across the Atka Bay. In addition, the image shows the flights transect from the EM-Bird across the Atka Bay and a TerraSAR-X scene, which describes the ice conditions below the GEM-transect. Since the GEM and the AEM surveys are more or less on top of each other and both cover a large part of the bay, they are very suitable for the inter-comparison of data from the different sensors. Also the impact of the platelet ice on the signals of both methods can be evaluated by those data.

Tab. 3.2.1.2.1: Ground-based sea ice-thickness and snow depth measurements using different instrumentation (see also Table 3.2.1.2): SIT: sea thickness drillings with augers, GEM: total thickness with GEM-2, SDMP: snow depth with Magna Probe.

Date	Label	Length (km)	# Measurements
19/12/2014	PS89/030-5-SIT	-	11
	PS89/030-5-SDMP	0.47	199
20/12/2014	PS89/032-1-SIT	-	11
	PS89/032-1-GEM	1.96	-
	PS89/032-1-GEM	Calibration	-
	PS89/032-1-SDMP	1.96	1230
22/12/2014	PS89/035-1-SIT	-	11
	PS89/035-1-GEM	2.24	-
	PS89/035-1-GEM	Calibration	-
	PS89/035-1-SDMP	2.24	1482
27/12/2014	PS89/040-1-SIT	-	2
	PS89/040-1-GEM	2.77	-
	PS89/040-1-GEM	Calibration	-
	PS89/040-1-SDMP	2.77	1185
28/12/2014	PS89/040-2-GEM	22.10	-
31/12/2014	PS89/040-5-GEM	37.10	-
04/01/2015	PS89/046-1-SIT	-	10
	PS89/046-1-GEM	3.03	-
	PS89/046-1-GEM	Calibration	-
	PS89/046-1-SDMP	3.03	1055
11/01/2015	PS89/058-1-GEM	4.03	-

Data management

The sea-ice thickness, snow depth and freeboard data will be released following final processing after the cruise or depending on the completion of competing obligations (e.g. PhD projects), upon publication as soon as the data are available and quality-assessed. Data submission will be to the PANGAEA database.

3.2.1.3 Physical properties of (snow and sea ice) during ice stations

Objectives

Snow stratigraphy and physical snow properties are highly variable even on small horizontal scales. These spatial and temporal variations in the snow pack characteristics (e.g. temperature, density, salinity, stratigraphy) have a crucial impact on the (optical) properties of the sea ice cover below. Therefore, the snow pack on the different ice station during PS89 (ANT-XXX/2) is characterized in detail. Furthermore, the data will be used as ground truth for the interpretation of radar backscatter satellite imagery.

Physical properties of sea ice (salinity, temperature, texture) are a backbone data set in sea ice research since the early days. During this expedition, we continue the tradition of sea ice sampling by coring to obtain this basic information. This will help to interpret (in particular) the optical measurements (see Chapter 3.2.1.4) and build a strong link to the biological part of the SIPES project (Chapter 3.3.1).

Work at sea

All work on physical properties of snow and sea ice was performed during the ice stations (ICE). All sea ice cores were obtained by the sea ice biology group and all information (incl. labels) are summarized in Chapter 3.3.1. Also all optical measurements (Chapter 3.2.1.4) were performed during these stations. In order to relate all activities during, in particular on drifting sea ice, a local coordinate system (in meters) was established. All measurement sites on the floe were recorded with GPS and corrected for sea ice drift. The resulting station maps and x/y coordinates may be used to localize measurements relative to each other, while only one geographic coordinate (latitude, longitude) is recorded for each ice station (Table 3.2.1.1 and Fig.s 3.2.1.3.2 to 3.2.1.3.6). Weather conditions during each ice station are available through the *Polarstern* meteorological station.

The physical snow parameters as well as the snow stratigraphy were obtained from snow pits. These were taken once per ice station at a representative location of the floe. The measurements were taken on the undisturbed shaded working wall of the snow pit. At first, the temperature was measured every 2 cm from the top (snow-air interface) to the bottom (snow-ice interface) with a hand-held thermometer (Testo 110). In a next step the different layers in the snow pack and its stratigraphic parameters were described. For each layer the snow grain size and type (e.g. rounded crystals, faceted crystals, depth hoar) is determined by the magnifying glass and a 1-to-3-mm grid card. In addition, every layer was characterized by its hardness with the following categories: fist (F), 4 fingers (4f), 1 finger (1f), pencil (p), and knife (k). Afterwards, the density of each layer was measured volumetrically by removing a tube of snow from each layer (tube weight: 615 g, tube volume: 500 ml) and weighting it with a spring scale. Additional density measurements were performed with a Snow Fork (Toikka, Finland). Snow Fork measurements were performed twice every 2 cm from the top to the bottom. In addition to the density, the Snow Fork measures liquid water content (in Vol. %) through the dielectrical properties of the snow pack. Due to technical issues, the snow fork was only used for stations PS89/040-1, PS89/046-1, and PS89/050-1. Even at these stations the measurements worked only for the top part of the snow pack. In addition, salinity samples were taken from the top and bottom snow layer and were melted (and measured) on the ship (not for all stations, see Table 3.2.1.3.1).

Preliminary results

Table 3.2.1.3.1 gives an overview about the sampled snow pits during PS89 (ANT-XXX/2). In total 5 snow pits were sampled with a mean snow thickness of 30.4 ± 21.1 cm.

Satellite image coverage could be achieved for four of the five sampled stations (not for station PS89/035-1). This data is expected to increase our understanding of which snow properties influence the X-band radar backscatter and therefore, to validate recent data products (Paul et al., 2014). Beside, the acquired snow pit data is expected to contribute to the results of the entire SIPES working group on board of *Polarstern*.

Fig. 3.2.1.3.1 shows an example of the snow pit at station PS89/040-1 (27.12.2014). The 61 cm thick snow pack contained 7 different layers with the variety of snow grain types from small (0.5 to 1 mm) rounded crystals (RC) in the top (layer B) down to big (3 to 4 mm) well-developed depth hoar crystals (DH) (layer G) in the bottom. This obvious development of several layers in the snow pack is also shown in the strong temperature gradient from -1°C (top) to -3.2°C (bottom).

Tab. 3.2.1.3.1: Snow pits during PS89 (ANT-XXX/2). Possible measurements for each snow pit are temperature (T), volumetric density (D), stratigraphy (Str), Snow Fork density and liquid water content (Sf), and salinity (S). Measurements were performed in all layers (X), top (t) or bottom (b) layers only, or not at all (O). Abbreviation: zs: Snow depth.

Label	Location	zs (cm)	T	D	Str	SF	S
PS89/030-5-SPIT	Next to L-Arm site	45	X	X	X	O	t
PS89/032-1-SPIT	Next to L-Arm/Coring site	22	X	X	X	O	O
PS89/035-1-SPIT	Next to ROV grid	8	X	X	X	X	O
PS89/040-1-SPIT	On GEM calibration site	61	X	X	X	X	t,b
PS89/046-1-SPIT	On GEM calibration site	42	X	X	X	X	t,b

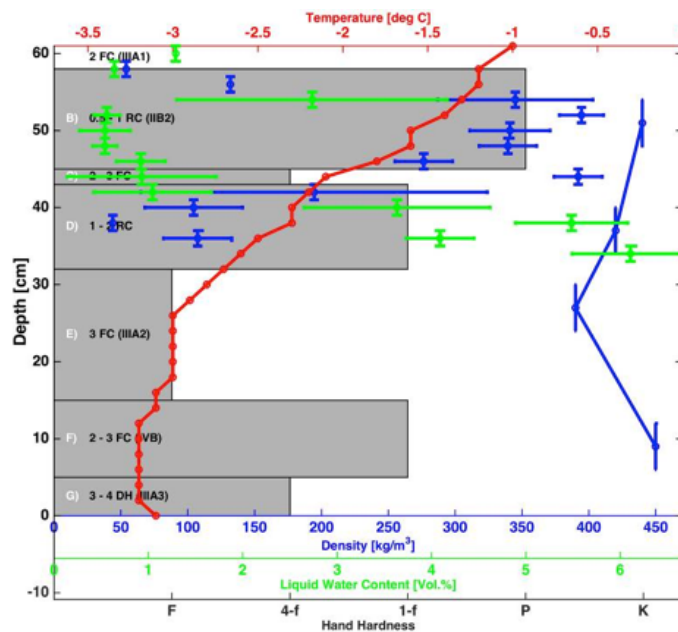


Fig. 3.2.1.3.1: Example of a snow pit analysis from Station PS89/040-1 (27.12.2014). Temperature measurements are marked in red, density measurements with the tube in blue (linked by straight lines), density measurements with the Snow Fork in blue, and liquid water content measurements in green. The grey bars indicate the vertical dimension of each layer and its hardness. The stratigraphy for each layer is given in the following sequence (example layer A): Layer label (A), grain size (2), grain type (FC(IIIA1)).

3.2 Sea ice physics

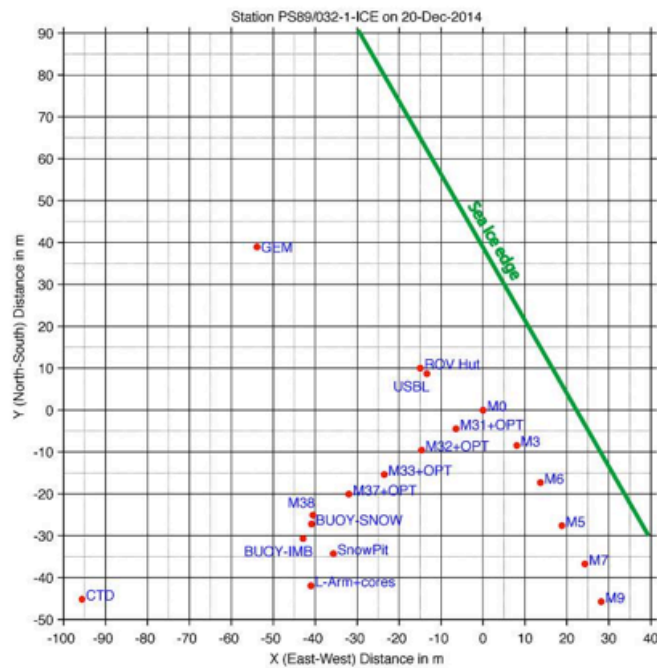


Fig. 3.2.1.3.2: Map of Station PS89/032-1 (20.12.2014). Markers (M) numbers refer to the orientation points for the ROV work. Position (P) numbers refer to surface markings for orientation, but without marker under sea ice.

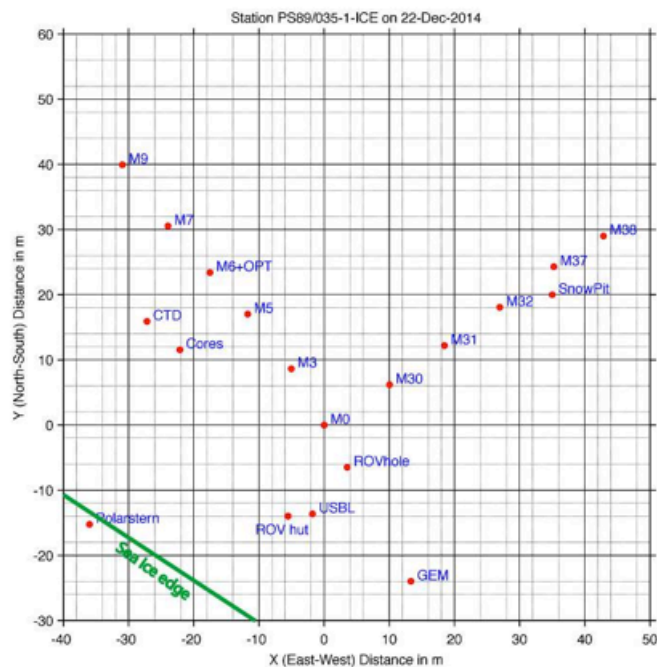


Fig. 3.2.1.3.3: Map of Station PS89/035-1 (22.12.2014). Markers (M) numbers refer to the orientation points for the ROV work. Position (P) numbers refer to surface markings for orientation, but without marker under sea ice.

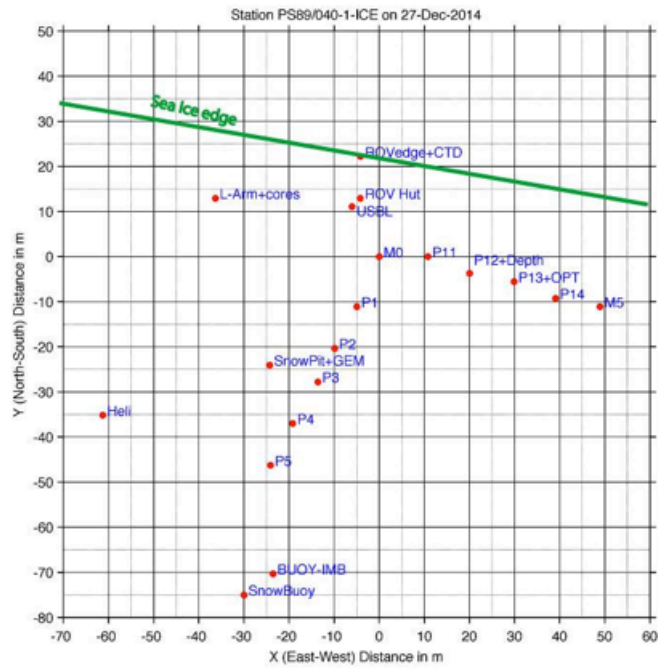


Fig. 3.2.1.3.4: Map of Station PS89/040-1 (27.12.2014). Markers (M) numbers refer to the orientation points for the ROV work. Position (P) numbers refer to surface markings for orientation, but without marker under sea ice.

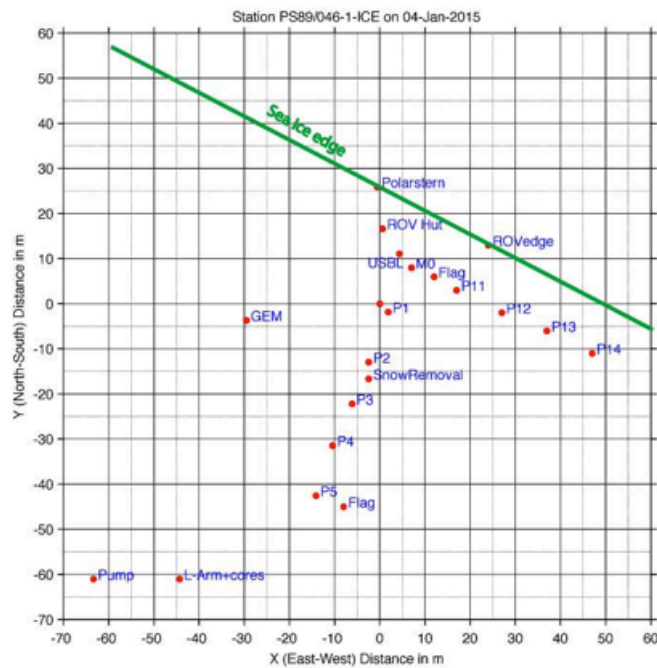


Fig. 3.2.1.3.5: Map of Station PS89/046-1 (04.01.2015). Markers (M) numbers refer to the orientation points for the ROV work. Position (P) numbers refer to surface markings for orientation, but without marker under sea ice.

3.2 Sea ice physics

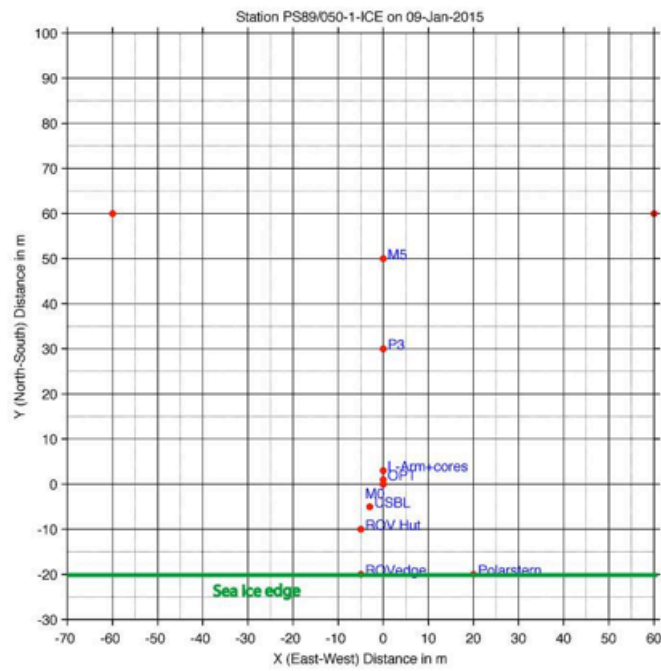


Fig. 3.2.1.3.6: Map of Station PS89/050-1 (09.01.2015) and PS89/058-1 (11.01.2015). Markers (M) numbers refer to the orientation points for the ROV work. Position (P) numbers refer to surface markings for orientation, but without marker under sea ice.

Data management

Data will be delivered to PANGAEA within two years after the cruise.

3.2.1.4 Optical properties of sea ice

Objectives

The amount of solar light transmitted through snow and sea ice plays a major role for the energy budget of ice-covered seas. In addition, the horizontal and vertical distribution of light under sea ice impacts biological processes and biogeochemical fluxes in the sea ice and the uppermost ocean. Due to their different absorption spectra, snow, sea ice, seawater, biota, sediments, and impurities affect the spectral composition of the light in its way from the atmosphere into the ocean. Especially the all-year snow-covered surface of Antarctic sea ice plays a crucial role for the amount of transmitted energy. To describe the influence of different sea ice surface properties (thin/thick snow layer, bare ice), we have performed comprehensive measurements of optical radiation under Antarctic sea ice with different surface layer characteristics during PS89 (ANT-XXX/2).

Work at sea

We measured spectral irradiance and radiance in the wavelength range from 350 to 920 nm with 3.3 nm resolution (mostly visible light) with Ramses spectral radiometers (Trios GmbH, Rastede, Germany). One irradiance sensor was installed above the ice as reference for incoming solar radiation, on radiance and one irradiance sensor were mounted on the ROV (Fig. 3.2.1.4.1). Radiance measurements (7° field of view) are best suited for studying the spatial variability of optical properties of sea ice. Irradiance measurements (cosine receptor) are best suited for studying the energy budget at the measured point, integrating all incident energy (from above) at this point. The optical measurements were done by operating our Remotely Operated Vehicle (ROV, Ocean Modules V8ii, Åtvidaberg, Sweden), called *Siri*, successfully during all 5 ice stations (Fig. 3.2.1.4.4 and Table 3.2.1.4.1).

The ROV system consisted of a surface unit (incl. power supply, control unit, monitor), a 200-m long tether cable, and the ROV itself. The ROV is controlled and moved by eight thrusters (allowing diving speed of up to 1.0 m/s). The speed varied during different profiles and was also depending on under-ice currents. The ROV was equipped with one upward-looking VGA video camera and one forward-looking HD camera (Fig. 3.2.1.4.1). Both cameras were used for navigation, orientation, and documentation of the dives. All video signals were recorded for the entire diving time. An altimeter (DST Micron Echosounder, Trittech, Aberdeen, UK) and a sonar (Micron DST MK2, Trittech, Aberdeen, UK) were mounted to support navigation and measure the distances to obstacles and markers (see below). The altimeter was particularly used to measure the distance between the radiometers (ROV) and the sea ice. Due to technical issues, the altimeter data were only recorded for the last station. Furthermore, an Ultra-Short-Base-Line positioning system (USBL, Trittech Micron Nav, Aberdeen, UK) was installed next to the ROV control hut through a 15cm-diameter hole (made with a sea ice corer). The transponder was installed on a solid pole right beneath the sea ice to generate a floe-fixed coordinate system for the moving vehicle. In addition, a modular logger system to measure water properties: salinity, temperature, and oxygen content. Finally, the ROV measured and recorded its depth, heading, roll, pitch, and turns constantly. Both cameras and all navigation features are displayed on the 4 screens in the ROV control hut (Fig. 3.2.1.4.3). The power supply for the ROV and its entire system was covered by the two coupled 3-kW generators.

From the radiometers on the ROV, we obtained horizontal transects and vertical profiles of under-ice irradiance and radiance. All data were directly recorded via an interface box into a PC running the sensors' software MSDA_xe. An additional reference irradiance sensor (type SAMIP) was mounted on a tripod on the sea-ice surface measuring incident solar radiation. All sensors were triggered in "burst mode" in intervals of 2 to 10 s, depending on light conditions under the ice.

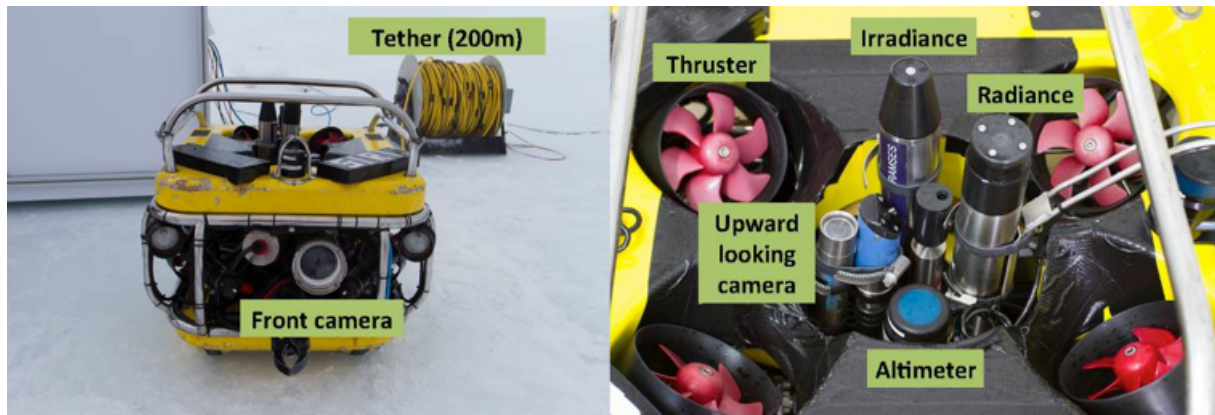


Fig. 3.2.1.4.1: Photograph of the ROV (left) and a close-up of the sensor side on top. The tether in the background contains the power line and allows for the communication between the vehicle and the ROV control hut (see Fig. 3.2.1.4.2).

All electronics were set up in our new ROV control hut (Fig. 3.2.1.4.2). The hut measured 3.03 x 2.02 x 2.123 m and weighed 680 kg including the ROV, the tether, all electronics, and a basic set of tools and accessories. The hut was stored on *Polarstern's* A-deck and lifted by crane either directly onto the sea ice or onto the helicopter deck, from where it was picked up by helicopter and transported onto the sea ice. This operation would have allowed ROV stations in up to 10 nm from the ship. Heavy additional equipment (e.g. generators, wooden boards, corer, augers, ice station tools) amounted to another 600 kg (incl. two Nansen sleds). This equipment was lifted by crane onto the ice and transported by snow scooter, if necessary.

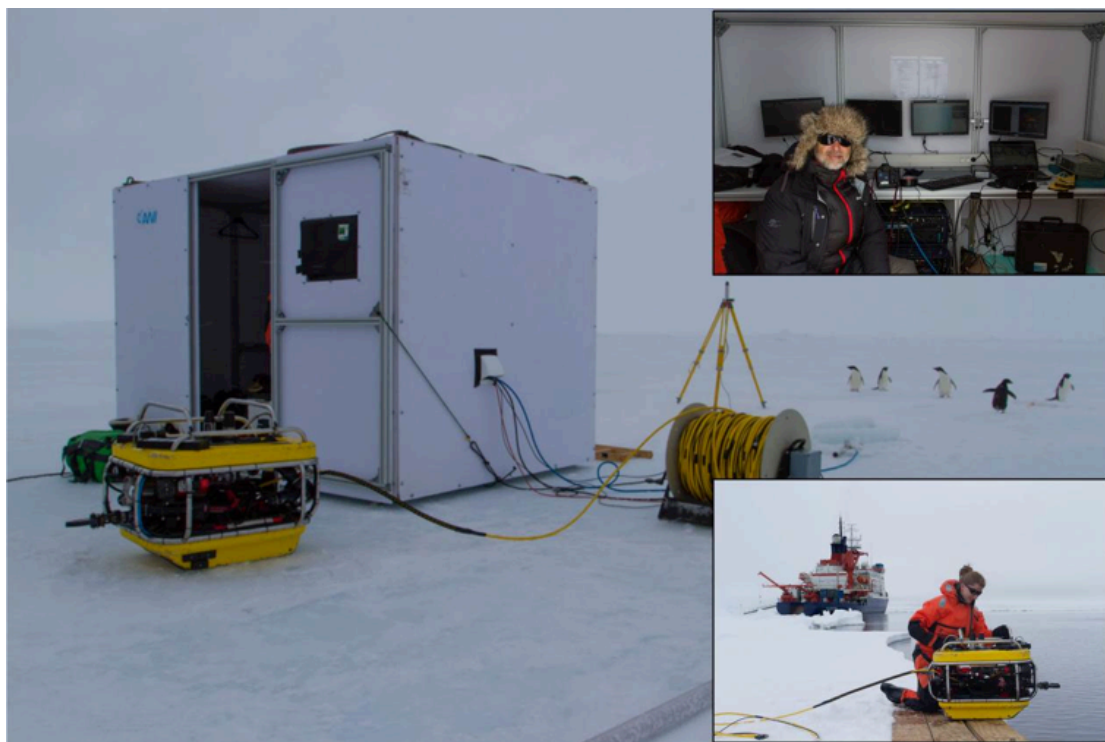


Fig. 3.2.1.4.2: Photograph of the ROV operating site. The big picture shows the ROV control hut with the tether on the right and the reference incoming radiance sensor in the back (next to the penguins). The upper small picture shows the set-up in the control hut with the four operating monitors in the back and the chief pilot in the front. The lower small picture gives an impression of the launch operation of the ROV.

Three persons operated the ROV: one pilot controlling the ROV, one co-pilot controlling the optical sensors and documenting the dive, and one person outside the hut, mostly handling the tether. The ROV was launched over the floe edge, except for station PS89-035-1, when a 1.5m*1.5m hole was sawn into the ice to launch the ROV. After an initial system check and test dive, the profiles (grid) were marked with numbered, red-white colored poles, hanging under the ice through drill holes. Sea-ice thickness, snow depth, and freeboard were measured at each hole. Additional measurements of total sea-ice thickness as well as snow depth were performed by GEM and Magna Probe transects above the selected grid (see Section 3.2.1.2). For station PS89-035, snow and ice thickness measurements were just done on the grid poles; GEM and Magna Probe transect around the ROV grid only. In addition, most optical measurements were co-located with physical, biological, and biogeochemical sampling of sea ice and water (see Chapter 3.2.2).

For the first three ice stations (PS89-032-1, PS89-035-1, PS89-040-1) we managed to operate the ROV in the marked 50m*50m (one marker every 10m) grid. Due to bad light conditions and strong currents, orientation and navigation was much more difficult afterwards. Hence, no similar regular grid could be achieved for station PS89-046-1 and PS89-050-1. Standard profiles were dived in a constant depth (per profile) between 2 and 4m depth, depending on the under-ice topography. Depth profiles (down to 20 to 70m) were performed by following a long line hanging under the ice. At station PS89-046-1, an additional snow-removal experiment was performed. After initial measurements, the snow was removed over an area of approx. 3m*10m to measure the difference in light transmittance between snow-covered ice and bare ice.

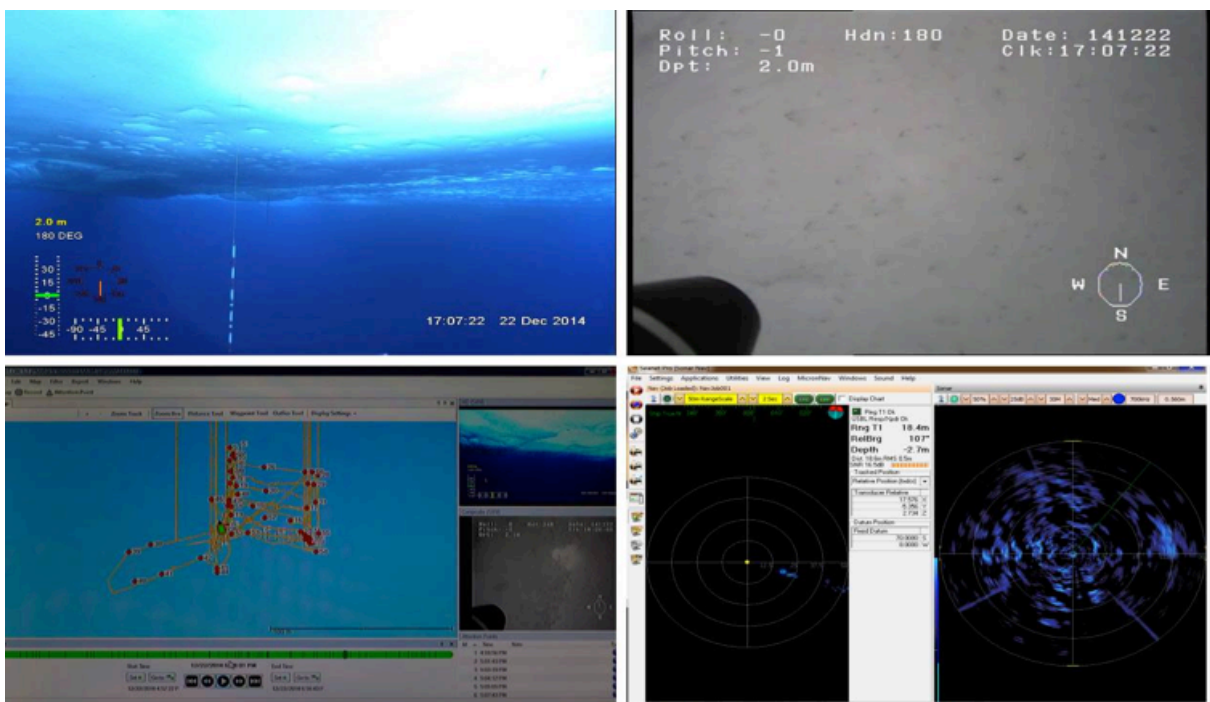


Fig. 3.2.1.4.3: Overview of the four operation screens. Upper left: Front camera. Upper right: Upward-looking camera. Lower left: Positioning system based on USBL. Lower right: Sonar signal and distance between ROV and sea ice (top right corner)

3.2 Sea ice physics

Tab. 3.2.1.4.1: Sea ice and snow conditions of all ROV stations. Mean sea ice thickness and snow depth are calculated from corresponding GEM and Magna Probe transects along the ROV grid (except for PS89-035-1-ROV). Abbreviations: zi: ice thickness; zs: snow depth; Plat: Platelett ice.

Label	Profile lines	zi (mean)	zs (mean)	Comment
PS89-032-1-ROV	2 x 50m (grid lines only)	0.9m	0.26m	ROV shut-down at 76m => end of measurements
PS89-035-1-ROV	9 x 50m (in ROV grid, incl. grid lines) 2 lines to the ice edge/ brash ice	(0.6 m)	(0.05 m)	Launch through hole Power-tube failure; Measurements after repair
PS89-040-1-ROV	4 x 50m (1 grid line, 3 parallel lines) 5 x 50m to the ice edge (parallel lines)	2.8 m (+ Plat.)	0.51 m	One thruster broke during measurements; repair on the floe
PS89-046-1-ROV	Random lines; Repeated lines under snow-free area	1.2 m (+ Plat.)	0.35 m	Bad orientation Snow removal (3m*10m) Tangle with marker pole
PS89-050-1-ROV	1 x 50m (1 grid line only)	2.2 m (+ Plat.)	Drift snow	Strong currents Bad orientation Strong pitch & roll

In addition to the ROV-based radiation measurements, two other types of spectral radiation data were recorded:

1) One irradiance sensor was mounted on the crow's nest, next to the meteorological station's radiation sensor (Label: PS89/OPT). This sensor recorded incident solar irradiance spectra from 04.12.2014 08:40 to 22.01.2015 19:00 in 5 min intervals (raster). In addition, this sensor was used as surface reference during SUIT hauls (Section 3.2.2). During these times it was set to burst mode. A total of 155.432 spectra was recorded during the expedition.

2) The ROV sensors were set up for inter-comparison measurements on the "Peildeck" of *Polarstern*. These measurements may be used, also in combination with the crow's nest sensor, to analyze differences between the sensors. Those differences were found in previous applications, in particular under low solar elevation angles.

Preliminary results

ROV measurements under the ice were performed during 5 ice stations. Depending on visibility and orientation 500 to 1,000 under-ice spectra were recorded per sensor and station. These spectra may be directly related to their position under the ice and along selected transects or depth profiles. Additional spectra were recorded during dives outside the grid or during general orientation and video dives. These may be included for statistical analyses of under-ice light conditions. Stations PS89-032-1, PS89-035-1, and PS89-040-1 resulted in the best data sets, covering the entire 50m*50m grid.

During the cruise, all radiation measurements (spectra) were processed from measured raw data to calibrated fluxes. However, results from sensor inter-comparisons were not applied yet. For the final data analysis and discussion only profile lines are taken into account. Profile

3.2 Sea ice physics

Stations PS89-032-1 and PS89-035-1 were performed on drifting sea ice (between 67.5 and 69°S on the Greenwich Meridian); while PS89-040-1, PS89-046-1, and PS89-050-1 were performed under land-fast sea ice (in the area of Atka Bay). The fast ice area was characterized by an additional layer of platelet ice beneath. Thickness and extent of the platelet layer were highly variable.

Light regimes differed strongly between light moving sea ice, resulting in a mean transmittance of approx. 1 % (Fig. 3.2.1.4.5), and fast ice with a varying platelet ice layer beneath, resulting in a mean transmittance of approx. 0.01 %. But there was no strong dependency of the surface properties, because the snow cover was optically thick on all stations. Instead, the size of the floe and the associated boarder effect has a strong impact on the vertical and horizontal light distribution beneath the sea ice.

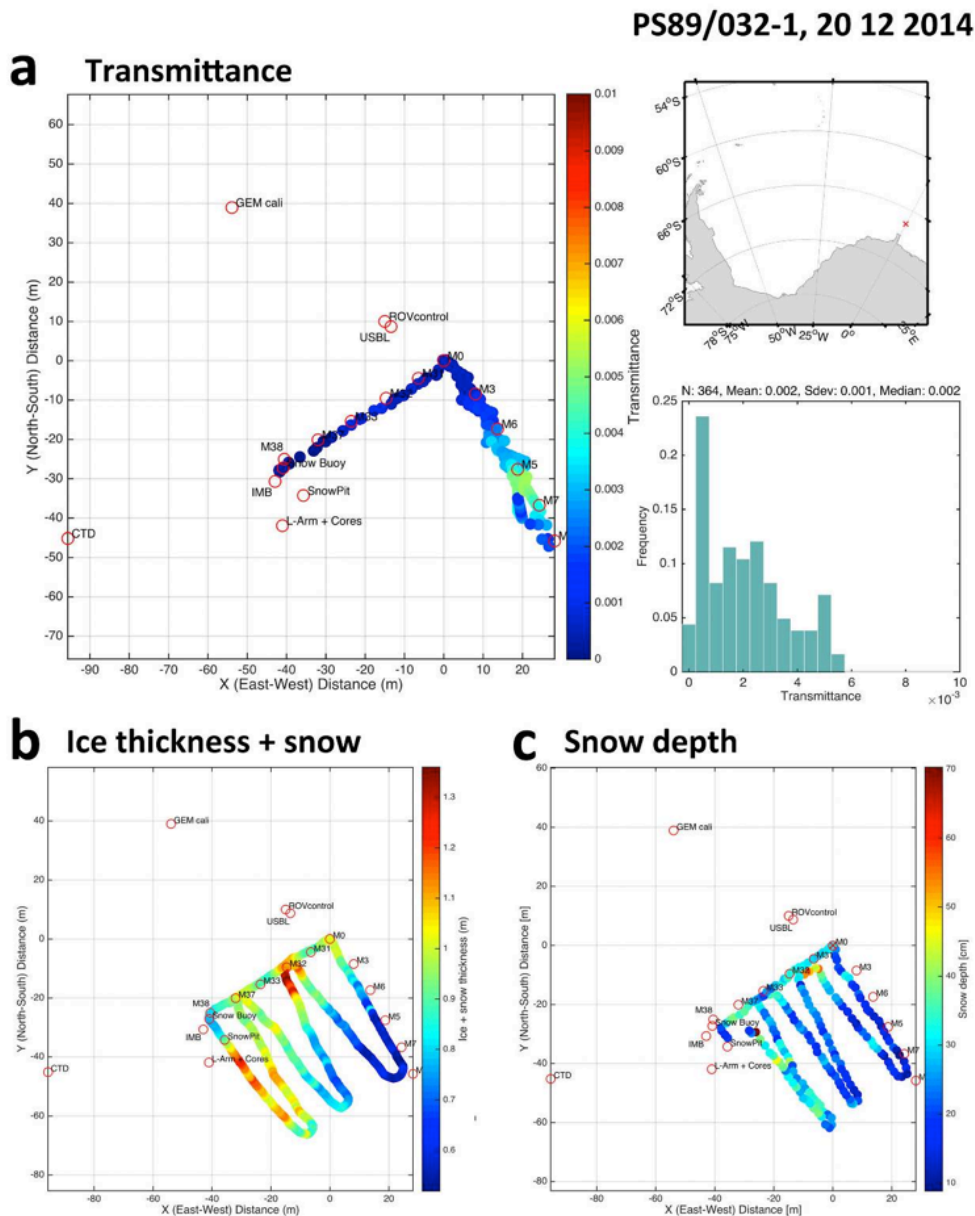


Fig. 3.2.1.4.5: Preliminary results of the example station PS89/032-1 (20.12.2014). (a) Left: Spatial distribution of the transmittance with the scale in fraction. Upper right: Location of the station. Lower right: Normalized histogram of the transmittance. (b) Spatial distribution of ice thickness (+snow) measured with GEM. (c) Spatial distribution of snow depth measured with magna probe. All maps contain the marker points of the ROV grid (M) and all other points of interest at the station.

Fig. 3.2.1.4.6 shows selected spectra of the spectral irradiance under sea ice and spectral transmittance of different ice types, as measured at station PS89/035-1 (22.12.2014). The transmittance spectra (Fig. 3.2.1.4.6b) show an increased absorption in the range of photosynthetically active radiation (PAR, 400 to 700 nm). This indicates high biological activity (photosynthesis) in sea ice and the water right under the ice. Hence, transmitted fluxes are reduced compared to bare sea ice. The maxima of the transmittance spectra are shifted towards longer wavelength.

Beyond the optical properties of sea ice, the ROV transects revealed the distribution of platelet ice under land-fast sea ice. The video recordings may be used for further insights into under-ice sea ice conditions, as well as for documentation and video-footage of the dives. Finally, the strong link between the ROV and SUIT (Section 3.2.2) sensors and approaches has to be highlighted, covering sea ice conditions on different scales.

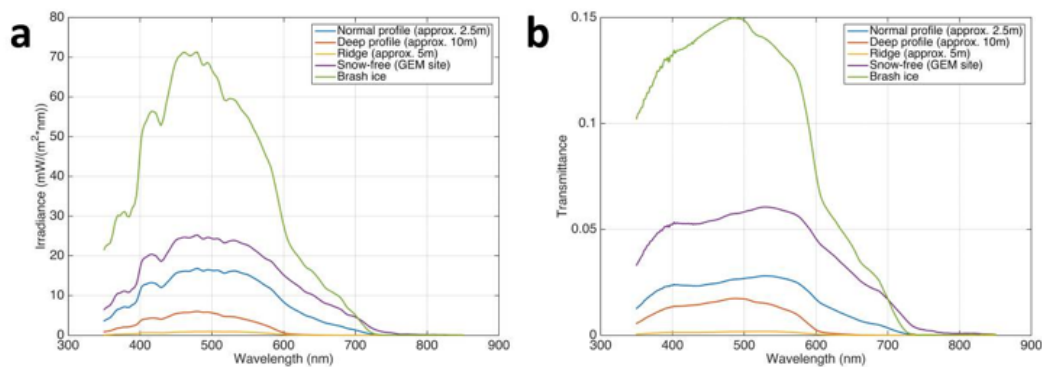


Fig. 3.2.1.4.6: Preliminary results (spectra) of station PS89/035-1 (22.12.2014). (a) Spectral irradiance under sea ice. (b) Spectral transmittance of snow and sea ice. In both figures spectra beneath different surface characteristics (or/and different depths) are shown: Level ice (diving depth: 2.5 m, blue), level ice (diving depth: 10 m, orange), old pressure ridge (diving depth: 5 m, yellow), snow free sea ice (diving depth: 2.5 m, purple), brash ice (2.5 m, green).

Data management

All ROV data will be released following final processing after the cruise. The processed data will be submitted to the PANGAEA database.

3.2.1.5 Deployments of autonomous ice tethered platforms (buoys)

Objectives

The investigation of physical sea-ice and snow parameters during station work can only give a snap-shot of the sea ice conditions. In order to obtain also information about the seasonal and inter-annual variability and evolution of the observed ice floes, we deploy autonomous ice tethered platforms (buoys), which measure the sea ice and snow characteristics also beyond the cruise. For that, we use different kinds of buoys. With ice mass-balance buoys (IMBs), the sea ice growth can be derived. Snow depth buoys measure the snow accumulation over the course of the year, and with surface velocity profilers (SVPs) we derive the sea-ice drift. In addition, buoys are partly equipped with air or body temperature and sea level pressure sensors. Combining the data from all these buoys, we will be able to better understand sea-ice processes and feedback mechanisms. Analyzing the drift of several buoys in the same region, deformation and dynamical processes of the pack ice may be derived.

3.2 Sea ice physics

Beyond the immediate value for our work, all SVP and snow buoys report their position together with measurements of surface temperature and atmospheric pressure directly into the Global Telecommunication System (GTS). Thus, these data may directly be used for weather prediction and numerical model applications.

Work at sea

In total, we deployed 6 SVP buoys and 3 sets of Snow Depth Buoys and IMBs in the eastern Weddell Sea (Fig. 3.2.1.5.1). For the SVPs we used the helicopter. During the first flight we could build up an array out of three buoys, each about 18 km apart from the ship. The other three buoys could not be deployed within an array and will be used for the sea-ice drift calculations only. The Snow Depth Buoy-IMB sets were deployed during sea-ice stations, two in the drift ice zone and one set on the fast ice in the Atka Bay. The fast-ice buoys are expected to break out of the bay and will be released to the drift ice zone by the end of austral summer. Sea-ice thickness, snow depth, and general sea-ice properties were noted down during deployment.

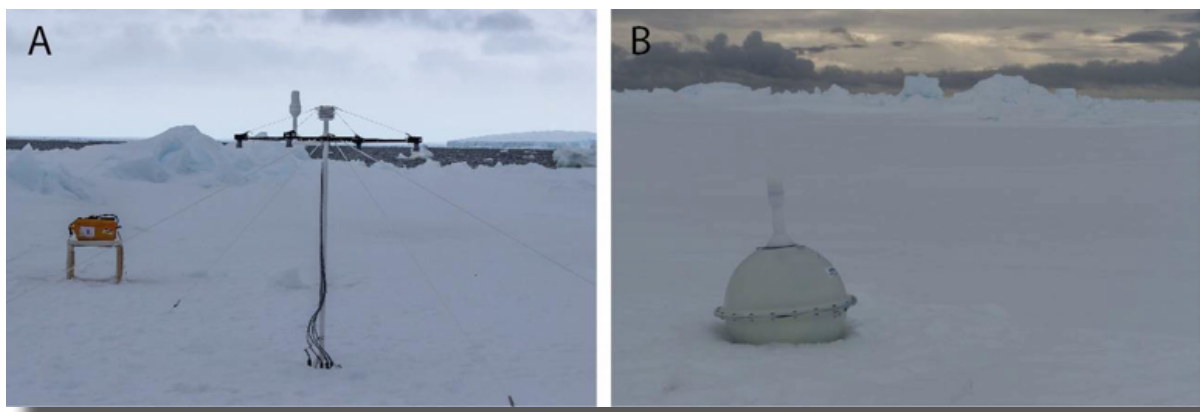


Fig. 3.2.1.5.1: a) Snow depth buoy combined with an IMB (yellow Pelicase), b) SVP buoy

Preliminary results

The SVP buoys will serve information on the sea-ice drift velocity and its seasonal behavior. Data will be transmitted as long as batteries will work. In case the sea ice doesn't survive the summer season, the SVPs will pass over to the sea and will measure ocean currents, as they are able to swim. Fig. 3.2.1.5.2 shows the drift velocities from the first three deployed SVP buoys over the measurement period from 03.01. - 24.01.2015. Although the buoys were originally deployed only few km apart from each other, their drift pattern varies already. Buoy PS89/H080-BUOY-SVP-1 drifted only very slowly, mostly with velocities less than 0.05 m/s. The total travelled distance of this buoy was 47 km in 21 days. PS89/H080-BUOY-SVP-2 velocities show a stronger variability. The travelled distance for the 3 week period was 200 km for that buoy. PS89/H080-BUOY-SVP-3 shows the highest drift velocities and highest variability for the drift. Accordingly, it travelled also the longest distance with 270 km for the three week period. Over the next months, the buoys will record further data from which we will calculate the sea-ice drift and deformation variability over the Weddell basin.

The snow depth buoys measure the snow accumulation at four spots by sonar sensors. Together with the IMBs, information on the snow depth changes, sea-ice growth and eventually estimates of flooding processes can be expected from the data. Fig. 3.2.1.5.2 shows an example for snow accumulation for the period 20.12.2014 to 24.02.2015. Due to the short time, there are barely any changes visible yet, neither in the snow depths nor in the meteorological data. Sea-ice growth data from the IMBs will be only processed after the cruise. Then, data

will also be combined with findings of former deployments during ANT-XXIX/6 and ANT-XXIX/9 and will help to understand the temporal and spatial variability of snow accumulation, sea-ice growth and eventually help to better understand flooding of Antarctic sea ice.

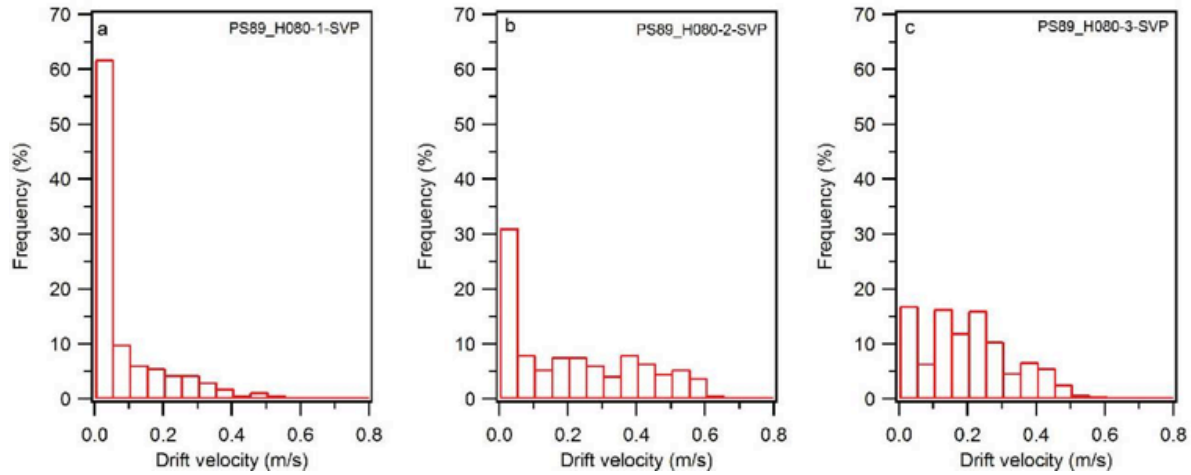


Fig. 3.2.1.5.2: Drift velocities of SVP a) PS89/H080-BUOY-SVP-1, b) PS89/H080-BUOY-SVP-2 and c) PS89/H080-BUOY-SVP-3. The figure demonstrates the spatial variability of drift velocities.

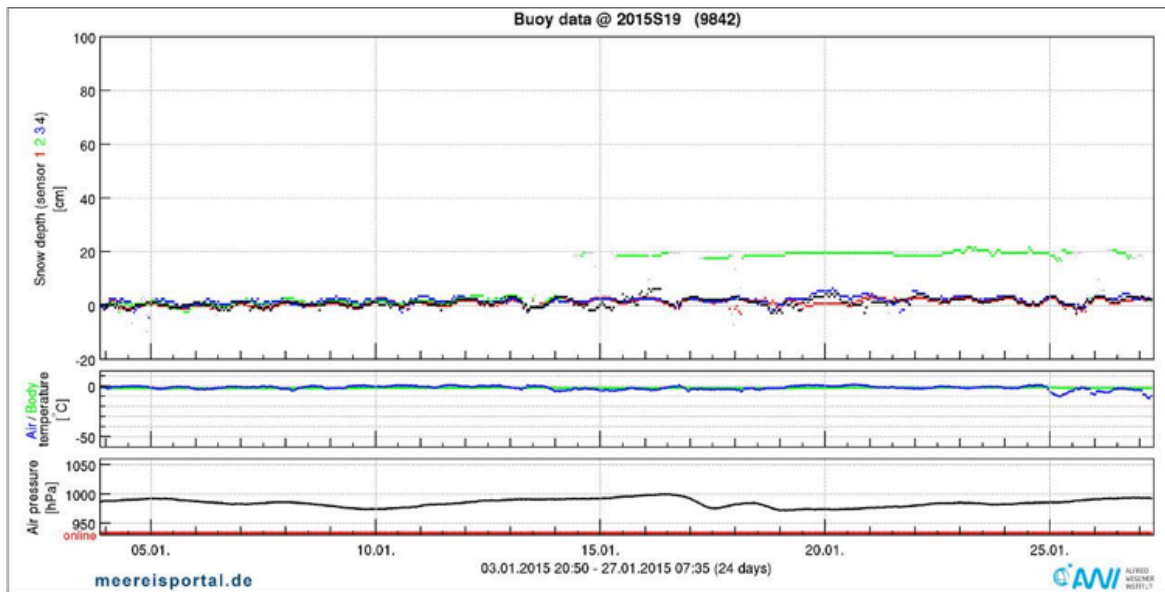


Fig. 3.2.1.5.3: Snow depth evolution combined with information on meteorological conditions for snow depth buoy 2014S19, deployed on 03.01.2014.

Tab. 3.2.1.5.1: List and initial positions of all deployed buoys during PS89 (ANT-XXX/2). Buoy names are identical to their name in www.meereisportal.de, where all data and buoy information is available in real time, and how the buoys report into international networks.

Label	Latitude	Longitude	Name	Date
PS89/032-1-BUOY-SNOW	-67.5772	0.1153	2014S17	20/12/2014
PS89/032-1-BUOY-IMB	-67.5772	0.1153	2014T3	20/12/2014
PS89/045-1-BUOY-SNOW	-70.4380	-8.2890	2015S18	03/01/2015
PS89/040-1-BUOY-IMB	-70.5274	-7.9584	2014FMI12	27/12/2014
PS89/044-1-BUOY-SNOW	-70.5270	-7.9590	2015S19	03/01/2015

3.2 Sea ice physics

Label	Latitude	Longitude	Name	Date
PS89/044-1-BUOY-IMB	-70.4380	-8.2890	2014FMI16	03/01/2015
PS89/H080-BUOY-SVP-1	-70.4272	-8.2762	2015P1	03/01/2015
PS89/H080-BUOY-SVP-2	-70.3314	-8.5850	2015P2	03/01/2015
PS89/H080-BUOY-SVP-3	-70.3186	-8.3763	2015P3	03/01/2015
PS89/H101-BUOY-SVP-1	-70.3558	-9.0408	2015P4	13/01/2015
PS89/H101-BUOY-SVP-2	-70.6083	-9.1917	2015P5	13/01/2015
PS89/H111-BUOY-SVP	-68.4940	-4.4888	2015P6	17/01/2015

Data management

All buoy positions and raw data are available in near real time through the sea-ice portal www.meereisportal.de. After the end of their lifetime (end of transmission of data) all data will be finally processed and made available in PANGAEA. All SVP and snow buoys report their position and atmospheric pressure directly into the Global Telecommunication System (GTS). Furthermore, all data are exchanged with international partners through the International Program for Antarctic Buoys.

3.2.1.6 Along track observations of sea ice conditions

Objectives

Over the last three decades, ship-based visual observations of the state of the sea ice and its snow cover have been performed over all seasons and serve the best-available observational data set of Antarctic sea ice. The recordings follow the Scientific Committee on Antarctic Research (SCAR) Antarctic Sea Ice Processes and Climate (ASPeCt) protocol and include information on sea-ice concentration, sea-ice thickness and snow depth as well as sea-ice type, surface topography and floe size. Those data are combined with information about meteorological conditions like air temperature, wind speed and cloud coverage. This protocol is a useful method to obtain a broad range of characterization and documentation of different sea-ice states and specific features during the cruise.

Work at sea

Every full hour during steaming, the sea-ice observations were carried out by trained scientists. The observations follow the ASPeCt protocol (Worby, 1999), with a newly developed software following the ASPeCt standard and being provided on a notebook on the ship's bridge. For every observation, pictures were taken in three different directions.

Date, time and position of the observation were obtained from the DSHIP system, along with standard meteorological data (current sea temperature, air temperature, true wind speed, true wind direction, visibility). The characterization of the ice conditions were then estimated by taking the average between observations to port side, ahead and to starboard side. Ice thicknesses of tilted floes were estimated by observing a stick attached to the ships starboard side.

Preliminary results

We performed hourly sea-ice observations as soon as we passed the first sea ice on 13 December 2014 at 60° 22.0' S and 0° 5.0' E. The ship left the sea-ice zone on 17 January 2015 at 68° 01.0' S and 3° 16.3' W. Over the 35 days, we did 214 individual observations. Sea-ice observations were skipped when the ship was stopped, for example at CTD stations and as long as we stayed in front of the shelf ice close to *Neumayer III*. The mean sea-ice

concentration was calculated as 65.3 % and the level sea-ice thickness to 0.9 m, which is comparable to the mode of EM-Bird measurements in the pack ice zone (see Chapter 3.2.1.1). Fig. 3.2.1.6.2 shows the variation of the sea-ice concentration and the sea-ice thickness along the cruise track. The sea-ice concentration varied between fully covered and open water in the polynya close to the shelf ice edge. Sea-ice thicknesses of up to 3 m were observed, but mostly it was between 0.7 m and 1.2 m on average.



Fig. 3.2.1.6.1: Example for pictures made to the portside, ahead and starboard showing different sea ice and weather conditions.

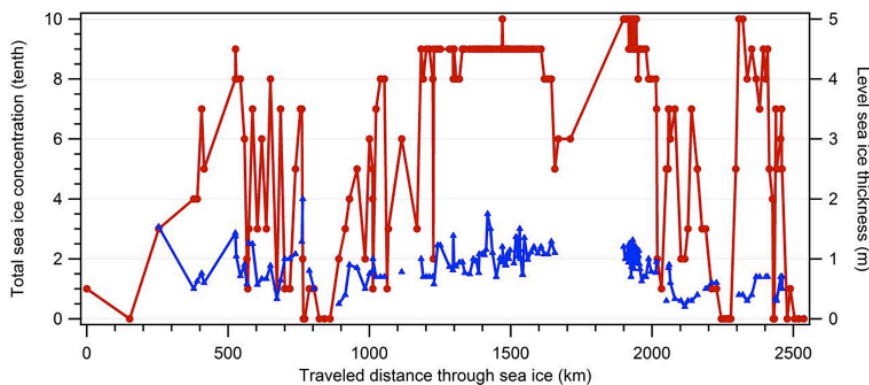


Fig. 3.2.1.6.2: Total sea-ice concentration and total level sea-ice thickness out of ASPeCt observations over travelled distance within the sea ice zone.

Data management

The visual sea-ice observations will be post-processed after the cruise and will be published together with the taken pictures in PANGAEA within two months after the cruise.

References

Worby AP (1999) Observing operating in the Antarctic sea ice: A practical guide for conducting sea ice observations from vessels operating in the Antarctic pack ice.

3.2.1.7 Retrieval of satellite remote sensing data

Objectives

One goal of this part was to improve our ability to interpret synthetic aperture radar (SAR) images of sea ice in order to gain additional knowledge about ice type composition and dynamical properties. From the combination of *in-situ* field measurements with coordinated satellite data acquisitions we aim to directly match both scales of observations. Based on the

3.2 Sea ice physics

ASPeCt-Ship observations, additional photographic documentation and coordinate satellite acquisitions over field sites we plan to investigate the influence that ice properties might have on the received radar signal both for X-Band (TerraSAR-X) as well as for C-Band (Sentinel-1).

A second goal was the coordinated acquisitions of TerraSAR-X images over buoy arrays deployed during the cruise to compare drift patterns of single buoys and the relative changes of distances between buoys with ice drift and deformation retrieved from a satellite image time series. This will help to validate the drift algorithms and contribute to the analysis of sea ice dynamics and deformation for larger areas at high spatial resolution.

Work at sea

During the cruise we acquired 12 TerraSAR-X scenes in total. Some of them were acquired for the purpose of ship navigation to further investigate the potential of Near-Real-Time data for supporting navigation of research vessels in the Polar Regions. The other images were acquired as complementary data source for stations or over the fast ice within one or two days. The acquired data is listed in Table 3.2.1.7.1.

Tab. 3.2.1.7.1: Acquired TerraSAR-X Images during PS89 (ANT-XXX/2)

Start Date/Time	End Date/Time	Sensor Mode	Polarization	Comment
2014-12-10 19:55:44,44	10.12.2014 19:55:59,59	ScanSAR	Single HH	Test scene
2014-12-19 04:31:08,08	19.12.2014 04:31:27,27	ScanSAR	Single HH	<i>Polarstern</i>
2014-12-20 04:14:24,24	20.12.2014 04:14:33,33	Stripmap	Single HH	Ice station
2014-12-21 03:57:37,37	21.12.2014 03:57:51,51	ScanSAR	Single HH	Ice conditions
2014-12-25 20:21:34,34	25.12.2014 20:21:41,41	Stripmap	Dual HH/VV	Fast ice
2014-12-26 04:06:59,59	26.12.2014 04:07:06,06	Stripmap	Single HH	Fast ice
2015-01-01 03:58:31,31	01.01.2015 03:58:32,32	Spotlight	Single HH	Fast ice
2015-01-10 04:32:01,01	10.01.2015 04:32:15,15	ScanSAR	Single HH	Fast ice
2015-01-10 04:32:19,19	10.01.2015 04:32:36,36	ScanSAR	Single HH	Ice conditions
2015-01-14 20:55:38,38	14.01.2015 20:55:51,51	ScanSAR	Single HH	TSX+S-1
2015-01-15 20:38:39,39	15.01.2015 20:38:48,48	Stripmap	Single HH	No <i>Polarstern</i>
2015-01-17 20:04:32,32	17.01.2015 20:04:46,46	ScanSAR	Single HH	<i>Polarstern</i>

The long stay at Atka Bay allowed us to acquire data in three different imaging modes in these regions, which are supplemented by the respective operationally acquired Sentinel-1 images in this area. For this purpose ESA provided us with the respective orbit plans for our cruise track. The long stay at Atka Bay might provide interesting possibilities for comparisons of different image products and detailed comparisons between C- and X- band. A list of acquired Sentinel-1 data is shown in Table 3.2.1.7.2.

The Sentinel-1 data were received using the Polarview portal for low-resolution images providing a general overview (resolution 375 x 375 m) and for special cases as processed jpeg2000 data from the EOS group at the AWI. In preparation to the cargo operations at *Neumayer III*, Sentinel-1 images were provided for the AWI logistics.

In contrast to the original plan we did not track the deployed buoy array. The adaption of the cruise plan and the lack of suitable ice conditions close to the adapted cruise track prevented the deployment of full buoy arrays suitable for studies of deformation. Since we had to return to Cape Town after directly after leaving the Atka Bay without crossing the Weddell Sea, we ordered fewer images than originally granted by DLR.

Data management

The TerraSAR-X data acquired during the cruise belongs to DLR. It will be available after the retention period via the electronic data catalogue of the DLR based on scientific proposals. The Sentinel-1 data acquired over *Polarstern* has been acquired by the European Space Agency (ESA) and is freely available for download from their Sentinel-1 Scientific Data Hub SciHub (<https://scihub.esa.int/>) without any retention period since the day of acquisition.

Tab. 3.2.1.7.2: Acquired Sentinel-1 Images during PS89 (ANT-XXX/2). All scenes were acquired in extra wide swath (EWS) mode with single HH polarization, and *Polarstern* was in the scene during acquisition.

Start Date/Time	End Date/Time
17.12.2014 19:59	17.12.2014 20:03
19.12.2014 19:44	19.12.2014 19:47
20.12.2014 20:23	20.12.2014 20:28
22.12.2014 20:07	22.12.2014 20:11
25.12.2014 20:31	25.12.2014 20:36
26.12.2014 21:12	26.12.2014 21:17
28.12.2014 20:56	28.12.2014 21:01
30.12.2014 20:40	30.12.2014 20:44
31.12.2014 21:20	31.12.2014 21:25
02.01.2015 21:04	02.01.2015 21:07
04.01.2015 20:48	04.01.2015 20:50
07.01.2015 21:12	07.01.2015 21:15
09.01.2015 20:56	09.01.2015 20:58
11.01.2015 20:40	11.01.2015 20:42
12.01.2015 21:21	12.01.2015 21:23
14.01.2015 21:04	14.01.2015 21:07
16.01.2015 20:48	16.01.2015 20:50

3.3 Biology

3.3.1 Sea ice ecology, pelagic food web and top predator studies

Hauke Flores^{1,2}, Jan Andries van Franeker³,
Anton Van de Putte⁴, Giulia Castellani¹,
Fokje Schaafsma³, Julia Ehrlich²,
Martina Vortkamp¹, André Meijboom³,
Bram Feij⁵, Michiel van Dorssen⁶

¹AWI
²UHH
³IMARES
⁴RBINS
⁵NIOZ
⁶van Dorssen Metaalbewerking

Grant No: AWI-PS89_02

Objectives

Sea ice ecology, pelagic food web and top predator studies during PS89 were a main contribution to the Sea Ice Physics and Ecology Study (SIPES). SIPES was designed as an inter-disciplinary field study focussing on the inter-connection of sea ice physics, sea ice biology, biological oceanography and top predator ecology. Pelagic food webs in the Antarctic sea ice zone can depend significantly on carbon produced by ice-associated microalgae. Future changes in Antarctic sea ice habitats will affect sea ice primary production and habitat structure, with unknown consequences for Antarctic ecosystems. Antarctic krill *Euphausia superba* and other species feeding in the ice-water interface layer may play a key role in transferring carbon from sea ice into the pelagic food web, up to the trophic level of birds and mammals (Flores et al. 2011, 2012). To better understand potential impacts of changing sea ice habitats for Antarctic ecosystems, the HGF Young Investigators Group *Iceflux* in cooperation with IMARES (*Iceflux-NL*), aim to quantify the trophic carbon flux from sea ice into the under-ice community and investigate the importance of sea ice in the support of living resources. This should be achieved by 1) quantitative sampling of the in-ice, under-ice and pelagic community in relation to environmental parameters; 2) using molecular and isotopic biomarkers to trace sea ice-derived carbon in pelagic food webs; 3) applying sea ice-ocean models to project the flux of sea ice-derived carbon into the under-ice community in space and time, and 4) studying the diet of sea ice-associated organisms.

In the Southern Ocean, the exploitation of marine living resources and the conservation of ecosystem health are tightly linked to each other in the management framework of the Convention for the Conservation of Antarctic Marine Living Resources (CCAMLR). Antarctic krill *Euphausia superba* is important in this context, both as a major fisheries resource, and as a key carbon source for Antarctic fishes, birds, and mammals. Similar to Antarctic krill, several abundant endothermic top predators have been shown to concentrate in pack-ice habitats in spite of low water column productivity (van Franeker et al. 1997). Investigations on the association of krill and other key species with under-ice habitats were complemented by systematic top predator censuses in order to develop robust statements on the impact of changing sea ice habitats on polar marine resources and conservation objectives.

The evolutionary processes supported by gene flow and genetic selection interact with ecological processes as they overlap temporally to some extent. While gene flow has the tendency to homogenise populations, selective pressure may lead to population differentiation over evolutionary time scales. Throughout the life history of marine organisms dispersal and connectivity play crucial roles in short and long term survival, fitness and evolution. Connectivity and dispersal are the result of interacting environmental limitations and dispersal capacity, which is influenced by physical and biological processes. The physical processes relate to hydrodynamics (barriers such as the Antarctic Polar Front (APF), transport routes (through deep-water formation) and geographical features (e.g., shallow land bridge of the Scotia Arc (Arntz et al. 2005; Ingels et al. 2006)). Biological processes include behavior, life-history traits,

trophic niche, size and other basic biological characteristics. The Southern Ocean forms a unique environment to study evolutionary patterns over different time scales. During this expedition fish and amphipods samples for molecular analysis were collected. These samples were used for Barcoding (species identification) and phylogeographic and population genetic work at RBINS.

Work at sea

SUIT sampling

A Surface and Under-Ice Trawl (SUIT: van Franeker et al. 2009) was used to sample the pelagic fauna down to 2 m under the ice and in open surface waters. The SUIT had two nets, one 0.3 mm mesh plankton net and a 7 mm mesh shrimp net. During SUIT tows, data from the physical environment were recorded using a bio-environmental sensor array, e.g. water temperature, salinity, ice thickness, and multi-spectral light transmission. Seven SUIT deployments were completed along the 0° meridian from open waters into the closed pack-ice. Six hauls directed at the investigation of the vertical distribution of zooplankton in open waters were conducted near Atka Bay. On the return trajectory from Atka Bay to Cape Town, another 5 hauls were completed in the marginal ice zone and the open Ocean (see appendix Table 3.3.1A1). An overview of the sampling locations is given in Fig. 3.3.1.1. Macrofauna samples from the SUIT shrimp net were sorted to the lowest possible taxonomic level. The catch was entirely preserved frozen (-20°C / -80°C), on ethanol (70 % / 100 %), or on 4 % formaldehyde/seawater solution, depending on analytical objectives. In euphausiids, the composition of size and sexual maturity stages was determined 48 hrs after initial preservation in formaldehyde solution.

Pelagic sampling

A Multiple opening Rectangular Midwater Trawl (M-RMT) was used to sample the pelagic community. During sampling, sampling depth, water temperature and salinity were recorded with a CTD probe attached to the bridle of the net. The standard sampling strata in offshore waters were 800-200 m, 200-50 m, and 50 m to surface. In the coastal waters near Atka Bay, sampling was conducted over the strata 200-100 m, 100-50 m, and 50 m to surface. We conducted 15 depth-stratified hauls with the M-RMT, each sampling 3 distinct depth layers. Five hauls were conducted between 57°S and 66°S on the 0° meridian (Station 18-30), 5 hauls were conducted near Atka Bay (Station 40-59), and 5 hauls were completed after leaving Atka Bay (Station 66-80; (Fig. 3.3.1.1)). The catch was sorted by depth stratum and taxon, and size measurements on euphausiids and fish larvae were performed in the analogous procedure described above for SUIT sampling.

Polarstern's EK60 echosounder recorded the distribution of acoustic targets continuously during sailing. Our sampling frequencies were 38 kHz, 70 kHz, 120 kHz, and 200 kHz. During station work, the EK60 was switched off to minimize potential risks for marine mammals approaching the ship. All EK60 data were backed up on the ship's mass storage server.

For biomarker analysis, Particulate Organic Matter (POM) was collected from filtered seawater obtained from the CTD rosette. Chlorophyll samples were filtered from CTD rosette water samples to calibrate fluorometers built in the ship's CTD, *Polarstern's* ferry box, and the SUIT's CTD (Table 3.3.1.1).

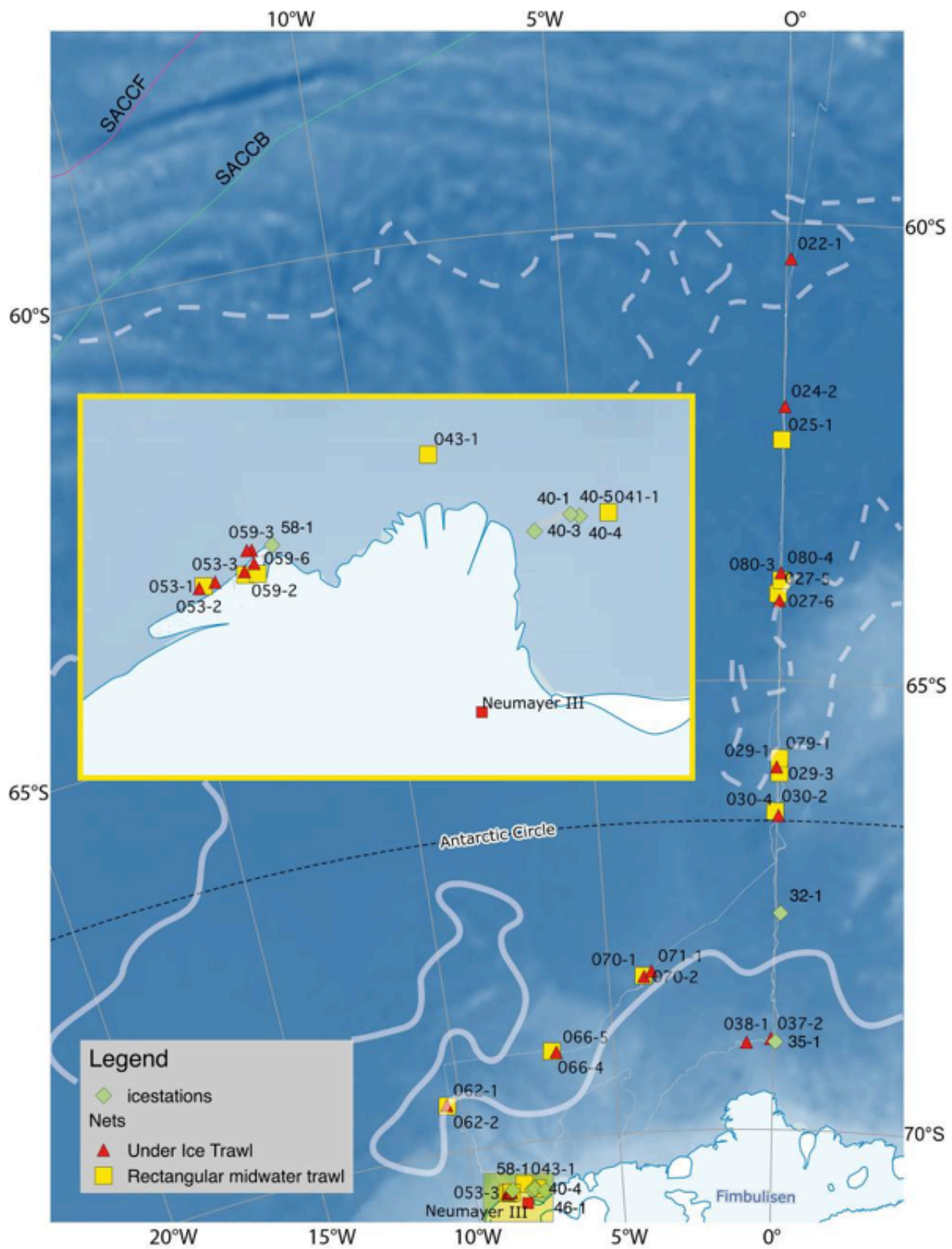


Fig. 3.3.1.1: Overview of stations sampled by the biological sampling of SIPES during PS89. The dashed white line indicates the position of the ice edge at the beginning of the sampling period; the position of the ice edge at the end of the sampling is indicated by a continuous white line. The cruise track is shown as a light-grey line.

Table 3.3.1.1: Summary of CTD casts performed and water samples collected. ferry: water sample from inflow of the ship's FerryBox system

Date	Time	Station	Gear	PositionLat	PositionLon	Depth [m]	Chl max depth [m]	Sampled depths [m]
07.12.2014	18:04:00	PS89/0006-1	CTD/rosette water sampler	46° 12.90' S	5° 40.50' E	4831.2	60	15,24,60,100
08.12.2014	07:43:00	PS89/0007-1	CTD/rosette water sampler	47° 40.28' S	4° 15.22' E	4540.5	50	15,25,50,100
09.12.2014	14:51:00	PS89/0009-1	CTD/rosette water sampler	50° 15.30' S	1° 25.53' E	3892.5	75	15,50,75,100,ferry
10.12.2014	11:48:00	PS89/0011-1	CTD/rosette water sampler	52° 28.72' S	0° 0.06' W	2597.6	80	35,50,80,100
11.12.2014	15:13:00	PS89/0014-1	CTD/rosette water sampler	54° 59.99' S	0° 0.02' W	1704.9	50	25,50,75,100,ferry
12.12.2014	23:17:00	PS89/0019-1	CTD/rosette water sampler	58° 0.08' S	0° 0.12' E	4528.3	25	15,25,50,100,ferry
14.12.2014	16:50:00	PS89/0023-1	CTD/rosette water sampler	60° 59.86' S	0° 0.38' W	5393.2	45	15,45,50,100,ferry
16.12.2014	00:14:00	PS89/0026-1	CTD/rosette water sampler	62° 59.37' S	0° 0.36' E	5310.9	40	9,40,60,100,ferry
19.12.2014	02:05:00	PS89/0030-1	CTD/rosette water sampler	66° 27.71' S	0° 1.49' W	4500.2	30	15,30,50,100,ferry
21.12.2014	02:49:00	PS89/0033-1	CTD/rosette water sampler	68° 0.03' S	0° 1.26' W	4512.9	40	5,40,75,120,ferry
22.12.2014	12:15:00	PS89/0035-1	CTD/ice	69° 0.14' S	0° 4.03' E			50
22.12.2014	23:23:00	PS89/0036-1	CTD/rosette water sampler	69° 0.61' S	0° 1.62' W	3369.4	25	15,25,50,100,ferry
27.12.2014	11:00:00	PS89/0040-1	CTD/ice	70° 5.27' S	7° 57.52' W			50
29.12.2014	11:00:00	PS89/0040-3	CTD/ice	70° 5.34' S	8° 4.54' W			50
30.12.2014	10:50:00	PS89/0040-4	CTD/ice	70° 5.27' S	7° 57.52' W			50
03.01.2015	00:24:00	PS89/0042-1	CTD/rosette water sampler	70° 34.46' S	9° 3.33' W	467	20	15,20,50,100,ferry
03.01.2015	05:17:00	PS89/0040-11	CTD/rosette water sampler	70° 31.40' S	7° 57.72' W	232	60	15,30,60,100,ferry
04.01.2015	10:00:00	PS89/0046-1	CTD/ice	70° 5.59' S	7° 38.56' W			50
07.01.2015	22:17:00	PS89/0049-1	CTD/rosette water sampler	70° 31.31' S	8° 45.46' W	156	20	20,ferry
08.01.2015	04:14:00	PS89/0049-7	CTD/rosette water sampler	70° 31.29' S	8° 45.44' W	153	10	10,ferry
08.01.2015	09:12:00	PS89/0049-12	CTD/rosette water sampler	70° 31.38' S	8° 45.58' W	179.2	25	25
09.01.2015	21:06:00	PS89/0052-1	CTD/rosette water sampler	70° 31.39' S	8° 45.58' W	168	30	30,ferry
10.01.2015	00:09:00	PS89/0052-4	CTD/rosette water sampler	70° 31.32' S	8° 45.42' W	155	15	15,ferry
10.01.2015	04:12:00	PS89/0052-8	CTD/rosette water sampler	70° 31.32' S	8° 45.48' W	157	15	15,ferry
10.01.2015	08:04:00	PS89/0052-12	CTD/rosette water sampler	70° 31.38' S	8° 45.49' W	163	50	50,ferry
11.01.2014	19:11:00	PS89/0058-1	CTD/ice	70° 30.80' S	8° 43.93' W			50
16.01.2015	10:55:00	PS89/0066-2	CTD/rosette water sampler	69° 0.31' S	6° 59.19' W	2948.8	50	15,25,50,100,ferry
20.01.2015	07:41:00	PS89/0080-1	CTD/rosette water sampler	63° 55.07' S	0° 0.44' E	5210.2	25	15,25,50,100,ferry
21.01.2015	10:48:00	PS89/0081-1	CTD/rosette water sampler	61° 0.02' S	0° 0.13' E	5384.6	15	15,25,50,100,ferry

Tab. 3.3.1.2. Parameters of SUIIT and M-RMT stations. SUIIT under ice = stations where SUIIT was trawled partly or entirely under ice; EcoRegion = broad biogeographical region: OW = open waters north of the ice edge; SIZ = Sea ice zone; Atka = shelf waters near Atka Bay

STATION	HAUL	GEAR	POSlat	POSITION	STRIT_TRAWL	END_TRAWL	SUIIT under ice	Eco Region	Comment
PS89/0022-1	1	SUIIT	-60.384	0.093	14.12.2014 08:48	14.12.2014 09:18	NO	OW	1st SUIIT station of survey; cable length only estimated visually
PS89/0024-2	2	SUIIT	-61.985	0.030	15.12.2014 09:47	15.12.2014 10:17	YES	SIZ	Problem with oxenauge of weight, weight has been pulked up between waypoint 011 and 012. Brown discolouration of ice visible.
PS89/0027-6	3	SUIIT	-64.110	-0.046	17.12.2014 17:52	17.12.2014 18:22	NO	SIZ	
PS89/0029-1	4	SUIIT	-65.948	-0.040	18.12.2014 09:28	18.12.2014 09:58	YES	SIZ	
PS89/0030-4	5	SUIIT	-66.492	0.048	19.12.2014 14:09	19.12.2014 14:49	YES	SIZ	
PS89/0037-2	6	SUIIT	-68.977	-0.091	23.12.2014 11:07	23.12.2014 11:17	YES	SIZ	Got stuck, hauled in after short time
PS89/0038-1	7	SUIIT	-69.017	-0.818	23.12.2014 17:41	23.12.2014 17:54	YES	SIZ	SUIIT lost due to broken cable at 17:54 , recovered, 1 cod end lost
PS89/0053-2	8	SUIIT	-70.541	-8.941	10.01.2015 10:53	10.01.2015 11:33	NO	Atka	Large open water 'puddle' near ice shelf. Surrounding ice approx. 2-3 thick but not close to trawl.
PS89/0053-3	9	SUIIT	-70.538	-8.901	10.01.2015 23:08	10.01.2015 23:39	NO	Atka	Large open water 'puddle' near ice shelf. Surrounding ice approx. 2-3 thick but not close to trawl.
PS89/0059-1	10	SUIIT	-70.534	-8.819	12.01.2015 01:12	12.01.2015 01:42	NO	Atka	Trawl in our 'puddle' near ice shelf. Surrounding ice approx. 2-3 thick approx. 300 m away.
PS89/0059-3	11	SUIIT	-70.518	-8.790	12.01.2015 08:16	12.01.2015 08:32	NO	Atka	Trawl in our 'puddle' near ice shelf. Surrounding sea ice approx. 2-3 thick.
PS89/0059-4	12	SUIIT	-70.516	-8.806	12.01.2015 12:42	12.01.2015 13:11	NO	Atka	Trawl in our 'puddle' near ice shelf. Surrounding sea ice approx. 2-3 thick.
PS89/0059-5	13	SUIIT	-70.531	-8.790	12.01.2015 20:06	12.01.2015 20:41	NO	Atka	Trawl in our 'puddle' near ice shelf. Surrounding sea ice approx. 2-3 thick.
PS89/0062-1	14	SUIIT	-69.462	-1.461	15.01.2015 15:35	15.01.2015 16:11	YES	SIZ	10 - 20 cm snow. Note that ice conditions change from waypoint 115 onwards.
PS89/0066-5	15	SUIIT	-69.027	-6.812	16.01.2015 17:27	16.01.2015 17:57	NO	OW	
PS89/0070-2	16	SUIIT	-68.259	-3.925	17.01.2015 14:07	17.01.2015 14:41	YES	SIZ	Lot of brown discolouration on underside of ice. Peak weight on cable: 44 tons. 10-20 cm snow.

3. Scientific Programmes

STATION	HAUL	GEAR	POSlat	POSITION	STRT_TRAWL	END_TRAWL	SUIT under ice	Eco Region	Comment
PS89/0071-1	17	SUIT	-68.203	-3.689	17.01.2015 16:36	17.01.2015 17:06	YES	SIZ	Lot of loose ice in between floes, occasionally small open water leads. Note change in cable length.
PS89/0080-4	18	SUIT	-63.814	-0.009	20.01.2015 14:48	20.01.2015 15:21	NO	OW	Last SUIT station!
PS89/0018-1		M-RMT	-57.44	0.11	12-12-2014 15:45	12-12-2014 16:44	NO	OW	
PS89/0025-1		M-RMT	-62.35	-0.04	15-12-2014 14:42	15-12-2014 15:12	NO	SIZ	
PS89/0027-5		M-RMT	-64.04	-0.07	17-12-2014 15:42	17-12-2014 16:19	NO	SIZ	
PS89/0029-3		M-RMT	-66.02	0.05	18-12-2014 14:43	18-12-2014 15:19	YES	SIZ	
PS89/0030-2		M-RMT	-66.45	-0.06	19-12-2014 04:36	19-12-2014 05:08	YES	SIZ	Voltage 316, current 0,02,
PS89/0040-2		M-RMT	-70.53	-7.89	27-12-2014 11:29	27-12-2014 11:35	NO	Atka	next to iceedge, Neumayer
PS89/0043-1		M-RMT	-70.46	-8.31	03-01-2015 13:46	03-01-2015 13:51	NO	Atka	
PS89/0053-1		M-RMT	-70.54	-8.91	10-01-2015 09:20	10-01-2015 09:26	NO	Atka	
PS89/0059-2		M-RMT	-70.53	-8.81	12-01-2015 03:02	12-01-2015 03:06	NO	Atka	
PS89/0059-6		M-RMT	-70.53	-8.78	12-01-2015 23:15	12-01-2015 23:19	NO	Atka	
PS89/0062-2		M-RMT	-69.47	-10.44	15-01-2015 17:49	15-01-2015 18:19	YES	SIZ	Bucket between the nets, all RMT 8 nets not complete open, RMT 1 ok
PS89/0066-4		M-RMT	-69.02	-6.94	16-01-2015 15:33	16-01-2015 16:08	NO	OW	
PS89/0070-1		M-RMT	-68.25	-3.95	17-01-2015 11:43	17-01-2015 12:13	YES	SIZ	Net 3 didn't released (not in the water and not on deck)
PS89/0079-1		M-RMT	-65.83	0.05	19-01-2015 11:01	19-01-2015 11:37	NO	OW	net not released
PS89/0080-3		M-RMT	-63.89	0	20-01-2015 12:08	20-01-2015 13:36	NO	OW	net 1 open in to the water, it fished from 0 - 800 and from 800- 200m depth

Sea ice work

Our sea ice work was conducted in close collaboration with the AWI sea ice physics group (M. Nicolaus & S. Schwegmann). A total of 8 sea ice stations were sampled during PS89, of which 2 were completed during the southward passage on the 0° meridian (Table 3.3.1.1). The majority of stations (6) focused on the landfast ice of the Atka Bay (Fig. 3.3.1.1). Depending on time availability and weather conditions, the following sampling procedure was completed during sea ice stations:

- a) We conducted measurements of the under-ice light field using a RAMSES spectroradiometer attached to an L-arm sampling light spectra under the sea ice well away from the drilling hole. At each L-arm site, a bio-optical core was taken straight above one RAMSES measurement point. Additional bio-optical cores were sampled above RAMSES measurement points along ROV transects of the sea ice physics group.
- b) Various ice cores were taken for analysis of physical, biogeochemical and biological properties: Archive, texture, salinity and chlorophyll *a* content, particulate organic matter (POM) for biomarker analysis, sea ice infauna, and DNA (eukaryote microbial communities). At each coring site, snow depth, ice thickness and freeboard were noted.
- c) We lowered a CTD probe equipped with a fluorometer through a coring hole down to 50 m depth, thus obtaining vertical profiles of temperature, salinity and chlorophyll *a* content in the upper 50 m under the sea ice.
- d) We collected under-ice water for the analysis of the phytoplankton and microzooplankton composition and DNA sequencing with a handheld Kemmerer water sampler lowered to approximately 1 m under the ice.
- e) At several ice stations in the Atka Bay, an *in-situ* pump was used to sample zooplankton from the platelet ice layer under the coastal fast-ice.
- f) In collaboration with Melchior Gonzales-Davila and Magdalena Santana-Casiano we collected additional water samples for carbonate studies at depths of 20 m, 15 m, 10 m, 7 m, 5 m, 3 m, and 1 m under the ice.

Archive and texture cores were stored in the ship's -20°C storage room and transported back to AWI. Retained sections of all other cores were carefully melted at 4°C in the ship's temperature-controlled laboratory container. In bio-optical cores, the bottom 10 cm were separated from the rest of the core, and both retained sections were processed for chlorophyll *a* content in order to determine the relationship of ice algal biomass with the under-ice spectral light properties. Additionally, subsamples from the melted bio-optical core sections were taken for pigment analysis (HPLC), POM, and microscopic analysis. Ice cores for salinity and chlorophyll *a* content were cut in 10 cm pieces to construct vertical profiles of these parameters. In cores for POM, sea ice infauna and DNA analysis, 10 cm sections from the bottom, the top and the inner part of the core were retained for sample collection. 200 ml filtered sea water per cm core section were added to melting sections of sea ice infauna cores. Filters for POM and pigment analysis obtained from melted ice core sections and water samples were frozen at -80°C. Microscopy samples from bio-optical cores, under-ice microzooplankton and sea ice infauna were stored at 2°C on 4 % formaldehyde/seawater solution.

Tab 3.3.1.3: List of the ice stations sampled, and number of ice cores taken at each sampling site. For each ice station it is specified if there have been conducted under ice radiation measurements (L-arm), under-ice water sampling, under-ice zooplankton sampling by using a self-constructed pump (Pump), water column sampling for CO₂ and pH measurements (CO₂ samples) and under-ice CTD profiles. Ice stations 32-1 and 35-1 were sampled on drifting sea ice floes, whereas stations 40-1 to 58-1 were sampled on fast ice in Atka Bay

Station N°	Position	Date	N° of cores	L-arm	Water Samp.	Pump	CO ₂ Samp.	CTD
32-1	67° 34.66' S 0° 8.86' E	20.12.2014	14	YES	NO	NO	NO	NO
35-1	69° 0.82' S 0° 4.03' E	22.12.2014	11	YES	YES	NO	YES	YES
40-1	70° 31.60' S 7° 57.52' W	27.12.2014	8	YES	NO	NO	NO	YES
40-3	70° 32.03' S 8° 4.54' W	29.12.2014	2	NO	YES	YES	YES	YES
40-4	70° 31.60' S 7° 57.52' W	30.12.2014	0	NO	YES	YES	YES	YES
40-5	70° 31.45' S 7° 58.83' W	31.12.2014	3	YES	NO	NO	NO	NO
46-1	70° 33.54' S 7° 38.56' W	04.01.2015	10	YES	YES	YES	YES	YES
58-1	70° 30.80' S 8° 43.93' W	11.01.2015	7	NO	NO	YES	NO	YES

Tab. 3.3.1.4: List of ice cores taken during PS89, with relative position on the ice floe (see Nicolauset al., this volume), and corresponding spectral, measurement site (Marker)

Station N°	LABEL	POSITION	MARKER
32-1	PS89/32-1-OPT-1	(-32,-20)	L-arm
"	PS89/32-1-OPT-2	(-23,-16)	M37
"	PS89/32-1-OPT-3	(-14,-9)	M33
"	PS89/32-1-OPT-4	(-7,-4)	M32
"	PS89/32-1-OPT-5	(-41,-42)	M31
"	PS89/32-1-LSI-1	(-41,-42)	L-arm
"	PS89/32-1-LSI-2	(-41,-42)	L-arm
"	PS89/32-1-DNA	(-41,-42)	L-arm
"	PS89/32-1-MEI-1	(-41,-42)	L-arm
"	PS89/32-1-MEI-2	(-41,-42)	L-arm
"	PS89/32-1-DEN	(-41,-42)	L-arm
"	PS89/32-1-ARC	(-41,-42)	L-arm

3.3 Biology

Station N°	LABEL	POSITION	MARKER
"	PS89/32-1-TEX	(-41,-42)	L-arm
"	PS89/32-1-SAL	(-22,11)	L-arm
35-1	PS89/35-1-OPT-1	(-17,23)	Coring
"	PS89/35-1-OPT-2	(-22,11)	M6
"	PS89/35-1-LSI-1	(-22,11)	Coring
"	PS89/35-1-LSI-2	(-22,11)	Coring
"	PS89/35-1-DNA	(-22,11)	Coring
"	PS89/35-1-MEI-1	(-22,11)	Coring
"	PS89/35-1-MEI-2	(-22,11)	Coring
"	PS89/35-1-DEN	(-22,11)	Coring
"	PS89/35-1-ARC	(-22,11)	Coring
"	PS89/35-1-TEX	(-22,11)	Coring
"	PS89/35-1-SAL	(-35,13)	Coring
40-1	PS89/40-1-BIO-1	(31,9)	Cores+L-arm
"	PS89/40-1-BIO-2	(-35,13)	M30m
"	PS89/40-1-LSI	(-35,13)	Cores+L-arm
"	PS89/40-1-MEI	(-35,13)	Cores+L-arm
"	PS89/40-1-DEN	(-35,13)	Cores+L-arm
"	PS89/40-1-ARC	(-35,13)	Cores+L-arm
"	PS89/40-1-TEX	(-35,13)	Cores+L-arm
"	PS89/40-1-SAL	-	Cores+L-arm
40-3	PS89/40-3-MEI-1	-	-
"	PS89/40-3-MEI-2	-	-
40-5	PS89/40-5-OPT	-	-
"	PS89/40-5-MEI	(-44,-61)	-
46-1	PS89/46-1-OPT-1	(-44,-61)	L-arm+Cores
"	PS89/46-1-LSI-1	(-44,-61)	L-arm+Cores
"	PS89/46-1-LSI-2	(-44,-61)	L-arm+Cores
"	PS89/46-1-DNA	(-44,-61)	L-arm+Cores
"	PS89/46-1-MEI-1	(-44,-61)	L-arm+Cores
"	PS89/46-1-MEI-2	(-44,-61)	L-arm+Cores
"	PS89/46-1-SED	(-44,-61)	L-arm+Cores
"	PS89/46-1-ARC	(-44,-61)	L-arm+Cores
"	PS89/46-1-TEX	(-44,-61)	L-arm+Cores
"	PS89/46-1-SAL	(-41,-42)	L-arm+Cores

Top predator censuses

During steaming of the ship, surveys of top predators (all marine birds and mammals) were made from open observation posts installed on the monkey-deck. Standard band transect survey methods were applied, in time blocks of 10 minutes with snapshot methodology for birds in flight, and additional line-transect methods for marine mammals. In addition to the ship-based surveys, helicopters were used for further band-transect censuses in sea ice areas. Flights were conducted at the standard seal survey altitude of 300 ft and speeds of 60 to 80 knots. For unbiased sampling, surveys followed pre-determined straight transect lines

to a maximum of 50 nautical miles away from the ship, with parallel outward and return tracks separated by at least 8 nautical miles. Helicopter counts were made in units of approximately 2 to 3 minutes flying time, identified by waypoints made on GPS. Bandwidth used in both ship based and aerial surveys was mostly 300 m (150 m to both sides of transect line), but was adapted according to conditions.

Densities of top predators were calculated from the number of densities of birds, seals and whales were then translated into food requirements using well established allometric formulas to calculate species-specific daily energy requirements. Energy requirements were translated to fresh food requirements using an energetic value of 4.5 KJ per gram fresh weight of food. For further methodological details see van Franeker et al. (1997). Data for the purpose of this cruise report could be analysed only for the southward leg to *Neumayer III*, 2 to 25 December. During this southward leg, 771 ship-based 10 minute counts were made, representing a survey surface of 688.6 km². Due to frequently poor weather conditions, only three helicopter surveys were made in the ice areas, with a total of 113 waypoint blocks representing a surveyed area of 179.1 km². Results from ship- and helicopter surveys were combined in the analyses, resulting in 884 count units representing a surface area of 867.7 km². On the return voyage to Cape Town at least a similar number of ship based observations has been made, but no additional helicopter surveys. Flying over denser sea ice was not possible due to a technical problem of *Polarstern*, preventing ship support in case of helicopter problems in dense sea ice sectors.

In addition to the at-sea density surveys of marine top predators, we conducted an aerial photographic survey of the emperor penguin colony in Atka Bay. The colony was not overflown. Instead, side angle photographs were taken from helicopter at 1,000 ft altitude, circling the colony at a radial distance of about 1,500 m from the concentration of birds. Photographs were analysed using the ITAG software produced by Sacha Viquerat.

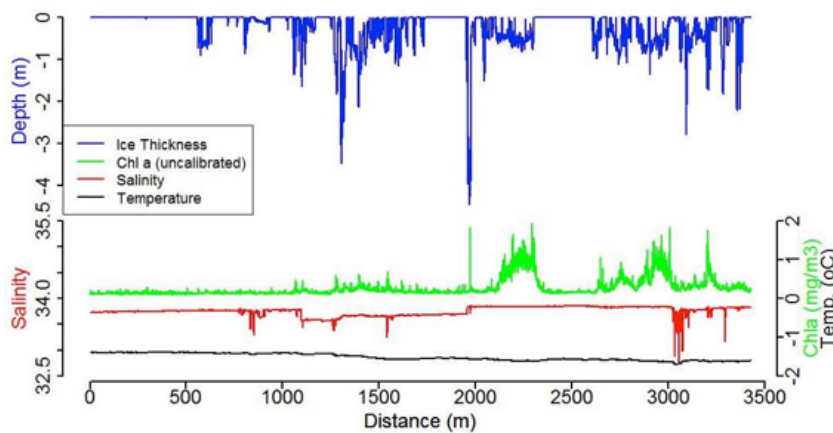


Fig.3.3.1.2: Example of environmental data profiles obtained from the SUIT's sensor array at station 30-4.

Preliminary results

SUIT sampling

SUIT sensors data. From the 18 SUIT hauls, 10 were conducted in open water, and 8 were conducted under various types of sea ice, including shattered ice floes in the marginal ice zone north of Atka Bay. Bio-environmental profiles were obtained from each SUIT haul (Fig. 3.3.1.2). The average ice coverage of the under-ice hauls was 90 %. Preliminary mean ice draft calculated based on pressure measurements of the SUIT's CTD ranged between 8 cm in the marginal ice zone, and 246 cm in heavy sea ice of the Coastal Current (Fig. 3.3.1.3 C).

3.3 Biology

The surface layer salinity increased towards the south. Near Atka Bay, the salinity was highly variable, which was possibly related to tidal currents. In a first analysis of surface chlorophyll-a content, a characteristic pattern of ice-free regions compared to ice-covered regions could not be identified. More insight on the biological productivity of the system, however, can be expected as soon as spectral data from the SUIT's RAMSES sensor can be related to the chlorophyll a content of sea ice derived from our L-arm measurements and associated ice core sampling.

SUIT catch composition. The catch from the 7 mm mesh shrimp net was counted and sorted on board. Fig. 3.3.1.3 A & B show an overview of the species found in the open water and under-ice hauls on the incoming and returning trajectories to and from Atka bay. In the first open water station, biomass was low and dominated by appendicularians. In ice-covered waters the catch was dominated by the euphausiids *Euphausia superba* and *Thysanoessa macrura*, and amphipods of the genus *Eusirus*. The latter were mainly *E. laticarpus* and *E. microps*, except in station 80-4, where *E. tridentatus* was found. In general species diversity was low compared to 2007/2008, when the open water and under ice surface layer was also investigated in this area (Flores et al. 2011). *Euphausia superba* shows an increased abundance at stations with thicker ice (Fig. 3.3.1.3 C). Fig. 3.3.1.3 D shows the mean properties of the sea water during trawling.

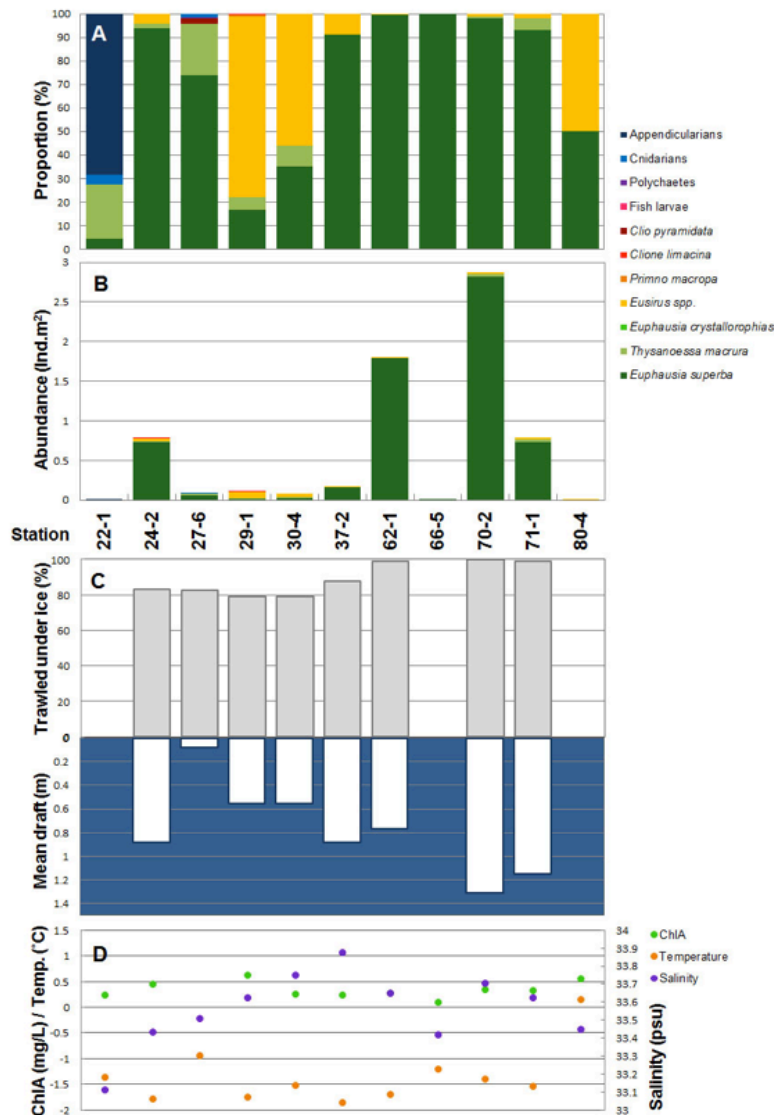


Fig. 3.3.1.3: SUIT catch, sea ice and under-ice water properties during trawling. A) Catch composition per station in percentage of total abundance. B) Abundance of major taxa at each SUIT station. C) Sea ice properties during SUIT hauls. The percentage of the haul that was conducted under ice is shown in grey bars. White bars represent the average ice draft during the haul. D) Mean surface water properties during each haul.

Near Atka Bay, the surface layer community was sampled over a 24 hour period to see if there were differences in the occurrence of macrofauna in the surface layer at different times of the day. In general the biomass in Atka Bay was very low (Fig. 3.3.1.4). Although also caught in the morning, *E. superba* seemed to be more abundant at night. All other species however were coming to the surface only at night time. These species included *Euphausia crystallorophias*, which is a known coastal species, *Eusirus* spp., fish larvae and polychaetes.

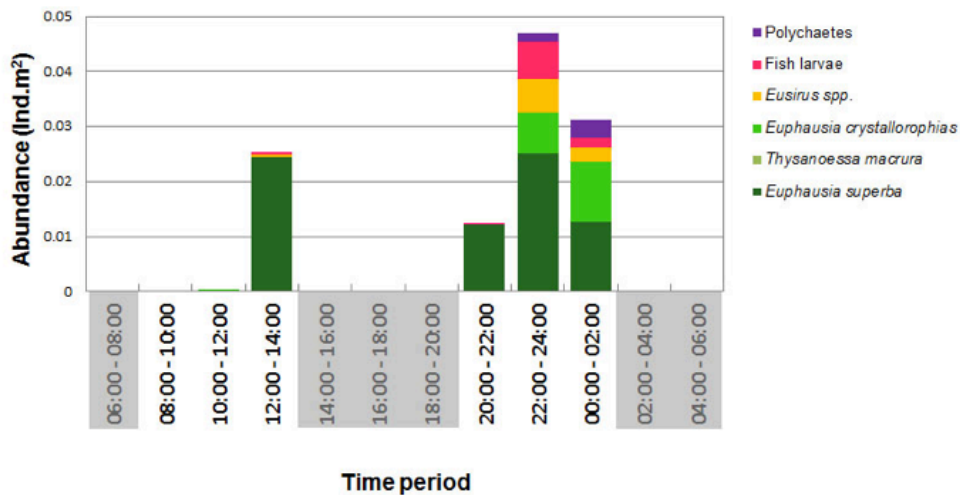


Fig. 3.3.1.4: Abundance of major taxa in the 0-2 m surface layer in Atka Bay per time period. The hauls at time periods 10:00 -12:00 hour and 22:00 – 24:00 hour were conducted on 10th January, while the others were conducted on the 12th. Time periods underlain in grey were not sampled.

The length frequency distribution of *E. superba* was analysed at the five stations completed along the southbound transect on the 0° meridian (Fig. 3.3.1.5). Three stations were dominated by juveniles with a modal length around 20 mm. Stations 24-2 and 38-1 were dominated by sub-adults with mean lengths of 31 and 34 mm. This is similar to the length distribution of 2007/2008 (Flores et al. 2012). The catch from station 38-1 also included larval krill (stage furcilia VI). This stage is often found in winter-early spring. There are, however, other studies that have found late stage furcilia in January and even until May (Marr 1962; Melnikov & Spiridonov 1996; Daly 2004).

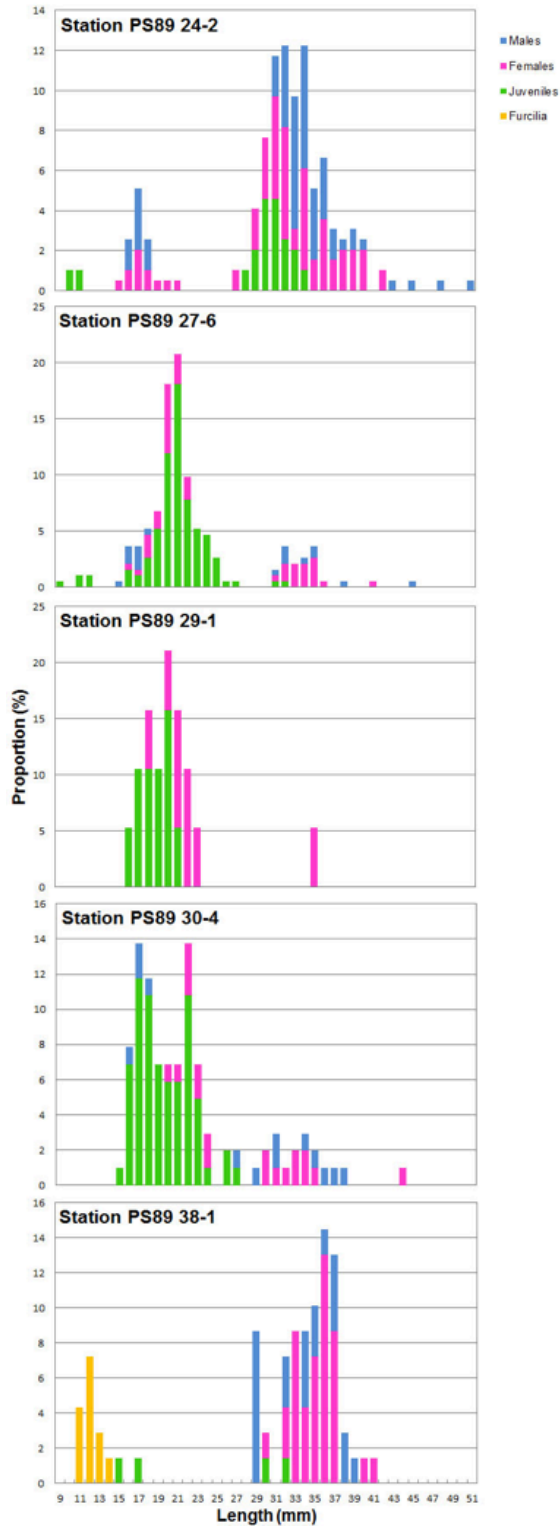
RMT sampling

We completed in total 15 M-RMT hauls, mostly in close proximity to SUIT sampling locations (Fig. 3.3.1.1). One haul had to be excluded from analysis due to entanglement of the net. At station 79, depth-stratified sampling was irregular due to malfunctioning of the release mechanism. Technical failure further precluded the analysis of 4 of the 39 remaining net samples (Fig. 3.3.1.7, Fig. 3.3.1.8). In this report we present preliminary data on macrozooplankton and micronekton collected by the RMT-8 nets. Data on siphonophores and chaetognaths were not included in this preliminary analysis.

Macrozooplankton communities. On the 0° meridian, cumulative macrozooplankton abundances in any of the 3 depth layers sampled were below 25 ind. 1,000 m⁻³ at stations north of 65°S. The highest M-RMT catch abundances of this survey (more than 250 ind. 1000 m⁻³) were obtained in the surface layer at Station 29, south-west of Maud Rise (Fig. 3.3.1.1, Fig. 3.3.1.6). South of 62°S, the macrozooplankton species composition was dominated by the euphausiid *Thysanoessa macrura*. Other abundant taxa were siphonophores and chaetognaths (both

3.3 Biology

not quantified), pteropods, amphipods and fish larvae. Antarctic krill *Euphausia superba* was surprisingly rare, its abundances ranging clearly below 2 ind. 1,000 m⁻³ in any of the 3 depth layers sampled (Fig. 3.3.1.6). The size of *T. macrura* ranged from 7 to 30 mm, with modes at 9 mm in juveniles, 18 mm in males, and 21 mm in females (Fig. 3.3.1.9 A).



3.3.1.5: Length frequency and stage distribution of *Euphausia superba* per station in percentage of numbers of individuals measured

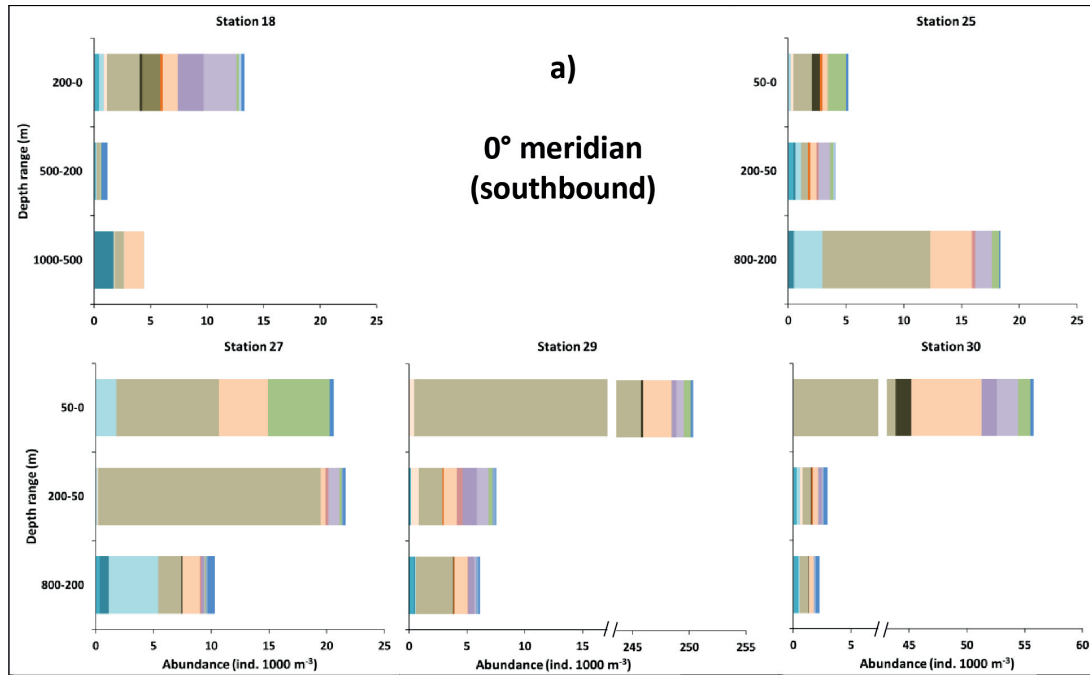


Fig. 3.3.1.6: Taxonomic composition and macrozooplankton abundance in M-RMT catches during the 0° meridian transect towards Neumayer III. The macrozooplankton community was sampled at 3 different depth layers. For figure legend refer to Fig. 3.3.1.8.

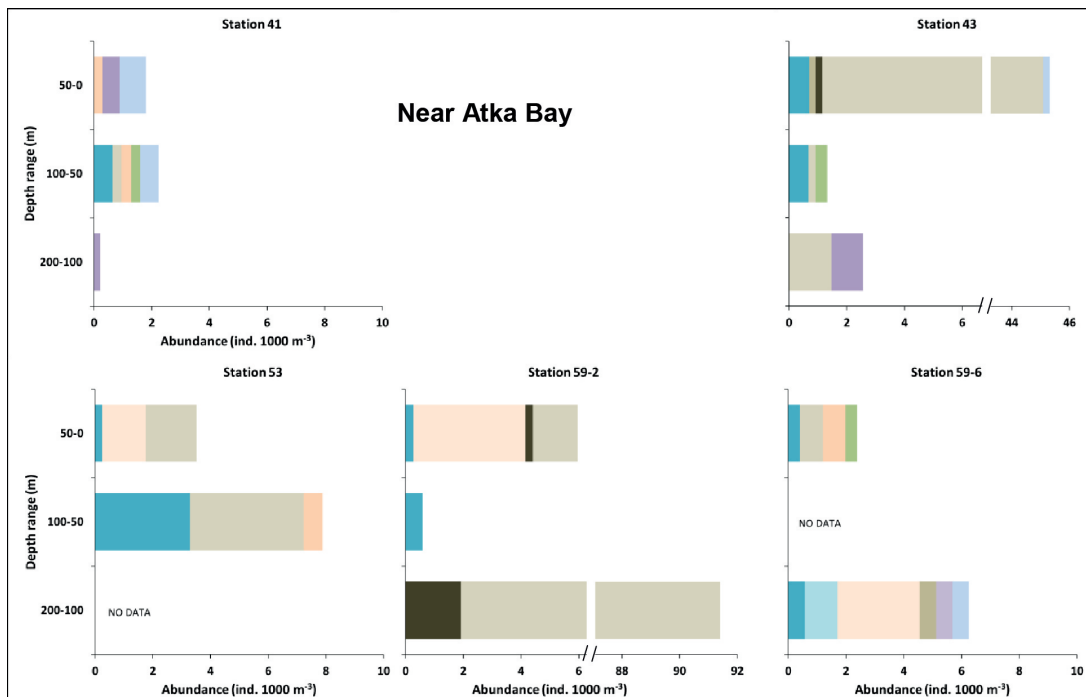


Fig. 3.3.1.7: Taxonomic composition and macrozooplankton abundance in M-RMT catches near Atka Bay. The macrozooplankton community was sampled at 3 different depth layers. For figure legend refer to 3.3.1.7.

3.3 Biology

Near Atka Bay, the macrozooplankton community was dominated by ice krill *Euphausia crystallorophias*. Peak abundances occurred both in the surface layer (Station 43: 45 ind. 1,000 m⁻³), and in the 100-200 m depth layer (Station 59-2: 91 ind. 1000 m⁻³) (Fig. 3.3.1.7). These 2 stations were also the only stations at which low numbers of Antarctic krill were caught. At the other 3 stations, cumulated macrozooplankton abundances were well below 10 ind. 1000 m⁻³ in any depth stratum (Fig. 3.3.1.7). There was a marked difference in the size distribution of *E. crystallorophias* caught in the 0-50 m surface layer at Station 43 versus the 100-200 m depth layer at Station 59. In the surface layer, the size composition was bimodal, with juveniles peaking at 19 mm and females at 30 mm. In the 100-200 m depth layer, the size composition was dominated by males, with a mode at 25 mm (Fig. 3.3.1.9 C, D). These vertical differences in the size distribution of ice krill were in line with similar observations made during PS82 in the Filchner region.

After leaving the Atka Bay area, 5 M-RMT stations were completed during the northbound transition to and on the 0° meridian. Unfortunately, only 3 of those stations were fully suitable for quantitative analysis due to technical problems during 2 hauls. Overall macrozooplankton abundances and species composition were similar to the catches during the southbound transect on the 0° meridian (Fig. 3.3.1.8). *Thysanoessa macrura* was again dominating in terms of abundance, and exhibited a similar size distribution (Fig. 3.3.1.8, Fig. 3.3.1.9 B). Station 79 and 80 were conducted at almost identical locations to Stations 29 and 27, respectively, during the southbound transect at the beginning of the expedition. Interestingly, the pattern of low abundances in the northern stations (27/80) versus high abundances in the southern stations (29/79) was confirmed during the return transect on the 0° meridian (Fig. 3.3.1.6, 3.3.1.8).

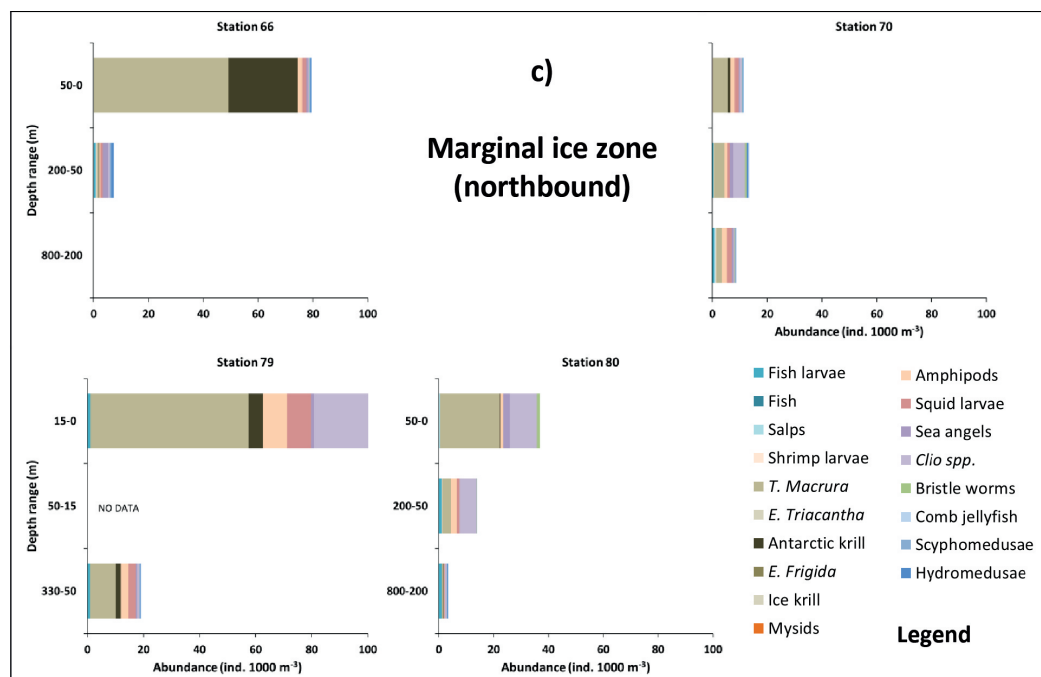


Fig. 3.3.1.8: Taxonomic composition and macrozooplankton abundance in M-RMT catches on the northbound leg after leaving the Atka Bay area. The macrozooplankton community was sampled at 3 different depth layers.

The vertical distribution of three euphausiid species in open and ice covered waters was investigated using SUIT and M-RMT data (Fig. 3.3.1.10). *E. superba* was most abundant in the surface layer under ice. In deeper layers, abundances were generally low. *T. macrura* was more abundant in deeper waters, especially in the upper 200 meters, with slightly higher abundances in ice-covered waters. These results are consistent with the results of 2007/2008 (Flores et al. 2012), demonstrating that abundances of Antarctic krill in the ice-water interface layer often far exceed integrated abundances of the 0-200 m layer. *E. crystallophias* was mostly found in low numbers near Atka bay. The highest abundance of this species was caught between 100 and 200 meter depth.

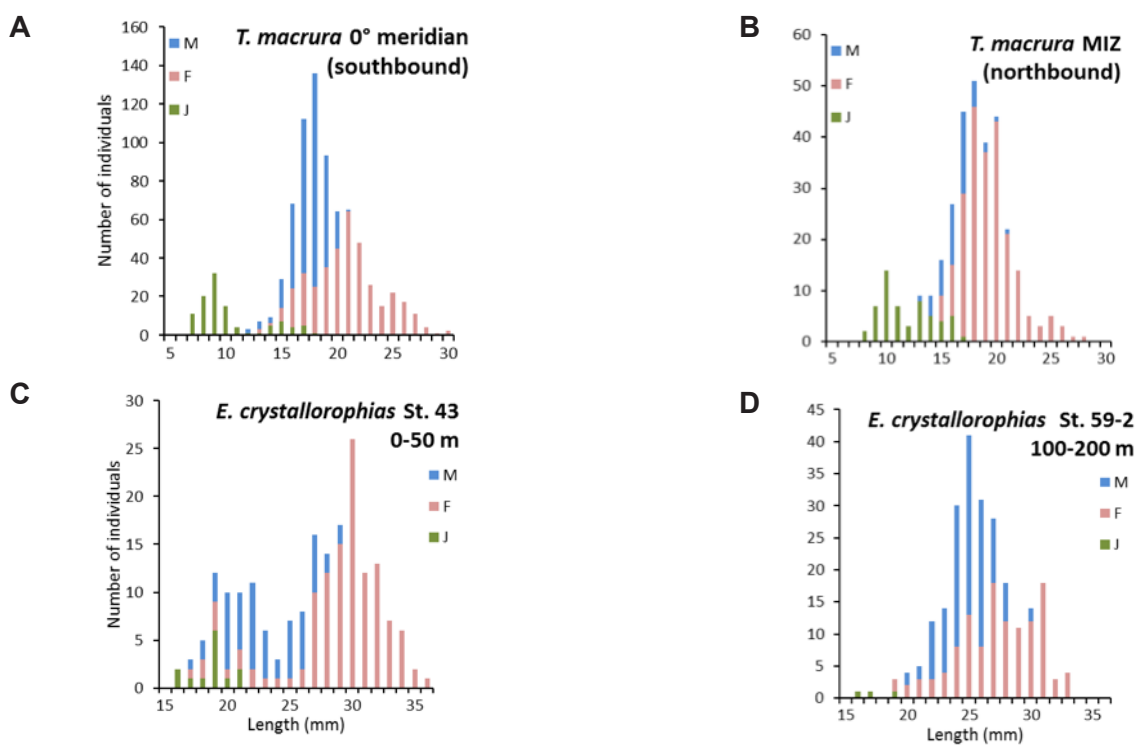


Fig. 3.3.1.9: Size composition of *Thysanoessa macrura* in the sea ice zone on the southbound 0° meridian and the northbound leg after leaving the Atka Bay area, and the size composition of *Euphausia crystallophias* at different depth layers at 2 stations near Atka Bay.

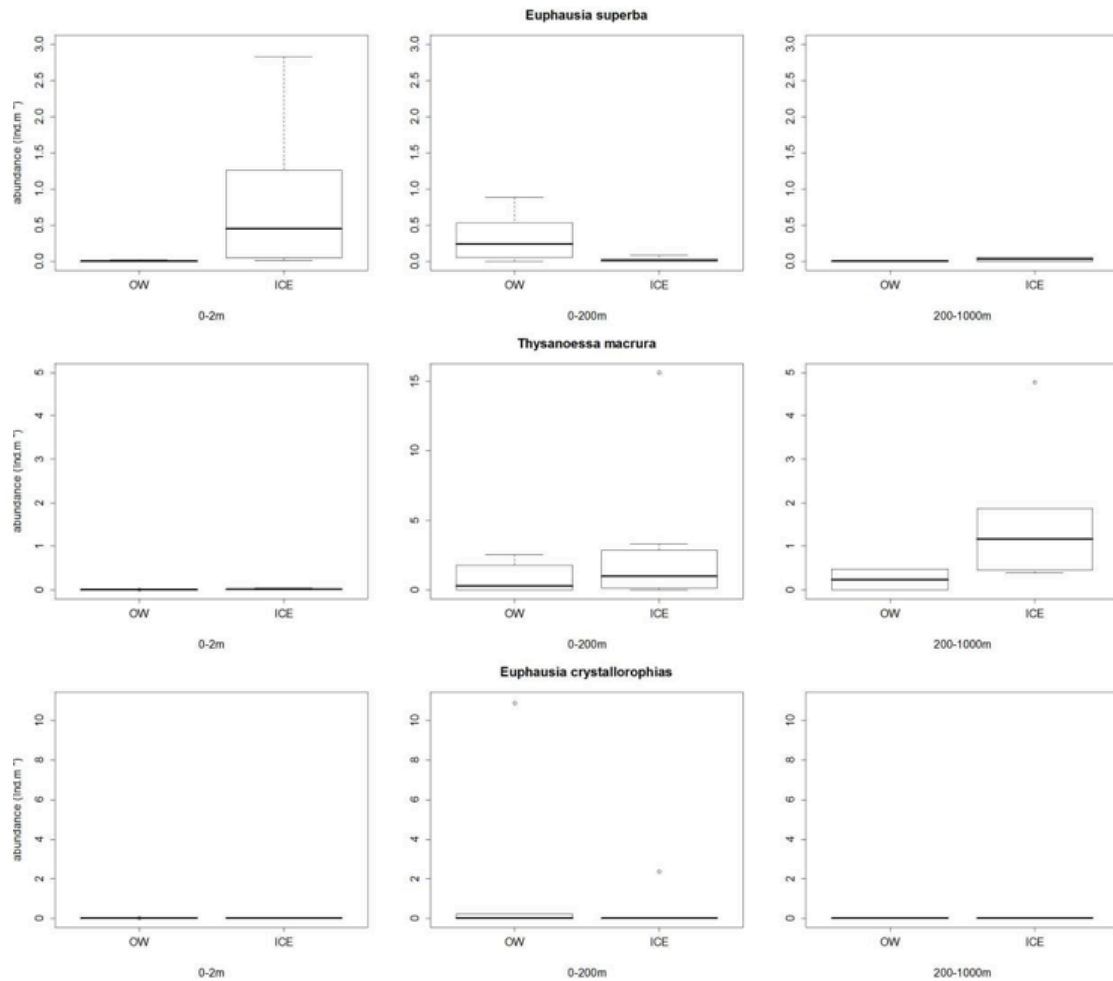


Fig. 3.3.1.10: Comparison of three euphausiid species sampled at different depth strata in open and ice-covered waters. Note the different scales in the *Thysanoessa macrura* plots. ICE = ice-covered SUIT stations and corresponding M-RMT stations; OW = open water SUIT stations and corresponding M-RMT stations

Larval Fish. In oceanic waters, larval stages of *Electrona antarctica* and *Notelepis coatsi* were caught frequently, while *Bathylagus antarcticus* larvae were caught infrequently. In coastal waters, icefish (Channichthyidae) larvae and unidentified Nototheniids were caught occasionally. Larval stages of *E. antarctica* showed peaks at 13 and 25 mm length (Fig. 3.3.1.11). Post-metamorphic and adults stages were also present but without displaying a clear pattern. This is likely due to the small number of these stages that were caught. *N. coatsi* covered a wide range from 12 up to 73 mm lengths, but most of them were between 28 and 43 mm in size. In coastal waters, the icefish and the unidentified Notothen showed similar size ranges peaking around 19 and 22 mm, respectively (Fig. 3.3.1.12).

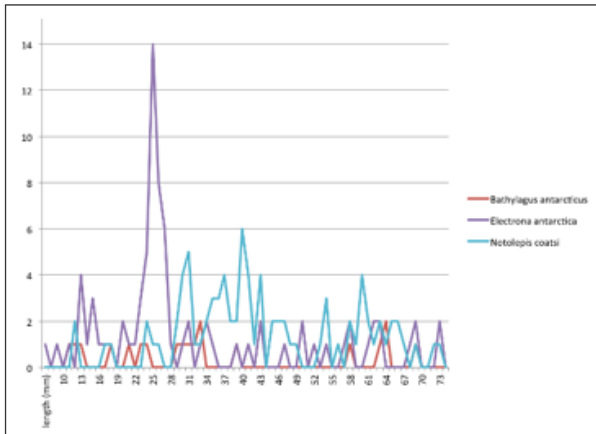


Fig.3.3.1.11: Length-frequency distribution of the most frequent oceanic fish, *Electrona antarctica*, *Notolepis coatsi* and *Bathylagus antarcticus* caught during PS89

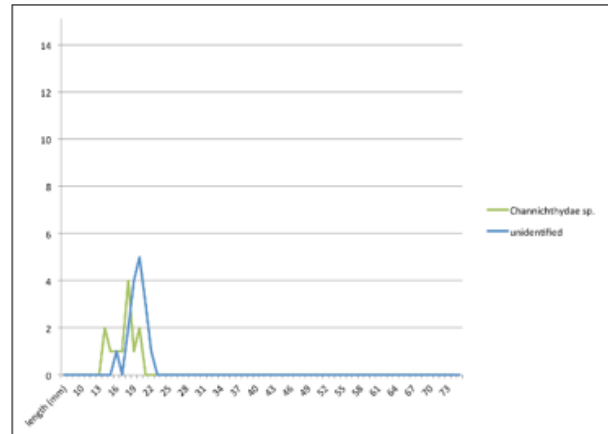


Fig. 3.3.1.12: Length-frequency distribution of the most frequent coastal fish, *Channichthyidae* and Nototheniid fish larvae caught during PS89

Samples for Genetic Analysis. Samples of amphipods, fish and other zooplankton were collected for further genetic analysis and will be integrated with other on-going efforts to collect samples of fish and amphipods around the Southern Ocean in order to perform phylogeographic and population genetic analyses (Table 3.3.1.3).

Tab. 3.3.1.3. Overview of samples collected for molecular Analysis

	100 % Ethanol	Frozen -20	Frozen -80°	Total
Amphipods	171			171
<i>Amphipod</i> sp.	1			1
<i>Cylopus lucasi</i>	9			9
<i>Eusirus laticarpus</i>	54			54
<i>Eusirus microps</i>	10			10
<i>Eusirus</i> spp.	31			31
<i>Hyperiella</i> sp.	10			10
<i>Hyperoche</i> sp.	1			1
<i>Primno macropa</i>	53			53
<i>Themisto gaudichaudii</i>	1			1
Fish	92	84	46	222
<i>Bathylagus antarcticus</i>	9	3	5	17
Channichthyidae spp.	6			6
<i>Electrona antarctica</i>	16	25	32	73
<i>Gymnoscoaphelus nicholsi</i>		1		1
<i>Gymnoscoaphelus</i> sp.		3		3
Myctophidae spp.		44		44
<i>Notolepis coatsi</i>	54	8	9	71
Nototheniid	1			1

3.3 Biology

Sea ice work

The sampled ice stations presented a very high variability in the majority of site parameters (Table 3.3.1.4). Ice thickness varied between ca 70 cm in sea ice on the 0° meridian, and more than 3 m in coastal fast ice at Atka Bay. The snow conditions were also highly variable, ranging from bare ice to more than 1 m snow cover. Thick snow cover was associated with negative freeboard (see stations 40-3, 40-5, and 48-1). Fig. 3.3.1.13 shows the typical coring grid taken at sites where also under-ice light measurements were performed.



Fig.3.3.1.13: Image of a typical coring grid taken at the L-arm site. The core hole on the right side was used to deploy the sensors attached to a L-arm underneath the ice. The ice cores were taken at the centre of the square in which the light measurements are performed. Picture by André Maijboom (IMARES).

Tab. 3.3.1.4: List of mean physical properties of the sampled ice for each sea ice station. The last 2 columns give information on the presence of a surface algae layer in the core holes and on the presence of (or signs of the presence of) platelet ice

Station	H (m)	H _{snow} (cm)	T (°C)	Salinity (psu)	Freeboard (cm)	Algae Layer	Platelet Ice
32-1	1.21	18	-1.73	11.65	6	NO	NO
35-1	0.73	6	-1.66	9.28	7	NO	NO
40-1	2.05	17	-2.73	9.04	8	YES	YES
40-3	3.51	119	-	-	-11	NO	YES
40-4	-	-	-	-	-	-	-
40-5	1.93	56	-2.1	-	-14	NO	YES
46-1	1.12	30	-1.24	10.19	-2	NO	NO
58-1	2.34	0	-	-	26	NO	Signs

Tab. 3.3.1 lists the number of ice cores taken for the physical, biogeochemical and biological analysis. High variability was also seen in the vertical profiles of in-ice temperature (Fig. 3.3.1.14) and salinity (Fig. 3.3.1.15). The stations in Atka Bay were characterized by the presence of platelet ice or by visible indications at the bottom of the ice cores that there had been platelet ice which was flushed away by the tidal movement of the water, or by the ship's propellers nearby. The only exception is station 46-1, where the ice was melting at the bottom, as was also evident from the temperature profile in Fig. 3.3.1.14. In general, the stations in

Atka Bay appeared to host higher biomass in the ice, visible by a brownish layer at the bottom of the cores, compared to the stations taken on ice sea floes. Further detailed analysis on sea-ice biogeochemistry and biological properties in the laboratory at AWI will give a complete picture on the sea-ice biomass.

Tab. 3.3.1.5: List of ice cores taken at each ice station for the analysis of physical (texture-TEX, Salinity-SAL, Sediment-SED), biogeochemical and biological analysis (Meiofauna-MEIO, DNA)

Station N°	BIO-OPT	LSI	DNA	MEIO	SED	ARC	TEX	SAL
32-1	5	2	1	2	1	1	1	1
35-1	2	2	1	2	1	1	1	1
40-1	2	1	1	1	1	0	1	1
40-3	0	0	0	2	0	0	0	0
40-4	-	-	-	-	-	-	-	-
40-5	1	0	0	1	0	0	1	0
46-1	1	2	1	2	1	1	1	1
58-1	2	2	1	2	0	0	0	0

The CTD profiles (Fig. 3.3.1.16) provided information on the water characteristics at the ice stations. The variability in the physical properties of the top 50 m of the water column resembled the high variability already found in the sea ice physical properties of sea ice. The sampling site of Station 40-1 was re-visited 4 days later (Station 40-4). At Station 40-1, the CTD profile showed a clear stratification in the upper about 18 m, where the uncalibrated chlorophyll *a* content reached levels of about 12 mg m⁻³ (Fig. 3.3.1.16 B). At the same spot four days later, no stratification was apparent, and chlorophyll *a* concentrations remained generally below 0.5 mg m⁻³ (Fig. 3.3.1.16 D). This pronounced difference in the vertical structure of the underlying water may have been related to the tidal movement of waters. This result highlights the high variability of the Atka Bay sea ice system, not only on a spatial scale, but also on a temporal scale.

At most stations we performed under-ice light field measurements. The high variability of the sampled places offers the possibility to study light transmission through ice of different types and thicknesses as well as through different snow covers. This will help to parameterize the under-ice radiation in relation to different sea-ice physical conditions and, once the further analysis on the chlorophyll *a* will be completed, with different biomass content.

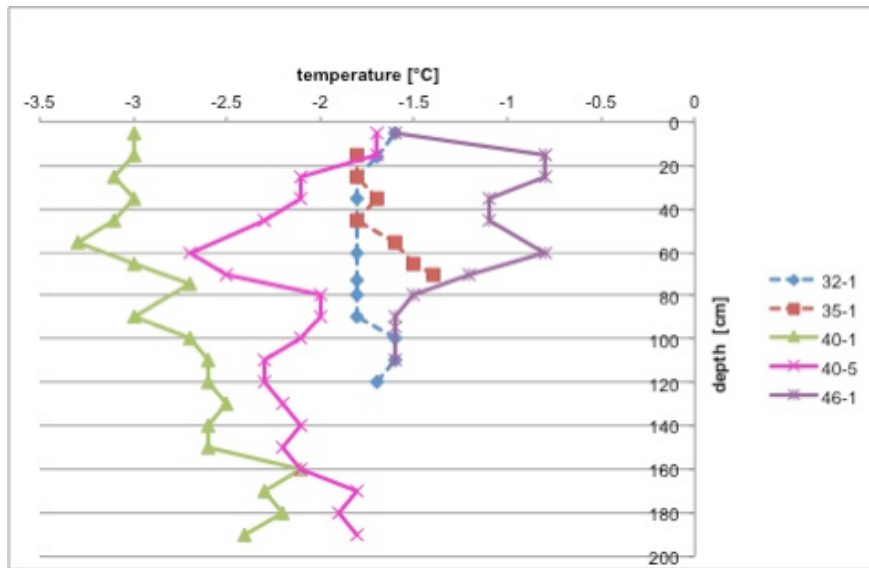


Fig.3.3.1.14: Temperature vertical profiles in the ice for stations 32-1, 35-1 (dashed line) on the ice floes and for stations 40-1, 40-5 and 46-1 (full line) on the fast ice.

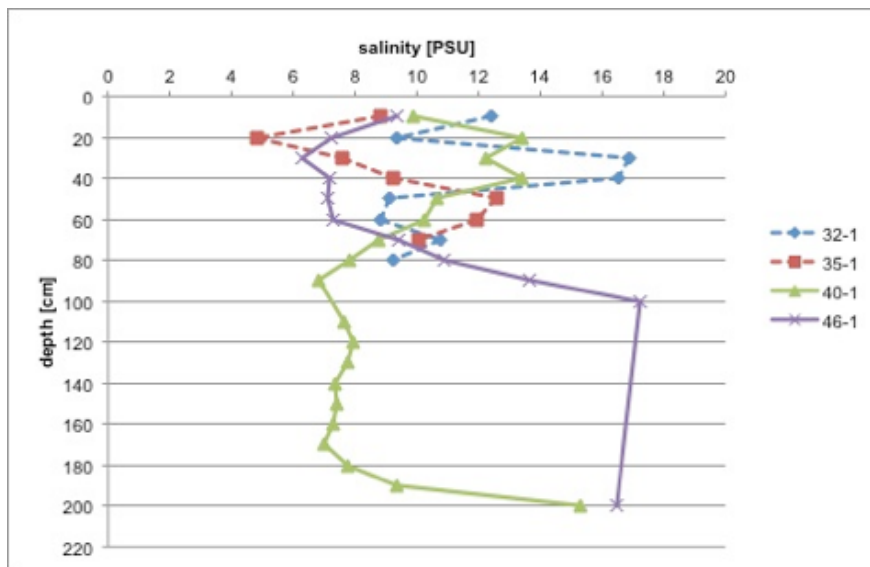


Fig. 3.3.1.15: Salinity vertical profiles in the ice for stations 1, 2 (dashed line) on the ice floes and for stations 40-1, 40-5 and 46-1 (full line) on the fast ice

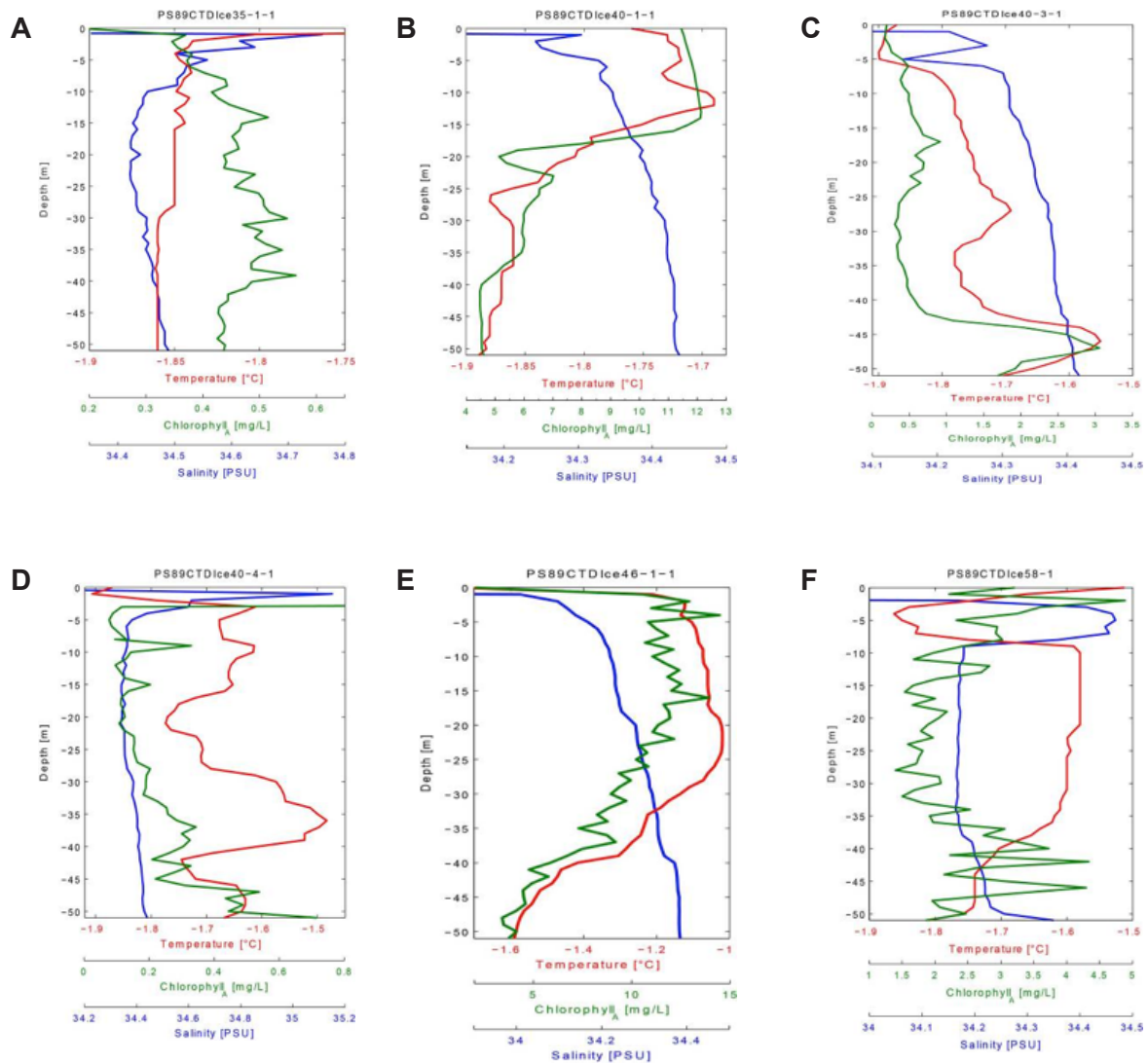


Fig. 3.3.1.16: CTD profiles in the 50 m water column under the ice at ice stations

Top predator censuses

Transect census. The southward leg of PS89 (ANT-XXX/2) was rather unusual in its pattern of food requirements of the top predators. In most earlier transects in this region, it was observed that birds, seals and whales had food requirements in ice covered waters that were much higher than in the open water further north. The background relates to a mix of increased numbers of individuals, larger sizes, and species restricted to life in sea ice. In the observations on this voyage, this pattern still holds for birds and seals. Fig. 3.3.1.17 A shows that flying seabirds, mainly tubenosed species, concentrated in the area of the Antarctic Polar Front around 49 to 50°S. Near and in the ice, penguins take over, with chinstrap penguins *Pygoscelis antarctica* in the outer zone, and Adélie penguins *Pygoscelis adeliae* and emperor penguins *Aptenodytes forsteri* further south. Apart from incidental fur seals *Arctocephalus gazella* in open waters, the crabeater seal *Lobodon carcinophagus* dominated in the sea ice. It concentrated in the far south but had remarkably low densities in the apparently suitable sea ice between 59°S and 64°S (Fig. 3.3.1.17 B). The overall picture of food requirements of top predators on this voyage (Fig. 3.3.1.17 C) was however dominated by larger whale species such as the fin whale

Balaenoptera physalus and the humpback whale *Megaptera novaeangliae*. Far north, these were rather incidental but influential observations, but just north of the ice edge observations became more regular. Deeper in the ice, the usually fairly abundant Antarctic minke whale *Balaenoptera bonaerensis* was not seen very frequently. The overall impression of top predator abundance in the sea ice was that it was relatively low compared to observations on earlier *Polarstern* cruises, but more detailed comparisons must await further analysis, including the data of the northward leg in mid-January, when the ice edge was positioned far south around 68°S. Data from that return trip have not been analysed yet, but the general impression is that abundances were still fairly low in denser sea ice. However, in the outer rim of the sea ice and north of it, whales were abundant, with both the Antarctic minke whale and several blue whales *Balaenoptera musculus* seen feeding around the ice edge, where also the SUIT net made its highest catches of Antarctic krill under the ice. Humpback whales were seen frequently over large parts of the zones that had been covered by sea ice in December.

Emperor Penguin colony census. On December 30, aerial photographs were made of the emperor penguin colony in Atka Bay near *Neumayer Station III* (Fig. 3.3.1.18). Preliminary counts of the *photos* sum up to approximately 3,200 chicks and 500 adults being present, with an additional presence of 22 Adélie penguins in adult plumage, apparently prospecting for breeding locations, which however are unavailable in the area. The number of emperor penguin chicks was much lower than made from a similar photo survey on 14 Dec 2007, when nearly 11,000 chicks and over 1,000 adults were counted. The lower number of chicks in the seasonally somewhat later 2014 survey cannot be explained by fledging of chicks. Only two fledged chicks were observed near the edge of the fast ice in 2014. In 2007, larger numbers of fledglings were seen only by mid-January. Reproductive success of Emperor penguin colonies is known to be extremely variable and dependent on winter weather, and position of the fast-ice edge during different critical phases of the breeding cycle. Undoubtedly, food availability will also vary and may have been low in this season or parts of it.

Concluding remarks

Based on the net catches, the area surveyed was characterized by low zooplankton abundances compared to earlier expeditions. The mere absence of Antarctic krill from pelagic M-RMT samples on the 0° meridian was remarkable. However, the well-known patchiness of zooplankton distribution in combination with the low number of net hauls accomplished during this expedition precludes any large-scale generalisation of this observation. Elevated abundances of juvenile Antarctic krill were only encountered in the ice-water interface layer, confirming earlier findings from the same region suggesting that Antarctic krill is often more abundant under sea ice than in the epipelagic layer. Patterns in top predator distribution resembled those of zooplankton, with elevated abundances of whales associated with relatively high under-ice krill abundances in the marginal ice zone on the northbound leg. Sea ice habitat properties evidently had a decisive impact on the distribution of animals in the investigation area. The high variability of sea ice properties found during our ice station work suggests that km-scale measurements of sea ice properties, such as those performed with SUIT, can be valuable in capturing this variability at more appropriate spatial scales.

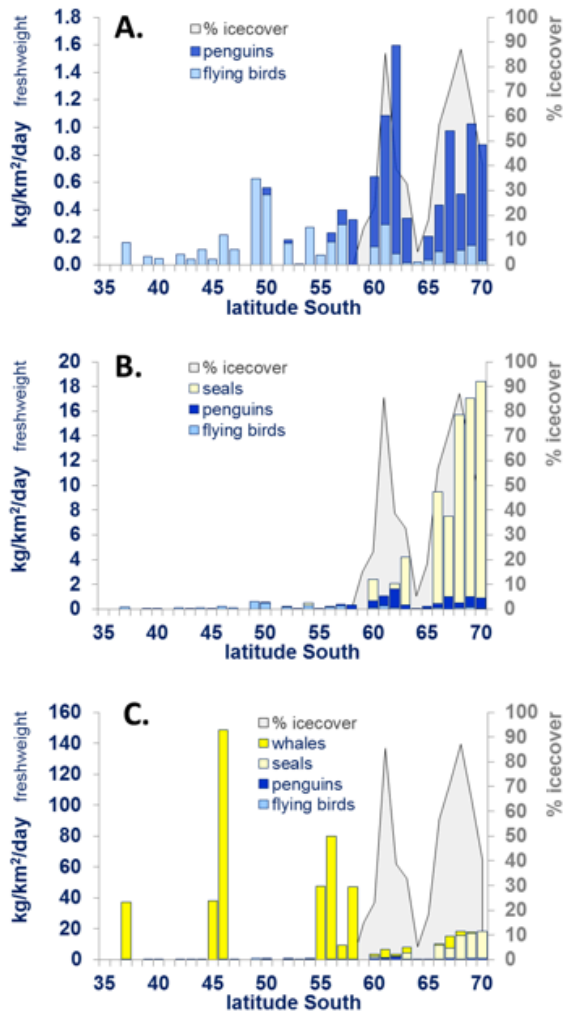


Fig. 3.3.1.17: Food requirement of top predators averaged by degree of latitude and in relation to average sea ice cover (884 ship based and aerial counts, 4-25 December 2014, Cape Town to Neumayer, largely following the 0° meridian). A. birds, B. birds and seals, C. birds, seals and whales.



Fig. 3.3.1.18: Overview of the emperor penguin colony on the fast ice in Atka Bay, with Neumayer Station III visible in the back (A). On the right (B), the first of the five aerial photographs used to count the number of chicks and adults in the colony. Based on details on the pictures, the drawn line shows the separation between counts of different photographs.

Data management

Almost all sample processing will be carried out in the home laboratories at AWI, IMARES and RBINS. This may take up to three years depending on the parameters as well as analytical methods (chemical measurements and species identifications and quantifications). As soon as the data are available they will be accessible to other cruise participants and research partners on request. Metadata will be shared at the earliest convenience; data will be published depending on the finalization of PhD theses and publications. Metadata will be submitted to PANGAEA, the Antarctic Master Directory (including the Southern Ocean Observation System), the Antarctic Biodiversity Portal www.Biodiversity.aq, and will be open for external use.

References

- Arntz WE, Thatje S, Gerdes D, Gili JM, Gutt J, Jacob U, Montiel A, Orejas C, Teixido N (2005) The Antarctic-Magellan connection: macrobenthos ecology on the shelf and upper slope, a progress report. *Scientia Marina* 69:237-269.
- Daly KL (2004) Overwintering growth and development of larval *Euphausia superba*: an interannual comparison under varying environmental conditions west of the Antarctic Peninsula, *Deep-Sea Research Part II* 51:2139–2168.
- Flores H, Van Franeker JA, Siegel V, Haraldsson M, Strass V, Meesters EHWG, Bathmann U, Wolff WJ (2012) The association of Antarctic krill *Euphausia superba* with the under-ice habitat. *PLoS one* 7:e31775.
- Flores H, Van Franeker JA, Cisewski B, Leach H, Van de Putte AP, Meesters EHWG, Bathmann U, Wolff WJ (2011) Macrofauna under sea ice and in the open surface layer of the Lazarev Sea, Southern Ocean. *Deep Sea Research Part II: Topical Studies in Oceanography* 58:1948–1961.
- Ingels J, Vanhove S, De Mesel I, Vanreusel A (2006) The biodiversity and biogeography of the free-living nematode genera *Desmodora* and *Desmodorella* (family Desmodoridae) at both sides of the Scotia Arc. *Polar Biology* 29:936-949.
- van Franeker JA, Bathmann U, Mathot S (1997) Carbon fluxes to Antarctic top predators. *Deep-Sea Research II* 44:435–455.
- van Franeker JA, Flores H, Van Dorssen M (2009) The Surface and Under Ice Trawl (SUIT), in: Flores, H. (Ed.), *Frozen Desert Alive - The Role of Sea Ice for Pelagic Macrofauna and its Predators*. PhD thesis. University of Groningen, pp. 181–188.
- Marr J (1962) The natural history and geography of the Antarctic krill (*Euphausia superba* Dana). *Discovery Reports* 32:37– 444.
- Melnikov IA, Spiridonov VA (1996) Antarctic krill under perennial sea ice in the western Weddell Sea. *Antarctic Science* 8(4):323-329.

3.3.2 Cetaceans in ice

Sacha Viquerat, Steve Geelhoed, Nicole Janinhoff, Shannon McKay, Sebastian Müller, Hans Verdaat
not on board: Helena Herr, Ursula Siebert

ITAW

Grant No: AWI-PS89_03

Objectives

Our work during this expedition was conducted as part of a project investigating the relationship of cetaceans and sea ice, aiming at density estimates in sea ice covered areas („*Modellierungen zu Populationsgrößen und räumlicher Verteilung von Zwergwalen im antarktischen Packeis auf der Grundlage von See- und luftgestützten Tiersichtungen*; Förderkennzeichen 2811HS002“). Knowledge on the density, distribution and habitat use of cetaceans in the Antarctic is comparably limited. Until today it is unknown to what extent cetaceans use the ice covered waters, though these waters are thought to play an important role in the sea-ice ecosystem and thus to contribute largely to biodiversity in this habitat. Knowledge on cetacean densities in relation to sea ice concentrations is central for understanding impacts of climate change on the Antarctic marine ecosystem as well as for Southern Ocean ecosystem management, including the conservation and management mandate of the International Whaling Commission (IWC). Especially, but not only, data on Antarctic minke whale (*Balaenoptera bonaerensis*) distribution in ice covered areas of Antarctica are urgently needed and requested by the IWC, as current abundance estimates of cetaceans in Antarctic waters are based on assessments conducted up to the marginal ice zone only. Without surveying for whales across the ice zone it is almost impossible to estimate their entire population sizes (both inside and outside of the ice) and how changes in climate and increasing human presence around the Antarctic will impact on whale populations in the coming decades.

Aerial surveys are currently the preferred method for obtaining quantitative data on cetacean occurrence in pack ice regions. Regional estimates of cetacean densities in selected areas of varying sea ice concentrations may allow to compare boundaries and magnitudes of abundances of cetaceans, both inside and outside of the sea ice region and provide valuable information in order to account for potential biases in current abundance estimates.

By means of dedicated cetacean sighting surveys, our project aims to contribute to base line data on cetacean occurrence and abundance, especially of Antarctic minke whales in selected areas of the Antarctic. Therefore we conduct aerial as well as ship-based cetacean sighting surveys following standard line-transect distance sampling methodology to obtain estimates of density for selected cetacean species with a special focus on Antarctic minke whales. In addition behavioural observations investigate response behaviour of cetaceans towards vessels in Antarctic waters.

Work at sea

We conducted dedicated cetacean sighting surveys, using the crow's nest (shipboard survey) and the on-board helicopters (aerial survey) as survey platforms. The same general methodology applied during aerial surveys and ship based surveys. Priority was given to the aerial surveys, but given the size of our team, both survey types could be run in parallel.

In addition to the distance sampling surveys, we conducted a tracking study from the crow's nest, i.e. focal follows of detected animal groups with high-powered binoculars („Big Eyes“), noting down their track (angle and distance to ship) as long as possible. This is a means to

3.3 Biology

evaluate cetacean behaviour, in particular responsive movement by cetaceans towards the ship (this being one of our survey platforms).

Aerial Survey

We conducted aerial surveys following standard line-transect distance sampling methodology (Buckland et al. 2001) with the two helicopters (BO 105) provided by HeliService on board of *Polarstern* between December 17, 2014 and January 20, 2015. All surveys were planned in an “ad-hoc” manner. Track lines were designed in a way that they could be surveyed depending on the current position and track of *Polarstern* as well as on weather conditions, aiming to achieve a good coverage of the survey area and applying basic principles of good survey design following Buckland et al. (2001).

All survey flights were conducted at an altitude of 600 feet and a speed of 80-90 knots. Two observers were positioned in the back seats of the helicopter on the right and left side and observed their side, concentrating on the area immediately below the helicopter. A third observer was seated in the front left seat of the helicopter next to the pilot, observing the area to the front, thus focusing on the transect line. The observer seated behind the pilot on the right side of the helicopter was also tasked with running the VOR software (Hiby & Lovell 1998) on a laptop computer, continuously storing GPS data, data on environmental conditions (sea state, cloud cover, glare, ice coverage, sighting conditions) and data on all sightings of marine mammals that were relayed by the observers.

The following attributes were collected for each sighting: species, distance to transect (via declination angle and in case of front observations, horizontal angle), group size, group composition, behaviour, cue and potential reaction to the helicopter. Inclinerometers were used to measure the declination angle to each sighting when abeam the helicopter, in order to later calculate the distance of the sighting to the transect line. Front observations additionally received a horizontal angle, measured by the front observer using an angle board, in order to calculate the distance to the transect line. The information on a sightings distance to the transect line is the crucial point for the estimation of the effectively covered strip width.

If a sighting occurred and the species or group size could not be determined immediately, the survey was paused in order to approach the sighting for closer inspection (closing mode). After identification, the helicopter returned to the transect line and the survey was resumed. Digital photography was used as an additional identification tool to aid in species identification and for Photo-ID purposes of specific cetacean species.

Ship based survey

We conducted a ship based survey following standard line-transect distance sampling methodology (Buckland et al. 2001) from the crow's nest of *Polarstern* at 29.5 m elevation above the sea surface.

Two observers were positioned on each side of the crow's nest and observed the area to the right and to the left respectively, concentrating on the area directly in front of the ship up to 90° abeam, using binoculars equipped with reticules and an angle board to measure the distance of a sighting to the track line. A third observer was seated inside the cabin of the crow's nest, using the VOR software (Hiby & Lovell 1998), running on a laptop computer, to continuously store GPS data, data on environmental conditions (sea state, glare, ice coverage, sighting conditions) and data on all sightings of marine mammals that were relayed by the observers.

For each sighting of a marine mammal in the water, the following data were collected: species, distance to transect (via horizontal angle and declination angle from the horizon), group size, group composition, behaviour, cue and any potential reaction to the presence of *Polarstern*.

Tracking survey

There was no opportunity for a tracking survey due to bad weather conditions and ship related problems that drastically changed the course track.

Preliminary results*Aerial Surveys*

A total of 14 flights were accomplished, resulting in 24 hours of flying time. The first flight on the 17th of December served as a calibration flight. The survey flights had an average duration of 1 hour and 45 minutes. We covered a total distance of 2,993.85 km on effort during 13 survey flights along the ship course. A total number of 24 cetacean sightings (Minke spec., fin whales and humpback whales, see Table 3.3.2.1) were recorded.

Tab. 3.3.2.1: Summary of cetacean sightings during helicopter surveys on PS89 (ANT-XXX/2). Minke spec. combines Antarctic (*Balaenoptera bonaerensis*), and dwarf (*B. acutorostrata*) minke whales.

Species	Number of Sightings	Number of Individuals
Minke spec.	7	7
Fin whale (<i>B. physalus</i>)	2	4
Humpback whale (<i>Megaptera novaeangliae</i>)	15	18
Total	24	29

Ship based Surveys

We covered a total distance of 855 km during 55 hours on effort in the crow's nest and observed a total number of 62 cetacean groups comprising 98 individuals between December 7, 2014 and January 21, 2015. We detected 51 individuals of minke whales (pooling *Balaenoptera acutorostrata*, *B. bonaerensis*) in 30 sightings. Worth mentioning are three blue whale (*B. musculus*) detections (Table 3.3.2.2).

Tab. 3.3.2.2: Summary of cetacean sightings during crow's nest surveys on board of *Polarstern* during PS89 (ANT-XXX/2). Minke spec. combines Antarctic (*Balaenoptera bonaerensis*), and dwarf (*B. acutorostrata*) minke whales.

Species	Number of Sightings	Number of Individuals
Minke spec.	30	51
Blue whale (<i>Balaenoptera musculus</i>)	3	3
Fin whale (<i>B. physalus</i>)	10	16
Hourglass dolphin (<i>Lagenorhynchus cruciger</i>)	1	8
Humpback whale (<i>Megaptera novaeangliae</i>)	18	20
Total	62	98

Long periods of unfeasible weather conditions and ship related issues limited our opportunities to conduct surveys. In spite of these circumstances, we were able to collect valuable data from both platforms along the zero meridian contributing to the overall datasets of our study (Fig. 3.3.2.1). Together with data from previous expeditions, the collected data will contribute to our analysis especially of minke whale sea ice relationships in areas south of 60° (Fig. 3.3.2.2).

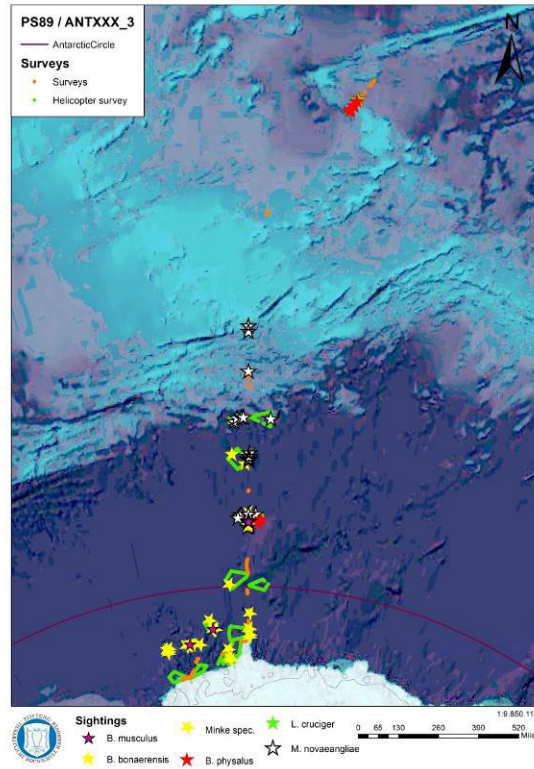


Fig. 3.3.2.1: Cetacean sightings and tracklines covered on effort during crow's nest and helicopter surveys on Polarstern PS89 (ANT-XXX/2)

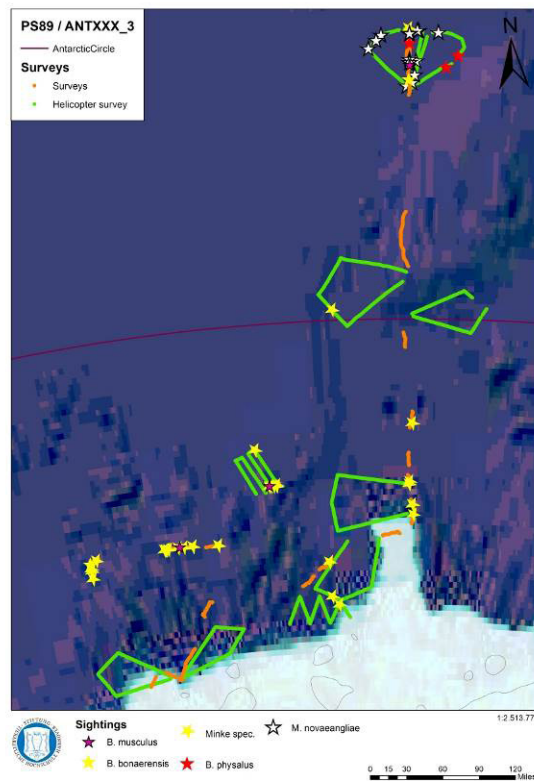


Fig. 3.3.2.2: Cetacean sightings and tracklines in the vicinity of 60° south and beyond covered on effort during crow's nest and helicopter surveys on Polarstern PS89 (ANT-XXX/2)

Data management

Publication in scientific journals in the fields of marine biology and zoology and presentation on scientific conferences will make the data obtained available for science and public. Survey results will be presented to the Scientific Committee of the International Whaling Commission. All datasets will be stored in the Antarctic Marine Mammal Survey Database of the Institute for Terrestrial and Aquatic Wildlife Research, Büsum, Germany. Pictures taken during the survey suitable for photo ID will be forwarded to the involved institutes.

Acknowledgement

We would like to thank Captain Wunderlich and the entire crew of *Polarstern* for their never-ending support throughout the whole survey.

Our survey would not have been possible without the excellent work, patience and support of the helicopter crew, Lars Vaupel, Martin Steffens, Fabian Gall and Thomas Heim.

We are grateful to the meteorological office on board, Max Miller and Hartmut Sonnabend. Their weather forecasts made it possible to conduct this survey in very variable weather conditions.

Our work was funded by the German Federal Ministry of Food and Agriculture within the project: „Modellierungen zu Populationsgrößen und räumlicher Verteilung von Zwergwalen im antarktischen Packeis auf der Grundlage von See- und luftgestützten Tiersichtungen (Förderkennzeichen 2811HS002)“.

References

- Buckland ST, Anderson DR, Burnham KP, Laake JL, Borchers DL, Thomas L (2001) Introduction to distance sampling: estimating abundance of biological populations. Oxford University Press, Oxford.
- Hiby AR, Lovell P (1998) Using aircraft in tandem formation to estimate abundance of harbour porpoise. *Biometrics* 54:1280–1289.

3.4 Geobiosciences

3.4.1 Culture experiments on trace metal incorporation in deep-sea benthic foraminifers from the Southern Ocean

Erik Wurz¹

¹AWI

not on board: Jutta Wollenburg¹

Grant No: AWI-PS89_04

Objectives

The Antarctic Ocean is one of our most important climate amplifiers: First, the production of Antarctic deep water drives the Global Thermohaline Conveyor Belt, thus, climate. Second, the Antarctic deep water during glacial time was/ disputably still is, the largest marine sink of atmospheric CO₂. Employment of effective sensitive and in geological sense preservable proxies to obtain precise information on changes in the polar deep oceans physical to geochemical properties are essential to assess past, modern, and future physical to geochemical changes in bipolar deep-waters. In this respect, analyses on trace metal (Mg/Ca, U/Ca, B/Ca) ratios recorded in tests of foraminifers to estimate calcification temperatures, salinity variations, carbonate ion saturation, pH and alkalinity became common methods. However, for the Southern Ocean deep-sea benthic foraminifera calibration curves constrained by culture experiments are lacking. During this expedition we will retrieve multiple corers from 1,500 m water depth and transfer the retrieved sediments into 15 different aquaria including newly developed high-pressure aquaria. These aquaria will in different experimental set-ups be used to cultivate our most trusted paleodeep-water recorders at different temperatures and in waters with different carbonate chemistries to establish species-specific trace metal calibration curves for the Antarctic Ocean.

Work at sea

Since our work is focused on epizooic Cibicides-type foraminifers, filter-feeding unilocular animals with maxima abundances in areas of high current activities, we will deploy 2-3 multiple cores at exposed sites with a water depth around 1,500 m. The retrieved cores will be transferred into a cold laboratory running at a site-alike bottom water temperature during the cruise. During the last day on board the sediments and overlaying water will be transferred into transfer-cores and storage systems. These storage systems will be transferred into special cold boxes ensuring a site-alike temperature during the flight to Bremerhaven. In Bremerhaven the sediments will immediately transferred into the respective aquaria and connected to respective supportive sea-water systems.

Preliminary results

Two multiple corers have been deployed successfully at the positions 69° 59,09' S 4° 4,54' W and 69° 59,26' S 4°4,39' W in a water depth of 2,307 m and 2,311 m, respectively. Cores have been transferred into a 0 °C refrigerated cold lab onboard *Polarstern*. 13 of 15 aquaria could be filled with cores from the multiple corers. During the cruise, sediment cores have been successfully provided with bottom-layer water from Niskin-bottles combined with a CTD and a suspension of *Spirulina* sp. Algae for food supply. A hose, connected to an air pumping device and submerged at the water surface of each aquarium ensured water circulation and oxygen supply. With this aquaria setup the sediment-associated meiobenthic community has been kept alive until the arrival of *Polarstern* in CapeTown.

Data management

This work is part of a bipolar DFG-project on the incorporation of trace metals in benthic deep-sea foraminifera. The results will be published in international journals within approx. 2 years after the expedition.

A.1 TEILNEHMENDE INSTITUTE / PARTICIPATING INSTITUTES

	Address
AWI	Alfred-Wegener-Institut Helmholtz-Zentrum für Polar- und Meeresforschung Am Handelshafen 12 27570 Bremerhaven / Germany
DWD	Deutscher Wetterdienst Seeschiffahrtsberatung Bernhard-Nocht Strasse 76 20359 Hamburg / Germany
GEOMAR	GEOMAR Helmholtz-Zentrum für Ozeanforschung Kiel Wischhofstr. 1-3 24148 Kiel / Germany
HAFRO	Marine Research Institute Skulagata 4 121 Reykjavik / Iceland
Heliservice	HeliService International GmbH, Deutschland Am Luneort 15 27572 Bremerhaven / Germany
ITAW	Institute for Terrestrial and Aquatic Wildlife Research University of Veterinary Medicine Hannover, Foundation Werftstr. 6 25761 Büsum / Germany
IMARES	IMARES Wageningen UR PO Box 167 1790AD DEN BURG / The Netherlands
IOCAG	Instituto de Oceanografía y Cambio Global Universidad de Las Palmas de Gran Canaria Campus Universitario de Tafira Edificio de Ciencias Básicas 35017 Las Palmas de Gran Canaria / Spain
Ludwig-Max. Univ. München	Ludwig-Max. Univ. München Professor-Huber-Platz 2 80539 München / Germany
Laeisz	Reederei F. Laeisz (Bremerhaven) GmbH Brückenstrasse 25 27568 Bremerhaven / Germany
MBARI	Monterey Bay Aquarium Research Institute 7700 Sandholdt Road Moss Landing, CA 95039 / USA

A.1 Teilnehmende Institute / Participating Institutes

	Address
NIOZ	Royal Netherlands Institute for Sea Research PO Box 59 1790 AB Den Burg Texel / The Netherlands
NOAA/PMEL	NOAA Pacific Marine Environmental Laboratory 7600 Sand Point Way NE Seattle, WA 98115 / USA
Oregon State	Oregon State University 104 CEOAS Admin Bldg. Corvallis, OR 97331 / USA
Princeton	Princeton University 306A Sayre Hall 08544 Princeton, NJ / USA
RBINS	Royal Belgian Institute of Natural Sciences Rue Vautier 29 Brussels 1000 / Belgium
SIO	Scripps Institution of Oceanography University of California, San Diego Oceans and Atmosphere Section Physical Oceanography Curricular Group 9500 Gilman Drive La Jolla, CA 92093-0230 / USA
SIO-ODF	Scripps Institution of Oceanography University of California, San Diego Ocean Data Facility 8855 Biological Grade San Diego, CA 92037 / USA
TU Hamburg-Harburg	TU Hamburg-Harburg Schwarzenbergstraße 95 21073 Hamburg, Germany
TU Braunschweig	TU Braunschweig Pockelsstraße 11 38106 Braunschweig/Germany
UHH	Universität Hamburg Biologiezentrum Grindel und Zoologisches Institut Martin-Luther-King Platz 3 20146 Hamburg / Germany

	Address
U Maine	University of Maine 458 Aubert Hall School of Marine Sciences Orono, ME 04469 / USA
U of Strathclyde	U of Strathclyde 16 Richmond St Glasgow G1 1XQ / United Kingdom
U Washington	University of Washington School of Oceanography Box 355351 Seattle, WA 98195 / USA
van Dorssen Metaalbe- werking	van Dorssen Metaalbewerking Stoompoort 7-I 1792 CT Oudeschild / The Netherland

A.2 FAHRTTEILNEHMER / CRUISE PARTICIPANTS

Name	Vorname/ First Name	Institut/ Institute	Beruf/ Profession
Arndt	Stefanie	AWI	Student
Boebel	Olaf	AWI	Oceanographer
Castellani	Giulia	AWI	Physicist
Ehrlich	Julia	UHH	Student
Feij	Bram	NIOZ	Captain
Flores	Hauke	AWUI, UHH	Biologist
Gall	Fabian	HeliTransair	Technician
Geelhoed	Steve	ITAW	Biologist
González-Dávila	Melchor	IOCAG	Chemist
Graupner	Rainer	AWI	Technician
Heim	Thomas	HeliTransair	Pilot
Hollands	Thomas	AWI	Ecologist
Ivanciu	Ioana	GEOMAR	Student
Janinhoff	Nicole	ITAW	Biologist
Kainz	Johannes	AWI	Student
Klebe	Stefanie	AWI	Technician
Lefering	Katerina	U of Strathclyde	Student
Lemke	Peter	AWI	Oceanographer
Lerchl	Christoph	Ludwig-Max. Univ. München	Student
McKay	Shannon	ITAW	Biologist
Meijboom	André	IMARES	Techniker
Meinhardt	Tim	TU Hamburg-Harburg	Student
Miller	Max	DWD	Meteorologist
Monsees	Matthias	AWI	Technician
Müller	Sebastian	ITAW	Biologist
Nicolaus	Marcel	AWI	Physicist
Rohardt	Friederike	TU Bergakademie Freiburg	Student
Rohardt	Gerd	AWI	Oceanographer
Rohde	Jan	TU Braunschweig	Student
Santana-Casiano	Magdalena	IOCAG	Chemist
Schaafsma	Fokje	IMARES	Student
Schiller	Martin	AWI	Technician
Schuller	Daniel	SIO-ODF	Technician
Schwegmann	Sandra	AWI	Physicist
Sonnabend	Hartmut	DWD	Technician
Spiesecke	Stefanie	AWI	Technician
Steffens	Marting	HeliTransair	Technician

Name	Vorname/ First Name	Institut/ Institute	Beruf/ Profession
Thomisch	Karolin	AWI	Student
van de Putte	Anton	RBINS	Biologist
van Dorssen	Michiel	van Dorssen Metaalbewerking	Techniker
van Franeker	Jan Andries	IMARES	Biologist
Vaupel	Lars	HeliTransair	Pilot
Verdaat	Hans	ITAW	Biologist
Viquerat	Sacha	ITAW	Biologist
Vortkamp	Martina	AWI	Technician
Wurz	Eric	AWI	Student
Zanowski	Hannah	Princetown University	Student
Zwicker	Sarah	AWI	Student

A.3 SCHIFFSBESATZUNG / SHIP'S CREW

	Name	Rank
1	Wunderlich, Thomas	Master
2	Spielke, Steffen	1st Offc.
3	Ziemann, Olaf	Ch.Eng.
4	Kentges, Felix	2nd Offc.
5	Lauber, Felix	2nd Offc.
6	Stolze, Henrik	2nd Offc.
7	Spilok, Norbert	Doctor
8	Hofmann, Jörg	Comm.Offc
9	Schnürch, Helmut	2nd Eng.
10	Westphal, Henning	2nd Eng.
11	Rusch, Torben	3rd Eng.
12	Brehme, Andreas	Elec.Eng.
13	Dimmler, Werner	ELO
14	Feiertag, Thomas	ELO
15	Ganter, Armin	ELO
16	Winter, Andreas	ELO
17	Schröter, Rene	Boatsw.
18	Neisner, Winfried	Carpenter
19	Burzan, Gerd-Ekkeh.	A.B.
20	Clasen, Nils	A.B.
21	Gladow, Lothar	A.B.
22	Hartwig-Lab.,Andreas	A.B.
23	Kretzschmar, Uwe	A.B.
24	Müller, Steffen	A.B.
25	Schröder, Horst	A.B.
26	Schröder, Norbert	A.B.
27	Sedlak, Andreas	A.B.
28	Beth, Detlef	Storek.
29	Dinse, Horst	Mot-man
30	Fritz, Günter	Mot-man
31	Krösche, Eckard	Mot-man
32	Plehn, Markus	Mot-man

33	Watzel, Bernhard	Mot-man
34	Meißner, Jörg	Cook
35	Tupy, Mario	Cooksmate
36	Völske, Thomas	Cooksmate
37	Luoto, Eija	1.Stwdess
38	Westphal, Kerstin	Stwdss/N.
39	Chen, Quan Lun	2.Steward
40	Hischke, Peggy	2.Stwdess
41	Hu, Guo Yong	2.Steward
42	Mack, Ulrich	2.Steward
43	Wartenberg, Irina	2.Stwdess
44	Ruan, Hui Guang	Laundrym.

A.4 STATIONSLISTE / STATION LIST PS89

Station	Date	Time	Gear	Action	Position Lat	Position Lon	Water depth (m)
PS89/1-1	04.12.2014	04:57:00	CTD/RO	on ground/ max depth	37° 6.17' S	12° 45.62' E	4890.0
PS89/1-2	04.12.2014	07:07:01	PIES	on ground/ max depth	37° 5.77' S	12° 45.23' E	4993.2
PS89/2-1	05.12.2014	00:56:00	CTD/RO	on ground/ max depth	39° 13.66' S	11° 20.03' E	5128.7
PS89/2-2	05.12.2014	03:41:00	PIES	on ground/ max depth	39° 13.68' S	11° 20.21' E	5128.5
PS89/2-3	05.12.2014	03:49:01	SOCCOM	on ground/ max depth	39° 13.74' S	11° 20.28' E	5130.2
PS89/3-1	05.12.2014	18:12:00	CTD/RO	on ground/ max depth	41° 9.88' S	9° 55.60' E	4610.0
PS89/3-2	05.12.2014	18:32:01	PIES	on ground/ max depth	41° 9.88' S	9° 55.60' E	4621.7
PS89/4-1	06.12.2014	09:05:00	CTD/RO	on ground/ max depth	42° 58.54' S	8° 30.56' E	3928.0
PS89/4-2	06.12.2014	10:59:00	CTD/RO	on ground/ max depth	42° 58.79' S	8° 30.35' E	3930.7
PS89/4-3	06.12.2014	11:20:00	PIES	on ground/ max depth	42° 58.81' S	8° 30.31' E	3932.0
PS89/5-1	07.12.2014	03:44:00	CTD/RO	on ground/ max depth	44° 39.47' S	7° 5.54' E	4585.2
PS89/5-2	07.12.2014	04:22:00	PIES	on ground/ max depth	44° 39.48' S	7° 5.57' E	4590.0
PS89/5-3	07.12.2014	05:54:59	SOCCOM	on ground/ max depth	44° 39.52' S	7° 5.58' E	4595.5
PS89/6-1	07.12.2014	18:04:00	CTD/RO	on ground/ max depth	46° 12.90' S	5° 40.50' E	4831.2
PS89/6-2	07.12.2014	18:36:00	PIES	on ground/ max depth	46° 12.91' S	5° 40.51' E	4800.0
PS89/7-1	08.12.2014	07:43:00	CTD/RO	on ground/ max depth	47° 40.28' S	4° 15.22' E	4540.5
PS89/7-2	08.12.2014	08:30:00	PIES	on ground/ max depth	47° 40.26' S	4° 15.13' E	4538.5
PS89/8-1	08.12.2014	23:19:00	CTD/RO	on ground/ max depth	49° 2.12' S	2° 51.60' E	4218.2
PS89/8-2	09.12.2014	01:02:59	SOCCOM	on ground/ max depth	49° 3.18' S	2° 52.10' E	4248.5
PS89/9-1	09.12.2014	14:51:00	CTD/RO	on ground/ max depth	50° 15.30' S	1° 25.53' E	3892.5
PS89/9-2	09.12.2014	15:23:01	PIES	on ground/ max depth	50° 15.40' S	1° 25.47' E	3895.7
PS89/10-1	10.12.2014	02:23:00	PIES	on ground/ max depth	51° 25.35' S	0° 0.92' E	2709.4
PS89/10-2	10.12.2014	03:41:00	CTD/RO	on ground/ max depth	51° 25.31' S	0° 0.58' E	2683.0

Station	Date	Time	Gear	Action	Position Lat	Position Lon	Water depth (m)
PS89/11-1	10.12.2014	11:48:00	CTD/RO	on ground/ max depth	52° 28.72' S	0° 0.06' W	2597.6
PS89/12-1	10.12.2014	19:07:00	PIES	on ground/ max depth	53° 31.35' S	0° 0.36' E	2640.6
PS89/12-2	10.12.2014	21:21:00	CTD/RO	on ground/ max depth	53° 31.46' S	0° 0.18' E	2647.1
PS89/12-3	10.12.2014	22:34:59	SOCCOM	on ground/ max depth	53° 30.96' S	0° 0.20' E	2644.7
PS89/13-1	11.12.2014	08:19:00	CTD/RO	on ground/ max depth	54° 15.26' S	0° 0.12' W	2733.5
PS89/14-1	11.12.2014	15:13:00	CTD/RO	on ground/ max depth	54° 59.99' S	0° 0.02' W	1704.9
PS89/15-1	11.12.2014	23:38:00	CTD/RO	on ground/ max depth	55° 59.96' S	0° 0.16' E	3685.1
PS89/15-2	12.12.2014	01:17:59	FLOAT	on ground/ max depth	56° 0.30' S	0° 0.17' W	3860.7
PS89/16-1	12.12.2014	08:11:00	CTD/RO	on ground/ max depth	56° 55.62' S	0° 0.35' E	3646.3
PS89/16-2	12.12.2014	08:42:00	PIES	on ground/ max depth	56° 55.63' S	0° 0.36' E	3646.3
PS89/17-1	12.12.2014	10:32:00	HYDRO	on ground/ max depth	56° 55.19' S	0° 1.02' E	3600.5
PS89/17-1	12.12.2014	10:33:00	HYDRO	profile start	56° 55.32' S	0° 0.86' E	3593.7
PS89/17-1	12.12.2014	10:41:00	HYDRO	profile end	56° 56.48' S	0° 0.24' W	3702.5
PS89/16-3	12.12.2014	11:00:59	SOCCOM	on ground/ max depth	56° 56.83' S	0° 0.30' W	3764.7
PS89/18-1	12.12.2014	15:23:00	RMT	profile start	57° 26.66' S	0° 4.77' E	3838.0
PS89/18-1	12.12.2014	17:30:01	RMT	profile end	57° 24.39' S	0° 14.55' E	4508.4
PS89/19-1	12.12.2014	23:17:00	CTD/RO	on ground/ max depth	58° 0.08' S	0° 0.12' E	4528.3
PS89/20-1	13.12.2014	07:15:00	MOR	on ground/ max depth	59° 2.60' S	0° 4.90' E	4647.6
PS89/20-2	13.12.2014	11:25:00	CTD/RO	on ground/ max depth	59° 2.24' S	0° 5.63' E	4639.0
PS89/20-3	13.12.2014	11:47:00	PIES	on ground/ max depth	59° 2.25' S	0° 5.76' E	4637.8
PS89/20-4	13.12.2014	13:45:00	HYDRO	profile start	59° 2.50' S	0° 6.33' E	4633.2
PS89/20-4	13.12.2014	13:52:00	HYDRO	profile end	59° 1.46' S	0° 5.01' E	4614.0
PS89/20-5	13.12.2014	16:38:00	MOR	on ground/ max depth	59° 2.67' S	0° 5.37' E	4645.9
PS89/20-6	13.12.2014	17:25:00	SOSO-C	on ground/ max depth	59° 3.37' S	0° 4.60' E	4660.2
PS89/20-7	13.12.2014	18:23:00	SOSO-C	on ground/ max depth	59° 3.34' S	0° 4.43' E	4661.5
PS89/21-1	14.12.2014	03:20:00	CTD/RO	on ground/ max depth	59° 59.09' S	0° 0.08' E	5374.5
PS89/21-2	14.12.2014	05:05:59	SOCCOM	on ground/ max depth	59° 59.01' S	0° 0.03' E	5373.7
PS89/22-1	14.12.2014	08:48:00	SUIT	profile start	60° 22.91' S	0° 5.75' E	5374.2

A.4 Stationsliste / station list PS89

Station	Date	Time	Gear	Action	Position Lat	Position Lon	Water depth (m)
PS89/22-1	14.12.2014	09:18:00	SUIT	profile end	60° 22.63' S	0° 8.15' E	5375.8
PS89/23-1	14.12.2014	16:50:00	CTD/RO	on ground/ max depth	60° 59.86' S	0° 0.38' W	5393.2
PS89/23-2	14.12.2014	19:32:00	SOSO-C	on ground/ max depth	61° 0.38' S	0° 0.70' W	
PS89/23-3	14.12.2014	20:29:00	SOSO-C	on ground/ max depth	61° 0.15' S	0° 0.44' W	
PS89/24-1	15.12.2014	07:11:00	CTD/RO	on ground/ max depth	61° 59.58' S	0° 0.84' E	5368.1
PS89/24-2	15.12.2014	09:47:00	SUIT	profile start	61° 59.30' S	0° 1.08' E	5368.8
PS89/24-2	15.12.2014	10:17:00	SUIT	profile end	61° 59.31' S	0° 1.02' W	5367.4
PS89/25-1	15.12.2014	14:43:00	RMT	profile start	62° 21.24' S	0° 2.60' W	5357.0
PS89/25-1	15.12.2014	15:40:00	RMT	profile end	62° 23.54' S	0° 2.89' W	5353.5
PS89/25-2	15.12.2014	16:30:00	SOSO-C	on ground/ max depth	62° 23.98' S	0° 2.52' W	5353.0
PS89/25-3	15.12.2014	17:28:00	SOSO-C	on ground/ max depth	62° 24.09' S	0° 1.89' W	
PS89/26-1	16.12.2014	00:14:00	CTD/RO	on ground/ max depth	62° 59.37' S	0° 0.36' E	5310.9
PS89/27-1	16.12.2014	11:06:00	CTD/RO	on ground/ max depth	64° 1.58' S	0° 1.04' W	5192.7
PS89/27-2	16.12.2014	18:27:00	MOR	on ground/ max depth	63° 59.57' S	0° 2.34' W	
PS89/27-3	17.12.2014	11:43:59	MOR	on ground/ max depth	64° 0.31' S	0° 0.22' W	
PS89/27-4	17.12.2014	14:38:00	PIES	on ground/ max depth	64° 0.99' S	0° 3.47' W	
PS89/27-5	17.12.2014	15:42:00	RMT	profile start	64° 2.54' S	0° 4.35' W	5194.5
PS89/27-5	17.12.2014	16:42:00	RMT	profile end	64° 5.24' S	0° 3.47' W	5190.5
PS89/27-6	17.12.2014	17:53:00	SUIT	profile start	64° 7.06' S	0° 2.29' W	
PS89/27-6	17.12.2014	18:22:00	SUIT	profile end	64° 8.10' S	0° 0.95' W	5185.5
PS89/28-1	18.12.2014	01:24:00	CTD/RO	on ground/ max depth	65° 0.02' S	0° 0.02' E	3735.4
PS89/28-2	18.12.2014	02:59:59	SOCCOM	on ground/ max depth	64° 59.68' S	0° 0.09' E	3780.0
PS89/29-1	18.12.2014	09:28:01	SUIT	profile start	65° 57.18' S	0° 2.15' W	3575.6
PS89/29-1	18.12.2014	09:58:00	SUIT	profile end	65° 58.37' S	0° 2.75' W	3576.9
PS89/29-2	18.12.2014	11:21:00	MOR	on ground/ max depth	66° 1.84' S	0° 3.00' E	
PS89/29-3	18.12.2014	14:52:00	RMT	profile start	66° 1.26' S	0° 2.76' E	3671.0
PS89/29-3	18.12.2014	15:50:00	RMT	profile end	66° 3.56' S	0° 2.80' E	3567.1
PS89/29-4	18.12.2014	18:25:00	CTD/RO	on ground/ max depth	66° 1.89' S	0° 2.87' E	3614.9
PS89/30-1	19.12.2014	02:05:00	CTD/RO	on ground/ max depth	66° 27.71' S	0° 1.49' W	4500.2
PS89/30-2	19.12.2014	04:36:00	RMT	profile start	66° 26.76' S	0° 3.36' W	4377.4
PS89/30-2	19.12.2014	05:39:00	RMT	profile end	66° 27.66' S	0° 9.30' W	4312.5

Station	Date	Time	Gear	Action	Position Lat	Position Lon	Water depth (m)
PS89/30-3	19.12.2014	09:24:00	MOR	on ground/ max depth	66° 30.68' S	0° 0.68' W	
PS89/30-4	19.12.2014	14:09:00	SUIT	profile start	66° 29.48' S	0° 2.12' E	
PS89/30-4	19.12.2014	14:50:00	SUIT	profile end	66° 29.41' S	0° 2.61' W	
PS89/30-6	19.12.2014	17:59:00	MOR	on ground/ max depth	66° 30.41' S	0° 0.66' W	
PS89/30-5	19.12.2014	18:01:00	ICE	on ground/ max depth	66° 30.41' S	0° 0.66' W	
PS89/31-1	20.12.2014	00:52:00	CTD/RO	on ground/ max depth	66° 58.75' S	0° 0.23' W	4709.8
PS89/31-2	20.12.2014	02:46:59	SOCCOM	on ground/ max depth	66° 58.73' S	0° 0.74' W	4700.0
PS89/32-2	20.12.2014	12:09:00	SOSO-C	on ground/ max depth	67° 34.81' S	0° 8.34' E	
PS89/32-3	20.12.2014	12:55:00	SOSO-C	on ground/ max depth	67° 34.62' S	0° 8.70' E	
PS89/32-4	20.12.2014	15:23:00	CTD/RO	on ground/ max depth	67° 34.18' S	0° 8.47' E	4153.5
PS89/32-1	20.12.2014	20:00:00	ICE	on ground/ max depth	67° 34.76' S	0° 6.31' E	
PS89/33-1	21.12.2014	02:49:00	CTD/RO	on ground/ max depth	68° 0.03' S	0° 1.26' W	4512.9
PS89/34-1	21.12.2014	21:52:00	MOR	on ground/ max depth	68° 59.70' S	0° 6.15' W	
PS89/35-2	22.12.2014	17:19:59	MOR	on ground/ max depth	69° 0.19' S	0° 2.43' W	
PS89/35-1	22.12.2014	20:00:00	ICE	on ground/ max depth	69° 0.17' S	0° 1.57' W	
PS89/36-1	22.12.2014	23:23:00	CTD/RO	on ground/ max depth	69° 0.61' S	0° 1.62' W	3369.4
PS89/37-1	23.12.2014	09:52:01	MOR	on ground/ max depth	68° 58.89' S	0° 5.00' W	
PS89/37-2	23.12.2014	11:16:00	SUIT	profile end	68° 58.72' S	0° 4.34' W	3408.4
PS89/38-1	23.12.2014	17:42:00	SUIT	profile start	69° 1.30' S	0° 50.06' W	2939.2
PS89/38-1	23.12.2014	17:55:02	SUIT	profile end	69° 1.60' S	0° 51.15' W	2945.5
PS89/39-1	24.12.2014	14:21:00	MUC	on ground/ max depth	69° 59.09' S	4° 4.54' W	2309.8
PS89/39-2	24.12.2014	16:26:00	MUC	on ground/ max depth	69° 59.26' S	4° 4.39' W	2315.1
PS89/41-1	27.12.2014	11:29:01	RMT	profile start	70° 31.61' S	7° 53.15' W	255.9
PS89/41-1	27.12.2014	11:49:00	RMT	profile end	70° 31.17' S	7° 55.12' W	245.8
PS89/40-1	27.12.2014	19:50:00	ICE	on ground/ max depth	70° 31.58' S	7° 57.44' W	240.6
PS89/40-2	28.12.2014	10:30:00	ICE	on ground/ max depth	70° 31.98' S	8° 3.91' W	217.0
PS89/40-3	29.12.2014	10:54:00	ICE	on ground/ max depth	70° 31.98' S	8° 4.32' W	214.0
PS89/40-4	31.12.2014	10:11:00	SOSO-C	on ground/ max depth	70° 31.98' S	8° 4.32' W	201.0

A.4 Stationsliste / station list PS89

Station	Date	Time	Gear	Action	Position Lat	Position Lon	Water depth (m)
PS89/40-5	31.12.2014	11:14:00	ICE	on ground/ max depth	70° 31.98' S	8° 4.33' W	201.0
PS89/40-6	31.12.2014	11:34:00	SOSO-C	on ground/ max depth	70° 31.98' S	8° 4.33' W	205.0
PS89/40-7	31.12.2014	12:54:00	SOSO-C	on ground/ max depth	70° 31.98' S	8° 4.33' W	203.0
PS89/40-8	01.01.2015	13:43:00	SOSO-C	on ground/ max depth	70° 31.99' S	8° 4.31' W	201.0
PS89/40-9	01.01.2015	14:47:00	SOSO-C	on ground/ max depth	70° 31.99' S	8° 4.31' W	202.0
PS89/40-10	01.01.2015	15:38:00	SOSO-C	on ground/ max depth	70° 31.99' S	8° 4.31' W	202.0
PS89/42-1	03.01.2015	00:24:00	CTD/RO	on ground/ max depth	70° 34.46' S	9° 3.33' W	467.0
PS89/40-11	03.01.2015	05:17:00	CTD/RO	on ground/ max depth	70° 31.40' S	7° 57.72' W	232.0
PS89/43-1	03.01.2015	13:50:00	RMT	profile start	70° 27.47' S	8° 18.76' W	355.0
PS89/43-1	03.01.2015	14:19:00	RMT	profile end	70° 27.09' S	8° 15.92' W	395.6
PS89/44-1	03.01.2015	18:20:00	ICE	on ground/ max depth	70° 26.27' S	8° 17.34' W	437.2
PS89/45-1	03.01.2015	20:12:00	ICE	on ground/ max depth	70° 31.58' S	7° 57.80' W	239.8
PS89/46-1	04.01.2015	08:04:00	ICE	on ground/ max depth	70° 33.49' S	7° 38.44' W	
PS89/47-1	05.01.2015	08:51:00	SOSO-C	on ground/ max depth	70° 22.52' S	8° 8.23' W	759.0
PS89/48-1	07.01.2015	14:13:00	SOSO-C	on ground/ max depth	70° 31.96' S	8° 50.79' W	363.0
PS89/48-2	07.01.2015	15:10:00	SOSO-C	on ground/ max depth	70° 31.98' S	8° 50.76' W	361.0
PS89/48-3	07.01.2015	16:54:00	SOSO-C	on ground/ max depth	70° 32.03' S	8° 50.60' W	360.0
PS89/48-4	07.01.2015	17:51:00	SOSO-C	on ground/ max depth	70° 32.21' S	8° 50.48' W	358.0
PS89/49-1	07.01.2015	22:17:00	CTD/RO	on ground/ max depth	70° 31.31' S	8° 45.46' W	156.0
PS89/49-2	07.01.2015	23:10:00	CTD/RO	on ground/ max depth	70° 31.32' S	8° 45.45' W	156.0
PS89/49-3	08.01.2015	00:09:00	CTD/RO	on ground/ max depth	70° 31.28' S	8° 45.29' W	154.0
PS89/49-4	08.01.2015	01:07:00	CTD/RO	on ground/ max depth	70° 31.25' S	8° 45.33' W	151.0
PS89/49-5	08.01.2015	02:06:00	CTD/RO	on ground/ max depth	70° 31.31' S	8° 45.46' W	155.0
PS89/49-6	08.01.2015	03:09:00	CTD/RO	on ground/ max depth	70° 31.31' S	8° 45.52' W	158.0
PS89/49-7	08.01.2015	04:14:00	CTD/RO	on ground/ max depth	70° 31.29' S	8° 45.44' W	153.0
PS89/49-8	08.01.2015	05:22:00	CTD/RO	on ground/ max depth	70° 31.32' S	8° 45.55' W	171.9

Station	Date	Time	Gear	Action	Position Lat	Position Lon	Water depth (m)
PS89/49-9	08.01.2015	06:22:00	CTD/RO	on ground/ max depth	70° 31.35' S	8° 45.52' W	174.1
PS89/49-10	08.01.2015	07:16:00	CTD/RO	on ground/ max depth	70° 31.34' S	8° 45.55' W	174.0
PS89/49-11	08.01.2015	08:10:00	CTD/RO	on ground/ max depth	70° 31.39' S	8° 45.53' W	177.5
PS89/49-12	08.01.2015	09:12:00	CTD/RO	on ground/ max depth	70° 31.38' S	8° 45.58' W	179.2
PS89/50-1	09.01.2015	10:35:00	ICE	on ground/ max depth	70° 30.87' S	8° 43.89' W	99.0
PS89/51-1	09.01.2015	17:03:00	SOSO-C	on ground/ max depth	70° 30.62' S	8° 51.75' W	420.0
PS89/51-2	09.01.2015	18:18:00	SOSO-C	on ground/ max depth	70° 31.10' S	8° 51.31' W	395.0
PS89/51-3	09.01.2015	19:25:00	SOSO-C	on ground/ max depth	70° 31.43' S	8° 51.18' W	388.0
PS89/52-1	09.01.2015	21:06:00	CTD/RO	on ground/ max depth	70° 31.39' S	8° 45.58' W	168.0
PS89/52-2	09.01.2015	22:04:00	CTD/RO	on ground/ max depth	70° 31.40' S	8° 45.56' W	168.0
PS89/52-3	09.01.2015	23:04:00	CTD/RO	on ground/ max depth	70° 31.39' S	8° 45.48' W	164.0
PS89/52-4	10.01.2015	00:09:00	CTD/RO	on ground/ max depth	70° 31.32' S	8° 45.42' W	155.0
PS89/52-5	10.01.2015	01:09:00	CTD/RO	on ground/ max depth	70° 31.31' S	8° 45.50' W	157.0
PS89/52-6	10.01.2015	02:08:00	CTD/RO	on ground/ max depth	70° 31.31' S	8° 45.38' W	154.0
PS89/52-7	10.01.2015	03:06:00	CTD/RO	on ground/ max depth	70° 31.32' S	8° 45.39' W	154.0
PS89/52-8	10.01.2015	04:12:00	CTD/RO	on ground/ max depth	70° 31.32' S	8° 45.48' W	157.0
PS89/52-9	10.01.2015	05:09:00	CTD/RO	on ground/ max depth	70° 31.35' S	8° 45.38' W	157.0
PS89/52-10	10.01.2015	06:09:00	CTD/RO	on ground/ max depth	70° 31.38' S	8° 45.39' W	159.0
PS89/52-11	10.01.2015	07:10:00	CTD/RO	on ground/ max depth	70° 31.40' S	8° 45.44' W	162.0
PS89/52-12	10.01.2015	08:04:00	CTD/RO	on ground/ max depth	70° 31.38' S	8° 45.49' W	163.0
PS89/53-1	10.01.2015	09:21:00	RMT	profile start	70° 32.31' S	8° 55.03' W	434.0
PS89/53-1	10.01.2015	09:37:00	RMT	profile end	70° 32.20' S	8° 53.27' W	426.0
PS89/53-2	10.01.2015	10:53:01	SUIT	profile start	70° 32.38' S	8° 55.75' W	437.0
PS89/53-2	10.01.2015	11:33:00	SUIT	profile end	70° 32.10' S	8° 51.25' W	387.3
PS89/54-1	10.01.2015	13:11:00	CTD/RO	on ground/ max depth	70° 31.31' S	8° 45.50' W	168.5
PS89/54-2	10.01.2015	14:09:00	CTD/RO	on ground/ max depth	70° 31.31' S	8° 45.47' W	166.4
PS89/54-3	10.01.2015	15:07:00	CTD/RO	on ground/ max depth	70° 31.29' S	8° 45.45' W	163.6

A.4 Stationsliste / station list PS89

Station	Date	Time	Gear	Action	Position Lat	Position Lon	Water depth (m)
PS89/55-1	10.01.2015	15:54:00	SOSO-C	on ground/ max depth	70° 30.25' S	8° 51.69' W	440.2
PS89/55-2	10.01.2015	16:52:00	SOSO-C	on ground/ max depth	70° 30.39' S	8° 51.40' W	436.4
PS89/55-3	10.01.2015	17:40:00	SOSO-C	on ground/ max depth	70° 30.64' S	8° 51.29' W	420.4
PS89/56-1	10.01.2015	19:08:00	CTD/RO	on ground/ max depth	70° 31.35' S	8° 45.45' W	
PS89/56-2	10.01.2015	20:02:00	CTD/RO	on ground/ max depth	70° 31.36' S	8° 45.43' W	157.0
PS89/56-3	10.01.2015	21:04:00	CTD/RO	on ground/ max depth	70° 31.34' S	8° 45.45' W	157.0
PS89/56-4	10.01.2015	22:04:00	CTD/RO	on ground/ max depth	70° 31.37' S	8° 45.36' W	157.0
PS89/53-3	10.01.2015	23:08:01	SUIT	profile start	70° 32.19' S	8° 53.23' W	439.3
PS89/53-3	10.01.2015	23:38:00	SUIT	profile end	70° 31.94' S	8° 49.50' W	353.4
PS89/57-1	11.01.2015	01:08:00	CTD/RO	on ground/ max depth	70° 31.28' S	8° 45.47' W	164.6
PS89/57-2	11.01.2015	02:07:00	CTD/RO	on ground/ max depth	70° 31.29' S	8° 45.51' W	166.5
PS89/57-3	11.01.2015	03:06:00	CTD/RO	on ground/ max depth	70° 31.30' S	8° 45.50' W	167.1
PS89/57-4	11.01.2015	04:07:00	CTD/RO	on ground/ max depth	70° 31.28' S	8° 45.45' W	164.6
PS89/57-5	11.01.2015	05:06:00	CTD/RO	on ground/ max depth	70° 31.36' S	8° 45.42' W	
PS89/57-6	11.01.2015	07:06:59	CTD/RO	on ground/ max depth	70° 31.30' S	8° 45.42' W	
PS89/57-7	11.01.2015	08:09:00	CTD/RO	on ground/ max depth	70° 31.32' S	8° 45.46' W	156.0
PS89/57-8	11.01.2015	09:06:00	CTD/RO	on ground/ max depth	70° 31.32' S	8° 45.51' W	158.0
PS89/57-9	11.01.2015	10:07:00	CTD/RO	on ground/ max depth	70° 31.35' S	8° 45.53' W	161.0
PS89/57-10	11.01.2015	11:07:00	CTD/RO	on ground/ max depth	70° 31.34' S	8° 45.43' W	157.0
PS89/57-11	11.01.2015	12:11:00	CTD/RO	on ground/ max depth	70° 31.34' S	8° 45.40' W	156.0
PS89/57-12	11.01.2015	13:06:00	CTD/RO	on ground/ max depth	70° 31.31' S	8° 45.47' W	155.0
PS89/57-13	11.01.2015	14:09:00	CTD/RO	on ground/ max depth	70° 31.26' S	8° 45.50' W	152.0
PS89/57-14	11.01.2015	16:09:00	CTD/RO	on ground/ max depth	70° 31.30' S	8° 45.53' W	156.0
PS89/57-15	11.01.2015	17:08:00	CTD/RO	on ground/ max depth	70° 31.30' S	8° 45.51' W	156.0
PS89/58-1	11.01.2015	17:59:00	ICE	on ground/ max depth	70° 30.87' S	8° 43.90' W	99.0
PS89/57-16	11.01.2015	19:10:00	CTD/RO	on ground/ max depth	70° 31.30' S	8° 45.49' W	154.0

Station	Date	Time	Gear	Action	Position Lat	Position Lon	Water depth (m)
PS89/57-17	11.01.2015	20:09:00	CTD/RO	on ground/ max depth	70° 31.31' S	8° 45.47' W	155.0
PS89/57-18	11.01.2015	21:07:00	CTD/RO	on ground/ max depth	70° 31.32' S	8° 45.51' W	158.0
PS89/57-19	11.01.2015	22:07:00	CTD/RO	on ground/ max depth	70° 31.33' S	8° 45.56' W	161.0
PS89/57-20	11.01.2015	23:06:00	CTD/RO	on ground/ max depth	70° 31.35' S	8° 45.48' W	159.0
PS89/57-21	12.01.2015	00:06:00	CTD/RO	on ground/ max depth	70° 31.35' S	8° 45.49' W	159.0
PS89/59-1	12.01.2015	01:12:00	SUIT	profile start	70° 31.89' S	8° 48.63' W	304.0
PS89/59-1	12.01.2015	01:42:00	SUIT	profile end	70° 30.88' S	8° 46.64' W	167.0
PS89/59-2	12.01.2015	03:02:00	RMT	profile start	70° 32.07' S	8° 48.57' W	310.0
PS89/59-2	12.01.2015	03:20:00	RMT	profile end	70° 31.61' S	8° 47.03' W	286.0
PS89/59-3	12.01.2015	08:16:01	SUIT	profile start	70° 30.89' S	8° 47.06' W	220.0
PS89/59-3	12.01.2015	08:31:00	SUIT	profile end	70° 30.55' S	8° 46.03' W	116.0
PS89/59-4	12.01.2015	12:42:00	SUIT	profile start	70° 30.87' S	8° 47.80' W	267.0
PS89/59-4	12.01.2015	13:11:00	SUIT	profile end	70° 30.39' S	8° 45.54' W	117.4
PS89/59-5	12.01.2015	20:06:01	SUIT	profile start	70° 31.56' S	8° 47.01' W	302.5
PS89/59-5	12.01.2015	20:41:00	SUIT	profile end	70° 30.28' S	8° 45.02' W	130.7
PS89/59-6	12.01.2015	23:15:01	RMT	profile start	70° 32.11' S	8° 46.70' W	317.5
PS89/59-6	12.01.2015	23:27:00	RMT	profile end	70° 31.78' S	8° 46.10' W	245.6
PS89/60-1	15.01.2015	11:40:59	FLOAT	on ground/ max depth	69° 46.55' S	10° 6.49' W	1860.0
PS89/61-1	15.01.2015	13:55:59	FLOAT	on ground/ max depth	69° 29.99' S	10° 32.49' W	
PS89/62-1	15.01.2015	15:36:00	SUIT	profile start	69° 27.59' S	10° 27.09' W	3772.9
PS89/62-1	15.01.2015	16:11:00	SUIT	profile end	69° 26.87' S	10° 23.60' W	3648.5
PS89/62-2	15.01.2015	17:49:01	RMT	profile start	69° 28.09' S	10° 26.54' W	3790.0
PS89/62-2	15.01.2015	18:46:00	RMT	profile end	69° 27.03' S	10° 20.91' W	3621.9
PS89/63-1	15.01.2015	21:01:59	FLOAT	on ground/ max depth	69° 13.66' S	10° 20.37' W	3977.6
PS89/64-1	15.01.2015	22:39:59	FLOAT	on ground/ max depth	69° 0.05' S	10° 18.39' W	4513.7
PS89/65-1	16.01.2015	04:18:59	FLOAT	on ground/ max depth	68° 59.99' S	7° 59.94' W	3544.5
PS89/66-1	16.01.2015	07:28:00	MOR	on ground/ max depth	69° 0.39' S	6° 59.43' W	
PS89/66-2	16.01.2015	10:55:00	CTD/RO	on ground/ max depth	69° 0.31' S	6° 59.19' W	2948.8
PS89/66-3	16.01.2015	14:20:00	MOR	on ground/ max depth	69° 0.34' S	6° 58.95' W	2946.2
PS89/66-4	16.01.2015	15:33:01	RMT	profile start	69° 0.91' S	6° 56.13' W	2870.9
PS89/66-4	16.01.2015	16:33:01	RMT	profile end	69° 1.44' S	6° 49.98' W	2806.1
PS89/66-5	16.01.2015	17:27:01	SUIT	profile start	69° 1.76' S	6° 47.97' W	2804.7
PS89/66-5	16.01.2015	17:57:00	SUIT	profile end	69° 2.34' S	6° 45.18' W	2792.5

A.4 Stationsliste / station list PS89

Station	Date	Time	Gear	Action	Position Lat	Position Lon	Water depth (m)
PS89/67-1	16.01.2015	20:01:00	MUC	on ground/ max depth	69° 2.31' S	6° 35.95' W	
PS89/68-1	16.01.2015	23:42:59	FLOAT	on ground/ max depth	69° 0.24' S	5° 45.97' W	
PS89/69-1	17.01.2015	03:03:59	FLOAT	on ground/ max depth	68° 39.92' S	5° 5.12' W	
PS89/70-1	17.01.2015	11:44:01	RMT	profile start	68° 15.07' S	3° 56.83' W	4094.8
PS89/70-1	17.01.2015	12:45:00	RMT	profile end	68° 15.48' S	4° 3.23' W	4084.8
PS89/70-2	17.01.2015	14:07:00	SUIT	profile start	68° 15.48' S	3° 56.07' W	4086.8
PS89/70-2	17.01.2015	14:42:00	SUIT	profile end	68° 15.35' S	4° 0.08' W	4091.8
PS89/70-3	17.01.2015	15:03:59	FLOAT	on ground/ max depth	68° 15.20' S	4° 0.40' W	4093.4
PS89/71-1	17.01.2015	16:35:01	SUIT	profile start	68° 12.21' S	3° 42.05' W	4124.7
PS89/71-1	17.01.2015	17:06:00	SUIT	profile end	68° 12.29' S	3° 45.56' W	4130.9
PS89/72-1	17.01.2015	22:08:59	FLOAT	on ground/ max depth	67° 59.92' S	3° 14.33' W	4214.4
PS89/73-1	18.01.2015	04:18:00	CTD/RO	on ground/ max depth	67° 39.99' S	1° 45.17' W	
PS89/73-2	18.01.2015	06:11:59	FLOAT	on ground/ max depth	67° 39.96' S	1° 45.36' W	
PS89/73-3	18.01.2015	06:16:59	FLOAT	on ground/ max depth	67° 39.91' S	1° 45.11' W	
PS89/74-1	18.01.2015	09:35:59	FLOAT	on ground/ max depth	67° 20.14' S	0° 56.37' W	
PS89/75-1	18.01.2015	13:52:59	FLOAT	on ground/ max depth	67° 0.17' S	0° 0.84' W	4500.0
PS89/76-1	18.01.2015	20:23:59	FLOAT	on ground/ max depth	66° 39.89' S	0° 0.56' E	
PS89/77-1	19.01.2015	00:36:59	FLOAT	on ground/ max depth	66° 20.17' S	0° 0.02' W	4022.0
PS89/78-1	19.01.2015	05:45:00	CTD/RO	on ground/ max depth	66° 2.13' S	0° 0.80' E	3642.3
PS89/78-2	19.01.2015	07:39:59	FLOAT	on ground/ max depth	66° 1.50' S	0° 2.03' E	
PS89/78-3	19.01.2015	07:46:59	FLOAT	on ground/ max depth	66° 1.29' S	0° 2.34' E	3677.8
PS89/79-1	19.01.2015	10:16:00	RMT	profile start	65° 51.44' S	0° 2.05' E	3613.2
PS89/79-1	19.01.2015	11:45:00	RMT	profile end	65° 47.99' S	0° 3.34' E	3654.7
PS89/80-1	20.01.2015	07:41:00	CTD/RO	on ground/ max depth	63° 55.07' S	0° 0.44' E	
PS89/80-2	20.01.2015	11:39:00	MOR	on ground/ max depth	63° 54.94' S	0° 0.17' E	
PS89/80-3	20.01.2015	12:10:00	RMT	profile start	63° 53.64' S	0° 0.15' E	5208.0
PS89/80-3	20.01.2015	14:05:00	RMT	profile end	63° 49.49' S	0° 0.61' W	5216.3
PS89/80-4	20.01.2015	14:49:00	SUIT	profile start	63° 48.59' S	0° 0.49' W	5218.2
PS89/80-4	20.01.2015	15:22:00	SUIT	profile end	63° 47.51' S	0° 0.12' W	5220.3
PS89/81-1	21.01.2015	12:34:00	CTD/RO	on ground/ max depth	61° 0.09' S	0° 0.14' W	5384.5

Station	Date	Time	Gear	Action	Position Lat	Position Lon	Water depth (m)
PS89/81-2	21.01.2015	14:38:59	SOCCOM	on ground/ max depth	61° 0.12' S	0° 0.08' W	5384.0
PS89/82-1	27.01.2015	14:01:00	CTD/RO	on ground/ max depth	49° 0.02' S	12° 56.05' E	4120.5
PS89/82-2	27.01.2015	15:40:00	CTD/RO	on ground/ max depth	49° 0.00' S	12° 55.95' E	4120.6
PS89/82-3	27.01.2015	17:08:59	FLOAT	on ground/ max depth	49° 0.07' S	12° 56.09' E	4124.3

Die **Berichte zur Polar- und Meeresforschung** (ISSN 1866-3192) werden beginnend mit dem Band 569 (2008) als Open-Access-Publikation herausgegeben. Ein Verzeichnis aller Bände einschließlich der Druckausgaben (ISSN 1618-3193, Band 377-568, von 2000 bis 2008) sowie der früheren **Berichte zur Polarforschung** (ISSN 0176-5027, Band 1-376, von 1981 bis 2000) befindet sich im electronic Publication Information Center (**ePIC**) des Alfred-Wegener-Instituts, Helmholtz-Zentrum für Polar- und Meeresforschung (AWI); see <http://epic.awi.de>. Durch Auswahl "Reports on Polar- and Marine Research" (via "browse"/"type") wird eine Liste der Publikationen, sortiert nach Bandnummer, innerhalb der absteigenden chronologischen Reihenfolge der Jahrgänge mit Verweis auf das jeweilige pdf-Symbol zum Herunterladen angezeigt.

The **Reports on Polar and Marine Research** (ISSN 1866-3192) are available as open access publications since 2008. A table of all volumes including the printed issues (ISSN 1618-3193, Vol. 1-376, from 2000 until 2008), as well as the earlier **Reports on Polar Research** (ISSN 0176-5027, Vol. 1-376, from 1981 until 2000) is provided by the electronic Publication Information Center (**ePIC**) of the Alfred Wegener Institute, Helmholtz Centre for Polar and Marine Research (AWI); see URL <http://epic.awi.de>. To generate a list of all Reports, use the URL <http://epic.awi.de> and select "browse"/ "type" to browse "Reports on Polar and Marine Research". A chronological list in declining order will be presented, and pdf icons displayed for downloading.

Zuletzt erschienene Ausgaben:

689 (2015) The Expedition PS89 of the Research Vessel POLARSTERN to the Weddell Sea in 2014/2015, edited by Olaf Boebel

688 (2015) The Expedition PS87 of the Research Vessel POLARSTERN to the Arctic Ocean in 2014, edited by Rüdiger Stein

687 (2015) The Expedition PS85 of the Research Vessel POLARSTERN to the Fram Strait in 2014, edited by Ingo Schewe

686 (2015) Russian-German Cooperation CARBOPERM: Field campaigns to Bol'shoy Lyakhovsky Island in 2014, edited by Georg Schwamborn and Sebastian Wetterich

685 (2015) The Expedition PS86 of the Research Vessel POLARSTERN to the Arctic Ocean in 2014, edited by Antje Boetius

684 (2015) Russian-German Cooperation SYSTEM LAPTEV SEA: The Expedition Lena 2012, edited by Thomas Opel

683 (2014) The Expedition PS83 of the Research Vessel POLARSTERN to the Atlantic Ocean in 2014, edited by Hartwig Deneke

682 (2014) Handschriftliche Bemerkungen in Alfred Wegeners Exemplar von: Die Entstehung der Kontinente und Ozeane, 1. Auflage 1915, herausgegeben von Reinhard A. Krause

681 (2014) Und sie bewegen sich doch ...Alfred Wegener (1880 – 1930): 100 Jahre Theorie der Kontinentverschiebung – eine Reflexion, von Reinhard A. Krause

680 (2014) The Expedition PS82 of the Research Vessel POLARSTERN to the southern Weddell Sea in 2013/2014, edited by Rainer Knust and Michael Schröder

679 (2014) The Expedition of the Research Vessel 'Polarstern' to the Antarctic in 2013 (ANT-XXIX/6), edited by Peter Lemke

Recently published issues:



ALFRED-WEGENER-INSTITUT
HELMHOLTZ-ZENTRUM FÜR POLAR-
UND MEERESFORSCHUNG

BREMERHAVEN

Am Handelshafen 12
27570 Bremerhaven
Telefon 0471 4831-0
Telefax 0471 4831-1149
www.awi.de

